United States Nuclear Regulatory Commission

Protecting People and the Environment

NUREG/CR-7109
ORNL/TM-2011/514

An Approach for Validating Actinide and Fission Product Burnup Credit Criticality Safety Analyses—Criticality (k_{eff}) Predictions

Office of Nuclear Regulatory Research

AVAILABILITY OF REFERENCE MATERIALS IN NRC PUBLICATIONS

NRC Reference Material

As of November 1999, you may electronically access NUREG-series publications and other NRC records at NRC's Public Electronic Reading Room at http://www.nrc.gov/reading-rm.html. Publicly released records include, to name a few, NUREG-series publications; *Federal Register* notices; applicant, licensee, and vendor documents and correspondence; NRC correspondence and internal memoranda; bulletins and information notices; inspection and investigative reports; licensee event reports; and Commission papers and their attachments.

NRC publications in the NUREG series, NRC regulations, and *Title 10, Energy*, in the Code of *Federal Regulations* may also be purchased from one of these two sources.

1. The Superintendent of Documents
   U.S. Government Printing Office
   Mail Stop SSOP
   Washington, DC 20402–0001
   Internet: bookstore.gpo.gov
   Telephone: 202-512-1800
   Fax: 202-512-2250
2. The National Technical Information Service
   Springfield, VA 22161–0002
   www.ntis.gov
   1–800–553–6847 or, locally, 703–605–6000

A single copy of each NRC draft report for comment is available free, to the extent of supply, upon written request as follows:

Address: U.S. Nuclear Regulatory Commission
Office of Administration
Publications Branch
Washington, DC 20555-0001
E-mail: DISTRIBUTION.RESOURCE@NRC.GOV
Facsimile: 301–415–2289

Some publications in the NUREG series that are posted at NRC's Web site address http://www.nrc.gov/reading-rm/doc-collections/nuregs are updated periodically and may differ from the last printed version. Although references to material found on a Web site bear the date the material was accessed, the material available on the date cited may subsequently be removed from the site.

Non-NRC Reference Material

Documents available from public and special technical libraries include all open literature items, such as books, journal articles, and transactions, *Federal Register* notices, Federal and State legislation, and congressional reports. Such documents as theses, dissertations, foreign reports and translations, and non-NRC conference proceedings may be purchased from their sponsoring organization.

Copies of industry codes and standards used in a substantive manner in the NRC regulatory process are maintained at—

The NRC Technical Library
Two White Flint North
11545 Rockville Pike
Rockville, MD 20852–2738

These standards are available in the library for reference use by the public. Codes and standards are usually copyrighted and may be purchased from the originating organization or, if they are American National Standards, from—

American National Standards Institute
11 West 42nd Street
New York, NY 10036–8002
www.ansi.org
212–642–4900

Legally binding regulatory requirements are stated only in laws; NRC regulations; licenses, including technical specifications; or orders, not in NUREG-series publications. The views expressed in contractor-prepared publications in this series are not necessarily those of the NRC.

The NUREG series comprises (1) technical and administrative reports and books prepared by the staff (NUREG–XXXX) or agency contractors (NUREG/CR–XXXX), (2) proceedings of conferences (NUREG/CP–XXXX), (3) reports resulting from international agreements (NUREG/IA–XXXX), (4) brochures (NUREG/BR–XXXX), and (5) compilations of legal decisions and orders of the Commission and Atomic and Safety Licensing Boards and of Directors' decisions under Section 2.206 of NRC's regulations (NUREG–0750).

DISCLAIMER: This report was prepared as an account of work sponsored by an agency of the U.S. Government. Neither the U.S. Government nor any agency thereof, nor any employee, makes any warranty, expressed or implied, or assumes any legal liability or responsibility for any third party's use, or the results of such use, of any information, apparatus, product, or process disclosed in this publication, or represents that its use by such third party would not infringe privately owned rights.

United States Nuclear Regulatory Commission

Protecting People and the Environment

NUREG/CR-7109
ORNL/TM-2011/514

An Approach for Validating Actinide and Fission Product Burnup Credit Criticality Safety Analyses—Criticality (k_{eff}) Predictions

Manuscript Completed: December 2011
Date Published: April 2012

Prepared by
J. M. Scaglione
D. E. Mueller
J. C. Wagner
W. J. Marshall

Oak Ridge National Laboratory
Managed by UT-Battelle, LLC
Oak Ridge, TN 37831-6170

Don Algama, NRC Project Manager

Prepared for
Division of Systems Analysis
Office of Nuclear Regulatory Research
U.S. Nuclear Regulatory Commission
Washington, DC 20555-0001

NRC Job Code V6005

Office of Nuclear Regulatory Research

ABSTRACT

Taking credit for the reduced reactivity of spent nuclear fuel (SNF) in criticality analyses is referred to as burnup credit (BUC). Criticality safety evaluations require validation of the computational methods with critical experiments that are as similar as possible to the safety analysis models, and for which the k_{eff} values are known. This poses a challenge for validation of BUC criticality analyses, as critical experiments with actinide and fission product (FP) nuclides similar to SNF are not available. To address the issue of validation for nuclides that lack experimental data (e.g., minor actinides and FPs) the US Nuclear Regulatory Commission initiated a project with the Oak Ridge National Laboratory to establish and demonstrate an approach that could be used for commercial SNF criticality safety evaluations based on best-available data and methods. This report describes how model-specific sensitivity data can be used to translate nuclear data uncertainties into uncertainty in the model k_{eff} value.

TABLE OF CONTENTS

Section **Page**

ABSTRACT iii
LIST OF FIGURES vii
LIST OF TABLES ix
EXECUTIVE SUMMARY xiii
ACKNOWLEDGMENTS xv
ACRONYMS AND UNITS xvii
1. INTRODUCTION 1
2. BACKGROUND 3
3. ANALYSIS METHODS 5
3.1 COMPUTER CODES AND DATA USED 7
3.1.1 Depletion Analyses 8
3.1.2 Criticality Analyses 9
3.1.3 Sensitivity/Uncertainty Analyses 9
3.2 DESCRIPTION OF ANALYSIS 9
3.2.1 Application and Critical Experiment Modeling 10
3.2.2 Similarity of Application and Critical Experiment Models 10
3.2.3 Sensitivity Analysis of Application and Critical Experiment Models 11
3.2.4 Similarity Analysis Using Sensitivity Data 11
3.2.5 Model-Specific k_{eff} Uncertainties Due to Nuclear Data Uncertainties 12
3.2.6 Trending Analysis and Bias and Bias Uncertainty Determination 19
3.2.7 Fission Product Bias Analysis Techniques 21
4. APPLICATION MODELS 25
4.1 PWR SPENT NUCLEAR FUEL POOL APPLICATIONS 26
4.2 CASK APPLICATION 29
4.3 BWR SPENT NUCLEAR FUEL POOL APPLICATION 32
5. CRITICAL EXPERIMENTS 37
5.1 LOW-ENRICHMENT URANIUM EXPERIMENTS 37
5.2 MIXED URANIUM AND PLUTONIUM EXPERIMENTS 39
5.3 HAUT TAUX DE COMBUSTION MOX EXPERIMENTS 41
5.4 FRENCH FISSION PRODUCT PROGRAM EXPERIMENTS 41
6. BIAS AND BIAS UNCERTAINTY 43
6.1 BIAS AND BIAS UNCERTAINTY DETERMINATION 43
6.2 BIAS AND BIAS UNCERTAINTY USING S/U ANALYSIS FOR SIMILARITY AND c_K TRENDING 47
6.2.1 Similarity Determination Using Sensitivity and Uncertainty Analysis 47
6.2.2 Bias and Bias Uncertainty Using Sensitivity and Uncertainty Analysis 51
6.3 COMPARISON OF BIAS AND UNCERTAINTY WITH NUCLEAR DATA UNCERTAINTY VALUES 53
6.4 BIAS AND BIAS UNCERTAINTY FOR FISSION PRODUCTS 57
6.4.1 Fission Product Experiment Analysis 61

TABLE OF CONTENTS
(Continued)

Section **Page**

6.4.2 Application of Fission Product Bias and Bias Uncertainty 77
6.5 CONCLUSIONS ON CALCULATION OF BIAS AND BIAS UNCERTAINTY 80

7. BIAS AND BIAS UNCERTAINTY SENSITIVITY STUDY 83
7.1 PARAMETRIC EVALUATION 83
7.2 REFERENCE MODEL PARAMETERS 83
7.3 PARAMETRIC APPLICATIONS 83
7.4 SENSITIVITY ANALYSIS RESULTS AND DISCUSSION 88
7.4.1 Conventional Bias and Bias Uncertainty Assessment Impacts 88
7.4.2 Sensitivity and Uncertainty Based Benchmark Selection Bias and Bias Uncertainty Impacts 96
7.4.3 Nonapplicable LCE Nuclide Validation Assessment 101
7.5 SENSITIVITY ANALYSIS SUMMARY 106

8. CONCLUSIONS AND RECOMMENDATIONS 107

9. REFERENCES 109

APPENDIX A. SPENT NUCLEAR FUEL ASSEMBLY BENCHMARK DATA SUMMARY OF EXPERIMENTAL AND CALCULATED RESULTS A-1

APPENDIX B. SIMILARITY ASSESSMENT RESULTS B-1

APPENDIX C. BIAS AND BIAS UNCERTAINTY USING GLLSM C-1

APPENDIX D. EXAMPLE TRITON DEPLETION CODE INPUT D-1

LIST OF FIGURES

Figure **Page**

Figure 3.1 Overview of burnup credit validation process. 6

Figure 3.2 Comparison of calculated biases and experiment-specific nuclear data uncertainty in k_{eff} for 124 LEU LCEs. 15

Figure 3.3 Comparison of calculated biases and experiment-specific nuclear data uncertainty in k_{eff} for 194 Pu+U LCEs. 16

Figure 3.4 Comparison of calculated biases and experiment-specific nuclear data uncertainty in k_{eff} for 156 French HTC LCEs. 17

Figure 3.5 Comparison of calculated biases and experiment-specific nuclear data uncertainty in k_{eff} for 135 French FP LCEs. 18

Figure 3.6 (*Top*) samarium-149 k_{eff} sensitivity, *(center)* (n,γ) cross sections, and *(bottom)* (n,γ) cross-section uncertainty. 22

Figure 3.7 Samarium-149 (n,γ) cross-section correlation matrix. 23

Figure 4.1 PWR SFP application model. 27

Figure 4.2 Burnup credit loading curves for PWR SFP application models. 28

Figure 4.3 Cutaway view of the GBC-32 cask showing the cask bottom half with a quarter of the model removed. 30

Figure 4.4 Burnup credit loading curves for GBC-32 application models. 31

Figure 4.5 Burnup credit and BWR peak SCCG k_∞. 33

Figure 4.6 Relationship between hot full-power k_∞ and SCCG k_∞. 34

Figure 4.7 BWR SFP application model. 35

Figure 6.1 Similarity of 10 GWd/MTU PWR SFP model and each critical experiment. 48

Figure 6.2 Similarity of 40 GWd/MTU PWR SFP model and each critical experiment. 49

Figure 6.3 Similarity of 10 GWd/MTU GBC-32 cask model and each critical experiment. 49

Figure 6.4 Similarity of 40 GWd/MTU GBC-32 cask model and each critical experiment. 50

Figure 6.5 Similarity of BWR SFP model at peak SCCG burnup (11 GWd/MTU) and each critical experiment. 50

Figure 6.6 FP experiment k_{eff} values. 60

LIST OF FIGURES
(Continued)

Figure **Page**

Figure 6.7 Reference HNO_3 trending of k_{eff} versus EALF. 61

Figure 6.8 Reference HNO_3 trending of k_{eff} versus leakage fraction. 62

Figure 6.9 Reference HNO_3 trending of k_{eff} versus neutron mean free path. 62

Figure 6.10 Reference HNO_3 trending of k_{eff} versus critical water height. 63

Figure 6.11 Reference HNO_3 trending of k_{eff} versus fuel rod number. 63

Figure 6.12 Trending analysis of k_{eff} versus EALF. 65

Figure 6.13 Trending analysis of k_{eff} versus neutron leakage fraction. 66

Figure 6.14 Trending analysis of k_{eff} versus mean free path. 67

Figure 6.15 Trending analysis of k_{eff} versus water level. 68

Figure 6.16 Trending analysis of k_{eff} versus rod number. 69

Figure 6.17 Net FP bias and uncertainty using reported experimental uncertainty. 76

Figure 6.18 Net FP bias and uncertainty using adjusted experimental uncertainty. 76

Figure 6.19 FP bias and uncertainty comparison against cross-section covariance as a function of burnup for PWR SFP application model. 80

Figure 7.1 Percentage change in bias as a function of decay time. 92

Figure 7.2 Percentage change in bias from rack design variations. 93

Figure 7.3 Percentage change in bias for different soluble boron concentrations. 94

Figure 7.4 Percentage change in bias for assembly and cross-section library parameter variations. 95

Figure C.1 Net FP bias and bias uncertainty compared against bounding FP covariance uncertainty. C-14

LIST OF TABLES

Table **Page**

Table 4.1 Key parameters from PWR SFP application models 28

Table 4.2 Key parameters from application models (GBC-32) 31

Table 6.1 Bias and uncertainty as a function of EALF using only IHECSBE experiments 44

Table 6.2 Bias and uncertainty as a function of EALF using IHECSBE and HTC experiments 44

Table 6.3 Bias and uncertainty as a function of final enrichment using IHECSBE experiments 45

Table 6.4 Bias and uncertainty as a function of final enrichment using HTC and IHECSBE experiments 45

Table 6.5 Bias and uncertainty as a function of final Pu content [wt %, g Pu/(g Pu + g U)] using IHECSBE experiments 46

Table 6.6 Bias and uncertainty as a function of final Pu content [wt %, g Pu/(g Pu + g U)] using HTC and IHECSBE experiments 46

Table 6.7 Similarity assessment summary 48

Table 6.8 Bias and bias uncertainty results using S/U analysis 52

Table 6.9 Nonparametric bias and bias uncertainty 52

Table 6.10 Uncertainty in k_{eff} due to uncertainty in nuclear data for BUC application models 54

Table 6.11 Uncertainty in k_{eff} due to uncertainty in nuclear data for SFP model as a function of burnup 55

Table 6.12 k_{eff} uncertainty due to uncertainty in nuclear data for ENDF/B-V, -VI, and -VII nuclear data libraries 56

Table 6.13 FP experiment evaluation data 58

Table 6.14 Rhodium-103 bias evaluation 71

Table 6.15 Cesium-133 bias evaluation 72

Table 6.16 Samarium-149 bias evaluation 73

Table 6.17 Samarium-152 bias evaluation 73

Table 6.18 Gadolinium-155 bias evaluation 74

LIST OF TABLES
(Continued)

Table **Page**

Table 6.19 Neodymium bias evaluation 74

Table 6.20 FP experiment bias and bias uncertainty (Δk) (reported experimental uncertainty) 75

Table 6.21 FP experiment bias and bias uncertainty (Δk) (adjusted experimental uncertainty) 75

Table 6.22 PWR SFP application model sensitivity-adjusted FP bias (EALF) and uncertainty (Δk) 78

Table 6.23 PWR SFP application model sensitivity-adjusted FP bias (leakage fraction) and uncertainty (Δk) 78

Table 6.24 PWR SFP application model sensitivity-adjusted FP bias (mean free path) and uncertainty (Δk) 78

Table 6.25 PWR SFP application model sensitivity-adjusted FP bias (water height) and uncertainty (Δk) 79

Table 6.26 PWR SFP application model sensitivity-adjusted FP bias (fuel rods) and uncertainty (Δk) 79

Table 6.27 Summary bias and uncertainty results for actinide-only validation 81

Table 6.28 Uncertainty in k_{eff} due to minor actinide and fission product nuclear data uncertainties 81

Table 6.29 Summary bias and uncertainty results for actinide and fission product BUC validation 82

Table 7.1 Parameters selected for sensitivity analyses 83

Table 7.2 Sensitivity case key parameters 85

Table 7.3 Bias and uncertainty as a function of EALF 89

Table 7.4 Bias and uncertainty as a function of final uranium enrichment 90

Table 7.5 Bias and uncertainty as a function of final plutonium content 91

Table 7.6 Bias and uncertainty based on c_k trending 97

Table 7.7 Bias and uncertainty based on *EALF* trending 98

Table 7.8 Bias and uncertainty based on final plutonium content trending 99

LIST OF TABLES
(Continued)

Table		Page
Table 7.9	Bias and uncertainty based on final uranium enrichment trending	100
Table 7.10	Summary of one sigma uncertainty results for PWR SFP parametric application models	102
Table 7.11	Unvalidated nuclide uncertainty-to-worth ratios (Δk) results for PWR SFP application model using all isotopes BUC	105
Table 7.12	Unvalidated nuclide uncertainty to worth ratios (Δk) results for GBC32 application models	105
Table A.1	Critical experiments from IHECSBE and ENDF/B-VII 238 group library results	A-1
Table B.1	Critical experiment similarity assessment c_k values for applications	B-1
Table C.1	TSURFER results using actinide + 16 FP isotopes	C-3
Table C.2	TSURFER total bias and bias uncertainty (1σ)	C-4
Table C.3	TSURFER FP isotope bias	C-5
Table C.4	TSURFER FP residual uncertainty (1σ)	C-8
Table C.5	TSUNAMI-IP seven FP bounding uncertainty in k_{eff} at 1σ confidence	C-11

EXECUTIVE SUMMARY

One of the most significant remaining challenges associated with expanded implementation of burnup credit in the United States is the validation of depletion and criticality calculations used in the safety evaluation—in particular, the availability and use of applicable measured data to support validation, especially for fission products. This report presents an approach for addressing validation of minor actinides and fission products in burnup credit criticality safety analyses of commercial spent nuclear fuel (SNF) storage and transportation systems.

This approach (1) uses available laboratory critical experiment (LCE) data from the *International Handbook of Evaluated Criticality Safety Benchmark Experiments* (IHECSBE) and the French Haut Taux de Combustion (HTC) program to demonstrate use of existing laboratory critical experiments for validation of the major actinide isotopes, and (2) uses calculated sensitivities and nuclear data uncertainties to predict individual biases for relevant nuclides (e.g., minor actinides and fission products) where applicable critical experiments are unavailable.

The methodology for determining the nuclide biases based on nuclear data uncertainties is described in Section 3.2.5, results are provided in Sections 6.3 and 7.4.3, and recommendations for applying the cross section uncertainty data to minor actinides and fission products are provided in Section 8.

Reference bias and bias uncertainty results are provided for representative criticality safety analyses of pressurized water reactor (PWR) and boiling water reactor SFP systems and a representative PWR storage cask.

Mixed plutonium-uranium oxide configurations from the IHECSBE and the HTC experiment configurations, collectively, provide sufficient data for validation of burnup credit analyses with major actinides and hence should be used for validation. LEU critical configurations should not be used in a conventional validation analysis to validate spent fuel systems because they do not include any bias contribution from the plutonium present in burned fuel. For minor actinide and fission product nuclides for which adequate critical experiment data are not available, calculations of k_{eff} uncertainty due to nuclear data uncertainties can be used to establish a bounding bias value which was approximately 1.5% of the worth of the minor actinides and fission products for the representative safety analyses used in this report. This value is considered applicable when using the ENDF/B-V, -VI, or –VII cross-section libraries.

ACKNOWLEDGMENTS

This work was performed under contract with the US Nuclear Regulatory Commission (NRC) Office of Nuclear Regulatory Research. The authors thank D. Algama, the NRC Project Manager, M. Aissa and R. Y. Lee of the Office of Nuclear Research (RES), K. A. L. Wood of the Office of Nuclear Reactor Regulation (NRR), A. B. Barto and Z. Li of the Office of Nuclear Material Safety and Safeguards (NMSS), and C. N. Van Wert of the Office of New Reactors (NRO) for their support and guidance. Many valuable review comments were received from NRC staff members of RES, NRR, NMSS, and NRO. The authors also wish to thank Chris Perfetti and Georgeta Radulescu for their reviews, and D. Counce, A. Harkey, and D. Weaver for assistance in editing, formatting, and preparing the final document.

ACRONYMS AND UNITS

1D	One-dimensional
2D	Two-dimensional
3D	Three-dimensional
BA	burnable absorber
BNL	Brookhaven National Laboratory
BPR	burnable poison rod
BUC	burnup credit
B&W	Babcock and Wilcox Company
BWR	boiling water reactor
CFR	*Code of Federal Regulations*
DOE	US Department of Energy
DUN	depleted uranyl-nitrate
EALF	energy of average lethargy of neutrons causing fission (unit of neutron energy)
ENDF/B	*Evaluated Nuclear Data Files, Part B*
EOL	end of life
eV	electron volts (unit of energy)
FP	fission product
GLLSM	generalized linear least squares method (e.g., TSURFER)
GWd/MTU	gigawatt-days per metric ton of uranium (unit of fuel burnup)
HTC	Haut Taux de Combustion experiments, French for high burnup experiments
H/X	ratio of hydrogen to fissile nuclide atoms
IHECSBE	*International Handbook of Evaluated Criticality Safety Benchmark Experiments*
IRSN	Institut de Radioprotection et de Sûreté Nucléaire
keV	kilo-electron volts (unit of energy)
LANL	Los Alamos National Laboratory
LCE	Laboratory Critical Experiment
LEU	low-enrichment uranium
LWR	light water reactor
MeV	megaelectron volts (unit of energy)
MOX	mixed uranium and plutonium oxides
NRC	US Nuclear Regulatory Commission
OFA	optimized fuel assembly
ORNL	Oak Ridge National Laboratory
ppm	parts per million
PWR	pressurized water reactor
RCA	radiochemical analysis
ROP	range of parameters
SCALE	Standardized Computer Analyses for Licensing Evaluation
SCCG	standard cold core geometry
SDF	sensitivity data file
SFP	spent nuclear fuel pool
SNF	spent nuclear fuel
SRP	standard review plan
S/U	sensitivity and uncertainty
USL	upper subcritical limit

W	Westinghouse Electric Company
WABA	wet annular burnable absorber rods

1. INTRODUCTION

Criticality safety analyses are performed to show that a proposed fuel storage or transport configuration meets the applicable requirements of Title 10, *Code of Federal Regulations* (CFR), Parts 50, 52, 70, 71, and 72 (Ref. 1) and that it includes calculations to demonstrate that the proposed configuration will meet the maximum effective neutron multiplication factor (k_{eff}) limits specified in the applicable requirements and guidance. For commercial spent nuclear fuel (SNF), the reduced reactivity associated with the net depletion of fissile isotopes and the creation of neutron-absorbing isotopes when the fuel is irradiated in the reactor can reduce the criticality potential of the SNF configurations. Taking credit for the reduced reactivity potential of SNF in criticality analyses is referred to as burnup credit (BUC).

Consistent with applicable industry standards (i.e., ANSI/ANS-8 [Refs. 2 and 3]) and regulatory guidance (Refs. 4 and 5), criticality safety evaluations require validation of the calculational method with critical experiments that are as similar as possible to the safety analysis models, and for which the k_{eff} values are known. This poses a challenge for validation of BUC criticality analyses, as critical experiments with actinide and fission product (FP) nuclides similar to SNF are not available. As a result, validation for SNF pools (SFPs) has typically relied on critical experiments without FPs (Ref. 6), and BUC for transportation has been limited to actinide-only, based on Ref. 5. Credit for FPs is needed for high-density SNF storage in SFPs and is beneficial for enabling storage and transportation of most discharged SNF assemblies in casks (i.e., dry storage casks and transportation packages) (Ref. 7). Therefore, this report explores a physics-based, defensible approach to establishing a bounding estimate for bias in k_{eff} prediction for cases in which critical experiment data are lacking or nonexistent.

The purpose of this report is to establish a validation approach for nuclides that lack experimental data (minor actinides and FPs) for commercial SNF criticality safety evaluations. Some additional information is provided to demonstrate acceptable methods for determining k_{eff} bias and bias uncertainty for major actinide nuclides using existing experimental data. This report uses the best-available data and methods and applies the approach to representative SNF storage and transport configurations/conditions to demonstrate its usage and applicability, as well as to provide reference bias results. Validation of SNF composition calculations is addressed in a companion report (Ref. 8).

The work presented in this report involved (1) validation of several representative BUC safety analysis models, hereafter also referred to as “applications,” (2) consideration of selecting appropriate critical experiments for the application, (3) examination of the variation in bias and bias uncertainty with variation of some analysis parameters, (4) examination of the potential impacts of validation gaps and weaknesses (most notably inadequate validation of FPs), and (5) establishment of a methodology on how to address the validation gaps and weaknesses. This report is organized with sections on analysis methods (Section 3), representative safety analysis models considered (Section 4), critical experiments used for validation (Section 5), validation of the safety analysis models (Section 6), evaluation of the potential impact of poor FP and minor actinide validation (Sections 6.3 and 6.4), a parametric evaluation of SFP application model differences and associated impacts on calculated biases and uncertainties (Section 7), and conclusions and recommendations for BUC validation (Section 8). The specific methodology for calculating k_{eff} uncertainties from the nuclear data uncertainties is described in Section 3.2.5, results are provided in Sections 6.3 and 7.4.3, and recommendations for applying the minor actinide and FP cross-section uncertainty data are provided in Section 8.

2. BACKGROUND

Ideally, computer calculations would yield results that predict reality. However, computational modeling of real-world systems requires the use of simplified and approximate descriptions of the systems being modeled to facilitate attaining solutions on available computing systems. For k_{eff} calculations, the nuclear data used include errors associated with data measurement, evaluation, and representation in forms usable by computer programs. As a result, calculated results typically do not exhibit exact agreement with expectations. Hence, the goal of validation is to establish a predictable relationship between calculated results and reality. The main goal of a validation study is a quantitative understanding of the difference or "bias" between calculated and expected results and the uncertainty in this difference (bias uncertainty).

Critical experiments, which are used to validate criticality (k_{eff}) calculations, are arrangements of fissionable and structural materials in various forms and configurations that are carefully assembled to approach a critical state (i.e., $k_{eff} \approx 1$). Information describing critical experiments is found in a variety of sources, such as technical reports generated to support the criticality safety of nuclear operations and the *International Handbook of Evaluated Criticality Safety Benchmark Experiments* (IHECSBE [Ref. 9]).

Criticality validation will yield an appropriate bias for the safety application only if the critical experiments and the safety application model are similar (i.e., use the same nuclear data in a similar energy-dependent manner). The same computational method must be used for both experiments and applications; otherwise, differences in the computational methods could produce biased results. The computational method is the combination of the computer code, the data used by the computer code, and the calculational options selected by the user. Materials present in only one of either the experiments or the applications could result in determination and application of an incorrect bias. Even if the same materials are present in an experiment and in an application, local variations in the energy-dependent neutron spectrum could cause different energy-ranges of the nuclear data to be exercised, resulting in an incorrect bias. It is not enough to simply have the same materials in both the experiments and the application. For example, in a water-moderated sphere of ^{235}U, the ^{235}U will not have the same neutron spectrum that a sphere of ^{235}U metal reflected by water would have; consequently, the bias is likely to be different. The high-energy ^{235}U nuclear data are very important in the metal sphere, whereas the thermal data are the most important in the water-moderated ^{235}U system.

A significant part of the bias and bias uncertainty calculated using critical experiment models is a result of deficiencies and errors in experiment descriptions. This can clearly be seen in comparing results from critical experiment models from different critical experiment series or different critical experiment facilities. Section 4 of the IHECSBE evaluations includes critical experiment model results prepared by the evaluation authors. In some cases, such as MIX-COMP-THERM-012 and PU-COMP-MIXED-001, the sample results are so far from critical that it is clear that a significant part of the variation from critical is caused by deficiencies in the experiment descriptions. This observation should not be read as a criticism of the experiments, experimentalists, or IHECSBE evaluators. These experiments were designed and performed consistent with the standards of the day and for the purposes of their time. The existence of bias components associated with critical experiment descriptions highlights the importance of using critical experiments from multiple sources to ensure that the bias calculated is not overly influenced by systematic deficiencies or errors in critical experiment descriptions. For example, the 156 critical configurations described in the French Haut Taux de Combustion (HTC)

experiment reports (Refs. 10, 11, 12, and 13) all use the same fuel rods. An error in determining the ^{235}U content would affect all 156 configurations and would contribute to the computational method bias even though this bias component has nothing to do with how well the computational method predicts reality. The intent of computational method validation is to quantify how well the method predicts reality. Inclusion of the bias and uncertainty associated with critical experiment descriptions increases the overall computational bias uncertainty, but this is an unavoidable aspect of using critical experiments for validation.

3. ANALYSIS METHODS

A general overview of the process for implementing BUC is outlined in Figure 3.1. This report focuses on the criticality code validation process and provides a validation approach for developing the information provided in the orange-shaded boxes. Examples for development of the unshaded boxes are also provided, but they are application-specific and need to be developed for each specific license application. The demonstration of adequate BUC validation involves development of an allowable neutron multiplication factor. For the sake of facilitating this discussion with a common terminology, the terms from ANSI/ANS-8.27 (Ref. 2) are being used in a slightly modified format as presented in Eq. (3.1).

$$k_p + \Delta k_p + \beta_i + \Delta k_i + \beta + \Delta k_\beta + \Delta k_x + \Delta k_m \leq k_{limit} \tag{3.1}$$

where

k_p is the calculated multiplication factor of the model for the system being evaluated.

Δk_p is an allowance for
- statistical or convergence uncertainties, or both, in the determination of k_p,
- material and fabrication tolerances,
- uncertainties due to geometric or material representation limitations of the models used in the determination of k_p.

β_i is the bias in k_p due to depletion code bias in the calculated nuclide compositions (this component is described in Ref. 8).

Δk_i is the uncertainty in k_p due to depletion code bias uncertainty in the calculated nuclide compositions (this component is described in Ref. 8).

β is the bias that results from the calculation of the benchmark criticality experiments using a particular calculation method and nuclear cross-section data.

Δk_β is bias uncertainty that includes
- statistical or convergence uncertainties, or both, in the computation of β,
- uncertainties in the benchmark criticality experiments,
- uncertainty in the bias resulting from application of the linear least-squares fitting technique to the critical experiment results,
- a tolerance interval multiplier to yield a single-sided 95% probability and 95% confidence level.

Δk_x is a supplement to β and Δk_β that may be included to provide an allowance for the bias and uncertainty from nuclide cross-section data that might not be adequately accounted for in the benchmark criticality experiments used for calculating β.

Δk_m is a margin for unknown uncertainties and is deemed adequate to ensure subcriticality of the physical system being modeled. This term is typically referred to as an administrative margin.

k_{limit} is the upper limit on the k_{eff} value for which the system is considered acceptable.

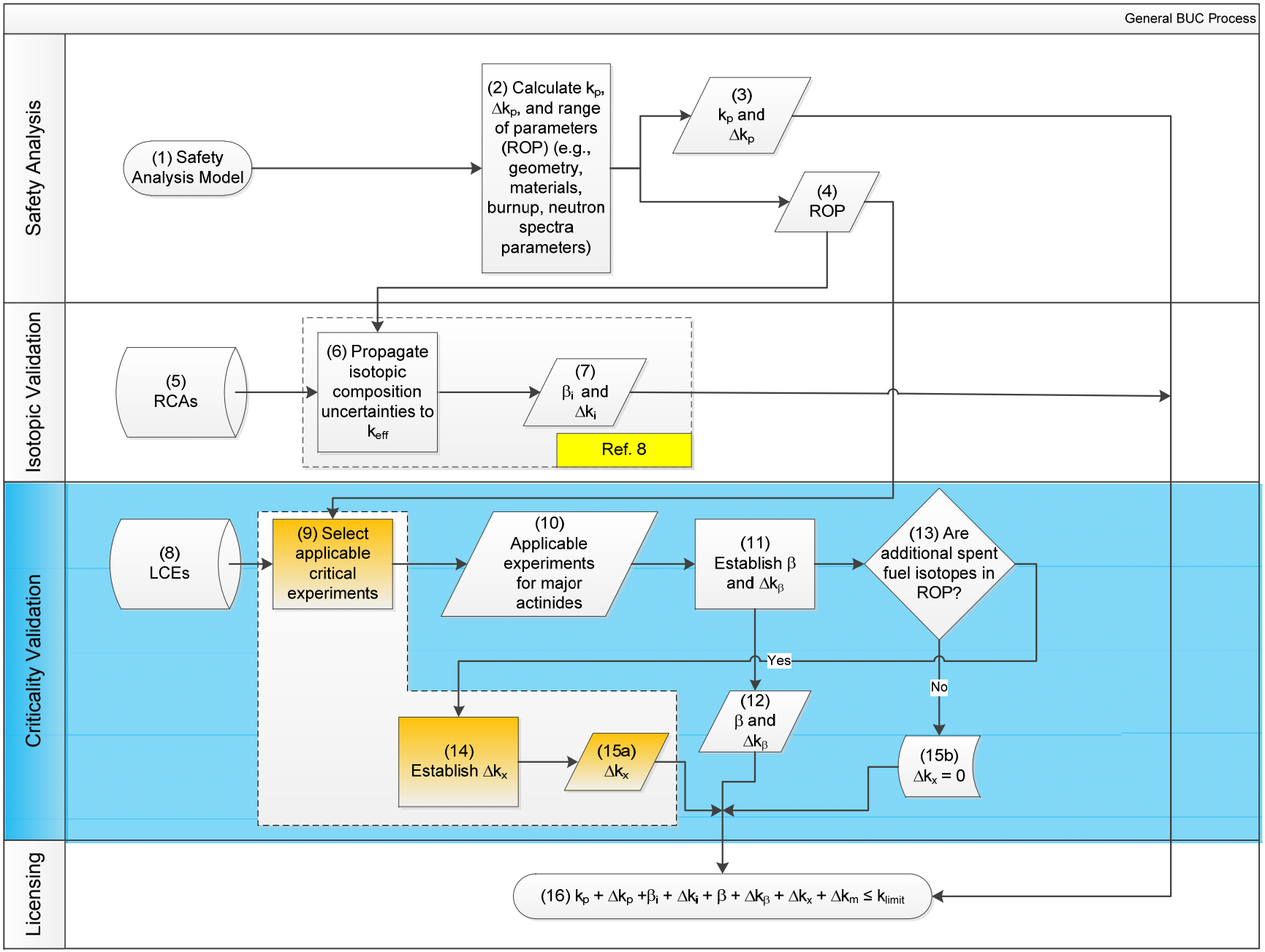

Figure 3.1 Overview of burnup credit validation process.

BUC computational validation starts with identification of a safety analysis model (Box 1 of Figure 3.1). Representative safety analysis models used in this report are described in Section 4. The safety analysis model is developed by an analyst using depletion and criticality computational tools and data of the analyst's choosing. Calculations are completed and relevant parameters of interest characterizing the application model are collected (Box 2; see Section 4 for representative examples in this report). The values for k_p and Δk_p (Box 3) are used for the licensing criterion (Box 16). Box 4 provides other parameters defining the application model that are used in the process steps identified as Boxes 6 and 9. Box 6 uses the range of parameters (ROP) data (Box 4) and the radiochemical assay (RCA) data (Box 5) to propagate isotopic uncertainties to k_{eff}; it is the subject of Ref. 8. The output from Box 6 are the β_i and Δk_i (Box 7) factors for the licensing criterion (Box 16). Box 9 uses information from the ROP (Box 4) for selecting applicable critical benchmark experiments (Box 10). Sections 3.2.2 and 3.2.4 provide a discussion of the benchmark selection process. Box 11 uses the critical benchmark experiments from Box 10 and establishes β and Δk_β. The values for β and Δk_β (Box 12) are used for the licensing criterion (Box 16). Methods for calculating these terms and example values are provided in Sections 6.1, 6.2, and 7.4. Note that β and Δk_β will be application-specific and need to be developed by the analyst with the tools that are being validated. Applicable critical benchmarks are available only for the major actinide isotopes. Therefore, if additional isotopes are being credited in the application model (Box 13), or if the neutron energy spectrum in which the common nuclides are present varies significantly between the application and laboratory critical experiments (LCEs), then Box 14 is implemented to establish Δk_x (Box 15a). (A method of determining this value is described in Section 3.2.5 with representative values presented in Sections 6.3 and 7.4.3). If additional isotopes are not being credited, then Δk_x is set to zero (Box 15b).

Applications crediting fuel burnup typically include some nuclides in the SNF material compositions for which little or no applicable critical experiment data is available (for SNF applications, typically FPs and minor actinides such as ^{243}Am, ^{237}Np, and ^{236}U). Therefore, a means of accounting for the unvalidated nuclides is necessary. This report demonstrates how the cross-section uncertainty data can be used to establish a bounding value using the following derivation to establish the Δk_x term in Eq. (3.1) above:

$$\Delta \mathrm{k_x} = \sqrt{\sum_{ACT} \sigma_i^2 + \sum_{FP} \sigma_i^2} \tag{3.2}$$

where

$\sum_{ACT} \sigma_i^2$ = sum of the squares of the uncertainty in k_{eff} due to the uncertainty in nuclear data for unvalidated and poorly validated actinide nuclides;

$\sum_{FP} \sigma_i^2$ = sum of the squares of the uncertainty in k_{eff} due to the uncertainty in nuclear data for unvalidated and poorly validated FP nuclides.

3.1 COMPUTER CODES AND DATA USED

A variety of computer codes and nuclear data sets have been and are being used by industry to perform BUC criticality safety analyses. Fuel depletion calculations are typically performed using flux solutions from either a cylindrical one-dimensional (1D) or two-dimensional (2D) lattice model, approximating an assembly, coupled with a zero-dimensional code used to calculate fuel compositions. Commonly used codes include SCALE (Ref. 14), CASMO (Ref. 15), and PARAGON (Ref. 16). Future methods are likely to include flux solutions from three-dimensional (3D) models. Access to some of the commonly used computer codes is controlled as proprietary

information. Burnup-dependent fuel compositions are then used in criticality codes such as SCALE or MCNP (Ref. 17) to determine k_{eff} for the system of interest.

The calculations performed for the work presented in this report were generated using a quality-assurance-controlled pre-release version of SCALE 6.1. All calculations were not updated with the version distributed through the Radiation Safety Information Computational Center, as differences in results were not expected.

3.1.1 Depletion Analyses

All depletion calculations were performed using either the TRITON (Ref. 14, Section T01) t-depl sequence or the STARBUCS (Ref. 14, Section C10) sequence. Model development is discussed in Section 4. Both the STARBUCS and TRITON sequences use the ORIGEN-S (Ref. 14, Section F07) program to calculate fuel compositions. The nuclear data in the ORIGEN-S libraries can be broadly classified as decay data, cross-section data, FP yields, photon emission data, and neutron emission data. In SCALE the nuclear decay data are derived from ENDF/B-VII.0 (hereinafter referred to as ENDF/B-VII), including the half-lives, branching fractions, and recoverable energy per disintegration. Decay branching fractions are included for the following decay modes: beta, electron capture and positron emission, isomeric transition, alpha, spontaneous fission, delayed neutron (β^-, n) emission, and double β^- decay.

The TRITON t-depl sequence uses the NEWT (Ref. 14, Section F21) computer code to obtain the detailed 2D flux solutions that are used in multiple ORIGEN-S depletion calculations to calculate fuel compositions that can be used directly in a criticality calculation and/or to generate ORIGEN/ARP libraries that are used by STARBUCS. The NEWT calculations were performed using the SCALE 238-energy-group ENDF/B-VII library (Ref. 14, Section M4).

The STARBUCS sequence was used to calculate fuel compositions for all pressurized water reactor (PWR) models. The automated fuel depletion built into STARBUCS was used to model fuel compositions that varied axially along the fuel assembly. The STARBUCS loading curve search options were used to determine the maximum acceptable initial fuel enrichment for a given fuel assembly burnup and target k_{eff} value. This process is discussed in the description of the model development in Section 4. STARBUCS uses the ORIGEN/ARP method, described in Section D01 of Ref. 14, to rapidly generate pointwise-specific fuel compositions for a range of conditions that are consistent with conditions used to generate the generic ORIGEN/ARP libraries. In other words, generic ORIGEN/ARP libraries are generated from TRITON calculations over a range of relevant enrichment and burnup values. The TRITON calculations required to generate the ORIGEN/ARP libraries can take several hours to complete. STARBUCS uses ORIGEN/ARP to give the specific enrichment and burnup isotopic compositions (e.g., initial enrichment of 2.63 wt % ^{235}U at 22.43 GWd/MTU burnup) with a few seconds of computer run-time based on the pregenerated ORIGEN/ARP libraries. The reason STARBUCS uses the ORIGEN/ARP code as opposed to TRITON is to reduce the total computational time needed. STARBUCS then uses the fuel compositions in CSAS5 (Ref. 14, Section C05) calculations with the SCALE ENDF/B-VII 238-energy-group library to determine k_{eff}. The boiling water reactor (BWR) application model fuel compositions were calculated directly with TRITON.

3.1.2 Criticality Analyses

Criticality or k_{eff} calculations were performed using the CSAS5 (Ref. 14, Section C05) or CSAS6 (Ref. 14, Section C06) sequences and the ENDF/B-VII 238-energy-group library. CSAS5 and CSAS6 use the KENO V.a and KENO-VI Monte Carlo transport codes, respectively. Both sequences were operated in multigroup mode. The primary difference between CSAS5 and CSAS6 is that the KENO-VI geometry inputs support more complex geometry descriptions. CSAS5 was used for all calculations with the exception of the BWR SFP model and some of the proprietary FP experiments.

3.1.3 Sensitivity/Uncertainty Analyses

The TSUNAMI-3D (Ref. 14, Section C09) analysis sequence was used to compute the sensitivity of k_{eff} to energy-dependent cross-section data for each reaction of each nuclide in a system model using linear perturbation theory as described in Sections C09 and F22 of Ref. 14. The 3D forward and adjoint calculations are performed with KENO V.a or KENO-VI. The energy-dependent sensitivity data are stored in a sensitivity data file (SDF) for subsequent analysis. TSUNAMI-3D was used to generate sensitivity data for all critical experiments and application models.

The TSUNAMI-IP (Ref. 14, Section M18) program was used to evaluate the similarity of critical experiments to application models and to compute the uncertainty in each system's k_{eff} value due to the cross-section uncertainty data (i.e., cross-section covariance data). Similarity and uncertainty analysis is discussed in more detail in following sections of this report.

TSURFER (Ref. 14, Section M21) is a bias and bias uncertainty prediction tool that implements the generalized linear least-squares method (GLLSM) approach to data assimilation and cross-section data adjustment. The data adjustments produced by TSURFER are not used to produce adjusted cross-section data libraries for subsequent use; rather, they are used to infer biases in application systems. The TSURFER tool was used with sensitivity data for the critical experiments and the application models to estimate biases associated with some FPs for a confirmatory analysis as described in Appendix C.

The TSUNAMI sequences and TSURFER program use energy-, nuclide-, and reaction-dependent nuclear data uncertainty information contained in the SCALE 44-neutron-energy-group cross-section covariance data file distributed with SCALE. The covariance data file is described in Section M19 of Ref. 14.

A final piece of software used was the USLSTATS computer code, which was used to calculate bias and bias uncertainty for application models using k_{eff} results for sets of critical experiment models. The USLSTATS program, which has been distributed with SCALE, was used to perform trending analysis and to calculate upper subcritical limits (USLs) from which the bias and bias uncertainties presented in this report were calculated. The USLSTATS program was derived from the V_STATS program (Ref. 18). The input for USLSTATS is described in Appendix C of Ref. 19.

3.2 DESCRIPTION OF ANALYSIS

The analyses performed to support the objective of this report involved the following:

- preparation of typical or representative safety analysis models, also referred to in this report as applications, and critical experiment models
- identification of critical experiments that are appropriate for use in validation studies for the applications
- generation of k_{eff} sensitivity data for the applications and for the critical experiments
- use of the sensitivity data to assess the neutronic similarity of the critical experiments and applications
- use of sensitivity data and nuclear data uncertainties to estimate the potential impact of nuclear data uncertainties on application k_{eff} values
- use of critical experiment calculated k_{eff} values to calculate bias and bias uncertainty as a function of trending parameters
- examination of FP critical experiment results to estimate FP biases

Note that the last analysis uses proprietary FP critical experiments only to confirm the approach of using nuclear data uncertainty information to address validation gaps and weaknesses.

3.2.1 Application and Critical Experiment Modeling

Application model development is described in Section 4 of this report. Critical experiment model development is described in Section 5. With the exception of the HTC [IRSN Proprietary Refs. 10, 11, 12, and 13] and French Fission Product Programme [IRSN Proprietary Refs. 20, 21, 22, 23, and 24] critical experiments, all critical experiments used in this work are described in the IHECSBE (Ref. 9). Section 5 provides a complete list of experiments used.

3.2.2 Similarity of Application and Critical Experiment Models

The primary objective of computational method validation is to establish the relationship between reality and calculated results. For validation of criticality calculations, this is accomplished with comparisons between measured critical conditions and calculated k_{eff} values of LCEs. The generally accepted guidance for critical experiment selection is that the critical experiments should be as similar to the application model as is practical and that the same computational method should be used for both critical experiment and application models. Unfortunately, a high degree of similarity occurs only in cases in which critical experiments were designed to simulate the real operational situation. Much more frequently, the analyst is confronted with validating an application model that varies from available critical experiment descriptions. This is particularly true for BUC application models because there are no LCEs that include enriched uranium, plutonium, other actinides, and FPs in the same proportions contained in commercial SNF. Hence, a combination of LCEs is necessary to yield an accurate calculation of the bias and bias uncertainty.

BUC application models involve fuel compositions that include low-enrichment uranium (LEU) and, especially at moderate to high burnup values, a significant amount of plutonium, which includes a significant ^{240}Pu fraction. Beyond the fuel composition issues, the fuel storage and

transport application models typically include steel and aluminum as structural materials and may include neutron absorbers. No LCEs are driven primarily by burned nuclear fuel; consequently, BUC critical experiment validation sets are typically composed of low-enrichment UO_2 critical experiments and mixed uranium and plutonium oxide (MOX) critical experiments. Unless one uses sensitivity and uncertainty (S/U) analysis techniques, the traditional approach is often used to determine which critical experiments are similar to a given application model, which is based primarily on qualitative characteristics, such as the presence of certain fissionable, moderating, and/or neutron-absorbing nuclides; the form and geometry of the fissionable material; and global quantitative characteristics such as the ratio of hydrogen to fissile nuclide atoms (H/X), fuel pin lattice pitch, and energy of average lethargy of neutrons causing fission (EALF).

3.2.3 Sensitivity Analysis of Application and Critical Experiment Models

The SCALE computer code system includes calculational sequences (i.e., TSUNAMI-1D, -2D, and -3D) that can be used to calculate the sensitivity of the k_{eff} value of a system to variation of the nuclear data used in the k_{eff} calculation. The fundamental principle evaluated, which can be evaluated with any criticality code, is how the response (e.g., system k_{eff}) changes with minor variations (i.e., perturbations) to input parameters used to calculate k_{eff}. The SCALE-generated sensitivities are calculated as a function of nuclide, nuclear reaction, and neutron energy group using first-order linear perturbation theory (Ref. 14, Section F22). As calculated by TSUNAMI, sensitivity is the fractional change in k_{eff} due to a fractional change in a nuclear data value, or $S \equiv (\Delta k/k) / (\Delta\sigma/\sigma)$. A sensitivity of +1.0 means a 1.0 % increase in the value of the nuclear data will result in a 1.0% increase in the system k_{eff} value. A feature unique to the SCALE sensitivity calculations is that the effects of the sensitivity of the multigroup problem-dependent resonance calculations to variations in data used in the resonance calculations are included and are referred to as the “implicit” contribution to sensitivity. For example, in water-moderated low-enrichment lattices, the ^{238}U resonance calculations are sensitive to the hydrogen-scattering cross sections. Consequently, the sensitivity of hydrogen scattering includes an explicit component related to its ability to thermalize neutrons and an implicit component that reflects hydrogen-scattering impact on ^{238}U resonance calculations.

TSUNAMI-3D calculations were performed for all application and critical experiment models. Direct perturbation calculations were used to confirm the adequacy of the sensitivity data. Direct perturbation calculations involve manually varying the composition information around the nominal value and using the resulting k_{eff} value variations to calculate the total sensitivity. Direct perturbation results were compared with TSUNAMI sensitivity results to confirm the adequacy of the sensitivity data.

3.2.4 Similarity Analysis Using Sensitivity Data

A technique implemented in the SCALE S/U tools can be used to perform detailed comparisons of application and critical experiment models. The technique compares the detailed sensitivity data for the two systems, giving greater weight to comparisons of sensitivities for nuclides and reactions with the highest nuclear data uncertainties. For each model, TSUNAMI-IP combines the sensitivity data and the cross-section covariance data to generate nuclide-, reaction-, and energy-dependent k_{eff} uncertainty data. A correlation coefficient, identified as the c_k value, is calculated and indicates the degree to which each application and critical experiment model pair

share k_{eff} uncertainty. A high c_k value, approaching one, indicates that the two compared systems share a similar sensitivity to the same nuclear data uncertainty. Based on the assumption that computational biases are due primarily to nuclear data errors and that the nuclear data uncertainty values should indicate the potential for such nuclear data errors, two highly correlated systems should exhibit the same computational bias.

Oak Ridge National Laboratory (ORNL) experience (Ref. 25) with the SCALE S/U tools has indicated that a critical experiment is similar to an application model if the c_k value ≥ 0.9. Critical experiments with c_k values between 0.8 and 0.9 are considered marginally similar, and use of experiments with c_k values below 0.8 is not recommended. The use of S/U techniques to assess similarity is discussed in more detail in Section 6.2.1.

3.2.5 Model-Specific k_{eff} Uncertainties Due to Nuclear Data Uncertainties

All nuclear data used in criticality calculations have some uncertainty. The amount of uncertainty varies with the type of data; the experimental apparatus used to measure the data; the quality and amount of measured data from which the nuclear data are derived; and the evaluation technique used to convert the experimental data into formats suitable for use in the computational method. Uncertainty associated with the latter includes uncertainties related to fitting sometimes conflicting data from multiple sources, interpolation between measurements, use of nuclear models to fill in gaps between sometimes sparse data, fitting of resonance data to nuclear data library formats, and creation of multigroup data from pointwise evaluated data. This nuclear data uncertainty can be correlated among different neutron energy groups, different nuclear reactions, and different nuclides. To quantify the degree of correlation and effects, covariance matrices are needed.

High-fidelity covariance data are available for only a limited number of nuclides. A collaborative effort involving nuclear data experts from Brookhaven National Laboratory (BNL), Los Alamos National Laboratory (LANL), and ORNL has developed approximate covariance data for nearly all other nuclides and reactions of interest. These high- and low-fidelity covariance data are combined in the SCALE 44-group covariance data file, which is a comprehensive covariance library representing 401 materials (Ref. 14, Section M19.1), including those relevant to BUC calculations. This information is in the form of variance and covariance information, where covariance is the degree to which different data and their uncertainties are related to each other. Model-specific sensitivity data, in units of $(\Delta k/k)/(\Delta\sigma/\sigma)$, can be used to translate nuclear data uncertainties, which are in units of $\Delta\sigma/\sigma$, into uncertainty in the model k_{eff} value.

Frequently, the use of 44-group covariance data with 238-group neutron transport calculations is questioned. Use of the 44-group data is acceptable because, whereas the nuclear data vary significantly within the 238 neutron-energy-group structure, the fractional uncertainty does not. Nuclear data uncertainties are more a product of the measurement and evaluation processes and do not vary as much over a broader range (see Section 3.2.7.1 for an illustrative example).

The SCALE TSUNAMI-IP module (Ref. 14, Section M18.1) was used to calculate detailed k_{eff} uncertainty information for each application model using the process described in Section F22.2.5 of Ref. 14. Note that the uncertainty calculation incorporates correlations in uncertainties among energy groups, among reactions, and, in some cases, among nuclides. Such correlations may exist because a measurement technique has been calibrated using one nuclide to measure the value for another. A different type of correlation is one in which nuclear

data are not measured but are calculated from two other measured quantities (e.g., the scattering cross section could be determined from the difference between the total cross section and the absorption cross section).

Conventional validation analyses use LCEs that are as similar as possible to the safety analysis models, and statistical analysis of the LCE results, to determine bias and bias uncertainty. Attention to the range of applicability of the LCEs is necessary to identify weaknesses in the validation. Such weaknesses may consist of missing materials, materials not present in the correct proportions, extra materials present only in the LCEs, geometry differences, neutron energy spectra differences, and others. Historically, when an analyst could not validate a particular material in a safety analysis model, the analyst typically either removed the material or used a Δk penalty or uncertainty based on engineering judgment (Ref. 6). The S/U analysis tools calculate the uncertainty in k_{eff} due to nuclear data uncertainties, creating a way to quantify k_{eff} bias associated with errors in the nuclear data in order to address these validation weaknesses using a quantifiable basis (Ref. 26).

Figures 3.2 through 3.5 present the individual calculated biases for 609 LCEs described and used in this report, along with the uncertainty in k_{eff} due to nuclear data for each experiment. In these figures, the *Bias* is the calculated k_{eff} minus the critical experiment evaluator expected k_{eff} (e.g., from IHECSBE); the *experiment uncertainty* is the evaluator-reported uncertainty for the expected k_{eff} value (e.g., from IHECSBE); and the *cross-section uncertainty* is the SCALE TSUNAMI-IP calculated k_{eff} uncertainty due to the cross-section uncertainties. Note that the Monte Carlo calculation uncertainty is not shown but would follow the *bias* and would be negligible compared with the uncertainties illustrated. Ignoring the contribution of experimental uncertainty to the bias and thereby assuming that the bias is due entirely to nuclear data errors, one would expect that around 67% of the individual critical experiment biases would be within one standard deviation of nuclear data uncertainty. Including the effect of critical experiment design and measurement uncertainty should spread the distribution of experiment-specific bias values somewhat. Figure 3.2 shows the results for 124 LEU LCEs. Note that 98% of the calculated bias values are within one standard deviation of the uncertainty in k_{eff} due to nuclear data uncertainty. This suggests that the nuclear data uncertainties are overestimated. The extreme outliers, such as experiment number 57, are probably the result of poor experiment description. Figures 3.3 through 3.5 show similar information for the 194 mixed Pu+U LCEs, the 156 French HTC LCEs, and the 135 French FP experiments. In the Pu+U configurations, 71% of the calculated biases are within one standard deviation. The average over the four sets, containing 609 LCEs, is that 90% of the LCE-calculated biases fall within one standard deviation of the expected value.

The purpose of these comparisons is to provide confidence that the uncertainty in k_{eff} due to nuclear data uncertainties can be used to provide bounding estimates of the actual bias values. Since each critical experiment uses the same nuclear data set, there is a significant source of common or systematic error. The impact of the systematic error is best quantified using the average or trended bias. The variability around the average bias reflects the variability in the critical experiment systems and does not reflect the ability of the computational method to accurately calculate k_{eff} for a safety analysis model. Based on Figures 3.2 through 3.5, the nuclear data uncertainty, even at the one-standard-deviation level, provides a good estimate for how large the computational bias could be, and using two or three standard deviations would provide a conservative bounding estimate for the bias.

The estimated bias values from the nuclear data uncertainties are related to the cross-section data measurements and evaluations. Since the various ENDF versions are derived from the same nuclear data measurements it is reasonable to believe that using other criticality codes with the same nuclear data should yield similar biases. Consequently, use of nuclear data uncertainties to provide a conservative estimate of the bias for commonly used criticality codes is appropriate. Cross-section processing may be different (e.g., continuous energy) for other criticality codes, but this will be captured through the validation process with applicable critical benchmark experiments. Confirmation of the applicability of this approach (i.e., the use of uncertainties in k_{eff} due to nuclear data uncertainties as a conservative estimate of the actual bias for unvalidated nuclides) for use with other criticality code systems could be demonstrated with nuclide worth comparisons.

This method will be applied below to the application models to yield information on the uncertainty in k_{eff} due to nuclear data uncertainty for the application models.

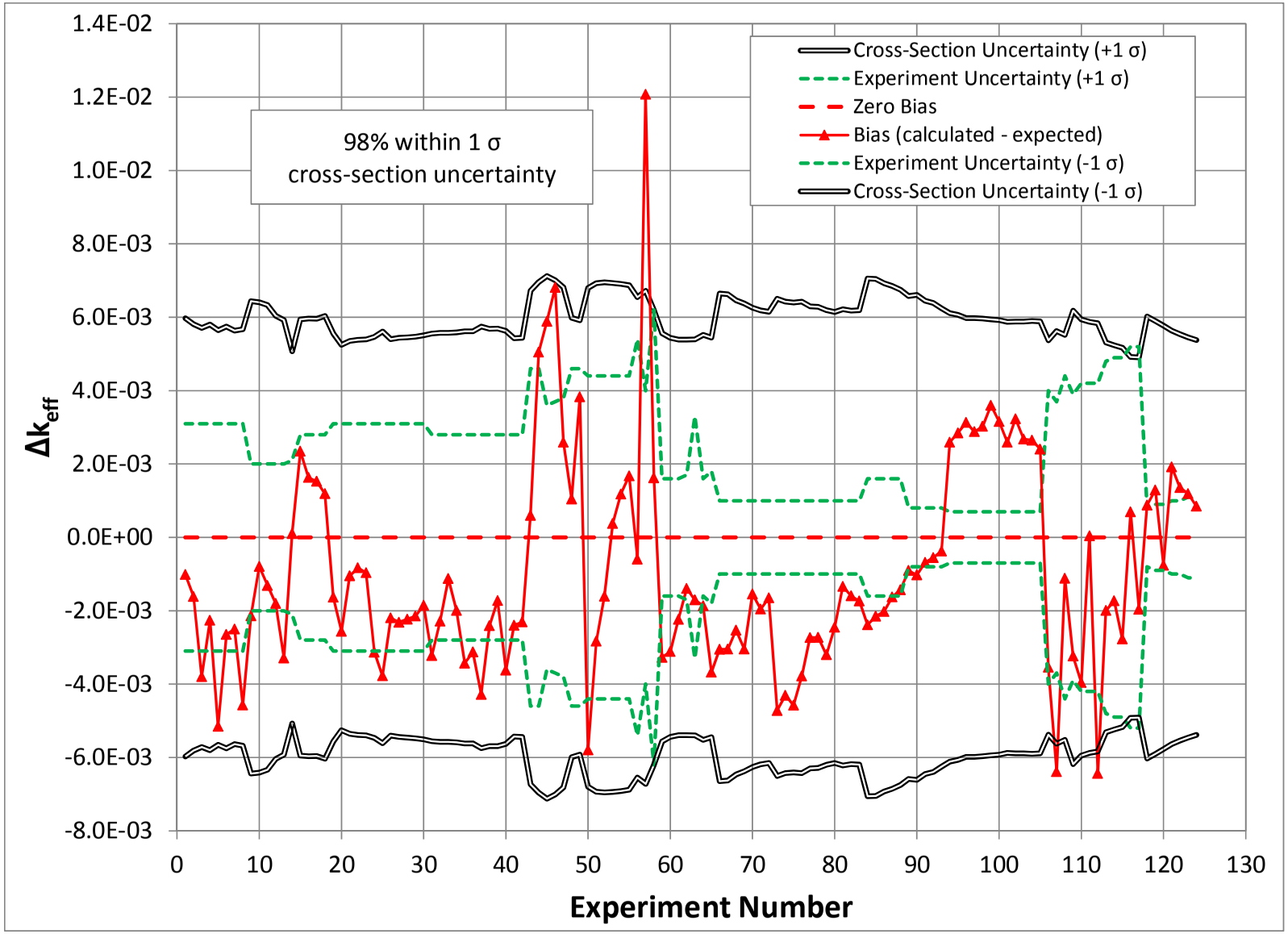

Figure 3.2 Comparison of calculated biases and experiment-specific nuclear data uncertainty in k_{eff} for 124 LEU LCEs.

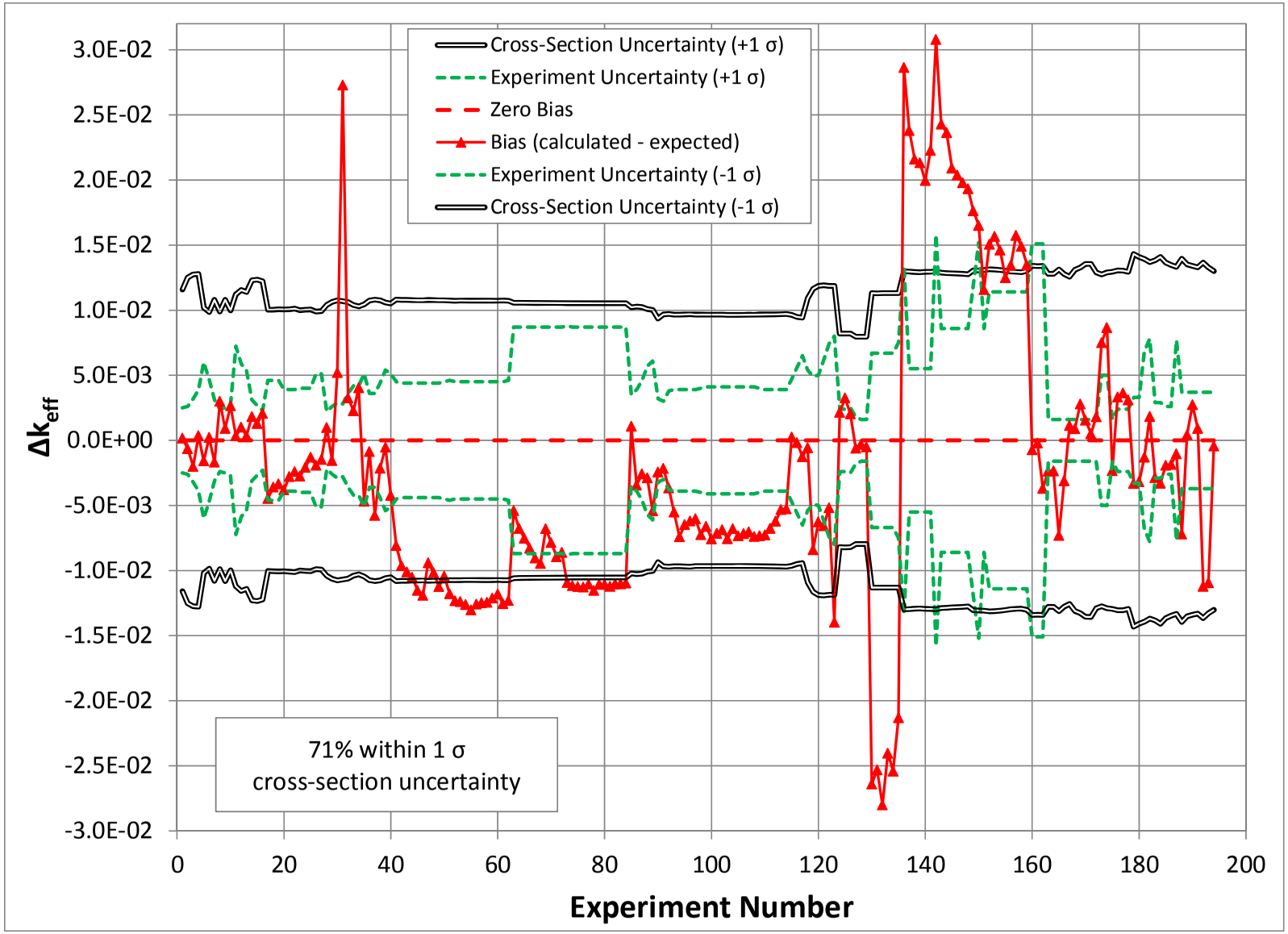

Figure 3.3 Comparison of calculated biases and experiment-specific nuclear data uncertainty in k_{eff} for 194 Pu+U LCEs.

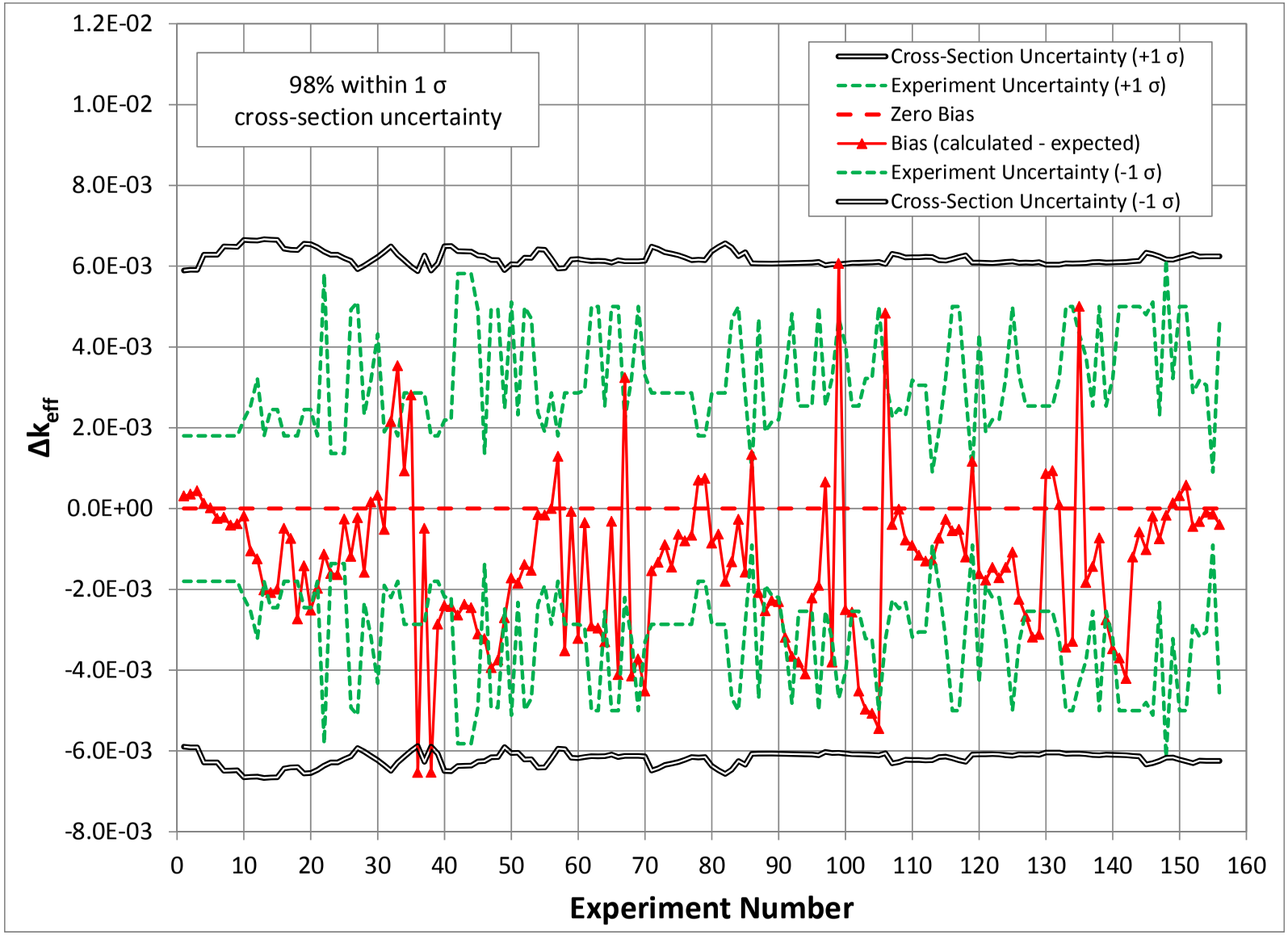

Figure 3.4 Comparison of calculated biases and experiment-specific nuclear data uncertainty in k_{eff} for 156 French HTC LCEs.

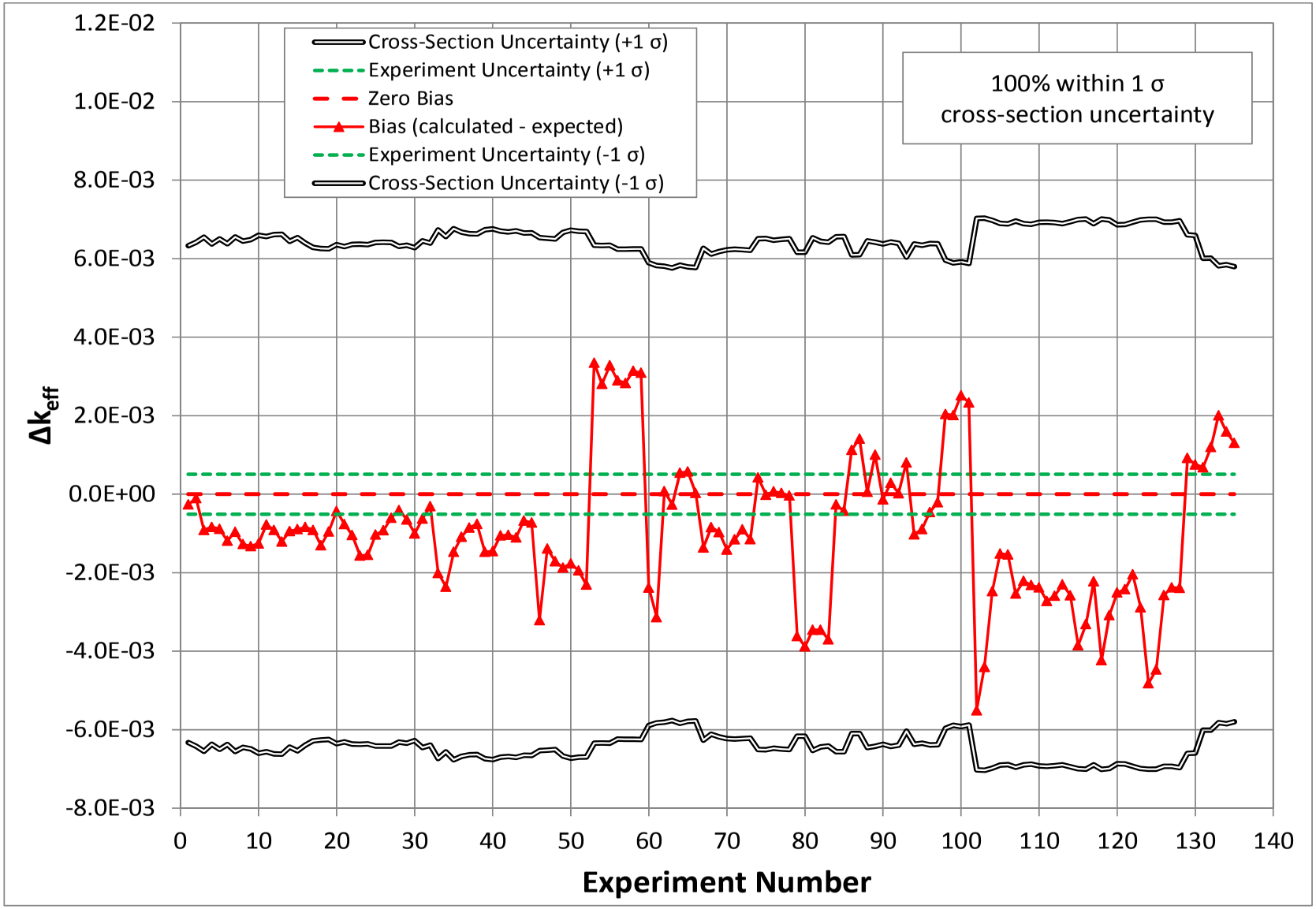

Figure 3.5 Comparison of calculated biases and experiment-specific nuclear data uncertainty in k_{eff} for 135 French FP LCEs.

3.2.6 Trending Analysis and Bias and Bias Uncertainty Determination

Computational method validation includes determination of bias and bias uncertainty based on statistical analysis of critical experiment simulation results. The bias and bias uncertainty sometimes vary significantly as a function of one or more characteristics of the critical experiments. For example, the bias and bias uncertainty may vary as a function of the soluble boron concentration used in the experiments, or as the neutron energy spectrum shifts to lower or higher energies. According to applicable standards and guidance (e.g., Refs. 3 and 27), the statistical analysis should include evaluation of the LCE results for trends occurring as functions of relevant parameters such as soluble boron concentration, EALF, fuel pin pitch, fissile concentration/enrichment, H/X atom ratios, and plutonium weight fraction (i.e., g Pu per g U+Pu) that may affect the bias and bias uncertainty. Since BUC analyses typically include fuel compositions that have a varying U to Pu ratio, and the biases associated with U and Pu may be significantly different, trending analysis for BUC validation should include a trend reflecting the in-growth of plutonium with fuel burnup.

Typically, trending analysis is performed by calculating a linear fit of the critical experiment results as a function of the trend parameters. Fits should include weighting with the uncertainty associated with each critical experiment result. NUREG/CR-6698, *Guide for Validation of Nuclear Criticality Safety Calculational Methodology* (Ref. 28), provides recipes and guidance that may be useful for trending analysis. For the work documented in this report, the USLSTATS (Refs. 18 and 19) computer code was used for single-parameter trending analyses.

An issue frequently encountered in examining trends is that the process yields multiple values for bias and bias uncertainty from the various fits, and it is not clear which bias and bias uncertainty should be used. Generally, to be conservative, the most restrictive bias and bias uncertainty resulting from the trending analyses is used. Exceptions should be thoroughly researched and justified.

An additional trending parameter, c_k, is used in this report. As discussed in Section 3.2.4, the c_k parameter is a correlation coefficient indicating how similar an experiment is to an application model. If the validation set includes a significant number of high-c_k-value critical experiments, trending and extrapolation of the bias and bias uncertainty to a c_k value of 1.0 should yield the most accurate value for the bias and bias uncertainty. A strength of the c_k value trending technique is that it includes the effects of all trends at the same time. Many other trending techniques either are 1D, considering only variation of the targeted parameter, or, as in the case of EALF, trend only global quantities. One might object to the extrapolation of the c_k trend to a value of 1.0 because extrapolation is typically not permitted unless the source of the trend is thoroughly understood. However, extrapolation of c_k to 1.0 is not really extrapolation, but rather interpolation to the center of an *n*-dimensional space. It can be thought of in three dimensions as interpolating to the center of a sphere along different rays. The c_k trending method should not be used unless there are a significant number of experiments with c_k values of no less than 0.9. Otherwise, the interpolation would be over too large a range. Reference 25 discusses how to determine what a significant number of experiments is, and recommends 25 to 40 experiments with c_k values of 0.8 or higher including 15 to 20 with c_k values of 0.9 or higher.

The bias is the best-estimate difference between calculated and expected k_{eff} values. A bias is called positive when the computational method calculates higher k_{eff} values than are expected. In general, credit is not taken for positive biases in safety analyses. This does not mean that

every positive contributor toward the bias should be discarded. The overall bias is a combination of many positive and negative biases. Discarding positive partial biases just because they have been explicitly quantified is not appropriate.

There are two components to the bias uncertainty: (1) the uncertainty in the mean bias value and (2) the sometimes overlooked uncertainty associated with spread of the critical experiment results. Including the uncertainty associated with the population variance is required to address the following requirements from 10 CFR 50.68 (b)(4):

> (4) If no credit for soluble boron is taken, the k-effective of the spent fuel storage racks loaded with fuel of the maximum fuel assembly reactivity must not exceed 0.95, at a 95 percent probability, 95 percent confidence level, if flooded with unborated water. If credit is taken for soluble boron, the k-effective of the spent fuel storage racks loaded with fuel of the maximum fuel assembly reactivity must not exceed 0.95, at a 95 percent probability, 95 percent confidence level, if flooded with borated water, and the k-effective must remain below 1.0 (subcritical), at a 95 percent probability, 95 percent confidence level, if flooded with unborated water.

Inclusion of the population variance is required because the probability and confidence level cited in 10 CFR 50.68(b)(4) is associated with a single configuration, which is assumed to be from the same population as the critical experiments, meeting the applicable k_{eff} criterion. It is required that if one additional calculation, assumed to be from the same distribution, is performed, the k_{eff} must be low enough that there is a 95% probability with a 95% confidence level that the k_{eff} value is below the applicable limit. Thus, ignoring the impact of discarded positive biases, the 95/95 bias and uncertainty should be below 95% of the critical experiment values; and it should be far enough below to support a 95% confidence band on the 95% probability level. Similar guidance is provided in the standard review plans (SRPs) for SNF dry storage facilities (Ref. 29), dry cask storage systems (Ref. 30), and transportation packages for SNF (Ref. 31).

Many techniques can be used to calculate bias and bias uncertainty. Some examples are provided in NUREG/CR-6698 (Ref. 28); the work presented in this report used the USLSTATS computer program (Refs. 18 and 19). Care must be taken to ensure that the application of the statistical method meets all assumptions and prerequisites associated with the method. For example, many methods rely on an assumption that the population of critical experiments is normally distributed. If the distribution is not normal, the uncertainty associated with the 95% probability and 95% confidence levels may be significantly in error. Typically, nonparametric methods are used when distribution normality cannot be established.

For the purposes of this report, the bias is the difference between the best-estimate fit of the adjusted calculated k_{eff} values and 1.0. The calculated k_{eff} values are adjusted by dividing each value by the “expected” value for the critical experiment model. The expected values, where available, include adjustments for modeling simplifications and approximations on the measured or inferred k_{eff} value. The IHECSBE (Ref. 9) evaluations describe recommended models and provide expected k_{eff} and experimental uncertainty values. Bias uncertainty values presented in this report will be either the 95/95 uncertainty, which includes the population variance and tolerance factor, or the uncertainty on the mean bias value.

3.2.7 Fission Product Bias Analysis Techniques

Laboratory critical experiments, including those with FPs, are described in Section 5. The FP LCEs are driven solely or primarily by ^{235}U fission, include insufficient or no plutonium, and/or include FPs in compositions that do not approximate those found in SNF. Hence, the FP LCEs do not support FP bias calculations with typical trending analysis techniques as described in Section 3.2.6. Consequently, it is necessary to use alternative techniques to estimate biases associated with FP nuclear data. These techniques include the use of nuclear data uncertainty information, qualitative examination of FP critical experiments for biases, and FP bias estimates using the GLLSM implemented in TSURFER, as described in Appendix C.

3.2.7.1 Fission Product Nuclear Data Uncertainty

The use of nuclear data uncertainty to estimate actual bias values is described in Section 3.2.5. Fission products do not fission and have an insignificant neutron scattering contribution compared with other materials present. They are also present only at low densities in commercial light water reactor (LWR) SNF, so the only relevant nuclear reaction is neutron capture (i.e., neutron absorption followed by γ emission). The neutron absorption contribution is primarily from thermal neutron absorption and absorption in a few resonances. Figure 3.6 shows the sensitivity of k_{eff} to the ^{149}Sm neutron capture cross section, the ^{149}Sm neutron capture cross sections, and the neutron capture cross-section uncertainties without associated covariances (note how the 44-group cross-section uncertainties are constant over the energy range where the 238-group cross-section data varies significantly, demonstrating the acceptability of using the 44-group covariance data with 238-group neutron transport calculations). Quantification of the uncertainty in k_{eff} due to ^{149}Sm nuclear data uncertainty involves combining the sensitivity data from the top plot in the figure with the uncertainty data in the bottom plot, including consideration of the nuclear data covariances. Figure 3.7 shows how the cross-section uncertainties are correlated among energy groups for the n,γ reaction data for ^{149}Sm. A mathematical description of how the uncertainties are calculated is included in Section F22.2.5 of Ref. 14.

Figure 3.7 shows that in the thermal neutron energy range (energy groups 25 to 44) and in the resonance region energy range (energy groups 15 to 24), cross-section uncertainties within each range are 100% correlated in the SCALE covariance library. In the fast neutron energy range (energy groups 1 to 14), the uncertainties are less correlated and negative correlations exist between some of the fast neutron energy groups. The combination of the k_{eff} sensitivity data and the nuclear data uncertainty information yields the uncertainty in the k_{eff} value for the application model due to the uncertainty in the ^{149}Sm cross sections. This uncertainty can then be used to provide a bounding estimate for how large the k_{eff} bias due to ^{149}Sm nuclear data errors could be.

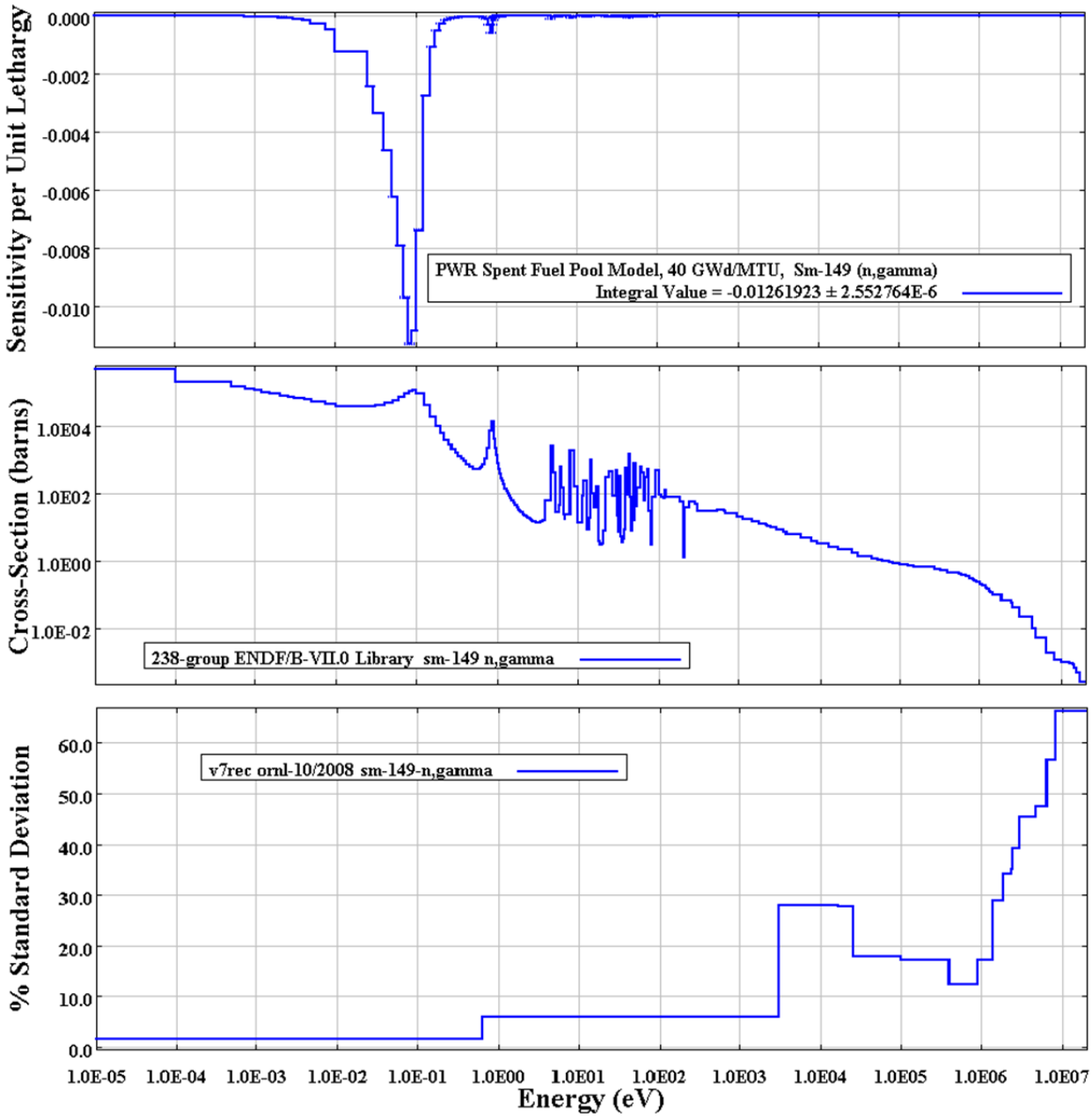

Figure 3.6 (*Top*) samarium-149 k_{eff} sensitivity, *(center)* (n,γ) cross sections, and *(bottom)* (n,γ) cross-section uncertainty.

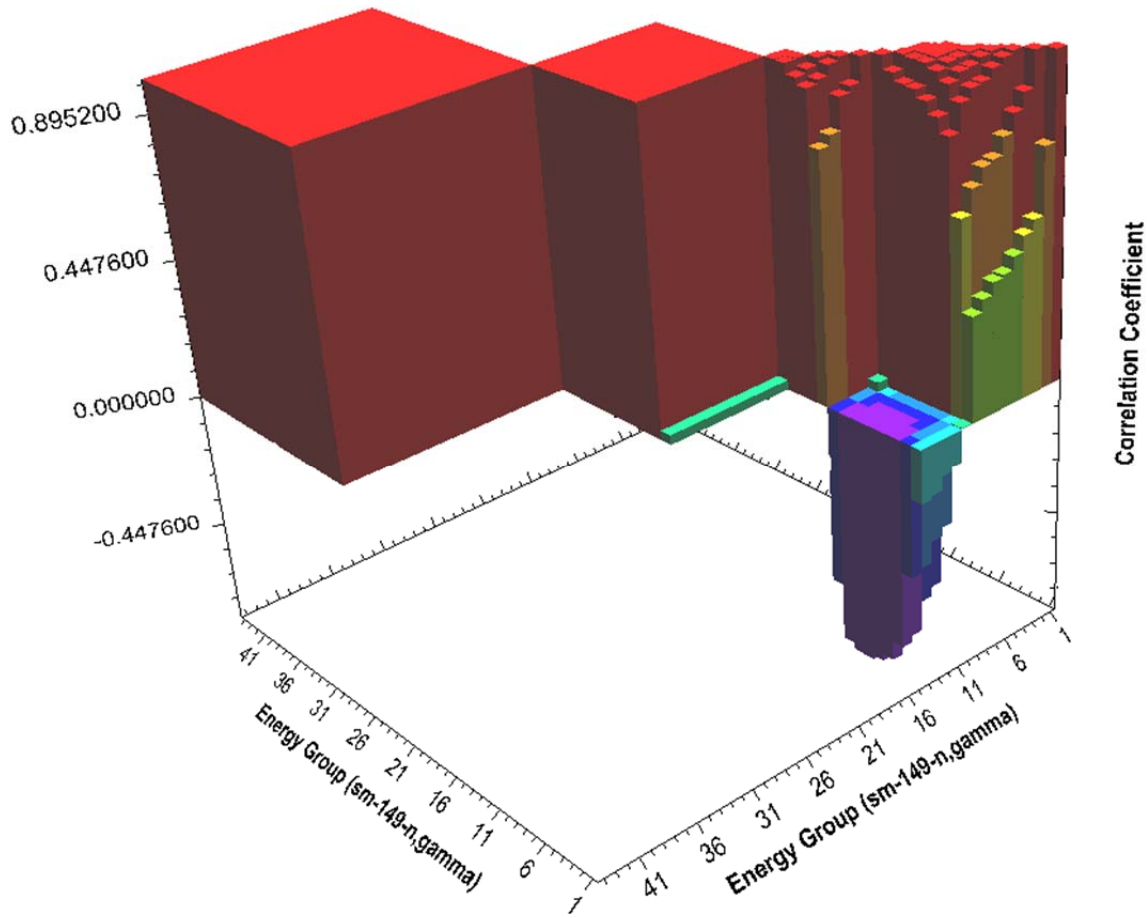

Figure 3.7 Samarium-149 (n,γ) cross-section correlation matrix.

3.2.7.2 Examination of FP LCE Results

Critical experiments that include FPs are described in Section 5. Although none of the existing critical experiments is directly applicable for bias determination for the BUC application models, the results can be examined for trends that may be useful in estimating FP biases. For example, examination of the LEU-COMP-THERM-050 ^{149}Sm LCE cases shows that as the amount of samarium is increased, the difference between calculated and experimental k_{eff} values rises. If there were no competing effects, this would indicate that the ^{149}Sm capture cross section is too small and that there is an increasingly positive (i.e., $k_{calc} - k_{expected} > 0$) computational bias associated with an increasing presence of ^{149}Sm in a thermal neutron energy spectrum. It should then be possible to estimate how much the computational bias changes as the amount of ^{149}Sm changes and thus to determine a bias applicable to the safety analysis model. The results for sets of FP critical experiments, appropriate for application to the BUC application models, were examined for trends and biases. Determination of FP biases from FP LCEs is discussed in detail in Section 6.4.

4. APPLICATION MODELS

Application models were generated representing PWR and BWR SFP configurations and a PWR cask configuration. The PWR configurations included a Westinghouse 17×17 optimized fuel assembly (OFA) burned from 0 to 70 GWd/MTU, whereas the BWR configuration included a generic 10×10 assembly design burned to about 11 GWd/MTU. These assembly designs were selected because they are used in many reactors and are considered to be representative of limiting fuel assembly designs in criticality safety applications. Example TRITON input files are provided in Appendix D showing the representative depletion parameters used for the PWR and BWR assemblies. The PWR SFP application models were generated without soluble boron in the SFP and a target k_{eff} value of 0.99. The 1% Δk reduction from 1.0 was included to approximate the impact of including bias and bias uncertainty. The GBC-32 target k_{eff} value was 0.94 and was represented as being flooded with full-density water. The BWR SFP configuration was representative of limiting SFP conditions (i.e., an assembly at peak reactivity).

PWR application models were developed for the following six cases:

- Actinides only
  - BUC with SNF composition consisting of actinide nuclides only (i.e., ^{234}U, ^{235}U, ^{236}U, ^{238}U, ^{237}Np, ^{238}Pu, ^{239}Pu, ^{240}Pu, ^{241}Pu, ^{242}Pu, ^{241}Am, and ^{243}Am). SFP model developed for 0 ppm soluble boron in the SFP with a target k_{eff} value of 0.99.
  - BUC in a cask configuration with a target k_{eff} value of 0.94.
- Actinides and 16 FPs
  - BUC with SNF composition consisting of “actinides-only” nuclides and 16 FPs (i.e., ^{95}Mo, ^{99}Tc, ^{101}Ru, ^{103}Rh, ^{109}Ag, ^{133}Cs, ^{143}Nd, ^{145}Nd, ^{147}Sm, ^{149}Sm, ^{150}Sm, ^{151}Sm, ^{152}Sm, ^{151}Eu, ^{153}Eu, and ^{155}Gd). SFP model developed for 0 ppm soluble boron in the SFP with a target k_{eff} value of 0.99.
  - BUC in a cask configuration with a target k_{eff} of 0.94.
- Actinides and all FPs
  - BUC with SNF composition consisting of all nuclides supported by the SCALE code system. SFP model developed for 0 ppm soluble boron in the SFP with a target k_{eff} value of 0.99.
  - BUC in a cask configuration with a target k_{eff} of 0.94.

The cask application model assumed a 5-year cooling period as is typical for dry storage cask and transportation package evaluations. The PWR SFP application models assumed a 3-day postirradiation decay period.

A single BWR SFP application BUC model was also developed using “actinides and all FPs” BUC for 0 ppm soluble boron at peak reactivity. The BWR SFP application assumed a 3-day postirradiation decay period.

Details of the application models are provided below. The application models are considered to be similar to or representative of models that applicants use in their criticality analyses.

4.1 PWR SPENT NUCLEAR FUEL POOL APPLICATIONS

The PWR fuel storage rack is modeled as a laterally infinite array of loaded fuel storage cells reflected on the top and bottom by 30 cm of full-density water. Each storage cell is a stainless steel box having an internal dimension of 22.352 cm (8.8 in.) and a wall thickness of 0.292 cm (0.115 in.). One 0.203-cm-thick (0.080-in.-thick) Boral® plate with a 0.020 g $^{10}B/cm^2$ loading is modeled between each storage cell. The center-to-center spacing for this model is 23.139 cm (9.110 in.). The 17 × 17 OFA is modeled as centered in the storage cell. Only the 365.76 cm (12 ft) of active fuel length of the assembly is modeled. The poison panels are also modeled to the same axial length.

Figure 4.1 shows an overhead view of the model, and Figure 4.2 shows three BUC loading curves, *Actinides-only*, *Actinides & 16 FP*, and *Actinides & all FP*. The numbers in the grid in Figure 4.2 identify the number of PWR assemblies within a given burnup and enrichment range as taken from the RW-859 database (Ref. 32), which includes data on the US commercial LWR SNF inventory as of 2002. Table 4.1 shows some key parameters for the application models at two burnups, 10 and 40 GWd/MTU, for evaluations of the potential for variation in biases as a function of burnup. The final uranium enrichment and plutonium fraction vary axially as a result of the use of axial burnup profiles. Two averages are presented for these parameters. One is the simple average from each of the 18 axial zones. The second uses the axial fission density fraction as a weighting factor, thus giving increased weight to the axial zones having the most impact on system neutron multiplication. For bias and bias uncertainty determination, use of the fission density weighted values is more appropriate.

The burned fuel compositions used in the SFP models were generated using the SCALE STARBUCS sequence and an ORIGEN/ARP library generated using TRITON and the ENDF/B-VII 238 energy group library. It included 24 wet annular burnable absorber (WABA) rods for the entire depletion. The WABA rods were included throughout the depletion because they cause the neutron spectrum to be harder during irradiation, resulting in a conservative representation of the SNF residual reactivity level. The STARBUCS loading curve search options were used to find the initial ^{235}U enrichment that, when depleted to the target assembly average burnup value, produced a rack model k_{eff} value of 0.99.

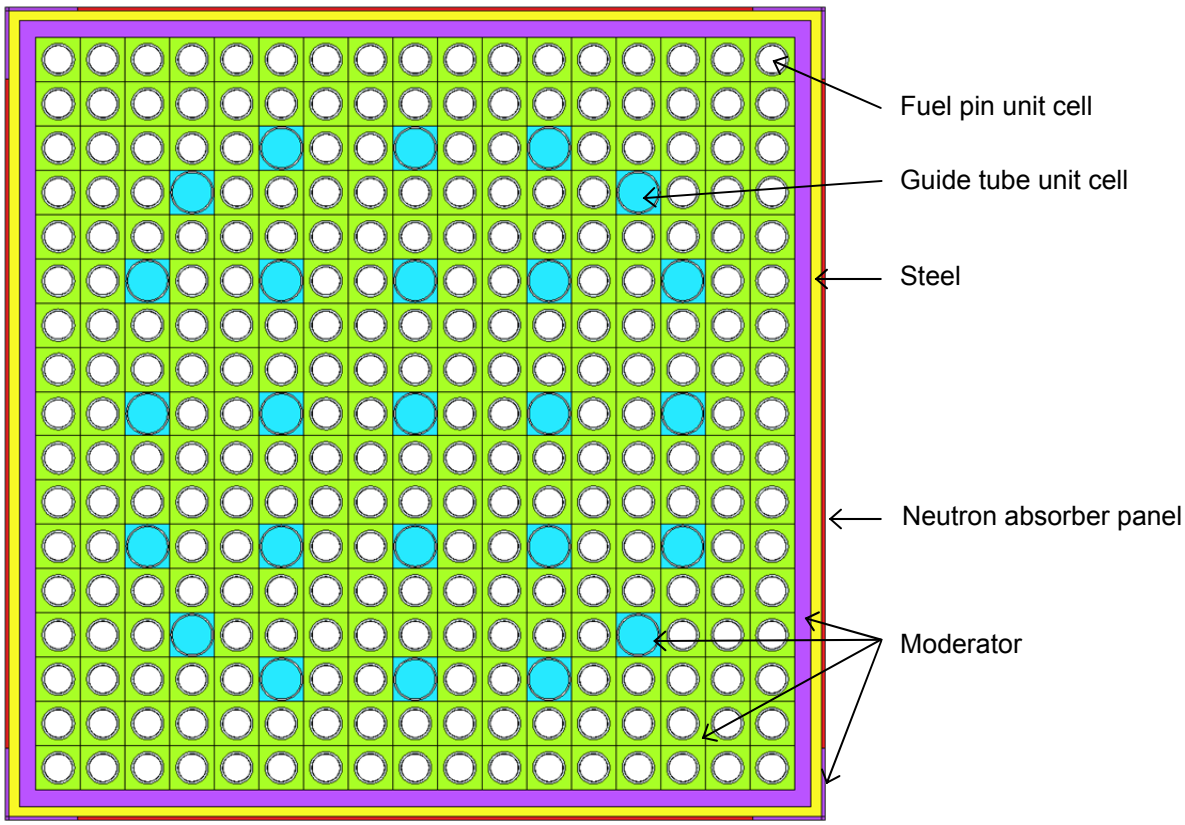

Figure 4.1 PWR SFP application model.

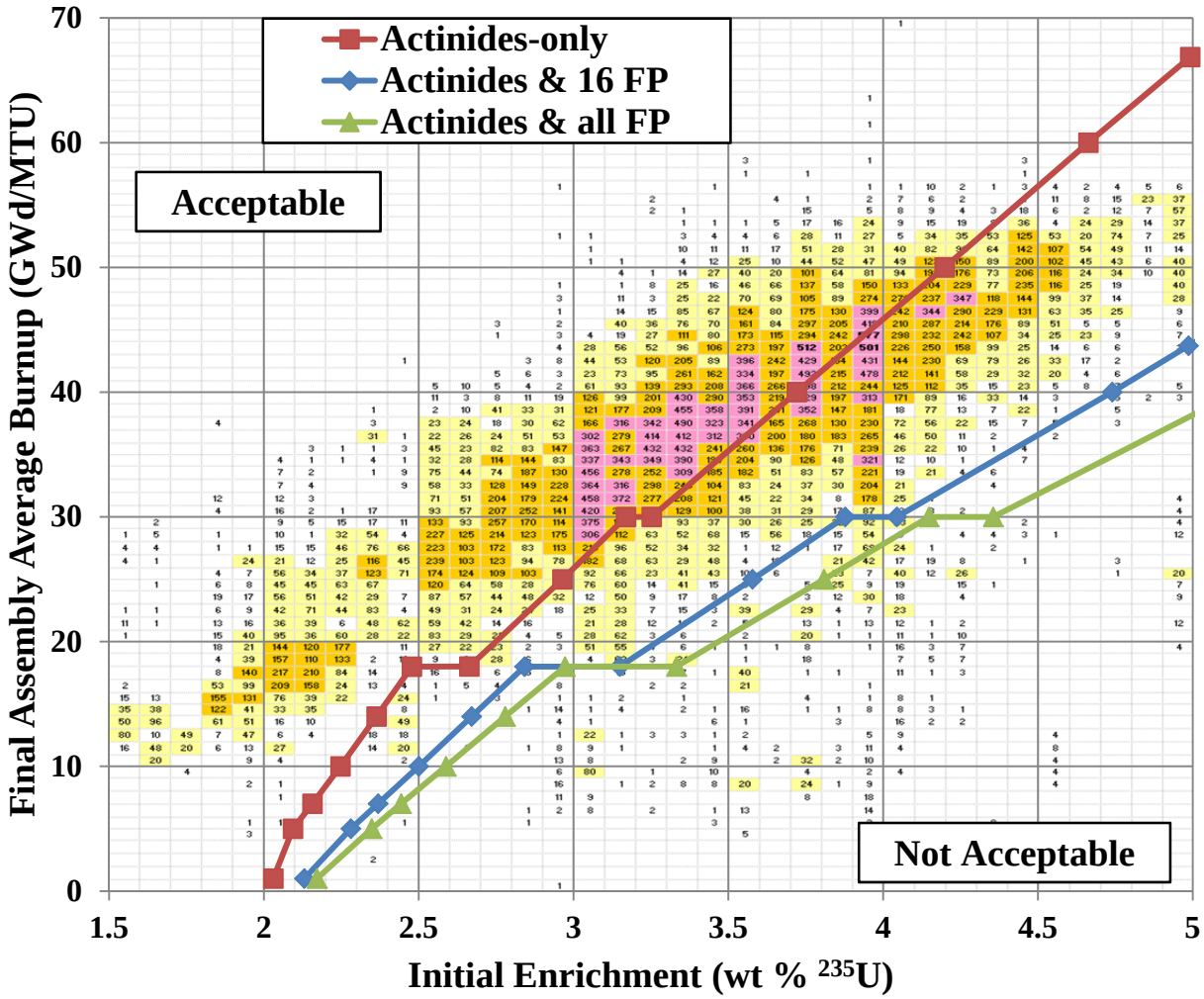

Figure 4.2 Burnup credit loading curves for PWR SFP application models.

Table 4.1 Key parameters from PWR SFP application models

				Simple average		Fission density weighted average	
BUC type	**Initial enr. (w/o ^{235}U)**	**BU (GWd/MTU)**	**EALF (eV)**	**Final enr. (w/o ^{235}U)**	**Pu/(Pu+U) (w/o Pu)**	**Final enr. (w/o ^{235}U)**	**Pu/(Pu+U) (w/o Pu)**
Actinides-only	2.25	10	0.190	1.440	0.579	1.548	0.507
Actinides-only	3.72	40	0.233	1.072	1.303	1.330	1.182
Actinides &16 FP	2.50	10	0.199	1.658	0.566	1.848	0.447
Actinides &16 FP	4.74	40	0.277	1.712	1.299	2.188	1.114
Actinides & all FP	2.59	10	0.202	1.735	0.562	1.956	0.427
Actinides & all FP	5.15	40	0.295	1.995	1.298	2.227	1.212

Note: w/o = weight percent

4.2 CASK APPLICATION

A generic cask model with a 32-PWR assembly capacity, referred to as the GBC-32 and described in NUREG/CR-6747 (Ref. 33), was previously developed to serve as a computational benchmark. The features of the GBC-32 model include 32 cells with 365.76-cm-tall and 19.05-cm-wide Boral® (0.0225 g $^{10}B/cm^2$) panels between and on the external faces of each cell. The cells have inner dimensions of 22 by 22 cm and are spaced on 23.76 cm centers. The cell walls are constructed of stainless steel. The cells sit 15 cm above the bottom of a stainless steel cask having an inner radius of 87.5 cm and internal height of 410.76 cm. The radial thickness of the side walls is 20 cm, and the cask bottom and lid are 30 cm thick. Figure 4.3 shows a cutaway view of the KENO V.a cask model, and Figure 4.4 shows the three BUC loading curves for the GBC-32 superimposed over the RW-859 database PWR inventory.

The cask was modeled as loaded with Westinghouse 17×17 OFA assemblies with assembly average burnups of up to 70 GWd/MTU. The fuel compositions were generated using the SCALE STARBUCS sequence and an ORIGEN/ARP library generated using TRITON and the ENDF/B-VII 238 energy group library. They included 24 WABA rods for the entire depletion. The STARBUCS loading curve search options were used to find the initial ^{235}U enrichment that, when depleted to the target assembly average burnup value, produced a k_{eff} value of 0.94. The target k_{eff} value was reduced from 0.95 by 0.01 Δk to leave margin for bias and bias uncertainty. Separate loading curves were determined and models generated for actinide-only BUC, actinide plus 16 FP BUC, and BUC using all actinides and FPs available in the SCALE ORIGEN and ENDF/B-VII 238-energy-group libraries. Table 4.2 shows some key parameters for the 32 PWR GBC application models at two burnups, 10 and 40 GWd/MTU, for evaluation of the potential for variation in biases as a function of burnup. The final uranium enrichment and plutonium fraction vary axially as a result of the use of axial burnup profiles. Two averages are presented for these parameters. One is the simple average from each of the 18 axial zones. The second uses the axial fission density fraction as a weighting factor, thus giving increased weight to the axial zones having the most impact on system neutron multiplication. As discussed earlier, for bias and bias uncertainty determination, use of the fission density weighted values is more appropriate.

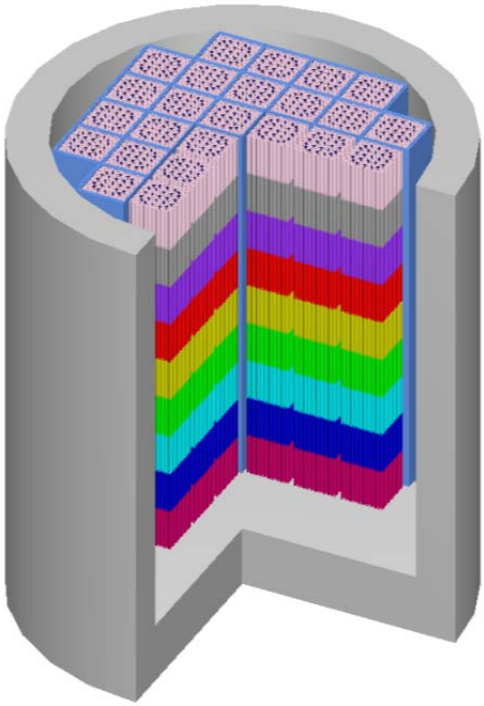

Figure 4.3 Cutaway view of the GBC-32 cask showing the cask bottom half with a quarter of the model removed.

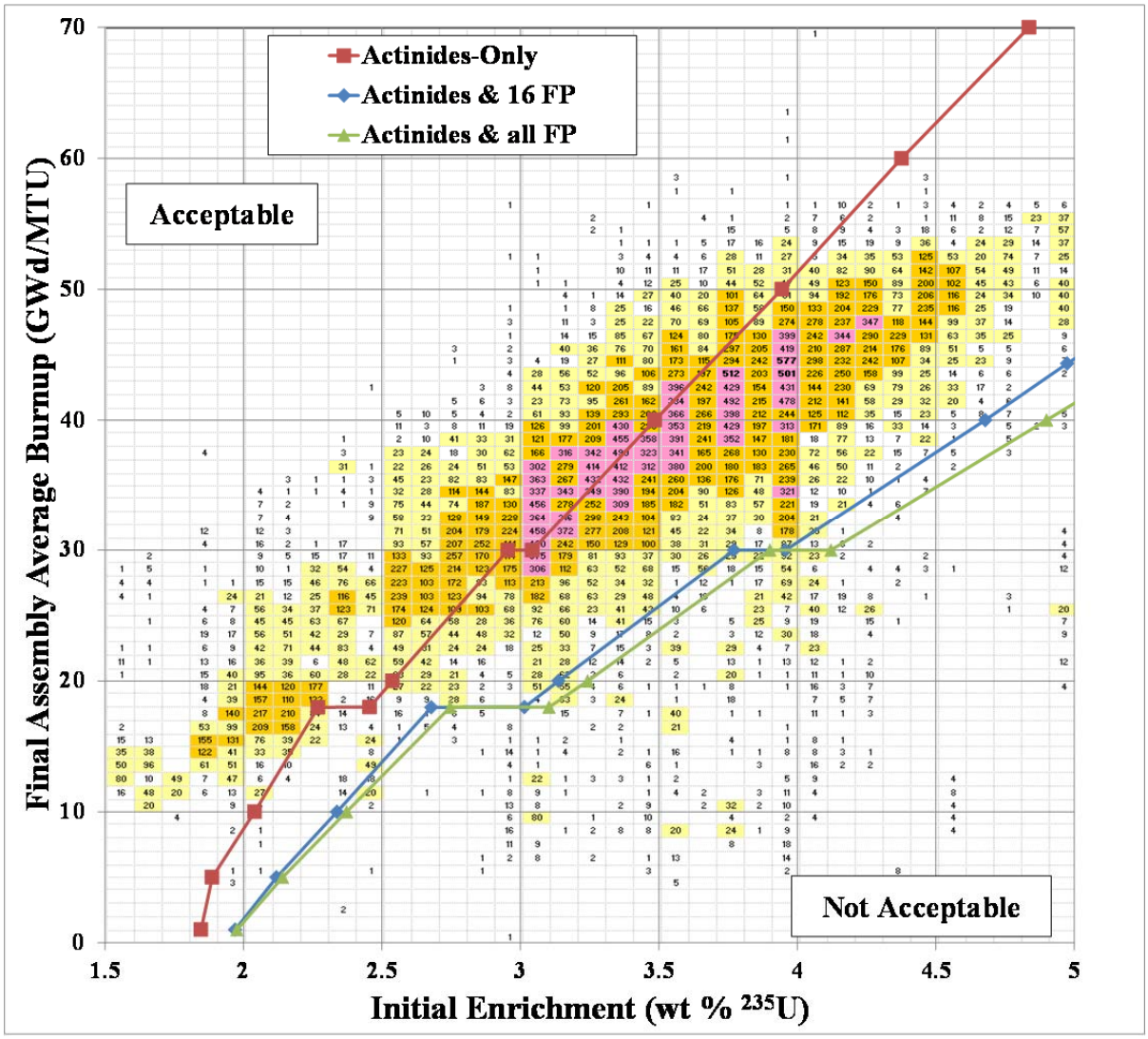

Figure 4.4 Burnup credit loading curves for GBC-32 application models.

Table 4.2 Key parameters from application models (GBC-32)

				Simple average		Fission density weighted average	
BUC type	**Initial enr. (w/o ^{235}U)**	**BU (GWd/MTU)**	**EALF (eV)**	**Final enr. (w/o ^{235}U)**	**Pu/ (Pu+U) (w/o Pu)**	**Final enr. (w/o ^{235}U)**	**Pu/(Pu+U) (w/o Pu)**
Actinides-only	2.04	10	0.190	1.262	0.588	1.480	0.433
Actinides-only	3.49	40	0.229	0.942	1.278	1.181	1.162
Actinides & 16FP	2.34	10	0.200	1.511	0.572	1.748	0.418
Actinides & 16FP	4.68	40	0.285	1.663	1.268	1.985	1.146
Actinides & all FP	2.37	10	0.201	1.540	0.570	1.780	0.416
Actinides & all FP	4.90	40	0.295	1.815	1.267	2.150	1.144

4.3 BWR SPENT NUCLEAR FUEL POOL APPLICATION

In BWRs, the fuel bundles typically include some fuel rods in which gadolinia (Gd_2O_3) is mixed with the UO_2 in the fuel pellets. Gadolinium is a strong neutron absorber that burns out relatively quickly. Gadolinium depletion causes the fuel bundle reactivity to rise to a peak value that, for the limiting fuel assemblies, occurs at assembly average burnup values below 20 GWd/MTU. Since reactivity initially increases with burnup, using the fresh fuel bundle in the fuel storage analysis would not be conservative if the gadolinium rods were modeled. However, analyses in which the gadolinium fuel rods are substituted with fresh, unpoisoned fuel rods will provide conservative results that are very restrictive over the first cycle of burnup. Consequently, criticality analyses of BWR fuel storage pools are usually performed with fuel at the maximum or "peak" reactivity point. Although some applicants have been working to credit fuel burnup beyond the peak reactivity point, this has not typically been done in BWR fuel storage rack analyses.

BWR fuel assemblies have initial ^{235}U enrichments that may vary axially and radially. The number of fuel rods with Gd_2O_3 and the weight fraction of the Gd_2O_3 in these rods may also vary. Modern BWR fuel assembly designs also use part-length fuel rods, allowing for additional water in the upper parts of the assembly. Because of the number of assembly lattice variations, BWR criticality analyses characterize each lattice, depleted in hot reactor conditions, according to its maximum 2D k_∞ in standard cold core geometry (SCCG) (i.e., an infinite lattice of assemblies with a 6 in. pitch at 20°C moderator temperature with no voids or control absorbers) (Ref. 34). After the peak k_∞ is identified, the fuel compositions from the peak k_∞ burnup are typically decayed for 3 days, to allow xenon decay, and then used in a fuel storage rack model to establish the relationship between peak SCCG k_∞ and the k_{eff} for the fuel storage rack model. This relationship identifies the maximum SCCG k_∞ that will result in a fuel storage rack k_{eff} that meets the regulatory requirement.

The red curve in Figure 4.5 shows the burnup-dependent behavior of the SCCG k_∞ for an assembly that contains eight Gd_2O_3 rods. The green curve shows the SCCG k_∞ for the same assembly without Gd_2O_3. The purpose of the figure is to illustrate the credit taken for fuel burnup in the BWR fuel storage rack analysis. Figure 4.6 shows the relationship between the SCCG k_∞ and the k_∞ at hot full-power reactor conditions.

The BWR application model is shown in Figure 4.7. Note that there are many variants of BWR assembly designs that could have been modeled, but the application model in this report is provided to be representative of commonly used BWR designs and will not exactly match an actual design. The modeled assembly is a 10×10 array of 5 wt % ^{235}U fuel rods burned to about 11 GWd/MTU. The assembly included eight 3 wt % Gd_2O_3 in UO_2 fuel rods and two water rods that displace eight fuel rods. The Gd_2O_3+UO_2 rods are modeled using five equal-volume radial regions to accurately model the gadolinium depletion. The assembly is stored in a 0.2-cm-thick Zircaloy fuel channel having an inner dimension of 12.95 cm. Each fuel storage rack cell is modeled as a square tube of steel that is 0.18 cm thick and has an inner dimension of 14.75 cm. A single B_4C plus aluminum plate (representative of Boral®) is placed between each storage cell. Each neutron-absorbing plate is 0.203 cm thick and 11.64 cm wide and has a neutron absorber loading of 0.020 g $^{10}B/cm^2$. The model has reflected boundary conditions on all sides and so is effectively infinite in all directions. The initial enrichment, number of gadolinium rods, gadolinium rod enrichment, and storage cell pitch were selected so that when the fuel is depleted to peak reactivity, the fuel storage rack model has a calculated k_{eff} value of 0.94. The target k_{eff} value was reduced from 0.95 by 0.01 Δk to leave margin for bias and bias uncertainty.

The peak SCCG was indentified and the burned fuel compositions calculated using the SCALE TRITON 2D depletion sequence. The in-rack k_{eff} value was calculated using the SCALE CSAS6 sequence. The EALF for the BWR application model is 0.456 eV. The burned fuel fission-density-weighted average composition included uranium with a ^{235}U enrichment of 3.82 wt % and a plutonium-to-uranium ratio of 0.331 wt % Pu.

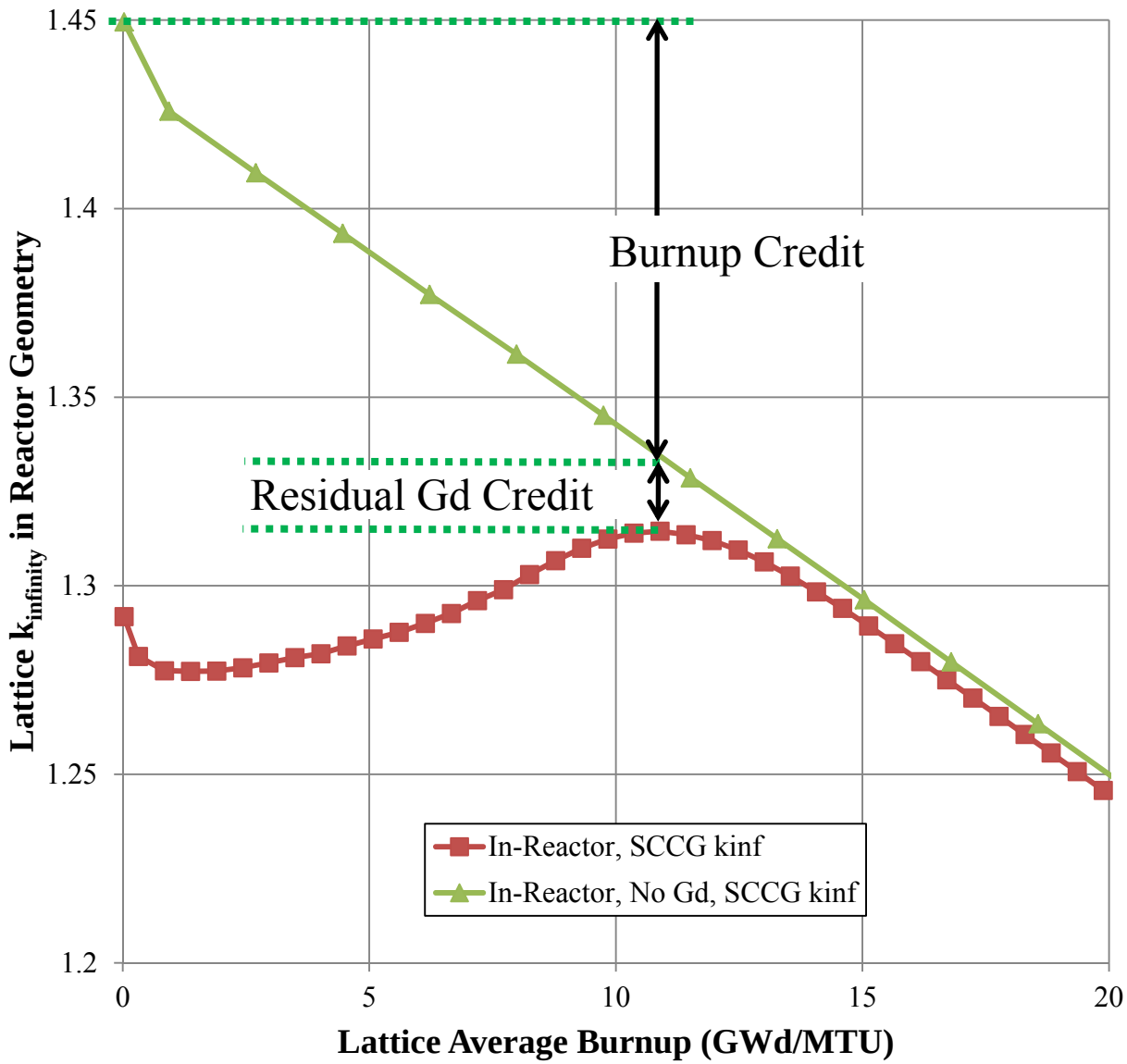

Figure 4.5 Burnup credit and BWR peak SCCG k_∞.

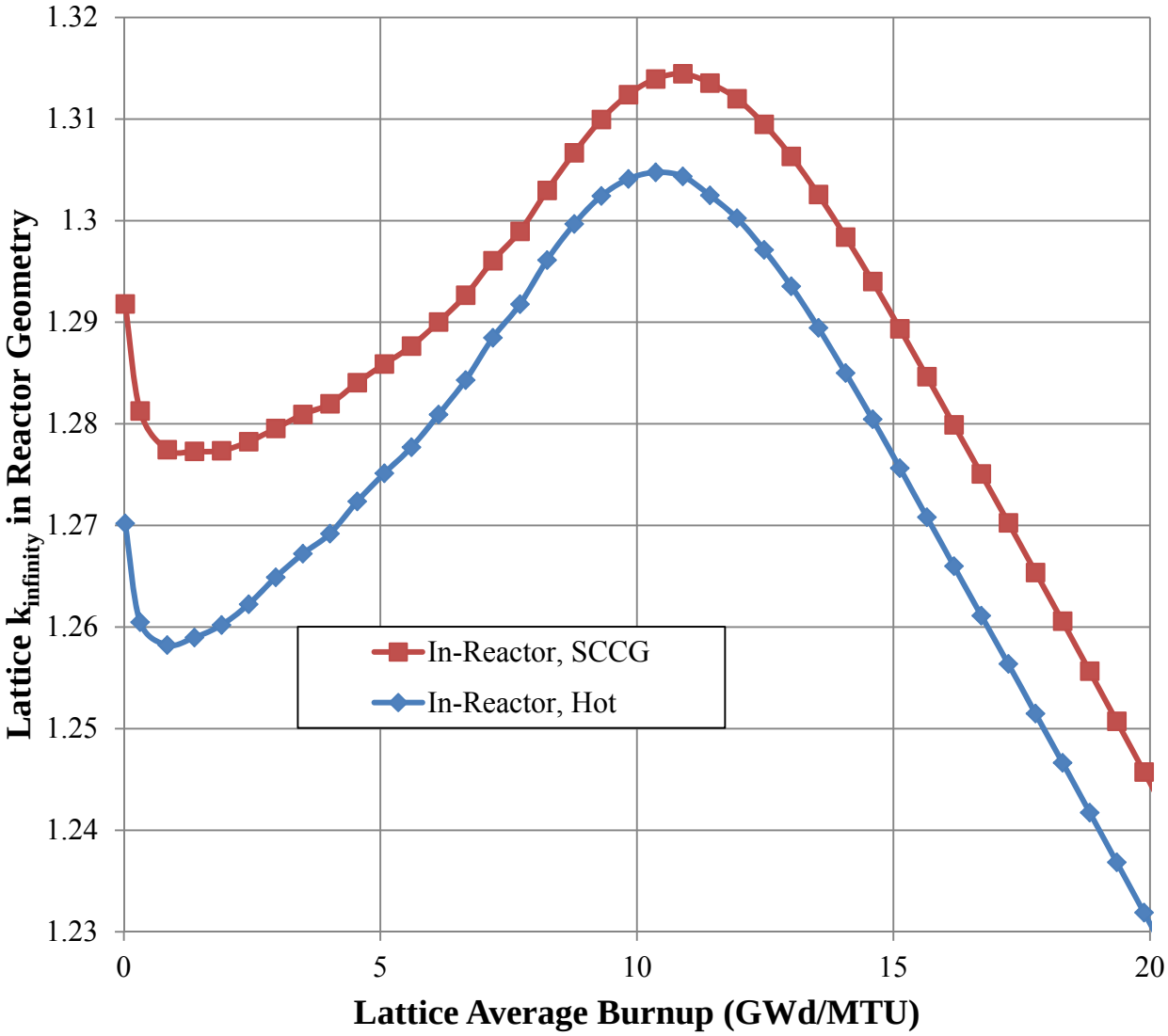

Figure 4.6 Relationship between hot full-power k_∞ and SCCG k_∞.

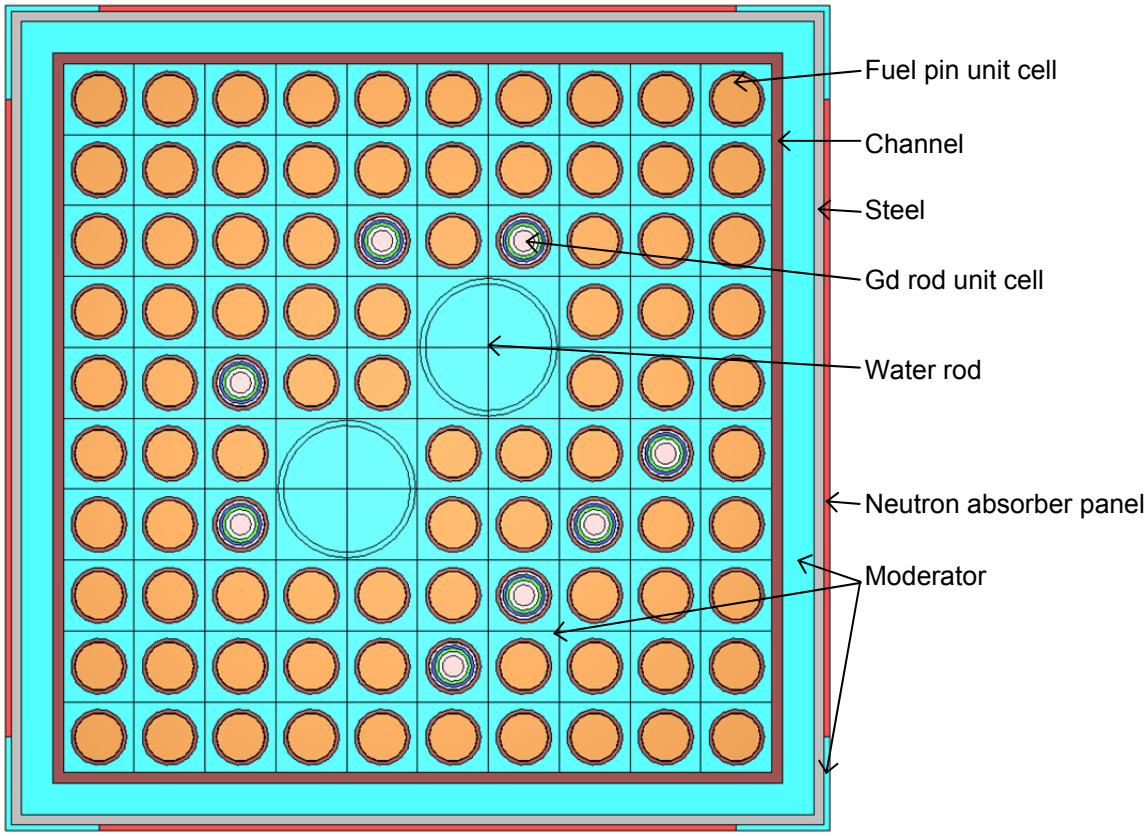

Figure 4.7 BWR SFP application model.

5. CRITICAL EXPERIMENTS

A total of 609 critical experiments were used as the initial validation set. As described below, the SCALE S/U analysis tools were used to down-select the validation set based on the c_k similarity correlation coefficient. The initial set included 124 LEU and 194 mixed uranium and plutonium critical configurations from the IHECSBE (Ref. 9). The critical configurations used are from the following IHECSBE evaluations:

- LEU-COMP-THERM-001, 002, 010, 017, 022, 023, 024, 026, 042, 050, and 079
- LEU-MISC-THERM-005
- LEU-SOL-THERM-002, 003, and 004
- MIXED-COMP-THERM-001, 002, 003, 004, 005, 006, 007, 008, 009, 011, and 012
- MIXED-SOL-THERM-001, 002, 004, and 005

Some of the configurations from LEU-COMP-THERM-050 and 079, and LEU-MISC-THERM-005 contain FPs.

The validation set also included 156 configurations from the HTC experiment set that includes actinide nuclides in proportions similar to those for a fuel assembly with an initial enrichment of 4.5 wt % ^{235}U burned to 37.5 GWd/MTU. The HTC experiment data were published in a series of four reports by the French Institut de Radioprotection et de Sûreté Nucléaire (IRSN). The experiment descriptions for this set are provided in Refs. 10 through 13 and are considered commercial proprietary. There are currently restrictions on who may use the data and for what purposes. Data recipients are required to sign a nondisclosure agreement, which includes provisions for release of the data to the US Nuclear Regulatory Commission (NRC) and the US Department of Energy.

The validation set also included 135 configurations from the French Fission Product Program experiments described in Refs. 20 through 24. The critical experiment descriptions are commercial proprietary and are not expected to be released for applicant use.

Summary descriptions are provided below for the critical experiments. All 609 critical configurations were modeled and analyzed with SCALE. Appendix A presents data derived from the experiment descriptions and from the calculational results for each critical configuration. Note that proprietary data are intentionally excluded from this report.

The ranges for the key parameters for these critical configurations are as follows:

0.0338	≤	EALF	≤	1.0 eV
0.145	≤	U enrichment	≤	59.7 wt % ^{235}U
0	≤	Pu/(Pu + U)	≤	96.8 wt % Pu
0	≤	Sol. boron concentration	≤	5030 ppm of B by weight

5.1 LOW-ENRICHMENT URANIUM EXPERIMENTS

Included in the initial validation set were 124 LEU critical configurations because applicants frequently include LEU configurations in their benchmarking analyses. These configurations are all documented in the IHECSBE.

The LEU configurations considered include the following:

- 8 configurations (cases 1–8) from LEU-COMP-THERM-001. These configurations are water-moderated U(2.35 wt %)O_2 fuel rods in 2.032-cm square-pitched arrays.

- 5 configurations (cases 1–5) from LEU-COMP-THERM-002. These configurations are water-moderated U(4.31 wt %)O_2 fuel rods in 2.54-cm square-pitched arrays.

- 5 configurations from LEU-COMP-THERM-010. These configurations are water-moderated U(4.31 wt %)O_2 fuel rods in square pitched arrays reflected by depleted uranium (case 5) or steel (cases 16–19).

- 24 configurations from LEU-COMP-THERM-017. These configurations are water-moderated U(2.35 wt %)O_2 fuel rods in square-pitched arrays reflected by lead (cases 3 and 23–25), depleted uranium (cases 4–9 and 28–29), or steel (cases 10–17 and 19–22).

- 7 configurations (cases 1–7) from LEU-COMP-THERM-022. These configurations are uniform water-moderated hexagonally pitched lattices of U(10 wt %)O_2 fuel rods.

- 6 configurations (cases 1–6) from LEU-COMP-THERM-023. These configurations are partially flooded, water-moderated hexagonally pitched lattices of U(10 wt %)O_2 fuel rods.

- 2 configurations (cases 1–2) from LEU-COMP-THERM-024. These configurations are water-moderated square-pitched lattices of U(10 wt %)O_2 fuel rods.

- 1 configuration (case 3) from LEU-COMP-THERM-026. This configuration is a water-moderated hexagonally pitched lattice of U(4.92 wt %)O_2 fuel rods.

- 7 configurations (cases 1–7) from LEU-COMP-THERM-042. These configurations are water-moderated square-pitched arrays of U(2.35 wt %)O_2 fuel rods separated by steel (case 1), borated(1.1% B)-steel (case 2), Boral (case 3), Boraflex (case 4), cadmium (case 5), copper (case 6), or copper with 1% cadmium (case 7) and reflected by steel walls.

- 18 configurations (cases 1–18) from LEU-COMP-THERM-050. These configurations are water-moderated, square-pitched lattices of U(4.738 wt %)O_2 fuel rods with a central tank that contains either water (cases 1–2), boron solution (cases 3–7), or one of three concentrations of samarium (enriched to 96.9 wt % ^{149}Sm) solution (cases 8–18).

- 10 configurations (cases 1–10) from LEU-COMP-THERM-079. These configurations are water-moderated, hexagonally pitched lattices of U(4.31 wt %)O_2 fuel rods with ^{103}Rh foils placed between fuel pellets in a fraction of the rods. Cases 3–5 and 8–10 contain ^{103}Rh foils.

The LEU systems also included the following solution configurations from four IHECSBE evaluations:

- 12 configurations (cases 1–12) from LEU-MISC-THERM-005. These configurations are square-pitched arrays of U(4.98 wt %)O_2 fuel rods sitting in uranyl (6 wt %) nitrate solution that includes one or more FP elements Sm, Cs, Rh, and Eu.

- 3 configurations (cases 1–3) from LEU-SOL-THERM-002. These configurations are uranium (4.9 wt %) oxyfluoride solution. Cases 1 and 3 are water reflected.

- 9 configurations (cases 1–9) from LEU-SOL-THERM-003. These configurations are bare spherical tanks containing aqueous uranyl (10 wt % ^{235}U) nitrate solutions.

- 7 configurations (cases 1–7) from LEU-SOL-THERM-004. These configurations are water-reflected uranyl (10 wt % ^{235}U) nitrate solutions in a cylindrical tank.

5.2 MIXED URANIUM AND PLUTONIUM EXPERIMENTS

Included in the initial validation set were 194 mixed uranium and plutonium critical configurations. These configurations are all documented in the IHECSBE. Burned fuel with initial enrichments and final burnups along a typical BUC loading curve generally have LEU and significant plutonium content. For example, the destructive assay composition measurement results for Takahama-3 sample SF95-4 from NUREG/CR-6811 (Ref. 35), which had an initial enrichment of 4.11 wt % ^{235}U and was burned to 36.69 GWd/MTU, show that the sample had a final enrichment of 1.57 wt % ^{235}U; a plutonium content of 1.1 wt % Pu (i.e., 100%×g Pu/(g Pu + g U)); and a plutonium isotopic vector of 59.2 wt % ^{239}Pu, 24.3 wt % ^{240}Pu, and 10.1 wt % ^{241}Pu. All of the mixed Pu + U systems include either natural or depleted uranium, and few have a plutonium isotopic vector that is close to the plutonium isotopics of burned fuel.

The mixed Pu + U systems validation set includes the following:

- 4 configurations (cases 1–4) from MIXED-COMP-THERM-001. These configurations involve MOX fuel pins in square-pitched lattices that are moderated and reflected by water. The fuel pins include natural uranium, and the plutonium was 86.2 wt % ^{239}Pu, 11.5 wt % ^{240}Pu, and 1.8 wt % ^{241}Pu.

- 6 configurations (cases 1–6) from MIXED-COMP-THERM-002. These configurations involve MOX fuel pins in square-pitched lattices that are moderated and reflected by water. The fuel pins include natural uranium, and the plutonium was 91.8 wt % ^{239}Pu, 7.8 wt % ^{240}Pu, and 0.4 wt % ^{241}Pu.

- 6 configurations (cases 1–6) from MIXED-COMP-THERM-003. These configurations involve MOX fuel pins in square-pitched lattices that are moderated and reflected by water. The fuel pins include natural uranium, and the plutonium was 90.6 wt % ^{239}Pu, 8.6 wt % ^{240}Pu, and 0.8 wt % ^{241}Pu.

- 11 configurations (cases 1–11) from MIXED-COMP-THERM-004. These configurations involve MOX fuel pins in square-pitched lattices that are moderated and reflected by water. The fuel pins include natural uranium, and the plutonium was 68.2 wt % ^{239}Pu, 22.0 wt % ^{240}Pu, and 7.3 wt % ^{241}Pu.

- 7 configurations (cases 1–7) from MIXED-COMP-THERM-005. These configurations involve MOX fuel pins in triangular-pitched lattices that are moderated and reflected by water. The fuel pins include natural uranium, and the plutonium was 75.5 wt % ^{239}Pu, 18.2 wt % ^{240}Pu, and 4.9 wt % ^{241}Pu.

- 50 configurations (cases 1–50) from MIXED-COMP-THERM-006. These configurations involve MOX fuel pins in triangular-pitched lattices that are moderated and reflected by water. The fuel pins include natural uranium, and the plutonium was 91.6 wt % ^{239}Pu, 7.7 wt % ^{240}Pu, and 0.6 wt % ^{241}Pu. The 7th through 50th cases include a hafnium, boron,

water, or air absorber rod in the center of the array. In cases 17–28 and 39–50, a cadmium sleeve was installed on the absorber rod.

- 5 configurations (cases 1–5 of 27) from MIXED-COMP-THERM-007. These configurations involve MOX fuel pins in triangular-pitched lattices that are moderated and reflected by water. The fuel pins include natural uranium, and the plutonium was 81.1 wt % ^{239}Pu, 16.5 wt % ^{240}Pu, and 1.8 wt % ^{241}Pu.

- 28 configurations (cases 1–28) from MIXED-COMP-THERM-008. These configurations involve MOX fuel pins in triangular-pitched lattices that are moderated and reflected by water. The fuel pins include natural uranium, and the plutonium was 71.7 wt % ^{239}Pu, 23.6 wt % ^{240}Pu, and 4.1 wt % ^{241}Pu. The 7th through 28th cases include an aluminum, hafnium, boron, water, or air absorber rod in the center of the array. In cases 17–28 a cadmium sleeve was installed on the absorber rod.

- 6 configurations (cases 1–6) from MIXED-COMP-THERM-009. These configurations involve MOX fuel pins in triangular-pitched lattices that are moderated and reflected by water. The fuel pins include depleted uranium, and the plutonium was 91.4 wt % ^{239}Pu, 7.9 wt % ^{240}Pu, and 0.7 wt % ^{241}Pu.

- 6 configurations (cases 1–6) from MIXED-COMP-THERM-011. These configurations involve MOX fuel pins in triangular-pitched lattices that are moderated and reflected by water. The fuel pins include uranium enriched to 59.7 wt % ^{235}U, and the plutonium was 89.3 wt % ^{239}Pu, 9.8 wt % ^{240}Pu, and 0.9 wt % ^{241}Pu.

- 33 configurations (cases 1–33) from MIXED-COMP-THERM-012. These configurations involve reflected and unreflected polystyrene-moderated mixed oxide cubes and slabs. All cases use depleted uranium. The fuel pins in cases 1–6 include plutonium that was 67.8 wt % ^{239}Pu, 23.0 wt % ^{240}Pu, and 5.6 wt % ^{241}Pu, and in cases 7–33 the plutonium was 91.2 wt % ^{239}Pu, 8 wt % ^{240}Pu, and 0.6 wt % ^{241}Pu.

The mixed uranium–plutonium systems also included the following solution configurations from four IHECSBE evaluations:

- 13 configurations (cases 1–13) from MIX-SOL-THERM-001. These configurations included depleted uranium nitrate mixed with plutonium nitrate in an annular tank with, in some cases, an additional bottle of solution located inside the annulus. The plutonium was 91 wt % ^{239}Pu, 8 wt % ^{240}Pu, and 0.4 wt % ^{241}Pu. Uranium concentrations varied from 2.3 to 380 g U/L, and the plutonium concentrations varied from 47 to 196 g Pu/L.

- 3 configurations (cases 1–3) from MIX-SOL-THERM-002. These configurations included depleted or natural uranium nitrate mixed with plutonium nitrate in a cylindrical tank. The plutonium was 91 wt % ^{239}Pu, 8 wt % ^{240}Pu, and 0.4 wt % ^{241}Pu. Uranium concentrations varied from 11 to 41 g U/L, and the plutonium concentrations were about 12 g Pu/L.

- 9 configurations (cases 1–9) from MIX-SOL-THERM-004. These configurations included depleted uranium nitrate and plutonium nitrate in a cylindrical tank that was either bare or reflected by water or concrete. The plutonium in these configurations was 91.1 wt % ^{239}Pu, 8.3 wt % ^{240}Pu, and 0.5 wt % ^{241}Pu. The uranium concentrations varied from 63 to 263 g U/L, and the plutonium concentrations varied from 42 to 173 g Pu/L.

- 7 configurations (cases 1–7) from MIX-SOL-THERM-005. These configurations included depleted uranium nitrate and plutonium nitrate in a slab tank that was either unreflected or reflected by water. The plutonium in these configurations was 91.1 wt % ^{239}Pu, 8.3 wt % ^{240}Pu, and 0.5 wt % ^{241}Pu. The uranium concentrations varied from 63 to 263 g U/L, and the plutonium concentrations varied from 41 to 173 g Pu/L.

5.3 HAUT TAUX DE COMBUSTION MOX EXPERIMENTS

In the 1980s, the HTC experiments were conducted by IRSN at the experimental criticality facility in Valduc, France. The plutonium-to-uranium ratio and the isotopic compositions of both the uranium and plutonium used in the simulated fuel rods were designed to be similar to what would be found in a typical PWR fuel assembly that initially had an enrichment of 4.5 wt % ^{235}U and was burned to 37.5 GWd/MTU. The fuel material also includes ^{241}Am, which is present from the decay of ^{241}Pu. The HTC experiments include configurations designed to simulate fuel handling activities, pool storage, and transport in casks constructed of thick lead or steel. The HTC critical experiments include the 156 critical configurations described in Refs. 10–13 and 36.

Rights of use for the HTC experiment data were purchased under an agreement that limits release of the information. Consequently, a detailed and complete description of the experiments is not presented in this report. The proprietary reports may be obtained from ORNL following completion of a nondisclosure agreement with UT-Battelle. An evaluation of the HTC experiment data is documented in NUREG/CR-6979 (Ref. 37).

5.4 FRENCH FISSION PRODUCT PROGRAM EXPERIMENTS

From 1998 to 2004, a series of critical experiments with FPs was conducted by IRSN at the experimental criticality facility in Valduc, France. The experiments focused on seven FP nuclides (either individually or as nuclide mixtures in various experiments): ^{103}Rh, ^{133}Cs, ^{143}Nd, ^{145}Nd, ^{149}Sm, ^{152}Sm, and ^{155}Gd. In all experiments with FPs, the test material was in the form of slightly acidic solutions. Three experimental phases (FP Phases 1–3) were performed, each distinguished by the manner in which the FP solutions were configured relative to the fuel rods. In some experiments, depleted uranium solution, with or without FPs, was used. Reference experiments (with dilute nitric acid replacing the FP solutions) were also performed. A total of 135 experiments are described in a set of five reports (Refs. 20 through 24). The NRC provided ORNL staff access to these reports for use in the present work. The reports are commercial proprietary information belonging to IRSN. It is not anticipated that these reports will be available to the US nuclear industry. Reference 38 provides some useful descriptions of the French Fission Product Program experiments.

In this work, these experiments were used in three ways. First, they were included in the initial validation set from which bias and bias uncertainty information was obtained. Second, trends in the calculational results for these experiments were used to estimate biases associated with individual FPs. Third, the experiments were used in SCALE TSURFER calculations to estimate FP biases as described in Appendix C.

6. BIAS AND BIAS UNCERTAINTY

Bias and bias uncertainty results are presented in this section for validation of the application models described in Section 4 using the LCEs described in Section 5 as a function of different trend parameters. Comparisons are provided in Section 6.1 using LCEs selected based on traditional techniques as discussed in Section 3.2.2. Results are presented using benchmark critical experiments from the IHECSBE only, and then also including the proprietary HTC LCEs for the application models. Section 6.2 presents bias and bias uncertainty results based on benchmark critical experiments selected using the SCALE S/U analysis tools, which is a more physics-based approach, as discussed in Section 3.2.4.

The k_{eff} results for the 474 HTC, IHECSBE Pu+U, and LEU critical configurations and for some of the subsets of configurations are not normally distributed. The distribution of the results is dependent upon the benchmark critical experiments selected for validation, and the non-normality of the distribution can be accounted for using either more sophisticated statistical analysis techniques or nonparametric analysis techniques. For the purposes of the demonstrations in this report, the data are assumed to follow a normal distribution because the bias and bias uncertainty results are provided for reference only and for examination of trends, and this allows a more equal comparison. Results using nonparametric analysis techniques (as provided in Ref. 28) for combined bias and bias uncertainty at a 95% probability and 95% confidence level are also provided; they are for illustration only, as they are specific to the respective critical benchmark experiment population sets used and the SCALE code system on the ORNL computer platform. Index values for the one-sided distribution-free tolerance limits were taken from Ref. 39.

6.1 BIAS AND BIAS UNCERTAINTY DETERMINATION

The USLSTATS computer program was used to determine the bias and bias uncertainty for the application models as a function of various trend parameters using LEU, mixed uranium–plutonium, and the HTC LCEs. The bias and bias uncertainty values presented in this section do not use S/U analysis tools and are representative of what would be developed in traditional analyses. In the tables that follow, “bias” is calculated as k_{eff} minus expected k_{eff} (i.e., 1.0 because calculated k_{eff} values were normalized to the experimental values). Thus a positive bias would imply the calculated values were higher than the expected values. Positive bias values are generally not credited in criticality safety analyses. The “fit uncertainty” is the one-standard-deviation uncertainty in the bias resulting from applying the linear least-squares fitting technique to the benchmark critical experiment results. The “bias uncertainty” includes the fit uncertainty and tolerance interval multiplier to yield a 95% probability and 95% confidence level. The bias results are presented with and without the HTC LCEs for the different trend parameters. Table 6.1, Table 6.3, and Table 6.5 provide results without including the HTC LCEs in the critical benchmarks used for the trending analysis; and Table 6.2, Table 6.4, and Table 6.6 provide results that incorporate the HTC LCEs in the trending analysis.

Table 6.1 Bias and uncertainty as a function of EALF using only IHECSBE experiments

BUC type	Initial enrichment (wt % ^{235}U)	BU (GWd/MTU)	EALF (eV)	k_{eff} versus EALF		Bias uncertainty
				Bias (Δk)	Fit uncertainty	
PWR SFP model						
Actinides-only	2.25	10	0.190	-1.53×10^{-3}	8.22×10^{-3}	1.71×10^{-2}
Actinides-only	3.72	40	0.233	-1.44×10^{-3}		
Actinides & 16 FP	2.50	10	0.199	-1.51×10^{-3}		
Actinides & 16 FP	4.74	40	0.277	-1.36×10^{-3}		
Actinides & all FP	2.59	10	0.202	-1.50×10^{-3}		
Actinides & all FP	5.15	40	0.295	-1.32×10^{-3}		
32 PWR GBC model						
Actinides-only	2.04	10	0.190	-1.53×10^{-3}	8.22×10^{-3}	1.71×10^{-2}
Actinides-only	3.485	40	0.229	-1.45×10^{-3}		
Actinides & 16 FP	2.338	10	0.200	-1.51×10^{-3}		
Actinides & 16 FP	4.679	40	0.285	-1.34×10^{-3}		
Actinides & all FP	2.372	10	0.201	-1.50×10^{-3}		
Actinides & all FP	4.9	40	0.295	-1.32×10^{-3}		
BWR SFP model						
Peak SCCG	5.0	11	0.456	-1.00×10^{-3}	8.22×10^{-3}	1.71×10^{-2}

Table 6.2 Bias and uncertainty as a function of EALF using IHECSBE and HTC experiments

BUC type	Initial enrichment (wt % ^{235}U)	BU (GWd/MTU)	EALF (eV)	k_{eff} versus EALF		Bias uncertainty
				Bias (Δk)	Fit uncertainty	
PWR SFP model						
Actinides-only	2.25	10	0.190	-1.45×10^{-3}	6.82×10^{-3}	1.44×10^{-2}
Actinides-only	3.72	40	0.233	-1.40×10^{-3}		
Actinides & 16 FP	2.50	10	0.199	-1.44×10^{-3}		
Actinides & 16 FP	4.74	40	0.277	-1.34×10^{-3}		
Actinides & all FP	2.59	10	0.202	-1.44×10^{-3}		
Actinides & all FP	5.15	40	0.295	-1.32×10^{-3}		
32 PWR GBC model						
Actinides-only	2.04	10	0.190	-1.45×10^{-3}	6.82×10^{-3}	1.44×10^{-2}
Actinides-only	3.485	40	0.229	-1.40×10^{-3}		
Actinides & 16 FP	2.338	10	0.200	-1.44×10^{-3}		
Actinides & 16 FP	4.679	40	0.285	-1.33×10^{-3}		
Actinides & all FP	2.372	10	0.201	-1.44×10^{-3}		
Actinides & all FP	4.9	40	0.295	-1.32×10^{-3}		
BWR SFP model						
Peak SCCG	5.0	11	0.456	-1.11×10^{-3}	6.82×10^{-3}	1.44×10^{-2}

Table 6.3 Bias and uncertainty as a function of final enrichment using IHECSBE experiments

BUC type	Initial enrichment (wt % ^{235}U)	BU (GWd/MTU)	Final enrichment (wt % ^{235}U)	k_{eff} vs. final enrichment		Bias uncertainty
				Bias (Δk)	Fit uncertainty	
PWR SFP model						
Actinides-only	2.25	10	1.548	-1.79×10^{-3}	8.21×10^{-3}	1.71×10^{-2}
Actinides-only	3.72	40	1.330	-1.81×10^{-3}		
Actinides & 16 FP	2.50	10	1.848	-1.77×10^{-3}		
Actinides & 16 FP	4.74	40	2.188	-1.75×10^{-3}		
Actinides & all FP	2.59	10	1.956	-1.76×10^{-3}		
Actinides & all FP	5.15	40	2.227	-1.74×10^{-3}		
32 PWR GBC model						
Actinides-only	2.04	10	1.480	-1.80×10^{-3}	8.21×10^{-3}	1.71×10^{-2}
Actinides-only	3.485	40	1.181	-1.82×10^{-3}		
Actinides & 16 FP	2.338	10	1.748	-1.78×10^{-3}		
Actinides & 16 FP	4.679	40	1.985	-1.76×10^{-3}		
Actinides & all FP	2.372	10	1.780	-1.77×10^{-3}		
Actinides & all FP	4.9	40	2.150	-1.75×10^{-3}		
BWR SFP model						
Peak SCCG	5.0	11	3.820	-1.63×10^{-3}	8.21×10^{-3}	1.71×10^{-2}

Table 6.4 Bias and uncertainty as a function of final enrichment using HTC and IHECSBE experiments

BUC type	Initial enrichment (wt % ^{235}U)	BU (GWd/MTU)	Final enrichment (wt % ^{235}U)	k_{eff} vs. final enrichment		Bias uncertainty
				Bias (Δk)	Fit uncertainty	
PWR SFP model						
Actinides-only	2.25	10	1.548	-1.60×10^{-3}	6.81×10^{-3}	1.46×10^{-2}
Actinides-only	3.72	40	1.330	-1.61×10^{-3}		
Actinides+FP	2.50	10	1.848	-1.58×10^{-3}		
Actinides+FP	4.74	40	2.188	-1.55×10^{-3}		
Actinides & all FP	2.59	10	1.956	-1.57×10^{-3}		
Actinides & all FP	5.15	40	2.227	-1.55×10^{-3}		
32 PWR GBC model						
Actinides-only	2.04	10	1.480	-1.60×10^{-3}	6.81×10^{-3}	1.46×10^{-2}
Actinides-only	3.485	40	1.181	-1.62×10^{-3}		
Actinides & 16 FP	2.338	10	1.748	-1.58×10^{-3}		
Actinides & 16 FP	4.679	40	1.985	-1.57×10^{-3}		
Actinides & all FP	2.372	10	1.780	-1.58×10^{-3}		
Actinides & all FP	4.9	40	2.150	-1.56×10^{-3}		
BWR SFP model						
Peak SCCG	5.0	11	3.820	-1.45×10^{-3}	6.81×10^{-3}	1.46×10^{-2}

Table 6.5 Bias and uncertainty as a function of final Pu content [wt %, g Pu/(g Pu + g U)] using IHECSBE experiments

BUC type	Initial enrichment (wt % ^{235}U)	BU (GWd/MTU)	Final Pu content (wt % Pu)	k_{eff} vs. final Pu content		Bias uncertainty
				Bias (Δk)	Fit uncertainty	
PWR SFP model						
Actinides-only	2.25	10	0.507	-2.44×10^{-3}	8.04×10^{-3}	1.67×10^{-2}
Actinides-only	3.72	40	1.182	-2.36×10^{-3}		
Actinides & 16 FP	2.50	10	0.447	-2.45×10^{-3}		
Actinides & 16 FP	4.74	40	1.114	-2.37×10^{-3}		
Actinides & all FP	2.59	10	0.427	-2.45×10^{-3}		
Actinides & all FP	5.15	40	1.212	-2.35×10^{-3}		
32 PWR GBC model						
Actinide-only	2.04	10	0.433	-2.45×10^{-3}	8.04×10^{-3}	1.67×10^{-2}
Actinide-only	3.485	40	1.162	-2.36×10^{-3}		
Actinide+FP	2.338	10	0.418	-2.45×10^{-3}		
Actinide+FP	4.679	40	1.146	-2.36×10^{-3}		
All	2.372	10	0.416	-2.45×10^{-3}		
All	4.9	40	1.144	-2.36×10^{-3}		
BWR SFP model						
Peak SCCG	5.0	11	0.331	-2.46×10^{-3}	8.04×10^{-3}	1.67×10^{-2}

Table 6.6 Bias and uncertainty as a function of final Pu content [wt %, g Pu/(g Pu + g U)] using HTC and IHECSBE experiments

BUC type	Initial enrichment (wt % ^{235}U)	BU (GWd/MTU)	Final Pu content (wt % Pu)	k_{eff} vs. final Pu content		Bias uncertainty
				Bias (Δk)	Fit uncertainty	
PWR SFP model						
Actinides-only	2.25	10	0.507	-2.04×10^{-3}	6.69×10^{-3}	1.42×10^{-2}
Actinides-only	3.72	40	1.182	-1.97×10^{-3}		
Actinides & 16 FP	2.50	10	0.447	-2.05×10^{-3}		
Actinides & 16 FP	4.74	40	1.114	-1.98×10^{-3}		
Actinides & all FP	2.59	10	0.427	-2.05×10^{-3}		
Actinides & all FP	5.15	40	1.212	-1.97×10^{-3}		
32 PWR GBC model						
Actinides-only	2.04	10	0.433	-2.05×10^{-3}	6.69×10^{-3}	1.42×10^{-2}
Actinides-only	3.485	40	1.162	-1.97×10^{-3}		
Actinides & 16 FP	2.338	10	0.418	-2.05×10^{-3}		
Actinides & 16 FP	4.679	40	1.146	-1.97×10^{-3}		
Actinides & all FP	2.372	10	0.416	-2.05×10^{-3}		
Actinides & all FP	4.9	40	1.144	-1.97×10^{-3}		
BWR SFP model						
Peak SCCG	5.0	11	0.331	-2.06×10^{-3}	6.69×10^{-3}	1.42×10^{-2}

The bias and bias uncertainty information presented in Table 6.1 through Table 6.6 was generated using a large set of LEU and mixed uranium–plutonium systems. No attempt was made to exclude critical configurations that might not be adequately similar to the application models. Doing so would probably be justifiable and could result in smaller 95/95 bias uncertainty values and data sets that are normally distributed. Applying nonparametric analysis techniques to account for the non-normality of the distribution resulted in a combined bias and bias uncertainty of −0.0306, which is nearly double the most restrictive combined bias and bias uncertainty based on the plutonium fraction trending parameter. The next section reports work that used S/U analysis tools to select critical experiments that are adequately similar to the application models and present the bias and bias uncertainty information for the down-selected sets of experiments.

6.2 BIAS AND BIAS UNCERTAINTY USING S/U ANALYSIS FOR SIMILARITY AND c_K TRENDING

SCALE S/U tools were utilized to quantify the similarity of each critical experiment and application model pair. This technique provides a physics-based approach to benchmark critical experiment selection and will result in a different validation set from that used in Section 6.1. The selected critical experiments were then used to calculate bias and bias uncertainty in a way similar to the method discussed in Section 6.1. In addition to the trending parameters used in Section 6.1, the trending was also performed using the c_k similarity index parameter.

6.2.1 Similarity Determination Using Sensitivity and Uncertainty Analysis

Calculating an accurate computational bias, one that accurately reflects the difference between the calculated and actual k_{eff} values for a safety analysis model, requires the use of critical experiments that are similar to the safety analysis model. The critical experiments need to use the same nuclear data in a similar energy-dependent manner. Thus the guidance usually cited (Ref. 3) is that the critical experiments used to validate a computational method must be as much like the application model as is possible. Historically, when critical experiments could not be created to simulate specific applications, analysts typically used qualitative and integral quantitative comparisons to select critical experiments as discussed in Section 3.2.2.

Section 3.2.4 describes a methodology for using S/U analysis techniques to assess the similarity of one model to another for a physics-based approach to critical experiment selection. S/U analysis was used to quantify the similarity of each application model described in Section 4 to each of the critical experiments identified in Section 5. A summary of the results (i.e., number of experiments within the c_k ranges) for the LEU, mixed uranium–plutonium, and HTC experiments is provided in Table 6.7. All of the 124 LEU experiments had c_k values below 0.8 and thus are not considered applicable for validation of the application models. Note that the highest c_k value for the BWR SFP application is 0.642, which was generated by comparing the application model to the HTC Phase 2, gadolinium solution experiment case 10. The lack of any experiments with c_k values as high as 0.8 suggests that further study is needed to identify critical experiments appropriate for validation of BWR SFP models. The larger number of applicable experiments for the 40 GWd/MTU PWR SFP and GBC-32 models is due to the increasing importance of plutonium at higher burnups. Figure 6.1 through Figure 6.5 show the c_k values for each experiment for each application.

Table 6.7 Similarity assessment summary

Model	Burnup (GWd/MTU)	Number meeting c_k criteria		
		$c_k < 0.8$	$0.8 \le c_k < 0.9$	$0.9 \le c_k$
PWR SFP	10	355	119	0
PWR SFP	40	250	128	96
GBC-32	10	318	152	4
GBC-32	40	197	122	155
BWR SFP	11	474	0	0

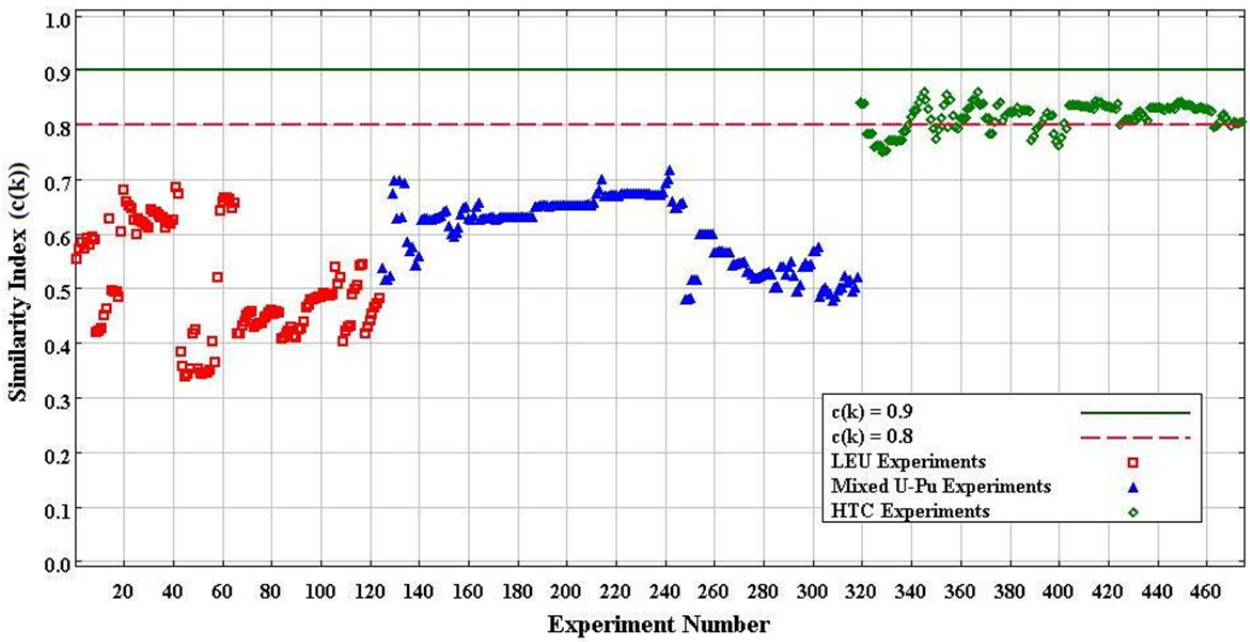

Figure 6.1 Similarity of 10 GWd/MTU PWR SFP model and each critical experiment.

From the similarity assessment results, only HTC experiments generated c_k values in excess of 0.9. IHECSBE evaluations MIX-COMP-THERM-002 through -009 and -012 generated some c_k values between 0.8 and 0.9. IHECSBE evaluations MIX-COMP-THERM-001 and -011 and MIX-SOL-THERM-001, -002, -004, and -005 generated some c_k values in the 0.7 to 0.8 range. Experiments in these evaluations could be considered as candidates for validation of other BUC application models.

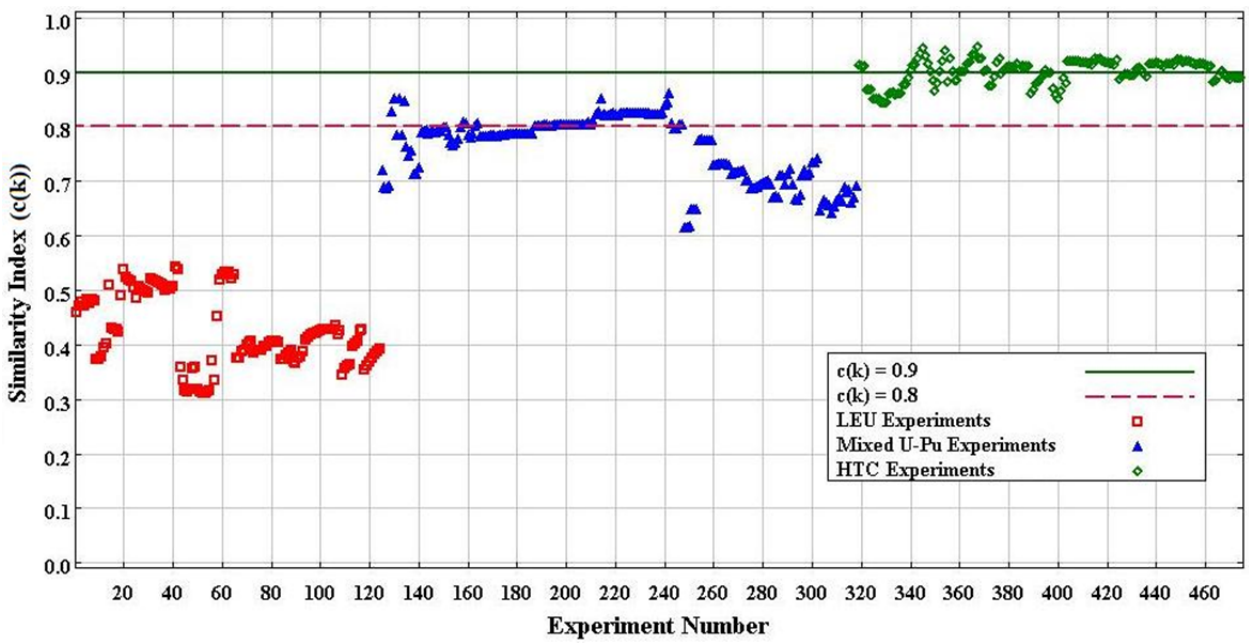

Figure 6.2 Similarity of 40 GWd/MTU PWR SFP model and each critical experiment.

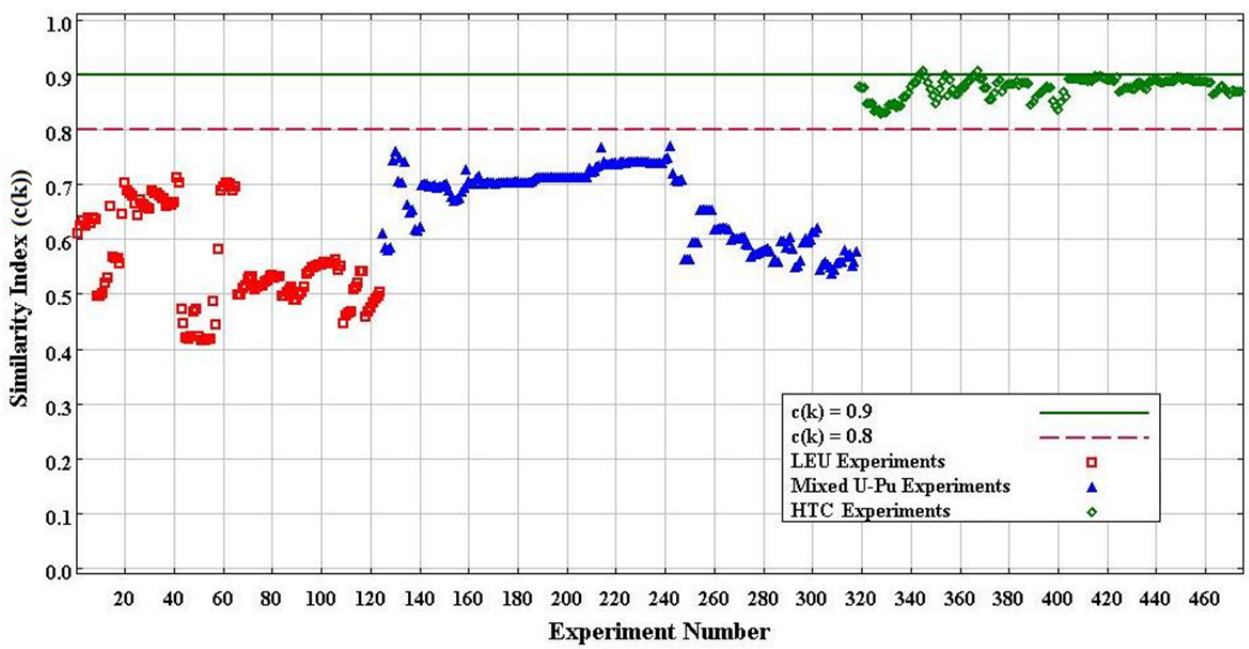

Figure 6.3 Similarity of 10 GWd/MTU GBC-32 cask model and each critical experiment.

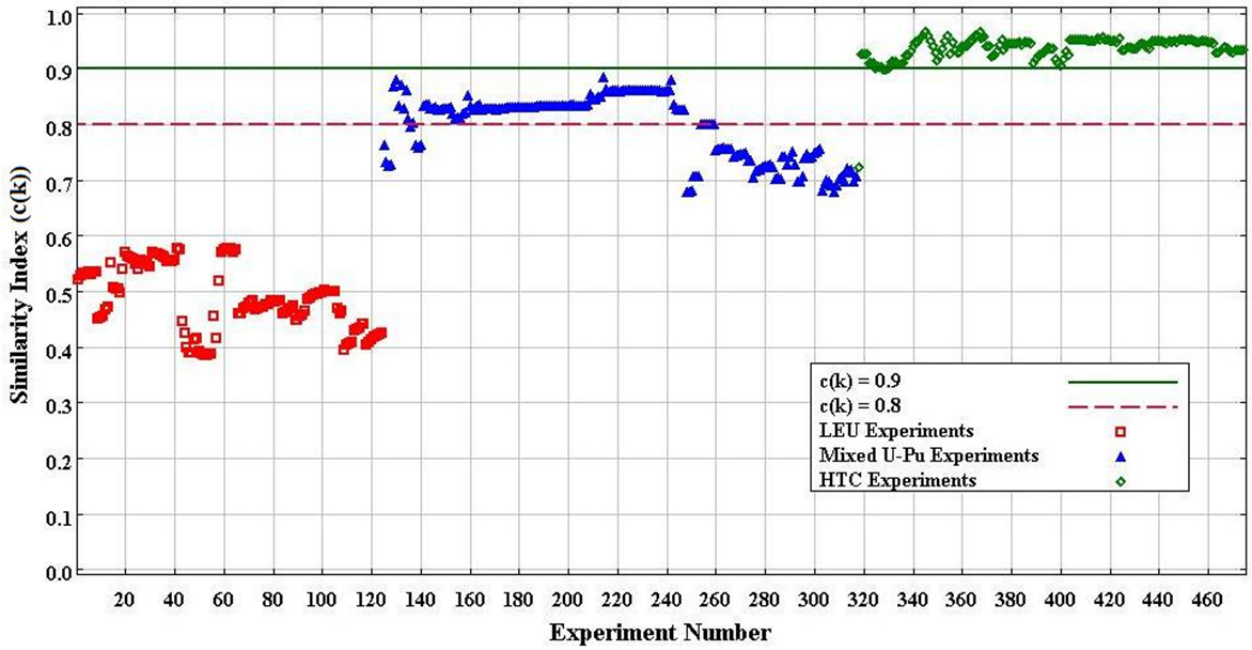

Figure 6.4 Similarity of 40 GWd/MTU GBC-32 cask model and each critical experiment.

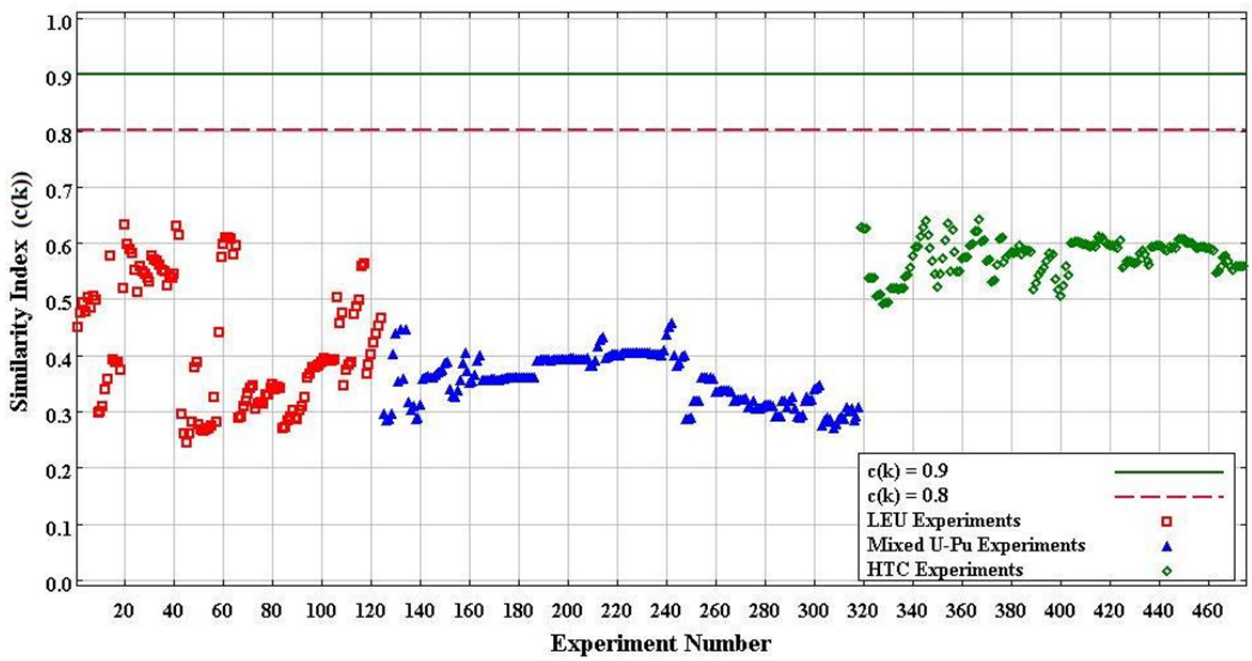

Figure 6.5 Similarity of BWR SFP model at peak SCCG burnup (11 GWd/MTU) and each critical experiment.

6.2.2 Bias and Bias Uncertainty Using Sensitivity and Uncertainty Analysis

In Section 6.2.1 S/U analysis was used to identify which critical experiments were similar to each application model. Results are presented in this section for calculation of the bias and bias uncertainty, similar to the work reported in Section 6.1, using only critical experiments that had a c_k value of at least 0.8. Bias and bias uncertainty are also calculated as a function of the c_k similarity index. No bias and bias uncertainty is presented in this section for the BWR application model because none of the critical experiments had a c_k value of at least 0.8 compared with the BWR model. As the information in Table 6.1 through Table 6.6 shows, the bias and bias uncertainty changes little as a function of the nuclides credited, because the additional isotopes have a very small influence on the application model parameters used for trending. Therefore, the bias and bias uncertainty information provided in this section is for BUC with actinides and all FPs credited. Table 6.8 presents the bias and bias uncertainty results for the PWR SFP and GBC-32 application models. The table shows a value of “none” for bias and bias uncertainty for the final enrichment and plutonium content trends, indicating that the value of the trend parameter for the application model was outside the range of parameter values for the critical experiments. Table 6.9 presents combined bias and bias uncertainty results when nonparametric analysis techniques are used to account for the non-normality of the distribution, which would replace $\beta + \Delta k_\beta$ in Eq. (3.1).

Table 6.8 Bias and bias uncertainty results using S/U analysis

Application model	Initial enrichment (wt % ^{235}U)	Final BU (GWd/MTU)	EALF (eV)	k_{eff} versus EALF		Bias uncertainty
				Bias	Fit uncertainty	
PWR SFP	2.59	10	0.202	-1.75×10^{-3}	2.10×10^{-3}	7.2×10^{-3}
	5.15	40	0.295	-1.68×10^{-3}	3.46×10^{-3}	1.04×10^{-2}
GBC-32	2.372	10	0.201	-1.71×10^{-3}	1.92×10^{-3}	6.6×10^{-3}
	4.9	40	0.295	-2.45×10^{-3}	5.42×10^{-3}	1.30×10^{-2}
Application model	**Initial enrichment (wt % ^{235}U)**	**Final BU (GWd/MTU)**	**Final enrichment (wt % ^{235}U)**	**k_{eff} vs. final enrichment**		**Bias uncertainty**
				Bias	**Fit uncertainty**	
PWR SFP	2.59	10	1.956	none	none	none
	5.15	40	2.227	none	none	none
GBC-32	2.372	10	1.780	none	none	none
	4.9	40	2.150	none	none	none
Application model	**Initial enrichment (wt % ^{235}U)**	**Final BU (GWd/MTU)**	**Final Pu content (wt % Pu)**	**k_{eff} vs. final Pu content**		**Bias uncertainty**
				Bias	**Fit uncertainty**	
PWR SFP	2.59	10	0.427	none	none	none
	5.15	40	1.212	-2.03×10^{-3}	2.95×10^{-3}	9.5×10^{-3}
GBC-32	2.372	10	0.416	none	none	none
	4.9	40	1.144	-2.35×10^{-3}	4.76×10^{-3}	1.10×10^{-2}
Application model	**Initial enrichment (wt % ^{235}U)**	**Final BU (GWd/MTU)**	**Application c_k value**	**k_{eff} vs. c_k**		**Bias uncertainty**
				Bias	**Fit uncertainty**	
PWR SFP	2.59	10	1	-6.12×10^{-3}	2.09×10^{-3}	1.07×10^{-2}
	5.15	40	1	3.08×10^{-3}	2.84×10^{-3}	8.9×10^{-3}
GBC-32	2.372	10	1	-4.03×10^{-3}	1.91×10^{-3}	7.47×10^{-3}
	4.9	40	1	1.92×10^{-3}	4.68×10^{-3}	1.08×10^{-2}

Table 6.9 Nonparametric bias and bias uncertainty

Model	Burnup (GWd/MTU)	Bias and bias uncertainty (Δk)
PWR SFP	10	N/A
PWR SFP	40	-1.99×10^{-2}
GBC-32	10	N/A
GBC-32	40	-3.06×10^{-2}

N/A – not applicable because data set was normally distributed

6.3 COMPARISON OF BIAS AND UNCERTAINTY WITH NUCLEAR DATA UNCERTAINTY VALUES

As is discussed in Section 3.2.3, methods have been implemented in the SCALE computer code system to calculate model-specific sensitivity data that relate how the model k_{eff} value varies as nuclear data are varied. Sensitivity data are calculated for each nuclide in each mixture as a function of reaction and neutron energy. The model-specific k_{eff} sensitivity data can then be combined with the nuclear data uncertainty information contained in the SCALE cross-section covariance data file to translate the nuclear data uncertainties into uncertainties in the model k_{eff} value. Since the k_{eff} uncertainty data are available on a per nuclide basis, the k_{eff} uncertainty information can be used to estimate biases for nuclides for which insufficient critical experiment data exist to determine the bias. Results in Section 3.2.5 demonstrate that the k_{eff} uncertainty data can be used to provide a bounding estimate for biases for nuclides when sufficient critical experiment information is not available. In this section, this approach is used to estimate bias for the application models and evaluate the use of the approach to estimate biases for nuclides, such as FPs, for which applicable LCEs are not available.

k_{eff} sensitivity data were generated for all application models described in Section 4 and for some variations of these models to support examination of how k_{eff} uncertainties vary with model variations. The k_{eff} uncertainty data were then generated for each application model with all actinides and FPs, using the SCALE TSUNAMI-IP program (Ref. 14, Section M18), the model-specific k_{eff} sensitivity data, and the SCALE 44-group cross-section covariance data. Table 6.10 presents the k_{eff} uncertainty data for each of the models. Table 6.11presents the k_{eff} uncertainty data for the PWR SFP as a function of burnup. Table 6.12 presents the k_{eff} uncertainty data for the PWR SFP pool at 10 and 40 GWd/MTU for ENDF/B-V, -VI, and -VII 238 neutron energy group nuclear data libraries. Note that the k_{eff} uncertainty associated with the FPs varies with burnup but does not vary much for different models at similar burnups, or when different nuclear data libraries are used for k_{eff} calculations.

Comparing the bias values from Table 6.1 though Table 6.6 with the total uncertainty value for “All nuclides” in Table 6.10 shows that the bias values calculated using statistical analysis of the critical experiment results are all within one standard deviation of the total uncertainty in k_{eff} due to nuclear data uncertainty. This suggests that, consistent with the study presented in Section 3.2.5, the uncertainty in k_{eff} due to nuclear data uncertainties could be used to conservatively estimate biases associated with nuclear data errors. Within Table 6.10, comparing the k_{eff} uncertainty for “All nuclides” with the uncertainty associated only with major actinides shows that the uncertainty associated with the major actinides contributes nearly all of the uncertainty in k_{eff}. This indicates that validation of the major actinides is most important. The next-highest contributor to the overall uncertainty is the category of structural materials. The data in Table 6.10 also indicate that bias in k_{eff} due to FP nuclear data errors is predicted to be small compared with the bias associated with the actinides.

The information provided in Tables Table 6.10 to Table 6.12 was used to develop the minor actinide and fission product uncertainty-to-worth ratios presented in Section 7.4.3 and the Δk_x recommendation provided in Section 8.

Table 6.10 Uncertainty in k_{eff} due to uncertainty in nuclear data for BUC application models

	BUC model k_{eff} uncertainty (Δk)				
Model	**SFP**	**SFP**	**GBC-32**	**GBC-32**	**BWR**
Burnup (GWd/MTU)	**10**	**40**	**10**	**40**	**11**
All nuclides	0.00471	0.00486	0.00468	0.00545	0.00402
Major actinides (9)	0.00463	0.00476	0.00455	0.00527	0.00393
^{234}U	0.00000	0.00000	0.00000	0.00000	0.00000
^{235}U	0.00270	0.00211	0.00246	0.00226	0.00293
^{238}U	0.00250	0.00189	0.00246	0.00216	0.00211
^{238}Pu	0.00000	0.00003	0.00000	0.00003	0.00000
^{239}Pu	0.00281	0.00377	0.00292	0.00420	0.00154
^{240}Pu	0.00017	0.00042	0.00018	0.00046	0.00011
^{241}Pu	0.00008	0.00037	0.00007	0.00033	0.00003
^{242}Pu	0.00001	0.00013	0.00001	0.00014	0.00000
^{241}Am	0.00000	0.00002	0.00003	0.00018	0.00000
Minor actinides (3)	0.00007	0.00027	0.00007	0.00029	0.00013
^{243}Am	0.00000	0.00001	0.00000	0.00001	0.00000
^{237}Np	0.00002	0.00009	0.00002	0.00010	0.00001
^{236}U	0.00007	0.00025	0.00007	0.00027	0.00013
FP (16)	0.00022	0.00052	0.00024	0.00058	0.00023
^{95}Mo	0.00001	0.00004	0.00001	0.00006	0.00002
^{99}Tc	0.00002	0.00007	0.00002	0.00008	0.00003
^{101}Ru	0.00002	0.00008	0.00002	0.00008	0.00003
^{103}Rh	0.00004	0.00019	0.00006	0.00022	0.00008
^{109}Ag	0.00000	0.00002	0.00000	0.00002	0.00000
^{133}Cs	0.00005	0.00016	0.00005	0.00018	0.00008
^{147}Sm	0.00000	0.00002	0.00002	0.00006	0.00000
^{149}Sm	0.00015	0.00018	0.00016	0.00022	0.00010
^{150}Sm	0.00001	0.00005	0.00001	0.00006	0.00002
^{151}Sm	0.00008	0.00013	0.00008	0.00013	0.00006
^{152}Sm	0.00002	0.00006	0.00002	0.00007	0.00003
^{143}Nd	0.00011	0.00033	0.00012	0.00036	0.00014
^{145}Nd	0.00004	0.00017	0.00004	0.00018	0.00008
^{151}Eu	0.00000	0.00000	0.00000	0.00000	0.00000
^{153}Eu	0.00001	0.00007	0.00001	0.00008	0.00002
^{155}Gd	0.00000	0.00000	0.00001	0.00004	*
Other actinides	0.00003	0.00003	0.00000	0.00001	0.00000
Other FP	0.00015	0.00034	0.00008	0.00027	0.00014
Structural materials	0.00081	0.00073	0.00106	0.00118	0.00080

*Gadolinium is included in structural materials because most is residual gadolinium from gadolinium fuel rods (i.e., gadolinium FP concentration is negligible at short decay times).

Table 6.11 Uncertainty in k_{eff} due to uncertainty in nuclear data for SFP model as a function of burnup

	SFP k_{eff} uncertainty (Δk) at various burnup values							
Burnup (GWd/MTU)	**5**	**10**	**18**	**30**	**40**	**50**	**60**	**70**
All nuclides	0.00464	0.00471	0.00485	0.00489	0.00486	0.00480	0.00485	0.00487
Major actinides (9)	0.00456	0.00463	0.00477	0.00480	0.00476	0.00469	0.00472	0.00473
^{234}U	0.00000	0.00000	0.00000	0.00000	0.00000	0.00000	0.00000	0.00000
^{235}U	0.00292	0.00270	0.00235	0.00216	0.00211	0.00209	0.00188	0.00169
^{238}U	0.00265	0.00250	0.00223	0.00201	0.00189	0.00180	0.00176	0.00172
^{238}Pu	0.00000	0.00000	0.00001	0.00002	0.00003	0.00004	0.00006	0.00007
^{239}Pu	0.00229	0.00281	0.00349	0.00374	0.00377	0.00373	0.00389	0.00400
^{240}Pu	0.00011	0.00017	0.00031	0.00039	0.00042	0.00043	0.00048	0.00051
^{241}Pu	0.00004	0.00008	0.00022	0.00035	0.00037	0.00040	0.00047	0.00054
^{242}Pu	0.00000	0.00001	0.00005	0.00010	0.00013	0.00016	0.00020	0.00023
^{241}Am	0.00000	0.00000	0.00000	0.00001	0.00002	0.00002	0.00003	0.00004
Minor actinides (3)	0.00005	0.00007	0.00014	0.00022	0.00027	0.00032	0.00035	0.00038
^{243}Am	0.00000	0.00000	0.00000	0.00001	0.00001	0.00001	0.00002	0.00003
^{237}Np	0.00001	0.00002	0.00004	0.00007	0.00009	0.00011	0.00013	0.00015
^{236}U	0.00005	0.00007	0.00013	0.00020	0.00025	0.00030	0.00033	0.00035
FP (16)	0.00018	0.00022	0.00033	0.00046	0.00052	0.00058	0.00062	0.00064
^{95}Mo	0.00000	0.00001	0.00002	0.00003	0.00004	0.00005	0.00006	0.00006
^{99}Tc	0.00002	0.00002	0.00004	0.00006	0.00007	0.00008	0.00008	0.00009
^{101}Ru	0.00001	0.00002	0.00004	0.00006	0.00008	0.00009	0.00010	0.00011
^{103}Rh	0.00002	0.00004	0.00010	0.00016	0.00019	0.00021	0.00022	0.00023
^{109}Ag	0.00000	0.00000	0.00001	0.00002	0.00002	0.00002	0.00003	0.00003
^{133}Cs	0.00003	0.00005	0.00009	0.00014	0.00016	0.00018	0.00020	0.00020
^{147}Sm	0.00000	0.00000	0.00000	0.00001	0.00002	0.00002	0.00002	0.00003
^{149}Sm	0.00015	0.00015	0.00017	0.00018	0.00018	0.00018	0.00018	0.00017
^{150}Sm	0.00001	0.00001	0.00003	0.00004	0.00005	0.00006	0.00006	0.00007
^{151}Sm	0.00007	0.00008	0.00010	0.00012	0.00013	0.00013	0.00014	0.00014
^{152}Sm	0.00001	0.00002	0.00004	0.00005	0.00006	0.00007	0.00007	0.00007
^{143}Nd	0.00006	0.00011	0.00020	0.00028	0.00033	0.00036	0.00040	0.00042
^{145}Nd	0.00003	0.00004	0.00009	0.00014	0.00017	0.00019	0.00021	0.00022
^{151}Eu	0.00000	0.00000	0.00000	0.00000	0.00000	0.00000	0.00000	0.00000
^{153}Eu	0.00001	0.00001	0.00003	0.00006	0.00007	0.00008	0.00010	0.00011
^{155}Gd	0.00000	0.00000	0.00000	0.00000	0.00000	0.00000	0.00000	0.00000
Other actinides	0.00003	0.00003	0.00003	0.00003	0.00003	0.00003	0.00004	0.00005
Other FP	0.00016	0.00015	0.00023	0.00030	0.00034	0.00037	0.00040	0.00043
Structural materials	0.00083	0.00081	0.00076	0.00073	0.00073	0.00074	0.00075	0.00077

Table 6.12 k_{eff} uncertainty due to uncertainty in nuclear data for ENDF/B-V, -VI, and -VII nuclear data libraries

	SFP k_{eff} uncertainty (Δk) for ENDF/B-V, -VI, and -VII libraries					
Library (ENDF/B-)	**V**	**VI**	**VII**	**V**	**VI**	**VII**
Burnup (GWd/MTU)	**10**	**10**	**10**	**40**	**40**	**40**
All actinides	0.00468	0.00471	0.00471	0.00483	0.00486	0.00486
Major actinides (9)	0.00462	0.00463	0.00463	0.00473	0.00475	0.00476
^{234}U	0.00000	0.00000	0.00000	0.00000	0.00000	0.00000
^{235}U	0.00264	0.00267	0.00270	0.00207	0.00209	0.00211
^{238}U	0.00249	0.00252	0.00250	0.00188	0.00191	0.00189
^{238}Pu	0.00000	0.00000	0.00000	0.00003	0.00003	0.00003
^{239}Pu	0.00285	0.00282	0.00281	0.00377	0.00377	0.00377
^{240}Pu	0.00018	0.00018	0.00017	0.00043	0.00042	0.00042
^{241}Pu	0.00009	0.00008	0.00008	0.00038	0.00037	0.00037
^{242}Pu	0.00001	0.00001	0.00001	0.00014	0.00013	0.00013
^{241}Am	0.00000	0.00000	0.00000	0.00002	0.00002	0.00002
Minor Actinides (3)	0.00007	0.00007	0.00007	0.00028	0.00027	0.00027
^{243}Am	0.00000	0.00000	0.00000	0.00001	0.00001	0.00001
^{237}Np	0.00002	0.00005	0.00002	0.00010	0.00010	0.00009
^{236}U	0.00007	0.00005	0.00007	0.00026	0.00026	0.00025
FP (16)	0.00022	0.00022	0.00022	0.00051	0.00052	0.00052
^{95}Mo	0.00001	0.00001	0.00001	0.00004	0.00004	0.00004
^{99}Tc	0.00002	0.00002	0.00002	0.00006	0.00006	0.00007
^{101}Ru	0.00002	0.00002	0.00002	0.00007	0.00008	0.00008
^{103}Rh	0.00005	0.00004	0.00004	0.00019	0.00019	0.00019
^{109}Ag	0.00000	0.00000	0.00000	0.00002	0.00002	0.00002
^{133}Cs	0.00004	0.00005	0.00005	0.00014	0.00016	0.00016
^{147}Sm	0.00000	0.00000	0.00000	0.00001	0.00001	0.00002
^{149}Sm	0.00015	0.00015	0.00015	0.00018	0.00019	0.00018
^{150}Sm	0.00001	0.00001	0.00001	0.00005	0.00005	0.00005
^{151}Sm	0.00008	0.00008	0.00008	0.00012	0.00013	0.00013
^{152}Sm	0.00002	0.00002	0.00002	0.00006	0.00006	0.00006
^{143}Nd	0.00011	0.00011	0.00011	0.00033	0.00033	0.00033
^{145}Nd	0.00004	0.00004	0.00004	0.00016	0.00017	0.00017
^{151}Eu	0.00000	0.00000	0.00000	0.00000	0.00000	0.00000
^{153}Eu	0.00001	0.00001	0.00001	0.00007	0.00007	0.00007
^{155}Gd	0.00000	0.00000	0.00000	0.00000	0.00000	0.00000
Other actinides	0.00002	0.00003	0.00003	0.00003	0.00003	0.00003
Other FP	0.00016	0.00016	0.00015	0.00038	0.00037	0.00034
Structural materials	0.00072	0.00080	0.00081	0.00065	0.00074	0.00073

6.4 BIAS AND BIAS UNCERTAINTY FOR FISSION PRODUCTS

Using FP LCE data (discussed in Section 5.4) for the nuclides ^{103}Rh, ^{133}Cs, ^{nat}Nd, ^{149}Sm, ^{152}Sm, and ^{155}Gd, biases were calculated for the individual FPs. The FP experiments are being used to confirm the relative merits of the method described in Section 3.2.5 for determining the individual FP biases and propagating them to the application models appropriately. The numbers of available critical experiments used to assess the FP bias and uncertainty are

- ^{103}Rh—11 experiments
- ^{133}Cs—15 experiments
- ^{149}Sm—9 experiments
- ^{152}Sm—7 experiments
- ^{155}Gd—10 experiments
- Nd—4 experiments (which consisted of natural neodymium)

As discussed in Section 5.4, the FP experiments were performed in three phases. Each phase had a number of baseline reference experiments with no FPs to test and check the experimental method. Phases 1 and 2 had 47 baseline experiments with a slightly acidic water (HNO_3) moderator, and Phase 3 used depleted uranyl-nitrate (DUN). The Phase 3 FP experiments consisted of combined FP mixtures; therefore, the Phase 3 experiments could not be used to establish individual FP biases based on traditional methods for this section.

Table 6.13 presents calculated values for the FP experiments as well as the overall FP worth within the experiment. For each experiment, the FP worth was calculated as the difference between the computed k_{eff} value for each experiment model and the computed k_{eff} value for the model with the FPs omitted. The phase in which they were performed is reflected in the experiment identifier, where FP1 indicates Phase 1, FP2 indicates Phase 2, and FP3 indicates Phase 3.

ORNL conducted an assessment of the FP experiment reports, which is reported in an NRC internal proprietary document (Ref. 40). Several unresolved issues remain for the experimental descriptions contained in the reference reports, leaving some unquantified uncertainties. Consequently, a total k_{eff} uncertainty for each Phase 1 and 2 FP experiment model and for each reference experiment model was recommended (Ref. 40) as follows:

- 2.00×10^{-3} for the total k_{eff} uncertainty for each FP experiment model and
- 1.00×10^{-3} for each reference experiment model.

The normalized k_{eff} (ratio of calculated to experimental [C/E]) values are presented in Figure 6.6. They identify a systematic bias between the Phase 1 and Phase 2 results when the FP benchmarks are grouped by FP and phase. In all cases except the ^{103}Rh experiments, the Phase 2 FP k_{eff} values are higher. This systematic bias indicates that these two experiment sets should be evaluated independently in performing trending analyses. The error bars in the figure include the adjusted experimental uncertainty.

Although the information presented above indicates some variability in the actual numeric values to be used for calculating biases and uncertainties, combined results will be presented using both the reported uncertainty information and the adjusted uncertainty values for comparative purposes.

Table 6.13 FP experiment evaluation data

Experiment	FP	k_{eff} (calc)	σ (calc)	FP worth (Δk)
FP1_173_01	^{103}Rh	1.000063	0.000100	0.0317
FP1_173_02	^{103}Rh	1.000464	0.000099	0.0288
FP1_173_03	^{103}Rh	0.999364	0.000099	0.0178
FP1_173_05	^{103}Rh	0.999716	0.000100	0.0199
FP2_174_HBC_01	^{103}Rh	0.998117	0.000099	0.0320
FP2_174_HBC_02	^{103}Rh	0.997367	0.000099	0.0326
FP2_174_UO2_06	^{103}Rh	0.996885	0.000099	0.0629
FP2_174_UO2_07	^{103}Rh	0.996620	0.000099	0.0632
FP2_174_UO2_08	^{103}Rh	0.997042	0.000099	0.0339
FP2_174_UO2_09	^{103}Rh	0.997044	0.000099	0.0350
FP2_174_UO2_10	^{103}Rh	0.996799	0.000099	0.0351
FP1_173_06	^{133}Cs	0.999884	0.000099	0.0207
FP1_173_07	^{133}Cs	0.999374	0.000099	0.0222
FP1_173_08	^{133}Cs	0.999599	0.000099	0.0193
FP1_173_09	^{133}Cs	0.999179	0.000100	0.0149
FP1_173_10	^{133}Cs	0.99908	0.000099	0.0153
FP1_173_11	^{133}Cs	0.999149	0.000099	0.0132
FP1_173_12	^{133}Cs	0.999537	0.000099	0.0138
FP1_173_13	^{133}Cs	0.999503	0.000100	0.0127
FP1_173_14	^{133}Cs	0.999226	0.000100	0.0125
FP1_173_15	^{133}Cs	0.999555	0.000099	0.0145
FP2_174_UO2_01	^{133}Cs	1.000927	0.000099	0.0278
FP2_174_UO2_02	^{133}Cs	1.000483	0.000099	0.0283
FP2_174_UO2_03	^{133}Cs	1.000571	0.000099	0.0287
FP2_174_UO2_04	^{133}Cs	1.000531	0.000099	0.0286
FP2_174_UO2_05	^{133}Cs	1.000465	0.000099	0.0288
FP1_173_31	^{149}Sm	0.999352	0.000100	0.0357
FP1_173_32	^{149}Sm	0.999761	0.000099	0.0214
FP2_174_HBC_05	^{149}Sm	1.001045	0.000099	0.0352
FP2_174_HBC_06	^{149}Sm	1.001075	0.000100	0.0353
FP2_174_UO2_13	^{149}Sm	1.001628	0.000100	0.0649
FP2_174_UO2_14	^{149}Sm	1.001914	0.000099	0.0647
FP2_174_UO2_15	^{149}Sm	1.000559	0.000099	0.0329
FP2_174_UO2_16	^{149}Sm	1.001505	0.000100	0.0334
FP2_174_UO2_17	^{149}Sm	1.000368	0.000100	0.0332
FP1_173_18	^{152}Sm	0.999552	0.000099	0.0432
FP1_173_19	^{152}Sm	0.999439	0.000099	0.0444
FP1_173_20	^{152}Sm	0.999291	0.000099	0.0451
FP1_173_21	^{152}Sm	1.00004	0.000099	0.0315
FP1_173_22	^{152}Sm	1.00002	0.000100	0.0319
FP2_174_UO2_18	^{152}Sm	1.000790	0.000098	0.0343
FP2_174_UO2_19	^{152}Sm	1.000522	0.000099	0.0352
FP1_173_23	^{155}Gd	0.999334	0.000100	0.0270
FP1_173_24	^{155}Gd	0.999093	0.000099	0.0278
FP1_173_25	^{155}Gd	0.998916	0.000099	0.0283
FP1_173_26	^{155}Gd	0.999384	0.000099	0.0181
FP1_173_27	^{155}Gd	0.999384	0.000099	0.0179
FP2_174_HBC_03	^{155}Gd	1.000577	0.000099	0.0355
FP2_174_HBC_04	^{155}Gd	1.000232	0.000100	0.0359

Table 6.13 FP experiment evaluation data (continued)

Experiment	FP	k_{eff} (calc)	σ (calc)	FP worth (Δk)
FP2_174_UO2_20	^{155}Gd	1.001308	0.000099	0.0709
FP2_174_UO2_21	^{155}Gd	0.999476	0.000099	0.0391
FP2_174_UO2_22	^{155}Gd	0.999607	0.000099	0.0392
FP1_173_28	Mix	0.999742	0.000099	0.0291
FP1_173_29	Mix	0.999884	0.000099	0.0314
FP1_173_30	Mix	0.999881	0.000100	0.0313
FP2_174_HBC_07	Mix	1.000533	0.000099	0.0349
FP2_174_UO2_23	Mix	1.000041	0.000097	0.0361
FP2_174_UO2_24	Mix	1.000291	0.000096	0.0367
FP2_174_UO2_25	Mix	1.002539	0.000099	0.0785
FP2_174_UO2_26	Mix	1.002514	0.000100	0.0792
FP2_174_UO2_27	Mix	1.003020	0.000099	0.0806
FP2_174_UO2_28	Mix	1.002835	0.000099	0.0810
FP1_173_16	^{nat}Nd	0.999678	0.000099	0.0173
FP1_173_17	^{nat}Nd	0.999502	0.000099	0.0198
FP2_174_UO2_11	^{nat}Nd	1.000237	0.000099	0.0173
FP2_174_UO2_12	^{nat}Nd	1.000076	0.000099	0.0176
FP3_177_04	DUN Mix	1.003398	0.000099	0.0447
FP3_177_05	DUN Mix	1.003332	0.000099	0.0449
FP3_177_06	DUN Mix	1.00364	0.000100	0.0446
FP3_177_07	DUN Mix	1.003592	0.000098	0.0446
FP2_175_13	DUN Mix	1.00201	0.000099	0.0231
FP2_175_14	DUN Mix	1.001594	0.000099	0.0279
FP2_175_15	DUN Mix	1.001308	0.000099	0.0283

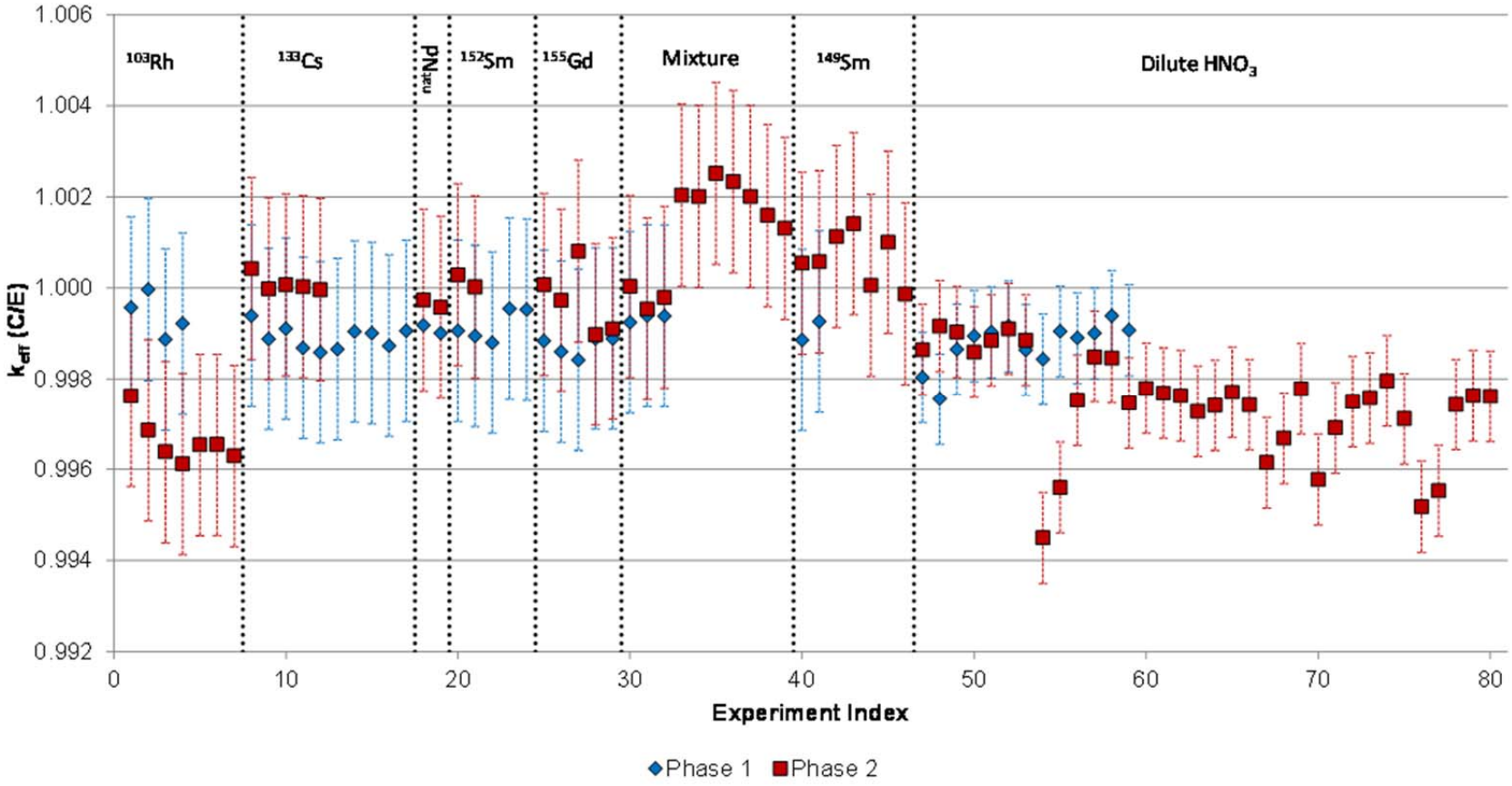

Figure 6.6 FP experiment k_{eff} values.

6.4.1 Fission Product Experiment Analysis

As discussed in Section 3.2.6, the typical evaluation of the computational biases and uncertainties of the computational methods and nuclear data is developed through the use of trending analyses.

The first step in the FP experiment evaluation was to evaluate for biases in the reference HNO_3 experiments. Because the true bias may change significantly as the neutronic characteristics of a system change, single-parameter trending analysis was performed to identify whether the bias is changing as other key parameters change. The k_{eff} results were examined for trends as a function of EALF, neutron leakage fraction, neutron mean free path, critical water height, and fuel rod number. Plots are illustrated in Figure 6.7 through Figure 6.11.

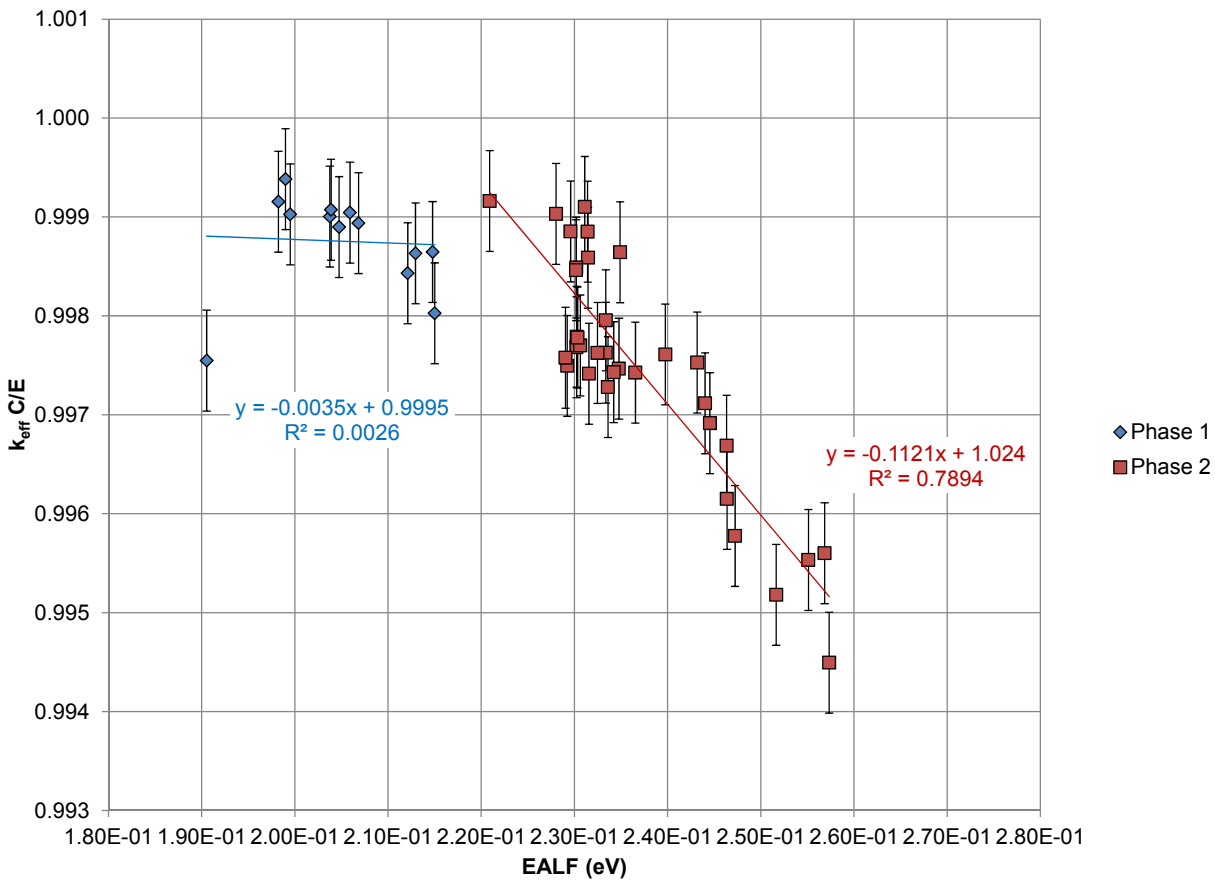

Figure 6.7 Reference HNO_3 trending of k_{eff} versus EALF.

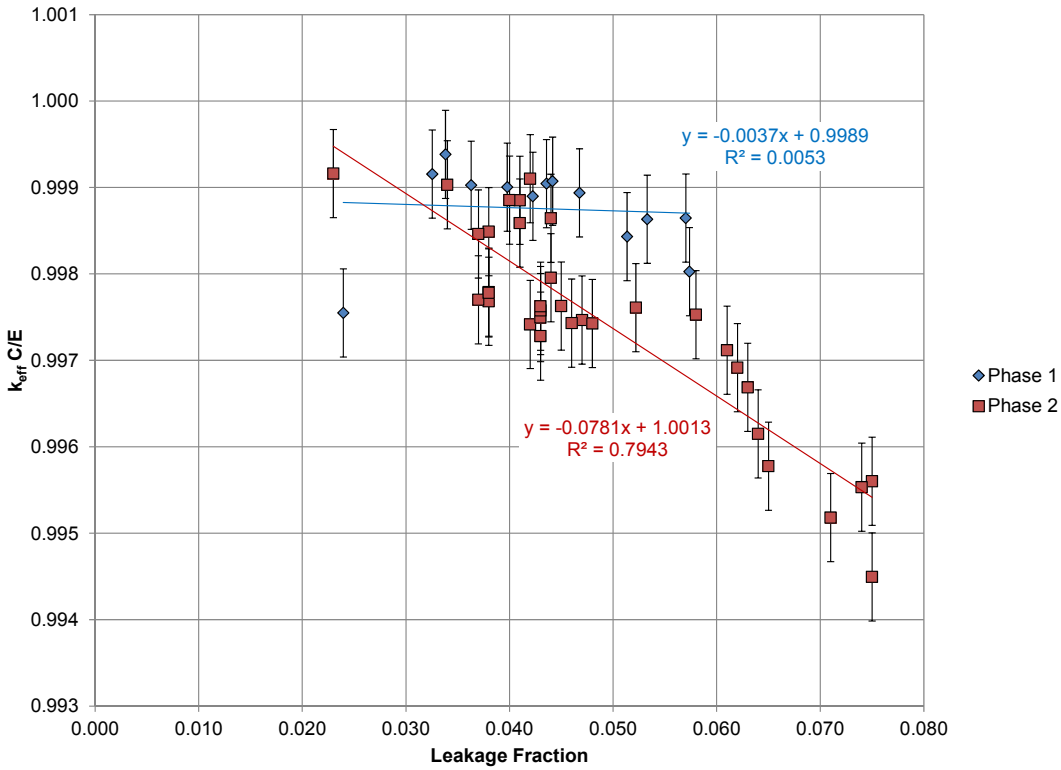

Figure 6.8 Reference HNO_3 trending of k_{eff} versus leakage fraction.

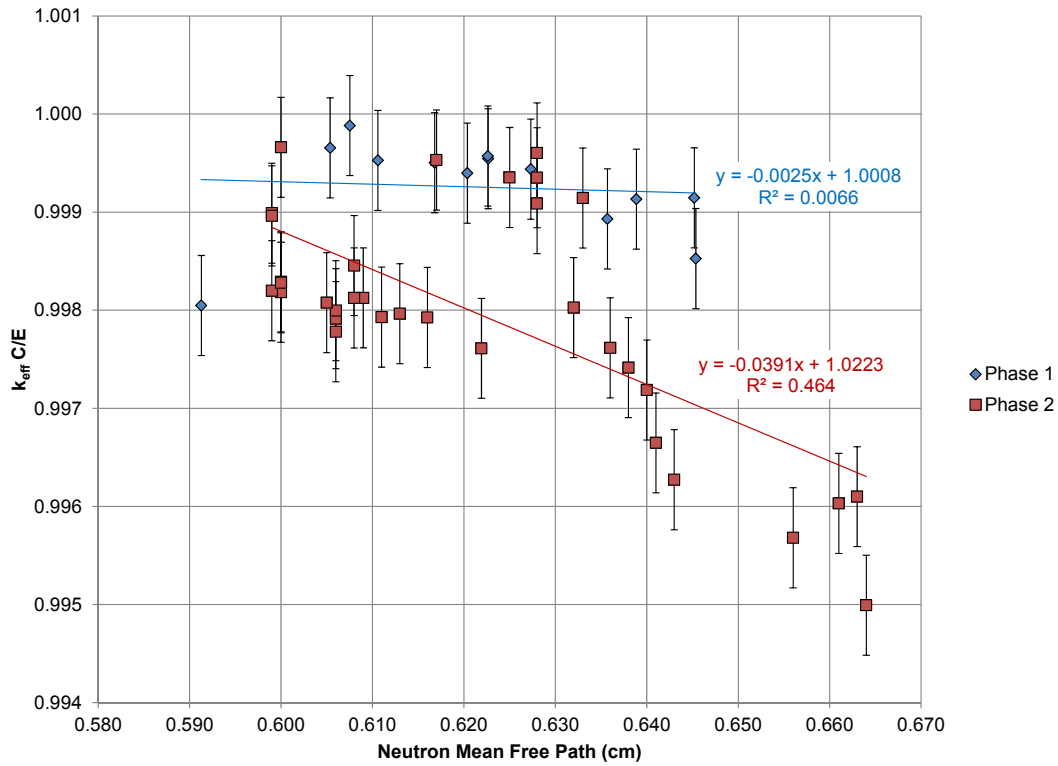

Figure 6.9 Reference HNO_3 trending of k_{eff} versus neutron mean free path.

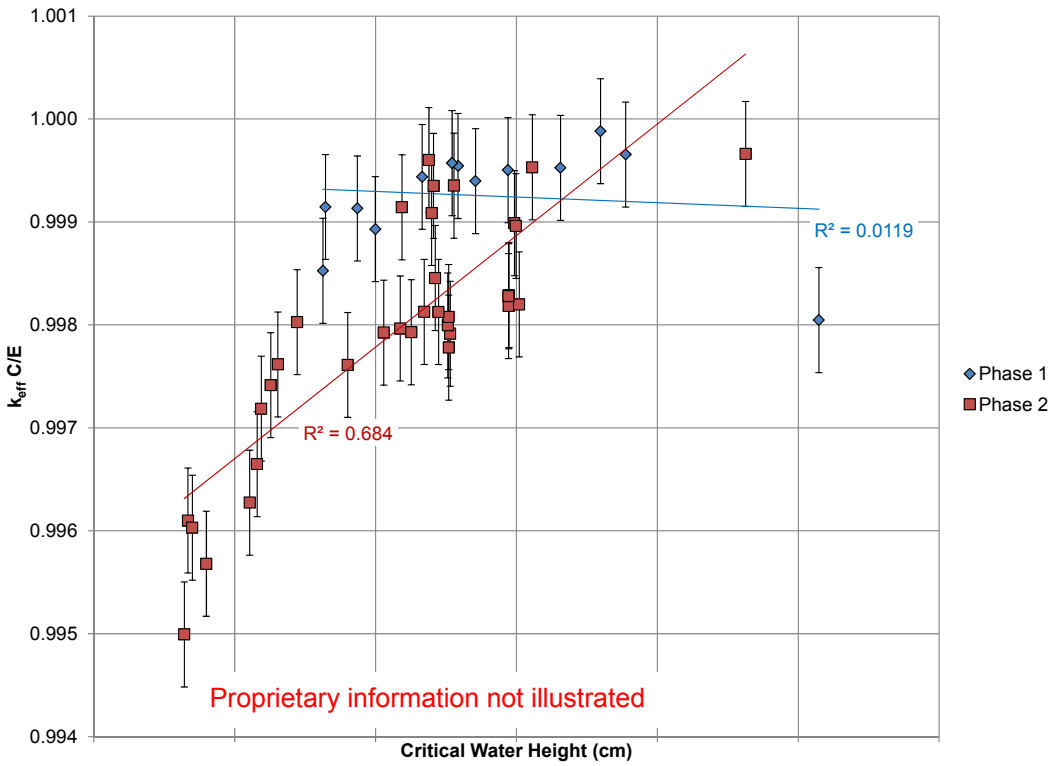

Figure 6.10 Reference HNO_3 trending of k_{eff} versus critical water height.

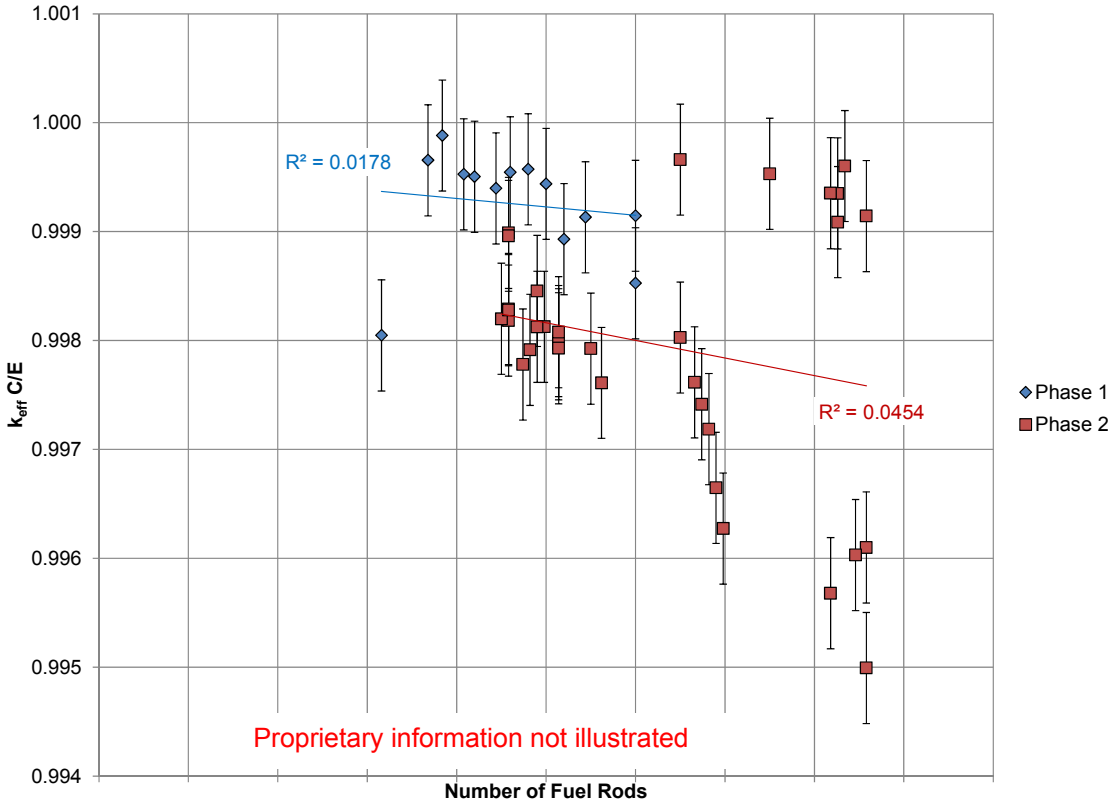

Figure 6.11 Reference HNO_3 trending of k_{eff} versus fuel rod number.

Examination of the FP experiment sets in Figure 6.7 through Figure 6.11 with the HNO_3 solution mix identifies apparent systematic biases for both the Phase 1 and Phase 2 experiment sets. Apparent trends are identified but are not well correlated (i.e., r^2 is low) because of several out-of-trend data points. In the Phase 1 data set, the data point that is consistently out of trend for all the parameters evaluated corresponds to a configuration with the lowest number of fuel rods and the highest critical water height. On average, the water level of this experiment is more than 25 cm greater than in the rest of the non-FP Phase 1 experiments; it is possibly out of trend as a result of the effects of increased water reflection in the experiment. Within the Phase 2 data set, the trending analysis indicates a strong trend with EALF and neutron leakage fraction. Apparent trends are identified with the other parameters; however, the trending results indicate that the experiments that included MOX fuel rods from the HTC experiments (referred to as HBC) have a distinctly different trend from the UO_2-only experiments. Therefore, the Phase 2 experiments will be analyzed separately when trended against neutron mean free path, critical water height, and number of fuel rods.

The trending analysis was completed for each of the data sets with one data point omitted from the Phase 1 experiment set, as discussed above, and one data point omitted from the Phase 2 data set. An apparent cause for this single experiment's being out of trend is unavailable at this time. Omission of the Phase 2 data point changed the r^2 correlation coefficient from 0.483 to 0.783, from 0.436 to 0.730, and from 0.455 to 0.782 in the trending analyses of mean free path, critical water height, and fuel rod number, respectively. The adjusted data set trending evaluations are provided in Figure 6.12 through Figure 6.16.

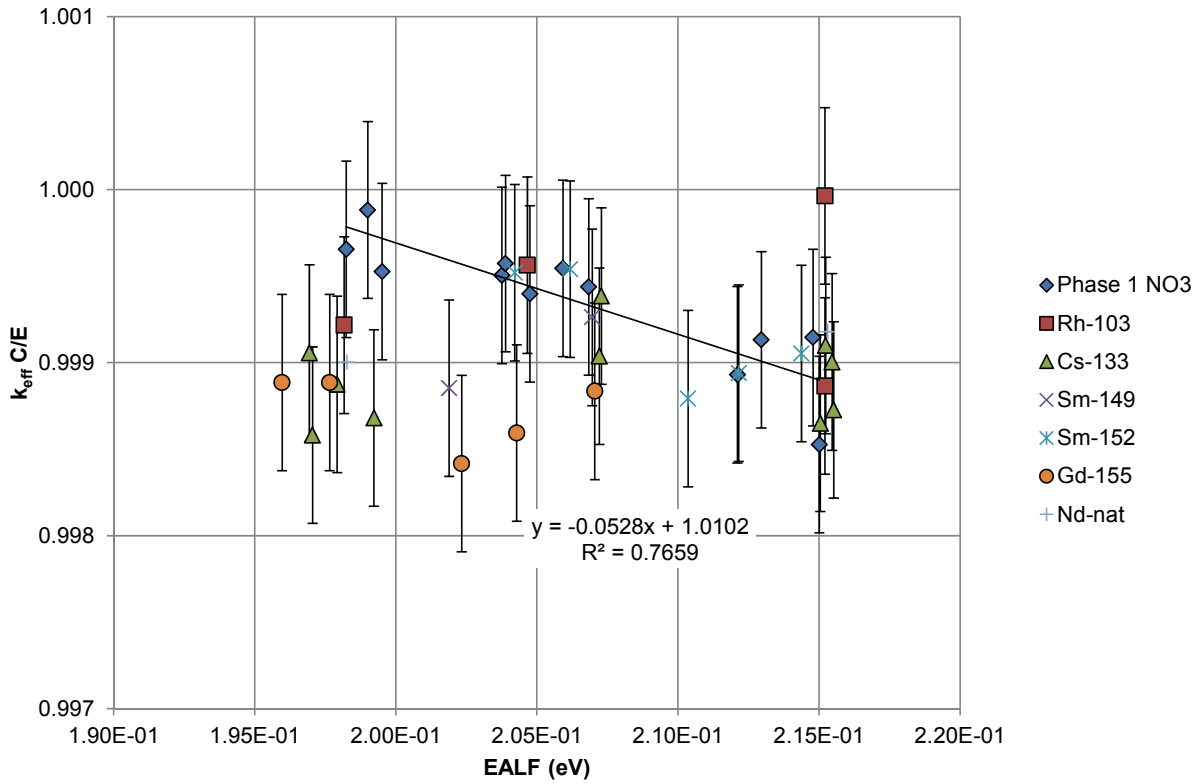

(a) Phase 1 experiments

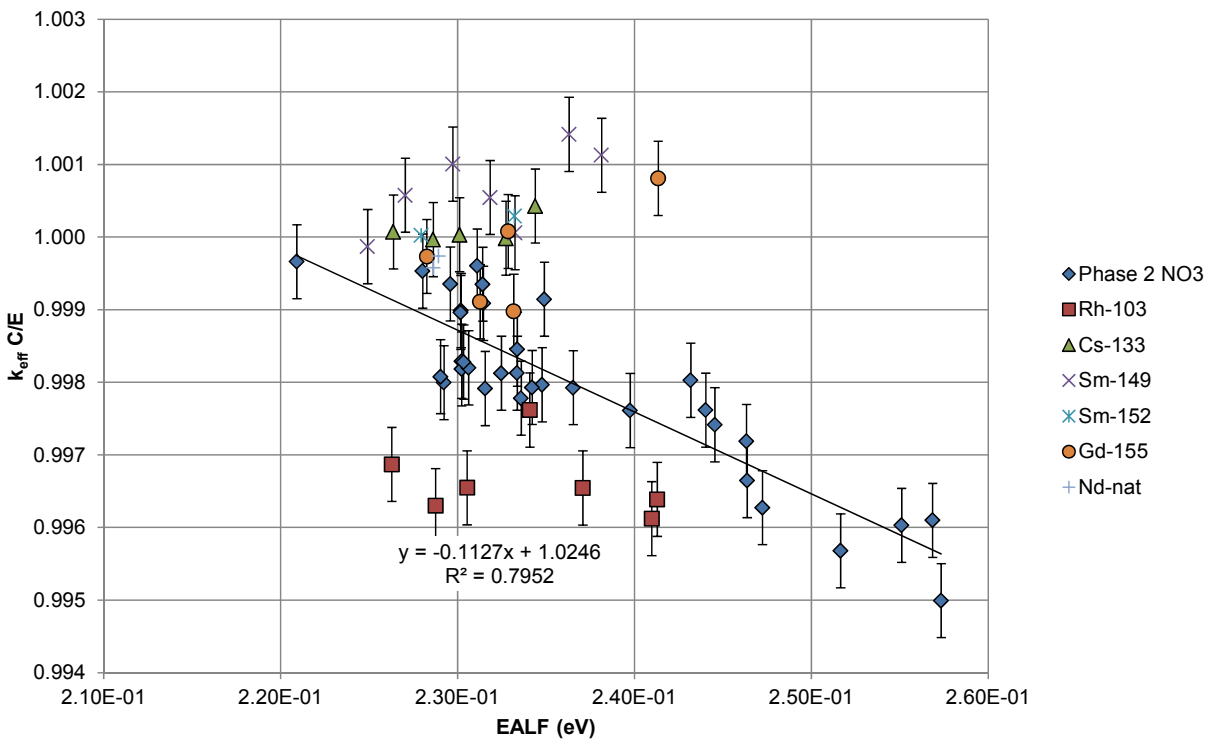

(b) Phase 2 experiments

Figure 6.12 Trending analysis of k_{eff} versus EALF.

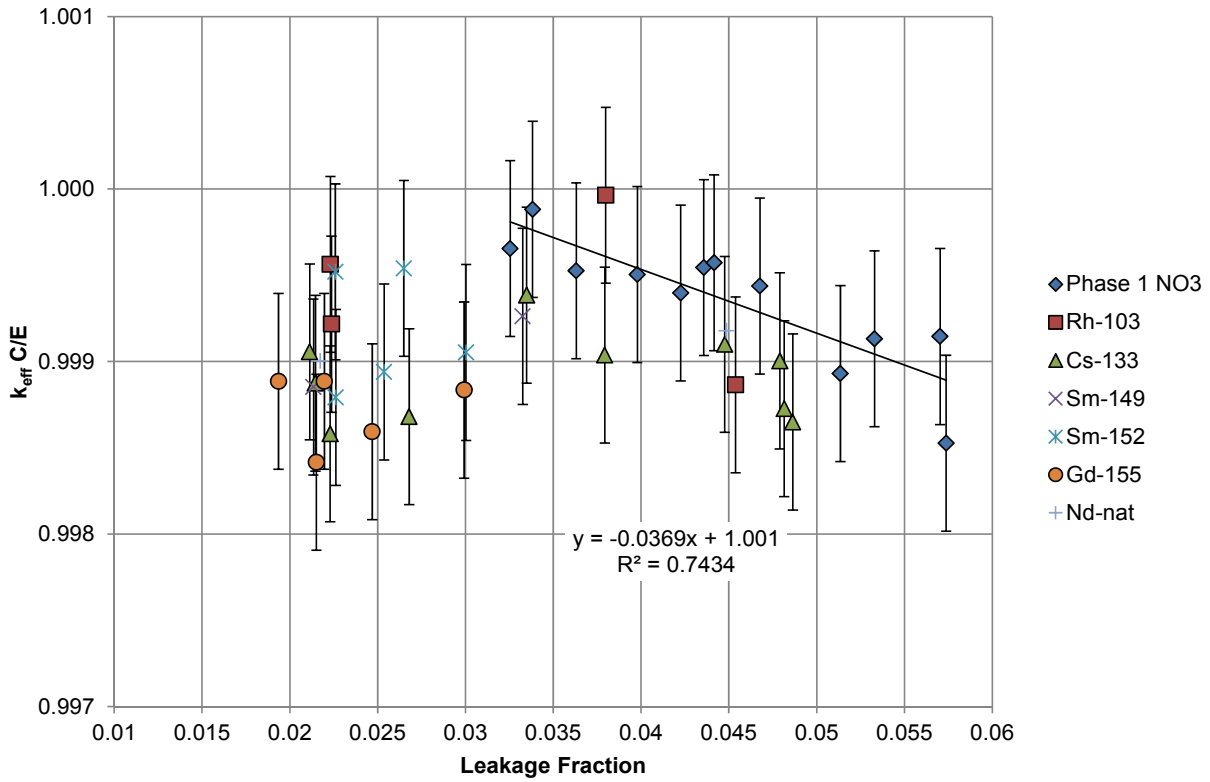

(a) Phase 1 experiments

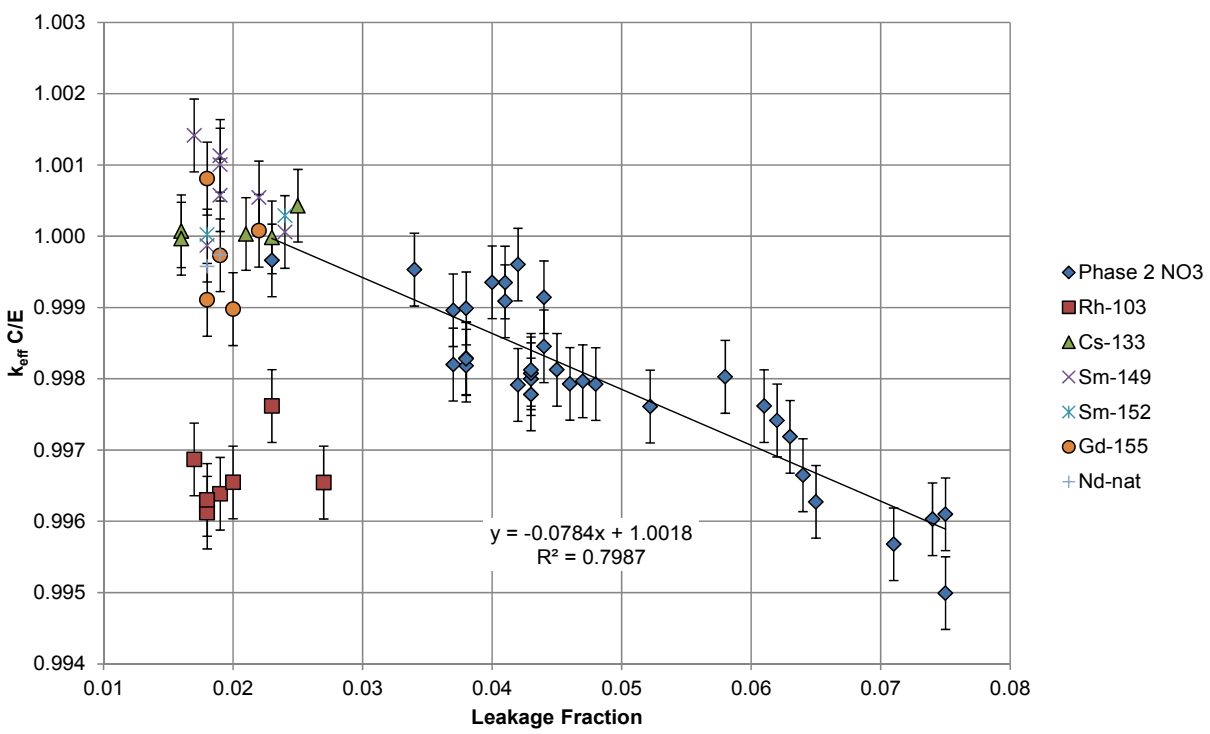

(b) Phase 2 experiments

Figure 6.13 Trending analysis of k_{eff} versus neutron leakage fraction.

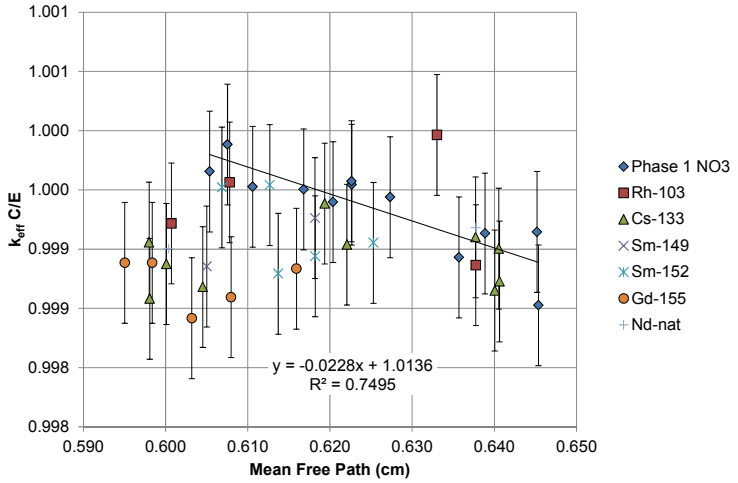

(a) Phase 1 experiments

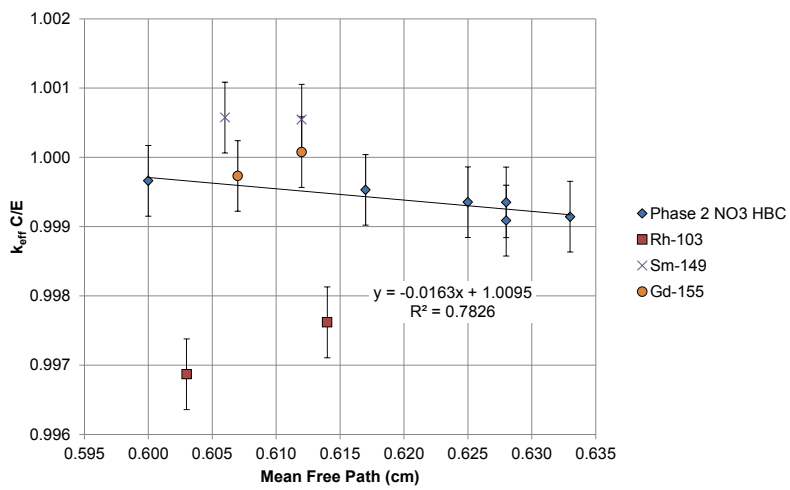

(b) Phase 2 experiments with HBC rods only

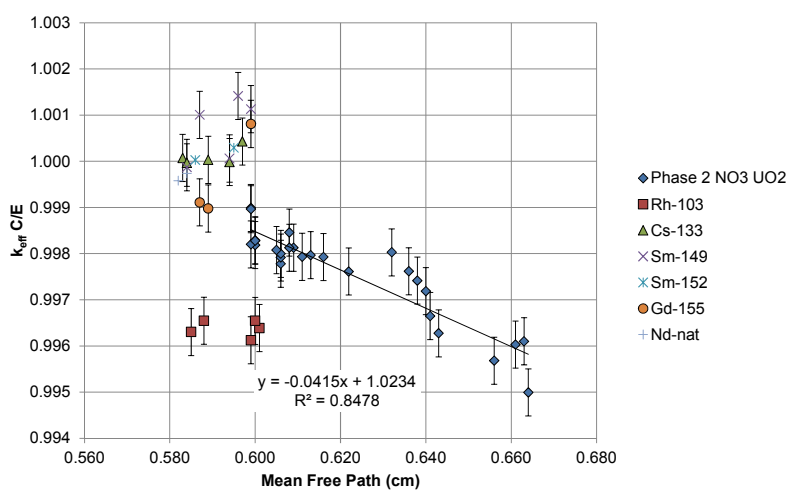

(c) Phase 2 experiments with UO_2 rods only

Figure 6.14 Trending analysis of k_{eff} versus mean free path.

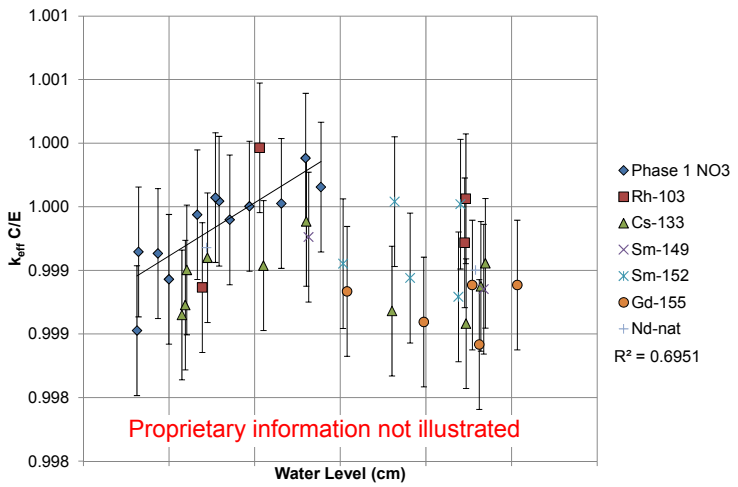

(a) Phase 1 experiments

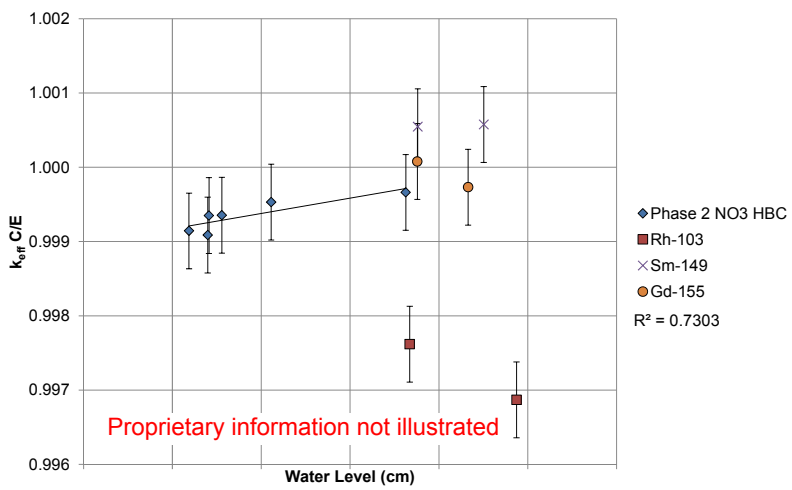

(b) Phase 2 experiments with HBC rods only

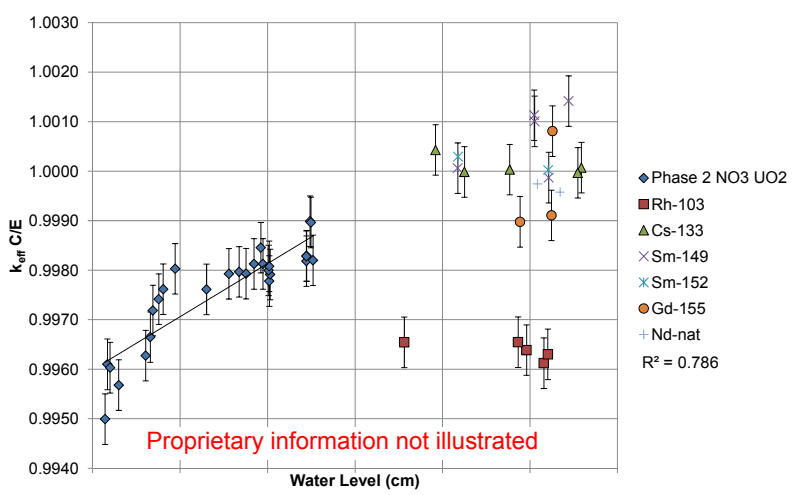

(c) Phase 2 experiments with UO_2 rods only

Figure 6.15 Trending analysis of k_{eff} versus water level.

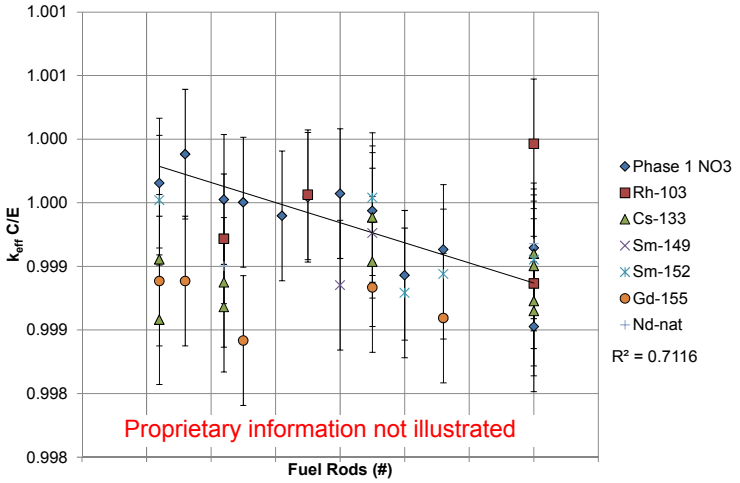

(a) Phase 1 experiments

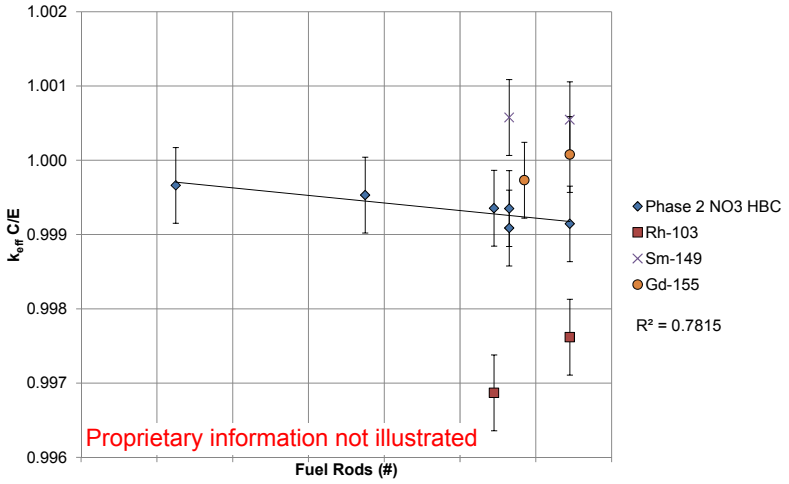

(b) Phase 2 experiments with HBC rods only

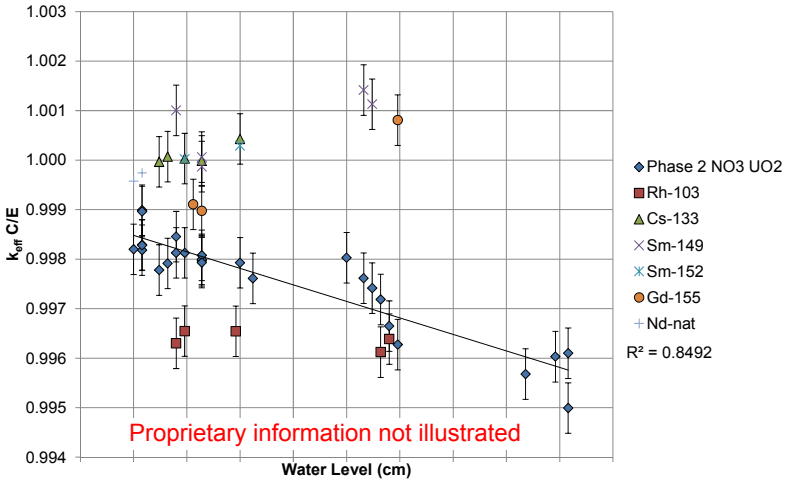

(c) Phase 2 experiments with UO_2 rods only

Figure 6.16 Trending analysis of k_{eff} versus rod number.

The FP experiment trending analysis evaluation results are presented in Table 6.14 through Table 6.19. The bias for an individual experiment was calculated by taking the difference between the expected k_{eff} value with no FPs, as determined from the trending analysis equations, and the calculated value for the experiment with FPs. Note that the bias can vary, depending on the trend parameter or if no trend is assumed.

The individual bias uncertainty values, s_b (referred to as "bias unc" in the tables below), were calculated as shown in Eq. (6.1):

$$s_b = \sqrt{\sigma_{FP}^{\ 2} + \sigma_{fit}^{\ 2}} \quad , \tag{6.1}$$

where

σ_{FP} = the standard deviation (σ_i) associated with the selected FP experiment k_{eff} values,

σ_{fit} = the mean of the sample standard deviations calculated as shown in Eqs. (6.2) and (6.3) (referred to as *Fit unc* in the tables below);

$$\sigma_i = \sqrt{\sigma_{\exp}^{\ 2} + \sigma_{calc}^{\ 2}} \quad , \tag{6.2}$$

where

i = 1 to the total number of samples (N),

$\sigma_{\exp}$ = the experimental uncertainty,

σ_{calc} = the calculated k_{eff} uncertainty;

$$\sigma_{fit}^{\ 2} = \frac{\frac{1}{N-2}\sum_{i=1}^{N}\left\{\frac{1}{\sigma_i^2}\left[k_{eff_i} - k_{fit}(x_i)\right]^2\right\}}{\frac{1}{N}\sum_{i=1}^{N}\frac{1}{\sigma_i^{\ 2}}} \quad , \tag{6.3}$$

where

k_{eff_i} = the FP critical experiment calculated k_{eff},

$k_{fit}(x_i)$ = the trend parameter (x_i) k_{eff} value.

Table 6.14 Rhodium-103 bias evaluation

Phase 1 ^{103}Rh experiments															
Trending parameter	EALF (Δk_{eff})			Leakage fraction (Δk_{eff})			Mean free path (Δk_{eff})			Water level (Δk_{eff})			Fuel rod number (Δk_{eff})		
Experiment	Bias	Fit unc	bias unc	Bias	Fit unc	bias unc	Bias	Fit unc	bias unc	Bias	Fit unc	bias unc	Bias	Fit unc	bias unc
FP1_173_01	6.69E-04	1.86E-04	5.43E-04	-1.76E-03	1.94E-04	5.46E-04	3.21E-04	1.92E-04	5.45E-04	-3.24E-04	2.12E-04	5.52E-04	7.03E-04	2.06E-04	5.50E-04
FP1_173_02	1.63E-03		5.42E-04	-1.94E-03		5.46E-04	1.30E-03		5.45E-04	1.04E-03		5.52E-04	1.66E-03		5.50E-04
FP1_173_03	5.27E-04		5.42E-04	-3.31E-03		5.46E-04	3.05E-04		5.45E-04	2.09E-04		5.52E-04	5.64E-04		5.50E-04
FP1_173_05	-2.06E-05		5.43E-04	-2.11E-03		5.46E-04	-1.88E-04		5.45E-04	-6.65E-04		5.52E-04	1.48E-04		5.50E-04
Phase 2 ^{103}Rh experiments															
FP2_174_HBC_01	-1.02E-04	5.32E-04	7.37E-04	-1.88E-03	5.28E-04	7.34E-04	-1.37E-03	1.15E-04	5.22E-04	-1.52E-03	1.28E-04	5.25E-04	-1.14E-03	1.15E-04	5.22E-04
FP2_174_HBC_02	-1.73E-03		7.37E-04	-3.10E-03		7.34E-04	-2.30E-03		5.22E-04	-2.51E-03		5.25E-04	-1.99E-03		5.22E-04
FP2_174_UO2_06	-5.22E-04		7.37E-04	-3.43E-03		7.34E-04	-1.57E-03	3.96E-04	6.46E-04	-3.78E-03	4.70E-04	6.93E-04	-2.17E-03	3.95E-04	6.45E-04
FP2_174_UO2_07	-8.22E-04		7.37E-04	-3.77E-03		7.34E-04	-1.92E-03		6.46E-04	-4.24E-03		6.93E-04	-2.47E-03		6.45E-04
FP2_174_UO2_08	-8.39E-04		7.37E-04	-2.64E-03		7.34E-04	-1.46E-03		6.46E-04	-2.22E-03		6.93E-04	-2.73E-03		6.45E-04
FP2_174_UO2_09	-1.57E-03		7.37E-04	-3.19E-03		7.34E-04	-1.95E-03		6.46E-04	-3.52E-03		6.93E-04	-2.97E-03		6.45E-04
FP2_174_UO2_10	-2.02E-03		7.37E-04	-3.59E-03		7.34E-04	-2.32E-03		6.46E-04	-4.11E-03		6.93E-04	-3.25E-03		6.45E-04

Table 6.15 Cesium-133 bias evaluation

Phase 1 ^{133}Cs experiments															
Trending parameter	EALF (Δk_{eff})			Leakage fraction (Δk_{eff})			Mean free path (Δk_{eff})			Water level (Δk_{eff})			Fuel rod number (Δk_{eff})		
Experiment	Bias	Fit unc	bias unc	Bias	Fit unc	bias unc	Bias	Fit unc	bias unc	Bias	Fit unc	bias unc	Bias	Fit unc	bias unc
FP1_173_06	6.29E-04	1.86E-04	5.42E-04	-2.35E-03	1.94E-04	5.46E-04	4.05E-04	1.92E-04	5.45E-04	2.43E-04	2.12E-04	5.52E-04	6.84E-04	2.06E-04	5.50E-04
FP1_173_07	-3.76E-04		5.42E-04	-2.42E-03		5.46E-04	-5.44E-04		5.45E-04	-1.08E-03		5.52E-04	-1.94E-04		5.50E-04
FP1_173_08	7.64E-04		5.42E-04	-3.05E-03		5.46E-04	5.39E-04		5.45E-04	4.19E-04		5.52E-04	7.99E-04		5.50E-04
FP1_173_09	-5.02E-04		5.43E-04	-2.81E-03		5.46E-04	-6.38E-04		5.45E-04	-8.63E-04		5.52E-04	-3.89E-04		5.50E-04
FP1_173_10	-7.16E-04		5.42E-04	-2.74E-03		5.46E-04	-8.84E-04		5.45E-04	-1.31E-03		5.52E-04	-6.48E-04		5.50E-04
FP1_173_11	3.04E-04		5.42E-04	-3.65E-03		5.46E-04	1.42E-04		5.45E-04	8.84E-05		5.52E-04	3.49E-04		5.50E-04
FP1_173_12	2.78E-04		5.42E-04	-2.86E-03		5.46E-04	1.20E-04		5.45E-04	9.54E-05		5.52E-04	3.37E-04		5.50E-04
FP1_173_13	6.80E-04		5.43E-04	-3.26E-03		5.46E-04	5.07E-04		5.45E-04	4.20E-04		5.52E-04	7.03E-04		5.50E-04
FP1_173_14	4.06E-04		5.43E-04	-3.55E-03		5.46E-04	2.32E-04		5.45E-04	1.50E-04		5.52E-04	4.26E-04		5.50E-04
FP1_173_15	-2.47E-04		5.42E-04	-2.22E-03		5.46E-04	-4.11E-04		5.45E-04	-9.23E-04		5.52E-04	-1.73E-04		5.50E-04
Phase 2 ^{133}Cs experiments															
FP2_174_UO2_01	2.74E-03	5.32E-04	7.37E-04	1.09E-03	5.27E-04	7.34E-04	2.30E-03	3.96E-04	6.46E-04	1.31E-03	4.70E-04	6.93E-04	1.18E-03	3.95E-04	6.45E-04
FP2_174_UO2_02	2.11E-03		7.37E-04	4.86E-04		7.34E-04	1.73E-03		6.46E-04	5.32E-04		6.93E-04	5.53E-04		6.45E-04
FP2_174_UO2_03	1.48E-03		7.37E-04	2.54E-05		7.34E-04	1.37E-03		6.46E-04	-7.17E-04		6.93E-04	4.81E-04		6.45E-04
FP2_174_UO2_04	1.87E-03		7.37E-04	3.77E-04		7.34E-04	1.57E-03		6.46E-04	6.29E-05		6.93E-04	5.21E-04		6.45E-04
FP2_174_UO2_05	1.63E-03		7.37E-04	-8.06E-05		7.34E-04	1.30E-03		6.46E-04	-7.81E-04		6.93E-04	3.35E-04		6.45E-04

Table 6.16 Samarium-149 bias evaluation

Phase 1 ^{149}Sm experiments															
Trending parameter	EALF (Δk_{eff})			Leakage fraction (Δk_{eff})			Mean free path (Δk_{eff})			Water level (Δk_{eff})			Fuel rod number (Δk_{eff})		
Experiment	Bias	Fit unc	bias unc	Bias	Fit unc	bias unc	Bias	Fit unc	bias unc	Bias	Fit unc	bias unc	Bias	Fit unc	bias unc
FP1_173_31	-1.88E-04	1.86E-04	5.43E-04	-2.44E-03	1.94E-04	5.46E-04	-4.54E-04	1.92E-04	5.45E-04	-1.12E-03	2.12E-04	5.52E-04	7.20E-05	2.06E-04	5.50E-04
FP1_173_32	4.89E-04		5.42E-04	-2.47E-03		5.46E-04	2.56E-04		5.45E-04	1.09E-04		5.52E-04	5.61E-04		5.50E-04
Phase 2 ^{149}Sm experiments															
FP2_174_HBC_05	2.57E-03	5.32E-04	7.37E-04	9.70E-04	5.27E-04	7.34E-04	1.52E-03	1.15E-04	5.22E-04	1.39E-03	1.28E-04	5.25E-04	1.79E-03	1.15E-04	5.22E-04
FP2_174_HBC_06	2.06E-03		7.37E-04	7.65E-04		7.34E-04	1.45E-03		5.23E-04	1.27E-03		5.26E-04	1.74E-03		5.23E-04
FP2_174_UO2_13	3.87E-03		7.37E-04	1.32E-03		7.34E-04	3.09E-03	3.96E-04	6.46E-04	8.80E-04	4.70E-04	6.94E-04	2.50E-03	3.95E-04	6.45E-04
FP2_174_UO2_14	3.95E-03		7.37E-04	1.45E-03		7.34E-04	3.25E-03		6.46E-04	7.72E-04		6.93E-04	2.74E-03		6.45E-04
FP2_174_UO2_15	2.25E-03		7.37E-04	6.41E-04		7.34E-04	1.81E-03		6.46E-04	6.84E-04		6.93E-04	6.29E-04		6.45E-04
FP2_174_UO2_16	2.80E-03		7.37E-04	1.19E-03		7.34E-04	2.47E-03		6.46E-04	7.52E-04		6.94E-04	1.45E-03		6.45E-04
FP2_174_UO2_17	1.12E-03		7.37E-04	-2.08E-05		7.34E-04	1.20E-03		6.46E-04	-5.47E-04		6.94E-04	4.38E-04		6.45E-04

Table 6.17 Samarium-152 bias evaluation

Phase 1 ^{152}Sm experiments															
Trending parameter	EALF (Δk_{eff})			Leakage fraction (Δk_{eff})			Mean free path (Δk_{eff})			Water level (Δk_{eff})			Fuel rod number (Δk_{eff})		
Experiment	Bias	Fit unc	bias unc	Bias	Fit unc	bias unc	Bias	Fit unc	bias unc	Bias	Fit unc	bias unc	Bias	Fit unc	bias unc
FP1_173_18	6.71E-04	1.86E-04	5.42E-04	-2.56E-03	1.94E-04	5.46E-04	2.09E-04	1.92E-04	5.45E-04	-2.61E-04	2.12E-04	5.52E-04	7.52E-04	2.06E-04	5.50E-04
FP1_173_19	4.41E-04		5.42E-04	-2.50E-03		5.46E-04	-6.60E-05		5.45E-04	-6.87E-04		5.52E-04	4.15E-04		5.50E-04
FP1_173_20	1.98E-04		5.42E-04	-2.54E-03		5.46E-04	-3.16E-04		5.45E-04	-1.06E-03		5.52E-04	1.71E-04		5.50E-04
FP1_173_21	7.26E-04		5.42E-04	-1.94E-03		5.46E-04	4.09E-04		5.45E-04	-1.40E-05		5.52E-04	8.40E-04		5.50E-04
FP1_173_22	6.03E-04		5.43E-04	-1.81E-03		5.46E-04	2.56E-04		5.45E-04	-3.41E-04		5.52E-04	2.92E-04		5.50E-04
Phase 2 ^{152}Sm experiments															
FP2_174_UO2_18	7.77E-04	5.32E-04	7.37E-04	8.72E-04	5.27E-04	7.33E-04	2.08E-03	3.96E-04	6.46E-04	9.12E-04	4.70E-04	6.93E-04	1.04E-03	3.95E-04	6.44E-04
FP2_174_UO2_19	7.09E-06		7.37E-04	1.33E-04		7.34E-04	1.44E-03		6.46E-04	-3.87E-04		6.93E-04	5.12E-04		6.45E-04

Table 6.18 Gadolinium-155 bias evaluation

Phase 1 ^{155}Gd experiments															
Trending parameter	EALF (Δk_{eff})			Leakage fraction (Δk_{eff})			Mean free path (Δk_{eff})			Water level (Δk_{eff})			Fuel rod number (Δk_{eff})		
Experiment	Bias	Fit unc	bias unc	Bias	Fit unc	bias unc	Bias	Fit unc	bias unc	Bias	Fit unc	bias unc	Bias	Fit unc	bias unc
FP1_173_23	6.65E-05	1.86E-04	5.43E-04	-2.77E-03	1.94E-04	5.46E-04	-2.23E-04	1.92E-04	5.45E-04	-4.98E-04	2.12E-04	5.52E-04	1.34E-04	2.06E-04	5.50E-04
FP1_173_24	-3.21E-04		5.42E-04	-2.82E-03		5.46E-04	-6.45E-04		5.45E-04	-1.10E-03		5.52E-04	6.90E-05		5.50E-04
FP1_173_25	-6.01E-04		5.42E-04	-2.88E-03		5.46E-04	-9.31E-04		5.45E-04	-1.53E-03		5.52E-04	-6.04E-04		5.50E-04
FP1_173_26	-4.69E-04		5.42E-04	-2.33E-03		5.46E-04	-6.49E-04		5.45E-04	-1.24E-03		5.52E-04	-3.44E-04		5.50E-04
FP1_173_27	-3.80E-04		5.42E-04	-2.43E-03		5.46E-04	-5.73E-04		5.45E-04	-1.03E-03		5.52E-04	-2.80E-04		5.50E-04
Phase 2 ^{155}Gd experiments															
FP2_174_HBC_03	2.22E-03	5.32E-04	7.37E-04	5.02E-04	5.27E-04	7.34E-04	1.05E-03	1.15E-04	5.22E-04	9.26E-04	1.28E-04	5.25E-04	1.32E-03	1.15E-04	5.22E-04
FP2_174_HBC_04	1.36E-03		7.37E-04	-7.84E-05		7.34E-04	6.26E-04		5.23E-04	4.66E-04		5.26E-04	9.17E-04		5.22E-04
FP2_174_UO2_20	3.91E-03		7.37E-04	9.19E-04		7.34E-04	2.77E-03	3.96E-04	6.46E-04	3.50E-04	4.70E-04	6.93E-04	2.30E-03	3.95E-04	6.45E-04
FP2_174_UO2_21	1.15E-03		7.37E-04	-7.56E-04		7.34E-04	5.19E-04		6.46E-04	-1.11E-03		6.93E-04	-4.54E-04		6.45E-04
FP2_174_UO2_22	1.07E-03		7.37E-04	-7.82E-04		7.34E-04	5.67E-04		6.46E-04	-1.34E-03		6.93E-04	-3.63E-04		6.45E-04

Table 6.19 Neodymium bias evaluation

Phase 1 Nd experiments															
Trending parameter	EALF (Δk_{eff})			Leakage fraction (Δk_{eff})			Mean free path (Δk_{eff})			Water level (Δk_{eff})			Fuel rod number (Δk_{eff})		
Experiment	Bias	Fit unc	bias unc	Bias	Fit unc	bias unc	Bias	Fit unc	bias unc	Bias	Fit unc	bias unc	Bias	Fit unc	bias unc
FP1_173_16	8.47E-04	1.86E-04	5.42E-04	-2.98E-03	1.94E-04	5.46E-04	6.19E-04	1.92E-04	5.45E-04	5.03E-04	2.12E-04	5.52E-04	8.78E-04	2.06E-04	5.50E-04
FP1_173_17	-2.29E-04		5.42E-04	-2.30E-03		5.46E-04	-4.09E-04		5.45E-04	-9.30E-04		5.52E-04	-6.60E-05		5.50E-04
Phase 2 Nd experiments															
FP2_174_UO2_11	1.44E-03	5.32E-04	7.37E-04	-7.34E-05	5.27E-04	7.34E-04	1.07E-03	3.96E-04	6.46E-04	-5.48E-04	4.70E-04	6.93E-04	2.70E-05	3.95E-04	6.45E-04
FP2_174_UO2_12	1.24E-03		7.37E-04	-3.13E-04		7.34E-04	8.29E-04		6.46E-04	-9.68E-04		6.93E-04	-1.74E-04		6.45E-04

The net bias and bias uncertainty results of the FP experiment evaluations are provided in Table 6.20 and Table 6.21 using the reported experimental uncertainties and the adjusted experimental uncertainties, respectively. The combined bias in the tables is the average of the individual FP experiment biases, and the bias uncertainty ("bias unc") is calculated from the pooled sample variance as shown in Eq. (6.4).

$$s_p^2 = \sum_{i=1}^{k} \frac{(N_i - 1)s_i^2}{N - k}, \tag{6.4}$$

where

N_i = number of samples within parameter space *i,*
s_i = mean standard deviation within parameter space *i,*
k = number of separate parameter spaces.

Table 6.20 FP experiment bias and bias uncertainty (Δk) (reported experimental uncertainty)

Trending parameter	EALF		Leakage fraction		Mean free path		Water level		Fuel rod number	
FP	Bias	bias unc	Bias	bias unc	Bias	bias unc	Bias	bias unc	Bias	bias unc
^{103}Rh	-4.40E-04	6.80E-04	-2.79E-03	6.80E-04	-1.02E-03	5.90E-04	-1.97E-03	6.20E-04	-1.24E-03	6.00E-04
^{133}Cs	7.40E-04	6.10E-04	-1.80E-03	6.10E-04	5.20E-04	5.80E-04	-1.60E-04	6.00E-04	3.30E-04	5.80E-04
^{149}Sm	2.10E-03	7.10E-04	1.60E-04	7.10E-04	1.62E-03	6.10E-04	4.70E-04	6.50E-04	1.33E-03	6.10E-04
^{152}Sm	4.90E-04	5.90E-04	-1.48E-03	5.90E-04	5.70E-04	5.70E-04	-2.60E-04	5.80E-04	5.70E-04	5.70E-04
^{155}Gd	8.00E-04	6.50E-04	-8.30E-04	6.50E-04	6.70E-04	5.70E-04	-3.30E-04	5.90E-04	5.60E-04	5.70E-04
^{nat}Nd	8.20E-04	6.50E-04	-1.42E-03	6.50E-04	5.30E-04	6.00E-04	-4.90E-04	6.30E-04	1.70E-04	6.00E-04

Table 6.21 FP experiment bias and bias uncertainty (Δk) (adjusted experimental uncertainty)

Trending parameter	EALF		Leakage fraction		Mean free path		Water level		Fuel rod number	
FP	Bias	bias unc	Bias	bias unc	Bias	bias unc	Bias	bias unc	Bias	bias unc
^{103}Rh	-4.40E-04	2.05E-03	-2.79E-03	2.05E-03	-1.02E-03	2.03E-03	-1.97E-03	2.03E-03	-1.24E-03	2.03E-03
^{133}Cs	7.40E-04	2.03E-03	-1.80E-03	2.03E-03	5.20E-04	2.02E-03	-1.60E-04	2.03E-03	3.30E-04	2.02E-03
^{149}Sm	2.10E-03	2.06E-03	1.60E-04	2.06E-03	1.62E-03	2.03E-03	4.70E-04	2.04E-03	1.33E-03	2.03E-03
^{152}Sm	4.90E-04	2.02E-03	-1.48E-03	2.02E-03	5.70E-04	2.02E-03	-2.60E-04	2.02E-03	5.70E-04	2.02E-03
^{155}Gd	8.00E-04	2.04E-03	-8.30E-04	2.04E-03	6.70E-04	2.02E-03	-3.30E-04	2.03E-03	5.60E-04	2.02E-03
^{nat}Nd	8.20E-04	2.04E-03	-1.42E-03	2.04E-03	5.30E-04	2.03E-03	-4.90E-04	2.04E-03	1.70E-04	2.03E-03

The FP bias uncertainty varies from 5.7×10^{-4} to 7.1×10^{-4} when the reported uncertainty values are used, and tends to show that some of the biases are considerably larger than expected (i.e., more than 2σ away from 0), as shown in Figure 6.17. When the adjusted uncertainty values are used in the analysis, the bias uncertainty varies from 2.02×10^{-3} to 2.06×10^{-3}. It is consistent with or exceeds the calculated experimental bias in all instances except the biases determined based on leakage fraction, as shown in Figure 6.18. As can be seen, the bias fluctuates with trending parameter, but the uncertainty remains about the same. The large fluctuations in bias may be an artifact of experimental uncertainties and/or recommended modeling simplifications that have not been sufficiently quantified. Considering that the uncertainty associated with the FP experiments is considered to be about 2.0×10^{-3}, the bias is consistent with or smaller than the uncertainty estimate, as shown in Figure 6.18.

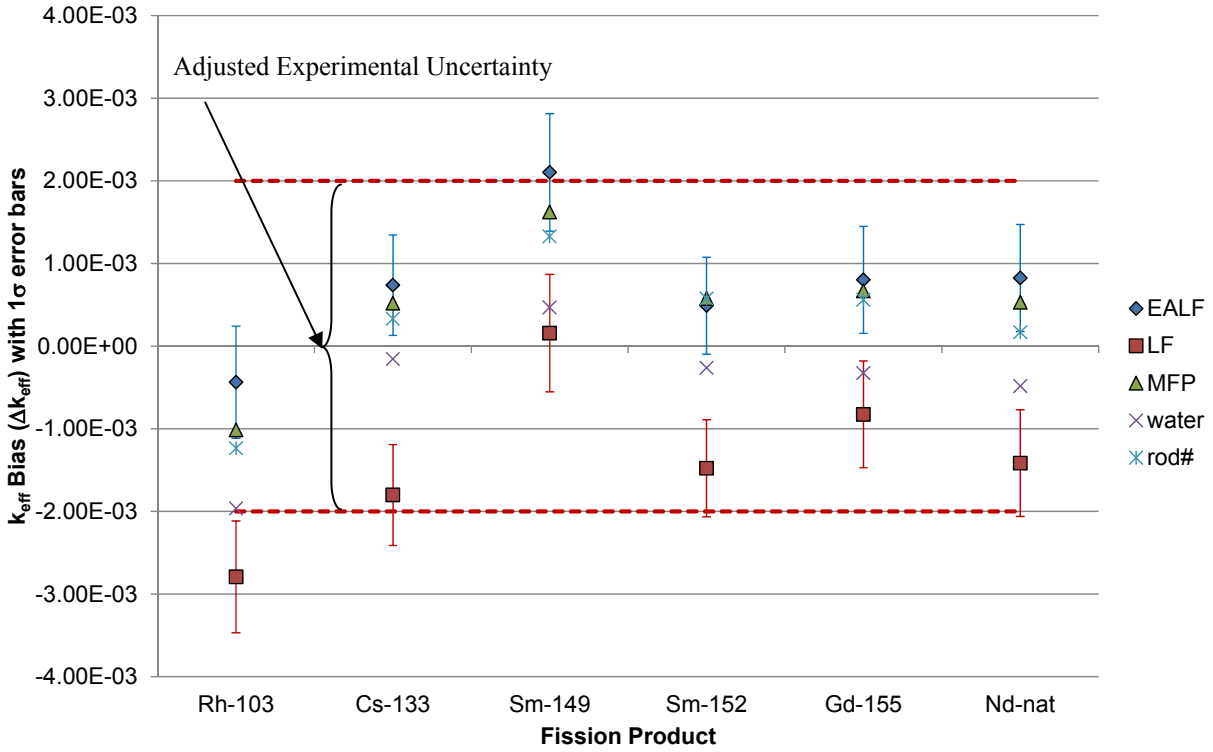

Figure 6.17 Net FP bias and uncertainty using reported experimental uncertainty.

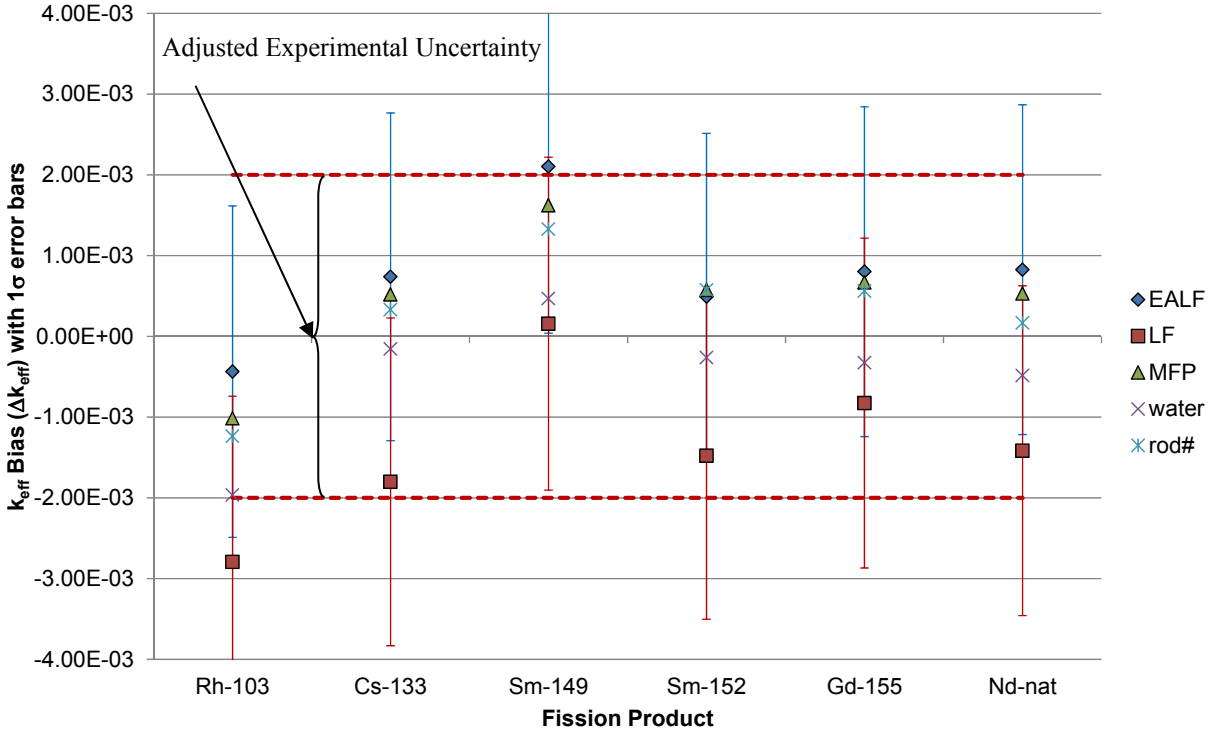

Figure 6.18 Net FP bias and uncertainty using adjusted experimental uncertainty.

6.4.2 Application of Fission Product Bias and Bias Uncertainty

As discussed in Section 3.2.7, the FP LCEs do not support bias calculations with typical trending analysis techniques because the same materials are not present in both the experiments and the application. A bias calculated for a FP using experiments that include only that FP, or include it in a system that is different than the application, may not be correct. Differences in neutron energy spectrum, as well as the presence of other FPs and other materials, may significantly affect the bias associated with the FP of interest.

The bias and uncertainty is typically calculated using a single-sided lower tolerance limit established so that there is 95% confidence that at least 95% of the population of critical experiment k_{eff} values are above the limit. One possible method of accounting for the FPs in the application model would be to add the individual FP biases to the computational bias developed using the non-FP experiments when the bias is negative. However, because the bias and bias uncertainty is developed on a 95% probability/95% confidence interval, the individual FP allowance factors (Δk_x from Section 3) would need to be similarly developed. This would result in very high penalties as a result of the low FP critical experiment sample sizes, requiring high tolerance factors to provide biases at the 95% probability/95% confidence interval. This method treats each FP bias independently, which is not the case in the application models. An alternative means of incorporating the FP biases into the application model is to adjust the individual FP biases by their respective k_{eff} sensitivities, as illustrated in Eq. (6.5). Using sensitivity data is more appropriate than using worth because some experiments could be saturated with the FP material and provide nonconservative adjustments. The sensitivities can be developed based on direct perturbation calculations or with the SCALE code system.

$$\boldsymbol{\beta_{FP}} = \sum_i \frac{S_i^{app}}{S_i^{exp}} \times \boldsymbol{\beta_i}, \tag{6.5}$$

where

β_{FP} = total FP bias for the application,
i = individual FP for which critical experiment data exist,
S_i^{app} = sensitivity of FP isotope (i) in application model,
S_i^{exp} = sensitivity of FP isotope (i) in critical experiment,
β_i = individual FP isotope bias taken as difference between calculated value and expected value.

Sensitivity-adjusted PWR SFP application model bias and bias uncertainty terms are provided in Table 6.22 through Table 6.26 for the different trend parameter biases at burnups of 10, 25, 40, and 57 GWd/MTU. The uncertainties ("unc") were developed using the FP experiment uncertainty value of 2.00×10^{-3}. Note that the FP experiments for neodymium were for the natural element. The total ^{nat}Nd sensitivity comprises several Nd isotopes, including ^{143}Nd and ^{145}Nd. Adjusting the ^{nat}Nd bias by the individual isotope sensitivities approximates the ^{143}Nd and ^{145}Nd isotope bias in the application model. However, because the ^{nat}Nd bias is within the experimental uncertainty estimate, it is expected that the individual isotope biases are, as well.

The combined results are illustrated in Figure 6.19 and compared against the combined FP nuclear data uncertainty developed from the cross-section covariance matrices. As can be seen, the bias fluctuates with trending parameter, but the uncertainty remains about the same for each burnup. Because of the large uncertainty component (compared with the bias value), the results do not definitively support or refute the use of nuclear data uncertainty to bound the FP bias. The results do show, however, that the bias values are generally of the same order of magnitude and that the bias values calculated with the experimental data are subsumed within

the nuclear data uncertainty band, hence supporting the premise that nuclear data uncertainty can be used to bound the bias for unvalidated nuclides. Use of additional critical experiment data with FPs may significantly reduce the bias uncertainty and thus provide more useful bias and bias uncertainty estimates from which to draw definitive conclusions.

Table 6.22 PWR SFP application model sensitivity-adjusted FP bias (EALF) and uncertainty (Δk)

Burnup (GWd/MTU)	10		25		40		57	
FP	β_{FP}	unc	β_{FP}	unc	β_{FP}	unc	β_{FP}	unc
^{103}Rh	−2.0E-05	1.6E-04	−5.0E-05	4.5E-04	−6.0E-05	6.4E-04	−8.0E-05	7.6E-04
^{133}Cs	5.0E-05	1.9E-04	1.1E-04	4.4E-04	1.5E-04	6.1E-04	1.8E-04	7.3E-04
^{149}Sm	6.6E-04	7.7E-04	7.5E-04	8.7E-04	8.4E-04	9.8E-04	8.5E-04	9.9E-04
^{152}Sm	3.0E-05	1.3E-04	7.0E-05	3.0E-04	9.0E-05	3.9E-04	1.0E-04	4.3E-04
^{155}Gd	0.0E+00	0.0E+00	0.0E+00	1.0E-05	0.0E+00	1.0E-05	0.0E+00	2.0E-05
^{143}Nd	2.6E-04	6.5E-04	5.7E-04	1.4E-03	7.6E-04	1.9E-03	8.9E-04	2.2E-03
^{145}Nd	2.8E-04	8.0E-04	6.2E-04	1.8E-03	8.8E-04	2.6E-03	1.1E-03	3.1E-03
Total	1.3E-03	1.3E-03	2.1E-03	2.6E-03	2.7E-03	3.5E-03	3.0E-03	4.1E-03

Table 6.23 PWR SFP application model sensitivity-adjusted FP bias (leakage fraction) and uncertainty (Δk)

Burnup (GWd/MTU)	10		25		40		57	
FP	β_{FP}	unc	β_{FP}	unc	β_{FP}	unc	β_{FP}	unc
^{103}Rh	−2.1E-04	1.6E-04	−5.8E-04	4.5E-04	−8.2E-04	6.4E-04	−9.7E-04	7.6E-04
^{133}Cs	−2.0E-04	1.9E-04	−4.6E-04	4.4E-04	−6.5E-04	6.1E-04	−7.7E-04	7.3E-04
^{149}Sm	−1.1E-04	7.7E-04	−1.2E-04	8.7E-04	−1.4E-04	9.8E-04	−1.4E-04	9.9E-04
^{152}Sm	−1.1E-04	1.3E-04	−2.4E-04	3.0E-04	−3.1E-04	3.9E-04	−3.5E-04	4.3E-04
^{155}Gd	0.0E+00	0.0E+00	0.0E+00	1.0E-05	−1.0E-05	1.0E-05	−1.0E-05	2.0E-05
^{143}Nd	−4.7E-04	6.5E-04	−1.0E-03	1.4E-03	−1.4E-03	1.9E-03	−1.6E-03	2.2E-03
^{145}Nd	−6.7E-04	8.0E-04	−1.5E-03	1.8E-03	−2.1E-03	2.6E-03	−2.6E-03	3.1E-03
Total	−1.8E-03	1.3E-03	−4.0E-03	2.6E-03	−5.5E-03	3.5E-03	−6.5E-03	4.1E-03

Table 6.24 PWR SFP application model sensitivity-adjusted FP bias (mean free path) and uncertainty (Δk)

Burnup (GWd/MTU)	10		25		40		57	
FP	β_{FP}	unc	β_{FP}	unc	β_{FP}	unc	β_{FP}	unc
^{103}Rh	−5.0E-05	1.6E-04	−1.5E-04	4.6E-04	−2.2E-04	6.5E-04	−2.6E-04	7.7E-04
^{133}Cs	3.0E-05	1.9E-04	7.0E-05	4.3E-04	9.0E-05	6.1E-04	1.1E-04	7.3E-04
^{149}Sm	5.0E-04	7.7E-04	5.6E-04	8.7E-04	6.3E-04	9.8E-04	6.3E-04	9.9E-04
^{152}Sm	3.0E-05	1.3E-04	6.0E-05	3.0E-04	8.0E-05	3.9E-04	9.0E-05	4.3E-04
^{155}Gd	0.0E+00	0.0E+00	0.0E+00	1.0E-05	0.0E+00	1.0E-05	0.0E+00	2.0E-05
^{143}Nd	1.7E-04	6.4E-04	3.6E-04	1.4E-03	4.9E-04	1.9E-03	5.7E-04	2.2E-03
^{145}Nd	1.7E-04	8.0E-04	3.8E-04	1.8E-03	5.5E-04	2.6E-03	6.6E-04	3.1E-03
Total	8.3E-04	1.3E-03	1.3E-03	2.6E-03	1.6E-03	3.5E-03	1.8E-03	4.1E-03

Table 6.25 PWR SFP application model sensitivity-adjusted FP bias (water height) and uncertainty (Δk)

Burnup (GWd/MTU)	10		25		40		57	
FP	β_{FP}	unc	β_{FP}	unc	β_{FP}	unc	β_{FP}	unc
^{103}Rh	−1.1E-04	1.6E-04	−3.1E-04	4.6E-04	−4.4E-04	6.5E-04	−5.2E-04	7.7E-04
^{133}Cs	−2.0E-05	1.9E-04	−4.0E-05	4.4E-04	−5.0E-05	6.1E-04	−6.0E-05	7.3E-04
^{149}Sm	1.3E-04	7.7E-04	1.5E-04	8.7E-04	1.7E-04	9.8E-04	1.7E-04	9.9E-04
^{152}Sm	−2.0E-05	1.3E-04	−4.0E-05	3.0E-04	−6.0E-05	3.9E-04	−6.0E-05	4.3E-04
^{155}Gd	0.0E+00	0.0E+00	0.0E+00	1.0E-05	0.0E+00	1.0E-05	−1.0E-05	2.0E-05
^{143}Nd	−1.4E-04	6.5E-04	−3.1E-04	1.4E-03	−4.2E-04	1.9E-03	−4.9E-04	2.2E-03
^{145}Nd	−1.5E-04	8.0E-04	−3.4E-04	1.8E-03	−4.8E-04	2.6E-03	−5.9E-04	3.1E-03
Total	−3.1E-04	1.3E-03	−9.0E-04	2.6E-03	−1.3E-03	3.5E-03	−1.6E-03	4.1E-03

Table 6.26 PWR SFP application model sensitivity-adjusted FP bias (fuel rods) and uncertainty (Δk)

Burnup (GWd/MTU)	10		25		40		57	
FP	β_{FP}	unc	β_{FP}	unc	β_{FP}	unc	β_{FP}	unc
^{103}Rh	−6.0E-05	1.6E-04	−1.7E-04	4.6E-04	−2.4E-04	6.5E-04	−2.8E-04	7.7E-04
^{133}Cs	3.0E-05	1.9E-04	6.0E-05	4.3E-04	8.0E-05	6.1E-04	1.0E-04	7.3E-04
^{149}Sm	4.3E-04	7.7E-04	4.8E-04	8.7E-04	5.4E-04	9.8E-04	5.5E-04	9.9E-04
^{152}Sm	4.0E-05	1.3E-04	8.0E-05	3.0E-04	1.0E-04	3.9E-04	1.1E-04	4.3E-04
^{155}Gd	0.0E+00	0.0E+00	0.0E+00	1.0E-05	0.0E+00	1.0E-05	0.0E+00	2.0E-05
^{143}Nd	6.0E-05	6.4E-04	1.4E-04	1.4E-03	1.8E-04	1.9E-03	2.1E-04	2.2E-03
^{145}Nd	9.0E-05	8.0E-04	2.1E-04	1.8E-03	3.0E-04	2.6E-03	3.6E-04	3.1E-03
Total	5.8E-04	1.3E-03	7.9E-04	2.6E-03	9.7E-04	3.5E-03	1.1E-03	4.1E-03

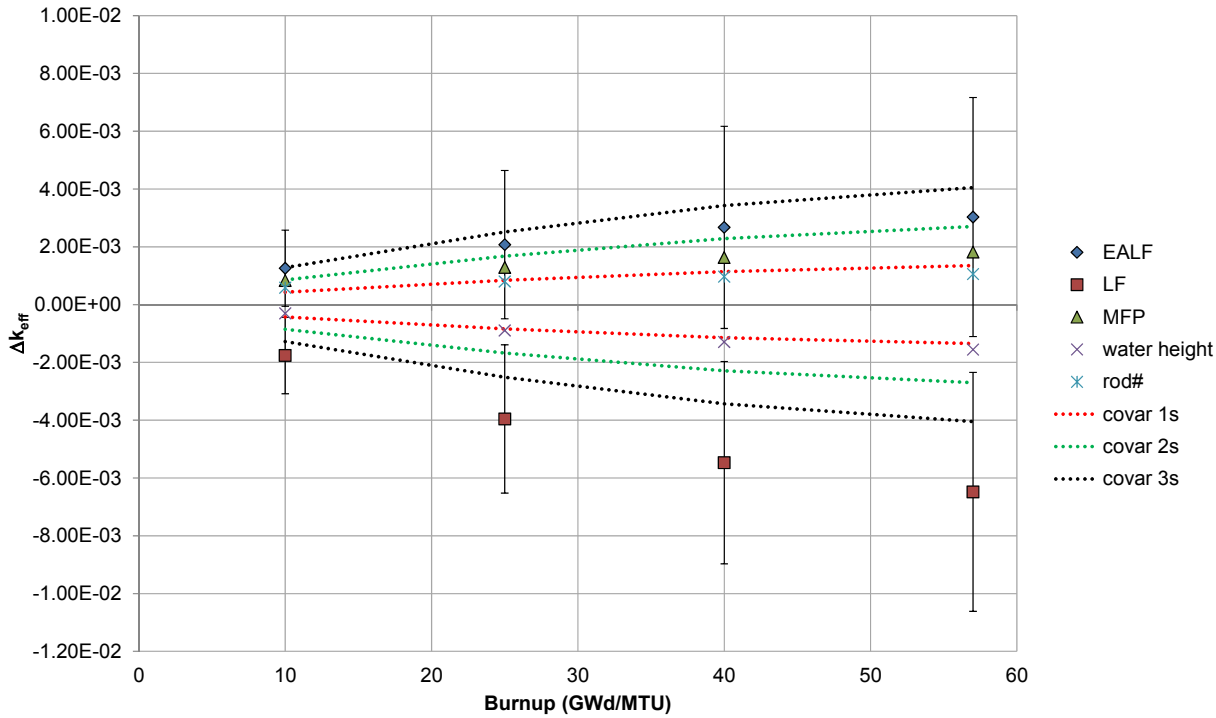

Figure 6.19 FP bias and uncertainty comparison against cross-section covariance as a function of burnup for PWR SFP application model.

6.5 CONCLUSIONS ON CALCULATION OF BIAS AND BIAS UNCERTAINTY

The calculated bias and bias uncertainty values presented in Sections 6.1 and 6.2.2 can vary significantly with burnup, the parameter used in the trending analysis, and the set of critical experiments used. The temptation exists to adopt the most conservative estimate for the bias and bias uncertainty. However, one needs to keep in mind that, provided that the statistical method bases and assumptions are met and an acceptable set of applicable critical experiments is used, each estimate is valid. The dominant factor in the bias and bias uncertainty is the critical experiment population variance. The spread of the critical experiment results is due to the inability to accurately describe critical experiments and is not related to the ability to calculate k_{eff}. Consequently, use of any validly determined bias and 95/95 bias uncertainty that includes the population variance and consideration of k_{eff} trends in the critical experiments results should be acceptable.

Table 6.27 provides a summary of the most restrictive combined bias and bias uncertainty results for the various application models that would be appropriate for validation of the actinide-only nuclides in the application models. These values represent the combined β and Δk_β terms in Eq. (3.1) in Section 3.

Table 6.27 Summary bias and uncertainty results for actinide-only validation

BUC type	Final BU (GWd/MTU)	Normality assumed		Nonparametric	
		w/HTC	wo/HTC	w/HTC	wo/HTC
Values calculated based on traditional LCE selection					
PWR SFP	10	−0.0163	−0.0192	−0.0306	−0.0306
PWR SFP	40	−0.0162	−0.0191	−0.0306	−0.0306
PWR cask	10	−0.0163	−0.0192	−0.0306	−0.0306
PWR cask	40	−0.0162	−0.0191	−0.0306	−0.0306
BWR SFP	11	−0.0163	−0.0192	−0.0306	−0.0306
Values calculated using S/U-based LCE selection					
PWR SFP	10	−0.0168		N/A	
PWR SFP	40	−0.0121		−0.0199	
PWR cask	10	−0.0115		N/A	
PWR cask	40	−0.0155		−0.0306	

N/A – not applicable because data set was normally distributed

The methodology presented in Section 3.2.5 was used to generate the results presented in Section 6.3 for the BUC application models. The minor actinide and FP results are provided in Table 6.28. The combined actinide, minor actinide, and FP bias and bias uncertainty values are presented in Table 6.29.

Table 6.28 Uncertainty in k_{eff} due to minor actinide and fission product nuclear data uncertainties

BUC type	Final BU (GWd/MTU)	Uncertainty
PWR SFP	10	0.00023
PWR SFP	40	0.00059
PWR cask	10	0.00025
PWR cask	40	0.00065
BWR SFP	11	0.00027

Table 6.29 Summary bias and uncertainty results for actinide and fission product BUC validation

BUC type	Final BU (GWd/MTU)	Normality assumed		Nonparametric	
		w/HTC	wo/HTC	w/HTC	wo/HTC
Values calculated based on traditional LCE selection					
PWR SFP	10	−0.0166	−0.0195	−0.0309	−0.0309
PWR SFP	40	−0.0169	−0.0198	−0.0313	−0.0313
PWR cask	10	−0.0166	−0.0195	−0.0309	−0.0309
PWR cask	40	−0.0169	−0.0198	−0.0313	−0.0313
BWR SFP	11	−0.0166	−0.0195	−0.0309	−0.0309
Values calculated based on S/U-based LCE selection					
PWR SFP	10	−0.0171		N/A	
PWR SFP	40	−0.0128		−0.0206	
PWR cask	10	−0.0118		N/A	
PWR cask	40	−0.0162		−0.0313	

N/A – not applicable because data set was normally distributed

7. BIAS AND BIAS UNCERTAINTY SENSITIVITY STUDY

7.1 PARAMETRIC EVALUATION

A parametric evaluation was conducted to determine if criticality code bias and bias uncertainty have any sensitivity to fuel design, SFP rack design, burnup, or other parameters important to criticality analyses. This section provides a parametric evaluation of SFP application model differences and the impacts on the calculated biases and uncertainties for a relatively wide range of variations that may be seen in SFP criticality safety analyses. The sensitivity of bias and bias uncertainty in k_{eff} was evaluated as a function of burnup for the following parameters important to criticality safety analyses: fuel assembly design, rack design, soluble boron concentration, fuel cooling time, axial representation of fuel burnup, and neutron cross-section data. These parameters were selected because they cover a broad range in neutron spectrum effects and geometric variations.

7.2 REFERENCE MODEL PARAMETERS

The base case SFP application model for the sensitivity studies is described in Section 4.1. The SNF compositions for assembly average burnups of 10, 25, 40, and 57 GWd/MTU were generated based on BUC with the SNF composition consisting of actinides and 16 FPs as listed in Section 4. Details of the parametric variation models are provided in the next section.

7.3 PARAMETRIC APPLICATIONS

Model parameters relevant to criticality analyses include fuel assembly design, rack design, SFP soluble boron concentration, fuel cooling time, axial representation of fuel burnup, and neutron cross-section data. The parametric variations considered in the sensitivity analysis are summarized in Table 7.1.

Table 7.1 Parameters selected for sensitivity analyses

Parameter	Reference value	Sensitivity analysis value
Assembly type	W 17×17 OFA	B&W 15×15 depleted with burnable absorbers (BAs), W 17×17 depleted with no BAs
Cell pitch size	9.110 in.	Reference value + 0.5 in.
^{10}B loading of Boral® panels	0.020 g/cm^2	0.022 g/cm^2 (10% increase from the reference value) 0.018 g/cm^2 (10% decrease from the reference value) 0 g/cm^2 (unpoisoned)
Soluble boron concentration	0 ppm	1000 ppm 303 ppm (10 GWd/MTU assembly burnup) 348 ppm (25 GWd/MTU assembly burnup) 393 ppm (40 GWd/MTU assembly burnup) 424 ppm (57 GWd/MTU assembly burnup)
Cooling time	3 days	0 days 1 year 5 years 20 years 40 years
Burnup axial representation	18-zone axial profile	Axially uniform burnup
Cross-section data library	ENDF/B-VII, 238 energy groups	ENDF/B-V, and ENDF/B-VI, 238 energy groups

The ENDF/B-V and ENDF/B-VI PWR application models were developed from the ENDF/B-VII cases. Nuclide compositions were omitted or modified from the original ENDF/B-VII files to be consistent with the different libraries. Only cases with burnups of 10 and 40 GWd/MTU were evaluated for comparative purposes against the ENDF/B-VII results. For actual safety analyses, application model bias and bias uncertainty should be developed using the same cross-section libraries as used in the critical benchmark evaluations.

For the 1000 ppm soluble boron concentration cases, the base case (i.e., 0 ppm boron) was modified to include 1000 ppm of boron, hence resulting in k_{eff} values much lower than 0.99. The end-of-life (EOL) fuel composition values should have been identical to those in the base case, but the 1000 ppm sensitivity cases were generated using the STARBUCS automation sequence with a more recent set of ORIGEN-ARP libraries, which resulted in minor variations in the SNF isotopic compositions. The observed variations are considered to have a negligible impact on the calculated bias and bias uncertainties (Figure 7.3, shown later in this section, confirms this). The same phenomenon and conclusion also apply to the soluble boron search cases that result in a system k_{eff} of 0.94.

Table 7.2 shows some key parameters for the different application models consistent with the results presented in Section 6. Calculated k_{eff} values are shown because at higher burnup, some of the variations do not result in a system k_{eff} of 0.99 without initial enrichments in excess of 6.0 wt % ^{235}U. For the purposes of this study, a cap of 5.99 wt % ^{235}U and an assembly average burnup of 57 GWd/MTU are used. The cap values represent the upper burnup and enrichment values for the base case application model to produce a k_{eff} value of 0.99. The k_{eff} values, EALF values, uranium enrichments, Pu/(U+Pu) ratios, and axially dependent fission densities were extracted from the CSAS5 calculations. As described in Section 3.1, SCALE TSUNAMI-3D calculations were used to generate SDFs for each application model, and TSUNAMI-IP was used to evaluate the neutronic similarity of the critical experiments with the application models.

Table 7.2 Sensitivity case key parameters

Description	Change from base	Initial enrichment (wt % ^{235}U)	Final BU (GWd/MTU)	k_{eff}/σ	EALF (eV)	Simple average		Fission density weighted average	
						Final enrichment (wt % ^{235}U)	Pu/(Pu+U) (wt %)	Final enrichment (wt % ^{235}U)	Pu/(Pu+U) (wt %)
Base case	--	2.500	10	0.99010 / 0.000072	0.199	1.650	0.567	1.840	0.447
		3.578	25	0.98989 / 0.000073	0.241	1.636	0.987	1.977	0.829
		4.740	40	0.99012 / 0.000071	0.277	1.701	1.301	2.179	1.114
		5.990	57	0.99002 / 0.000078	0.309	1.685	1.607	2.496	1.330
Assembly design	B&W 15×15	2.413	10	0.98998 / 0.000065	0.265	1.575	0.563	1.739	0.455
		3.502	25	0.99011 / 0.000082	0.330	1.584	0.994	1.890	0.846
		4.701	40	0.98995 / 0.000069	0.386	1.678	1.309	2.123	1.131
		5.962	57	0.98999 / 0.000064	0.438	1.706	1.611	2.468	1.344
	W 17×17 (no BAs)	2.614	10	0.99005 / 0.000069	0.192	1.703	0.477	1.938	0.356
		3.765	25	0.99002 / 0.000075	0.233	1.689	0.874	2.104	0.706
		4.975	40	0.99001 / 0.000069	0.266	1.746	1.161	2.321	0.969
		5.990	57	0.97746 / 0.000074	0.292	1.545	1.437	2.461	1.164
Rack design	Unpoisoned panels	1.356	10	0.99017 / 0.000053	0.160	0.721	0.620	0.814	0.532
		1.974	25	0.98988 / 0.000057	0.184	0.598	1.011	0.787	0.872
		2.719	40	0.98987 / 0.000061	0.203	0.565	1.298	0.816	1.137
		3.524	57	0.99019 / 0.000056	0.216	0.520	1.552	0.926	1.319
	Cell pitch increased 0.5 in.	2.723	10	0.99002 / 0.000079	0.178	1.844	0.548	2.044	0.430
		3.915	25	0.99004 / 0.000082	0.217	1.896	0.975	2.247	0.819
		5.177	40	0.99017 / 0.000068	0.249	2.008	1.291	2.511	1.106
		5.990	57	0.97031 / 0.000073	0.268	1.724	1.588	2.528	1.315
	Poison panel ^{10}B loading increased 10%	2.536	10	0.98994 / 0.000069	0.200	1.681	0.565	1.874	0.445
		3.628	25	0.98992 / 0.000075	0.243	1.674	0.986	2.016	0.828
		4.808	40	0.99007 / 0.00007	0.280	1.747	1.300	2.230	1.113
		5.990	57	0.98646 / 0.000073	0.311	1.685	1.607	2.497	1.331

Table 7.2 Sensitivity case key parameters (continued)

Description	Change from base	Initial enrichment (wt % ^{235}U)	Final BU (GWd/MTU)	k_{eff}/σ	EALF (eV)	Simple average		Fission density weighted average	
						Final enrichment (wt % ^{235}U)	Pu/(Pu+U) (wt %)	Final enrichment (wt % ^{235}U)	Pu/(Pu+U) (wt %)
	Poison panel ^{10}B loading decreased 10%	2.460	10	0.99010 / 0.000068	0.197	1.615	0.569	1.804	0.449
		3.521	25	0.99011 / 0.000073	0.239	1.594	0.988	1.933	0.829
		4.668	40	0.99000 / 0.00007	0.274	1.652	1.301	2.127	1.114
		5.902	57	0.98997 / 0.000072	0.306	1.632	1.606	2.435	1.330
Decay time	0 d	2.487	10	0.99014 / 0.000068	0.197	1.638	0.549	1.817	0.439
		3.544	25	0.99002 / 0.000078	0.239	1.613	0.974	1.939	0.822
		4.690	40	0.99014 / 0.000078	0.273	1.669	1.284	2.137	1.102
		5.873	57	0.99002 / 0.000071	0.304	1.653	1.578	2.435	1.311
	1 year	2.540	10	0.98996 / 0.000071	0.200	1.684	0.560	1.887	0.434
		3.660	25	0.99002 / 0.000068	0.245	1.700	0.981	2.066	0.812
		4.858	40	0.98994 / 0.000066	0.282	1.783	1.291	2.295	1.095
		5.990	57	0.98612 / 0.000067	0.313	1.724	1.586	2.560	1.301
	5 year	2.570	10	0.98996 / 0.000068	0.200	1.710	0.552	1.930	0.419
		3.786	25	0.99018 / 0.000071	0.248	1.796	0.959	2.209	0.778
		5.088	40	0.99003 / 0.000066	0.290	1.945	1.260	2.524	1.052
		5.990	57	0.97132 / 0.000074	0.318	1.724	1.546	2.627	1.250
	20 year	2.623	10	0.98995 / 0.000064	0.200	1.756	0.533	2.002	0.394
		3.998	25	0.98997 / 0.000071	0.252	1.961	0.908	2.449	0.718
		5.491	40	0.98995 / 0.000073	0.302	2.237	1.186	2.928	0.972
		5.990	57	0.94386 / 0.000069	0.323	1.725	1.447	2.739	1.148
	40 year	2.642	10	0.98980 / 0.000075	0.200	1.774	0.523	2.033	0.383
		4.094	25	0.99001 / 0.000066	0.254	2.039	0.879	2.560	0.690
		5.670	40	0.98986 / 0.000071	0.307	2.373	1.143	3.105	0.932
		5.990	57	0.92800 / 0.000070	0.324	1.690	1.396	2.761	1.102

Table 7.2 Sensitivity case key parameters (continued)

Description	Change from base	Initial enrichment (wt % ^{235}U)	Final BU (GWd/MTU)	k_{eff}/σ	EALF (eV)	Simple average		Fission density weighted average	
						Final enrichment (wt % ^{235}U)	Pu/(Pu+U) (wt %)	Final enrichment (wt % ^{235}U)	Pu/(Pu+U) (wt %)
Soluble boron	1000 ppm	2.506	10	0.84285 / 0.00006	0.278	1.654	0.557	1.816	0.457
		3.565	25	0.86156 / 0.000065	0.328	1.628	0.982	1.952	0.830
		4.731	40	0.87443 / 0.000062	0.369	1.697	1.292	2.168	1.109
		5.916	57	0.88311 / 0.000074	0.406	1.680	1.587	2.471	1.316
Soluble boron ppm for k_{eff} = 0.94	303	2.506	10	0.93933 / 0.000084	0.221	1.655	0.558	1.833	0.445
	348	3.565	25	0.93933 / 0.000068	0.269	1.629	0.983	1.958	0.828
	393	4.731	40	0.93992 / 0.000069	0.311	1.697	1.293	2.167	1.107
	424	5.916	57	0.94022 / 0.000073	0.348	1.679	1.587	2.466	1.318
Cross-section library	ENDF/B-V	2.500	10	0.98409 / 0.000068	0.215	1.650	0.567	1.831	0.453
		4.740	40	0.98500 / 0.000073	0.300	1.701	1.301	2.159	1.112
	ENDF/B-VI	2.500	10	0.98700 / 0.000076	0.204	1.650	0.567	1.839	0.448
		4.740	40	0.98694 / 0.000070	0.285	1.701	1.301	2.173	1.117
Axial burnup	1 node	2.600	10	0.98997 / 0.00013	0.211	1.725	0.572	N/A[a]	N/A
		3.773	25	0.99000 / 0.00011	0.256	1.764	0.998	N/A	N/A
		5.084	40	0.99007 / 0.00012	0.293	1.909	1.311	N/A	N/A
		5.990	57	0.95282 / 0.00016	0.319	1.633	1.622	N/A	N/A

[a]N/A = not applicable.

7.4 SENSITIVITY ANALYSIS RESULTS AND DISCUSSION

A consideration in determining biases and bias uncertainties is that the true bias may change significantly as the neutronic characteristics of a system change. Consequently, trending analysis is performed to identify whether the bias is changing as other key parameters change. To facilitate the evaluation in a manner applicable to real-world applications, the parameter change evaluations are broken down as follows.

Section 7.4.1 provides an evaluation of bias and bias uncertainty when the critical benchmark experiments are selected via traditional methods as discussed in Section 3.2.2. Results are presented using key parameters—EALF, EOL fission density weighted ^{235}U enrichment, and EOL fission density weighted plutonium fraction for developing bias and bias uncertainty terms. The trending analyses were performed on the HTC LCEs and the IHECSBE as listed in Section 5 (excluding the LEU-MISC-THERM-005 cases) for a total of 462 experiments. The proprietary FP critical benchmark data were excluded because the majority of applicants will not have access to this data set and, as discussed in Section 6.4.2, traditional techniques do not appear adequate for applying individual FP biases and bias uncertainties to BUC applications.

Section 7.4.2 provides an evaluation using the SCALE S/U analysis tools for selecting critical benchmarks applicable to the various applications, consistent with the information in Section 6.2. All 609 experiments listed in Section 5 were evaluated for similarity. The S/U analysis tools enable a more robust methodology for determining critical benchmark applicability compared with traditional techniques, which are based on engineering judgment.

Section 7.4.3 evaluates the application model parameter differences for the SNF nuclides when applicable LCE data are not available. The impacts on k_{eff} uncertainties generated based on the 44-group cross-section covariance matrices using TSUNAMI-IP, as described in Section 6.3, are provided.

7.4.1 Conventional Bias and Bias Uncertainty Assessment Impacts

The k_{eff} results were examined for trends as a function of enrichment, plutonium content, and EALF. Single-parameter trending analyses were performed using the USLSTATS computer code distributed with SCALE.

Table 7.3 to Table 7.5 show the bias and bias uncertainty calculated for each application model variant. The bias value is the difference between the best-estimate linear fit (BELF) of the critical experiment data as a function of the independent variable at the value from the application model and k_{eff} = 1 (bias = $k_{BELF} - 1$). The bias uncertainty in the tables is the total uncertainty including the variance of the population and a tolerance factor used to create the 95% probability/95% confidence interval based on sample population. The bias uncertainty is the same for a given trending parameter for the different cases (with the exception of the different cross-section library sensitivity cases) because the experimental data used in the trending analysis are the same. The bias uncertainty varies slightly for the different trending parameters and among experiment sets because the linear fit to the data varies.

Table 7.3 Bias and uncertainty as a function of EALF

Description	Change from base	Bias/bias uncertainty (Δk)			
		Final burnup (GWd/MTU)			
		10	25	40	57
PWR SFP model					
Base case	--	-1.57E-03 / 1.46E-02	-1.50E-03 / 1.46E-02	-1.44E-03 / 1.46E-02	-1.38E-03 / 1.46E-02
Assembly design	B&W 15×15	-1.46E-03 / 1.46E-02	-1.35E-03 / 1.46E-02	-1.26E-03 / 1.46E-02	-1.17E-03 / 1.46E-02
	W 17×17 no BAs	-1.58E-03 / 1.46E-02	-1.51E-03 / 1.46E-02	-1.46E-03 / 1.46E-02	-1.41E-03 / 1.46E-02
Rack design	Unpoisoned panels	-1.63E-03 / 1.46E-02	-1.59E-03 / 1.46E-02	-1.56E-03 / 1.46E-02	-1.54E-03 / 1.46E-02
	Cell pitch increased 0.5 in.	-1.60E-03 / 1.46E-02	-1.54E-03 / 1.46E-02	-1.49E-03 / 1.46E-02	-1.45E-03 / 1.46E-02
	Poison panel B10 +10%	-1.57E-03 / 1.46E-02	-1.49E-03 / 1.46E-02	-1.43E-03 / 1.46E-02	-1.38E-03 / 1.46E-02
	Poison panel B10 –10%	-1.57E-03 / 1.46E-02	-1.50E-03 / 1.46E-02	-1.44E-03 / 1.46E-02	-1.39E-03 / 1.46E-02
Decay time	0 d	-1.57E-03 / 1.46E-02	-1.50E-03 / 1.46E-02	-1.45E-03 / 1.46E-02	-1.39E-03 / 1.46E-02
	1 year	-1.57E-03 / 1.46E-02	-1.49E-03 / 1.46E-02	-1.43E-03 / 1.46E-02	-1.38E-03 / 1.46E-02
	5 year	-1.57E-03 / 1.46E-02	-1.49E-03 / 1.46E-02	-1.42E-03 / 1.46E-02	-1.37E-03 / 1.46E-02
	20 year	-1.57E-03 / 1.46E-02	-1.48E-03 / 1.46E-02	-1.40E-03 / 1.46E-02	-1.36E-03 / 1.46E-02
	40 year	-1.57E-03 / 1.46E-02	-1.48E-03 / 1.46E-02	-1.39E-03 / 1.46E-02	-1.36E-03 / 1.46E-02
Soluble boron	1000 ppm[a]	-1.44E-03 / 1.46E-02	-1.35E-03 / 1.46E-02	-1.29E-03 / 1.46E-02	-1.22E-03 / 1.46E-02
	ppm for k_{eff} = 0.94	-1.53E-03 / 1.46E-02	-1.45E-03 / 1.46E-02	-1.38E-03 / 1.46E-02	-1.32E-03 / 1.46E-02
Cross-section library	ENDF-B/V	-3.16E-03 / 1.54E-02	--	-4.14E-03 / 1.54E-02	--
	ENDF-B/VI	-3.04E-03 / 1.53E-02	--	-3.96E-03 / 1.53E-02	--
Axial burnup	1 node	-1.55E-03 / 1.46E-02	-1.47E-03 / 1.46E-02	-1.41E-03 / 1.46E-02	-1.37E-03 / 1.46E-02

[a]Parts per million boron by mass.

Table 7.4 Bias and uncertainty as a function of final uranium enrichment

Description	Change from base	Bias/bias uncertainty (Δk)			
		Final burnup (GWd/MTU)			
		10	25	40	57
PWR SFP model					
Base case	--	-1.69E-03 / 1.47E-02	-1.68E-03 / 1.47E-02	-1.67E-03 / 1.47E-02	-1.65E-03 / 1.47E-02
Assembly design	B&W 15×15	-1.70E-03 / 1.47E-02	-1.69E-03 / 1.47E-02	-1.67E-03 / 1.47E-02	-1.65E-03 / 1.47E-02
	W 17×17 no BAs	-1.69E-03 / 1.47E-02	-1.68E-03 / 1.47E-02	-1.66E-03 / 1.47E-02	-1.65E-03 / 1.47E-02
Rack design	Unpoisoned panels	-1.75E-03 / 1.47E-02	-1.75E-03 / 1.47E-02	-1.75E-03 / 1.47E-02	-1.75E-03 / 1.47E-02
	Cell pitch increased 0.5 in.	-1.68E-03 / 1.47E-02	-1.67E-03 / 1.47E-02	-1.65E-03 / 1.47E-02	-1.65E-03 / 1.47E-02
	Poison panel B10 +10%	-1.69E-03 / 1.47E-02	-1.68E-03 / 1.47E-02	-1.67E-03 / 1.47E-02	-1.65E-03 / 1.47E-02
	Poison panel B10 -10%	-1.69E-03 / 1.47E-02	-1.69E-03 / 1.47E-02	-1.67E-03 / 1.47E-02	-1.66E-03 / 1.47E-02
Decay time	0 d	-1.69E-03 / 1.47E-02	-1.69E-03 / 1.47E-02	-1.67E-03 / 1.47E-02	-1.66E-03 / 1.47E-02
	1 year	-1.69E-03 / 1.47E-02	-1.68E-03 / 1.47E-02	-1.66E-03 / 1.47E-02	-1.65E-03 / 1.47E-02
	5 year	-1.69E-03 / 1.47E-02	-1.67E-03 / 1.47E-02	-1.65E-03 / 1.47E-02	-1.64E-03 / 1.47E-02
	20 year	-1.68E-03 / 1.47E-02	-1.66E-03 / 1.47E-02	-1.63E-03 / 1.47E-02	-1.64E-03 / 1.47E-02
	40 year	-1.68E-03 / 1.47E-02	-1.65E-03 / 1.47E-02	-1.62E-03 / 1.47E-02	-1.64E-03 / 1.47E-02
Soluble boron	1000 ppm[a]	-1.69E-03 / 1.47E-02	-1.68E-03 / 1.47E-02	-1.67E-03 / 1.47E-02	-1.65E-03 / 1.47E-02
	ppm for k_{eff} = 0.94	-1.69E-03 / 1.47E-02	-1.68E-03 / 1.47E-02	-1.67E-03 / 1.47E-02	-1.65E-03 / 1.47E-02
Cross-section library	ENDF-B/V	-2.82E-03 / 1.57E-02	--	-2.80E-03 / 1.57E-02	--
	ENDF-B/VI	-2.82E-03 / 1.55E-02	--	-2.80E-03 / 1.55E-02	--
Axial burnup	1 node	-1.70E-03 / 1.47E-02	-1.70E-03 / 1.47E-02	-1.69E-03 / 1.47E-02	-1.70E-03 / 1.47E-02

[a]Parts per million boron by mass.

Table 7.5 Bias and uncertainty as a function of final plutonium content

Description	Change from base	Bias/bias uncertainty (Δk)			
		Final burnup (GWd/MTU)			
		10	25	40	57
PWR SFP model					
Base case	--	-2.25E-03 / 1.43E-02	-2.20E-03 / 1.43E-02	-2.17E-03 / 1.43E-02	-2.15E-03 / 1.43E-02
Assembly design	B&W 15×15	-2.25E-03 / 1.43E-02	-2.20E-03 / 1.43E-02	-2.17E-03 / 1.43E-02	-2.15E-03 / 1.43E-02
	W 17×17 no BAs	-2.26E-03 / 1.43E-02	-2.22E-03 / 1.43E-02	-2.19E-03 / 1.43E-02	-2.17E-03 / 1.43E-02
Rack design	Unpoisoned panels	-2.24E-03 / 1.43E-02	-2.20E-03 / 1.43E-02	-2.17E-03 / 1.43E-02	-2.15E-03 / 1.43E-02
	Cell pitch increased 0.5 in.	-2.25E-03 / 1.43E-02	-2.21E-03 / 1.43E-02	-2.17E-03 / 1.43E-02	-2.15E-03 / 1.43E-02
	Poison panel B10 +10%	-2.25E-03 / 1.43E-02	-2.20E-03 / 1.43E-02	-2.17E-03 / 1.43E-02	-2.15E-03 / 1.43E-02
	Poison panel B10 -10%	-2.25E-03 / 1.43E-02	-2.20E-03 / 1.43E-02	-2.17E-03 / 1.43E-02	-2.15E-03 / 1.43E-02
Decay time	0 d	-2.25E-03 / 1.43E-02	-2.21E-03 / 1.43E-02	-2.17E-03 / 1.43E-02	-2.15E-03 / 1.43E-02
	1 year	-2.25E-03 / 1.43E-02	-2.21E-03 / 1.43E-02	-2.17E-03 / 1.43E-02	-2.15E-03 / 1.43E-02
	5 year	-2.25E-03 / 1.43E-02	-2.21E-03 / 1.43E-02	-2.18E-03 / 1.43E-02	-2.16E-03 / 1.43E-02
	20 year	-2.25E-03 / 1.43E-02	-2.22E-03 / 1.43E-02	-2.19E-03 / 1.43E-02	-2.17E-03 / 1.43E-02
	40 year	-2.26E-03 / 1.43E-02	-2.22E-03 / 1.43E-02	-2.19E-03 / 1.43E-02	-2.17E-03 / 1.43E-02
Soluble boron	1000 ppm[a]	-2.25E-03 / 1.43E-02	-2.20E-03 / 1.43E-02	-2.17E-03 / 1.43E-02	-2.15E-03 / 1.43E-02
	ppm for k_{eff} = 0.94	-2.25E-03 / 1.43E-02	-2.20E-03 / 1.43E-02	-2.17E-03 / 1.43E-02	-2.15E-03 / 1.43E-02
Cross-section library	ENDF-B/V	-2.51E-03 / 1.50E-02	--	-2.51E-03 / 1.50E-02	--
	ENDF-B/VI	-2.51E-03 / 1.50E-02	--	-2.51E-03 / 1.50E-02	--
Axial burnup	1 node	-2.23E-03 / 1.43E-02	-2.19E-03 / 1.43E-02	-2.15E-03 / 1.43E-02	-2.11E-03 / 1.43E-02

[a]Parts per million boron by mass.

As can be seen, using conventional trending analysis techniques, the bias and bias uncertainty as a function of the respective trending parameters produce similar values for the different parametric evaluations, with the largest differences coming from use of different cross-section libraries. The biases generated based on the final plutonium fraction trending parameter provide the most conservative bias and bias uncertainty values for all cases except the different cross-section libraries. The impacts of SNF system parameter changes on the burnup-dependent base case biases, calculated in terms of percent difference using the final plutonium fraction trending parameter, are illustrated in Figure 7.1 to Figure 7.4. Note that the base case bias uncertainty is a factor of ~7 greater than the base case bias and hence subsumes the changes in the base case bias due to the system parameter changes.

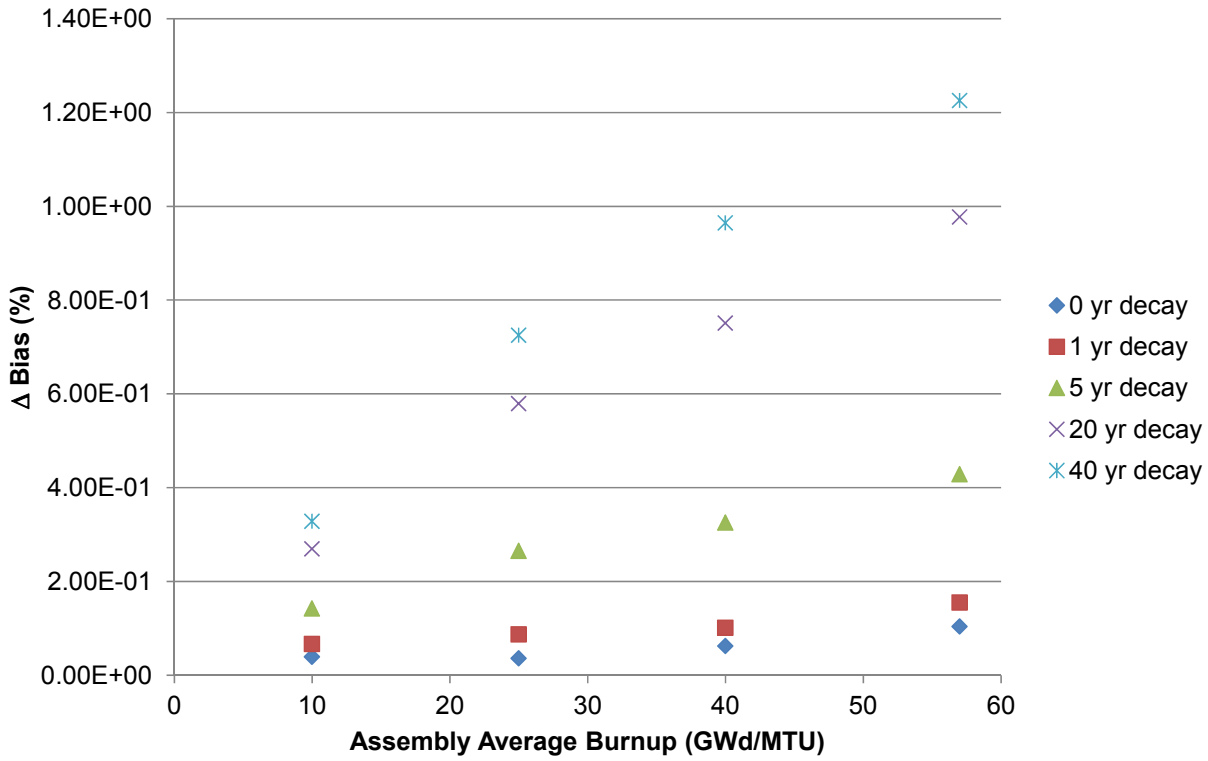

Figure 7.1 Percentage change in bias as a function of decay time.

The results in Figure 7.1 illustrate the effects on the bias of nuclide decay and buildup over a 40-year decay time for different burnups. The changes are greater at the higher burnups where the discharge plutonium fractions are higher. These results demonstrate that different decay times can have about a 1.2% effect on the calculated bias at high burnup. This effect is very small compared with the bias uncertainty values.

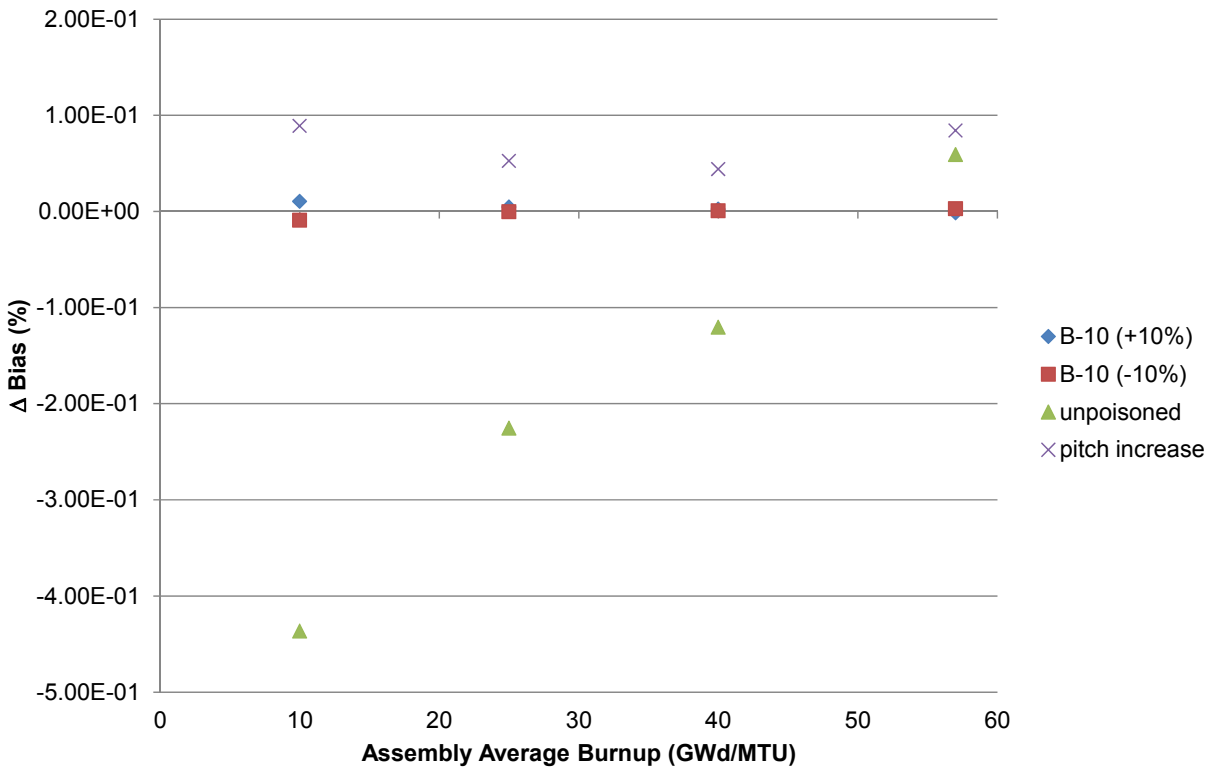

Figure 7.2 Percentage change in bias from rack design variations.

The results in Figure 7.2 illustrate the effects of variations in storage rack design and configuration. As can be seen, a rack design that does not rely on interstitial neutron absorbers for criticality control has increased reliance on BUC. Note the substantially lower initial enrichments in Table 7.2 needed to yield a target k_{eff} of 0.99. The changes are greater at the lower burnups in which the discharge SNF isotopic compositions have the greatest variation from the base case. As burnup increases, the ratio of net plutonium conversion/consumption decreases; therefore, the impact on the bias becomes less pronounced. Overall, these results indicate that variations in rack design have a small effect on the bias and that the impacts of the changes are very small compared with the base case bias uncertainty.

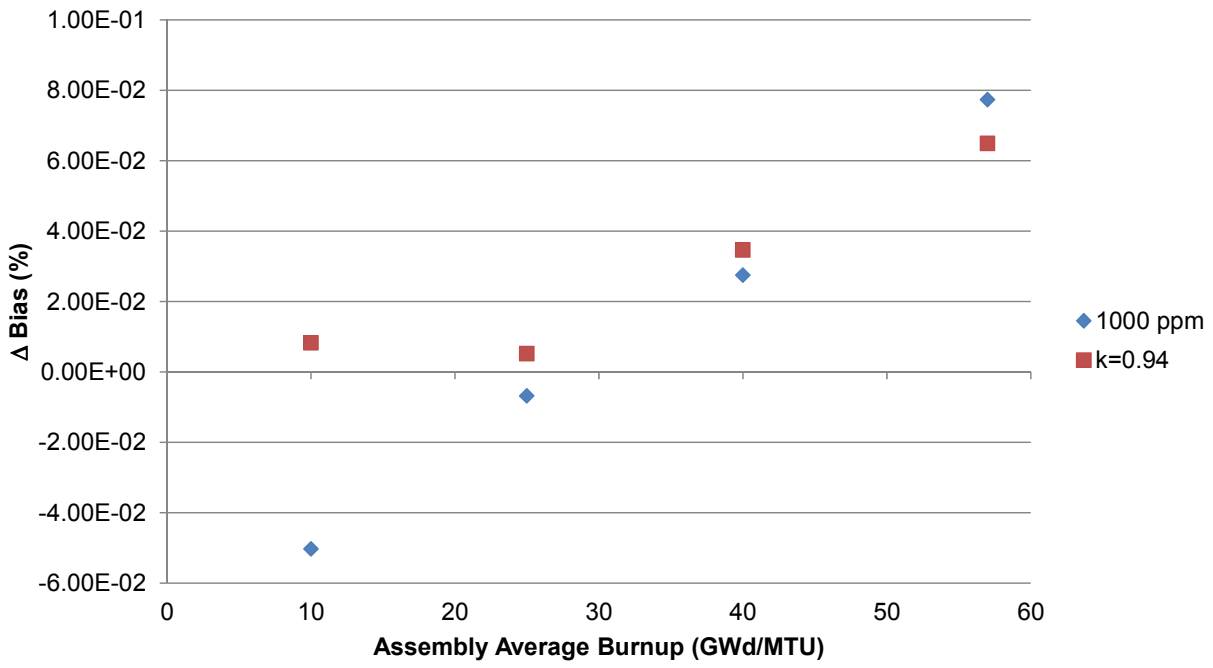

Figure 7.3 Percentage change in bias for different soluble boron concentrations.

The results in Figure 7.3 illustrate the effects of different soluble boron concentrations on the bias and bias uncertainty. As can be seen, the impact is negligible (<0.1%) and should actually be 0 because the boron concentration affects the neutron spectrum and would only have impacts on trending parameters that vary with neutron energy. The negligible differences observed are due to the minor variations in isotopic compositions introduced from the use of different ORIGEN-ARP libraries as indicated in Section 7.3.

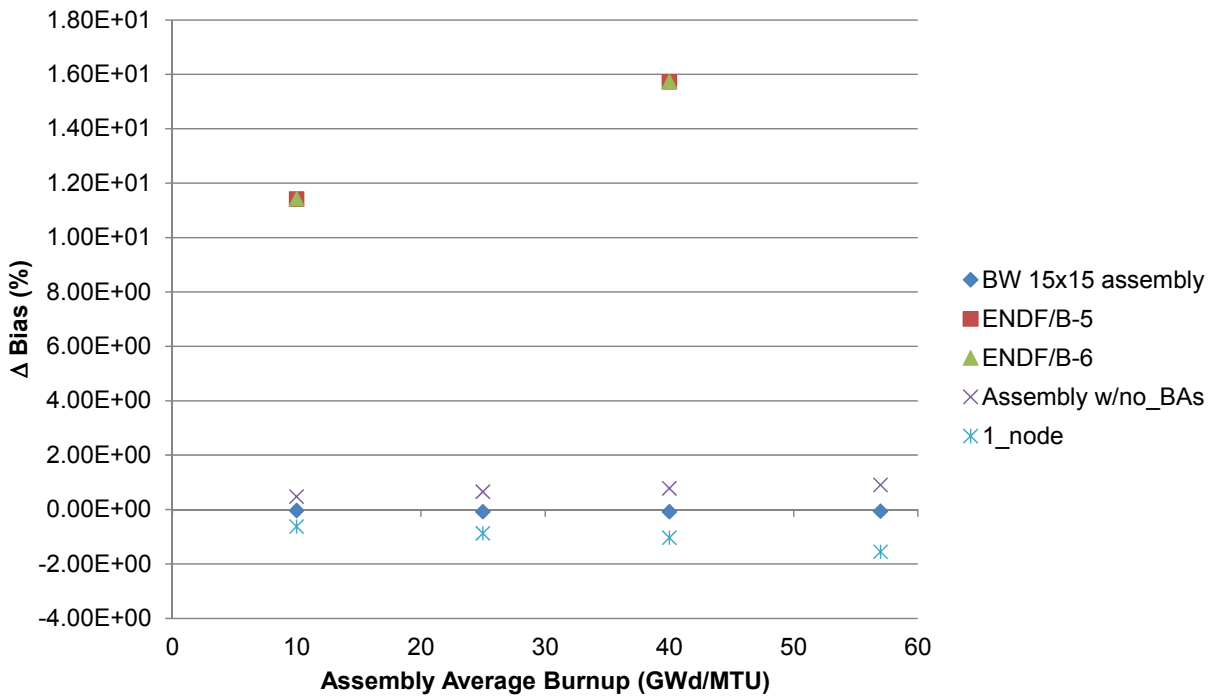

Figure 7.4 Percentage change in bias for assembly and cross-section library parameter variations.

The results in Figure 7.4 illustrate the effects on the bias of assembly design variations and cross-section library differences. As can be seen, the impact is small (~1%) for different assembly designs and slightly lower when a 1-node burnup profile is used but are ~11% to ~16% when different cross-section libraries are used. The change in bias is even greater for the different cross-section libraries when the EALF trending parameter is used. Historically, ENDF/B-V and -VI plutonium cross sections had a tendency to overpredict k_{eff} (slight positive bias), and U cross sections underpredicted k_{eff} (slight negative bias). Therefore, as the final plutonium fraction increases, the percentage change from the ENDF/B-VII cross-section libraries will increase.

7.4.2 Sensitivity and Uncertainty Based Benchmark Selection Bias and Bias Uncertainty Impacts

A weakness associated with single-parameter trending analysis is that the method assumes that the analyst has identified the most important trending parameter and that nothing is changing other than the parameter. In reality, the true bias varies as a function of many variables, some of which are not independent. As discussed in Section 3.2.4, the TSUNAMI-IP program was used to generate the c_k benchmark similarity metric. The similarity assessment results and bias and bias uncertainty based on c_k, EALF, final plutonium content, and final uranium content trending parameters for the PWR SFP parametric application models are presented in Table 7.6 to Table 7.9. Note that in the tables some cells are shaded. These particular application model variations were not within the range of applicability of the critical benchmark experiments and required extrapolation to calculate a bias and bias uncertainty. Typically, extrapolation is not recommended unless the source of the trend is thoroughly understood. Hence, these values are presented for comparative purposes only and would need to be evaluated more thoroughly as suggested in Appendix C of Ref. 3.

For the various parametric models, the number of similar experiments was fairly constant with the base case application model, with the exception at low burnup (i.e., 10 GWd/MTU) of the B&W 15×15 assembly design, the W 17×17 with no burnable absorbers (BAs) inserted during the depletion, and the 1000 ppm soluble boron concentration cases. These differences gradually became smaller as burnup increased. The most likely reason for this is variation in the discharge isotopic compositions for the B&W 15×15 and W 17×17 with no BAs. These assemblies experience very different spectral characteristics from the base case during the initial burnup. As the assemblies are burned for a longer time period, the differences in spectral characteristics become more smoothed out because the fuel isotopic composition has a stronger influence than the other reactor components (e.g., burnable poison rods are burned out). The differences between the 1000 ppm boron case and the base case are most likely attributable to the difference in k_{eff} (0.99 versus 0.84), causing the 1000 ppm case to have a much lower overall sensitivity to nuclear data uncertainty. Overall, the minimum number of at least marginally similar experiments for any application model was 69, compared with 134 for the base case model.

Table 7.6 Bias and uncertainty based on c_k trending

Description	Change from base	Bias/bias uncertainty (Δk) / No. of experiments with c_k > 0.8			
		Final burnup (GWd/MTU)			
		10	25	40	57
PWR SFP model					
Base case	--	NC[b]	1.89E-03 / 9.19E-03 / 198	3.62E-03 / 1.27E-02 / 259	4.20E-03 / 1.49E-02 / 281
Assembly design	B&W 15×15	NC	-1.54E-03 /7.06E-03 / 168	4.50E-03 / 1.36E-02 / 232	4.13E-03 / 1.32E-02 / 237
	W 17×17 no BAs	NC	-1.33E-03 /6.97E-03 / 165	1.47E-03 / 8.67E-03 / 200	2.95E-03 / 1.20E-02 / 268
Rack design	Unpoisoned panels	NC	7.39E-03 / 1.82E-02 / 252	5.46E-03 / 1.73E-02 / 285	5.11E-03 / 1.69E-02 / 286
	Cell pitch increased 0.5 in.	NC	1.45E-03 / 8.65E-03 / 198	2.86E-03 / 1.19E-02 / 272	3.01E-03 / 1.38E-02 / 284
	Poison panel B10 +10%	NC	1.89E-03 / 9.09E-03 / 198	3.16E-03 / 1.22E-02 / 250	4.19E-03 / 1.49E-02 / 281
	Poison panel B10 -10%	NC	2.13E-03 / 9.53E-03 / 199	3.72E-03 / 1.28E-02 / 264	4.25E-03 / 1.50E-02 / 281
Decay time	0 d	NC	1.89E-03 / 9.09E-03 / 198	2.85E-03 / 1.18E-02 / 247	4.13E-03 / 1.48E-02 / 281
	1 year	NC	1.84E-03 / 9.04E-03 / 198	2.84E-03 / 1.17E-02 / 241	3.97E-03 / 1.47E-02 / 281
	5 year	NC	-1.52E-03 / 6.98E-03 / 171	3.00E-03 / 1.18E-02 / 235	3.79E-03 / 1.45E-02 / 281
	20 year	NC	-1.71E-03 / 6.89E-03 / 167	1.79E-03 / 8.99E-03 / 198	4.13E-03 / 1.48E-02 / 281
	40 year	NC	1.36E-03 /6.94E-03 / 166	1.82E-03 / 9.02E-03 / 197	2.96E-03 / 1.21E-02 / 274
Soluble boron	1000 ppm[a]	NC	-1.33E-03 / 7.17E-03 / 169	4.25E-03 / 1.33E-02 / 235	6.29E-03 / 1.66E-02 / 264
	ppm for k_{eff} = 0.94	NC	2.01E-03 / 9.31E-03 / 198	3.31E-03 / 1.23E-02 / 241	5.27E-03 / 1.55E-02 / 279
Cross-section library	ENDF-B/V	N/A[c]	N/A	N/A	N/A
	ENDF-B/VI	N/A	N/A	N/A	N/A
Axial burnup	1 node	NC	NC	NC	NC

[a] Parts per million boron by mass.
[b] NC = not calculated, insufficient number of experiments with c_k > 0.9 for bias calculation.
[c] N/A = not available, only benchmark experiment SDFs using ENDF/B-VII are available.

Table 7.7 Bias and uncertainty based on *EALF* trending

Description	Change from base	Bias/bias uncertainty (Δk) / No. of experiments with $c_k > 0.8$			
		Final burnup (GWd/MTU)			
		10	25	40	57
PWR SFP model					
Base case	--	-1.47E-03 / 7.12E-03 / 134	-1.71E-03 / 8.30E-03 / 198	-2.04E-03 / 1.09E-02 / 259	-2.04E-03 / 1.29E-02 / 281
Assembly design	B&W 15×15	-1.84E-03 / 7.53E-03 / 91	-1.36E-03 / 7.73E-03 / 168	-7.33E-04 / 1.05E-02 / 232	-5.83E-04 / 1.04E-02 / 237
	W 17×17 no BAs	-1.47E-03 / 7.79E-03 / 69	-1.52E-03 / 7.24E-03 / 165	-1.67E-03 / 8.30E-03 / 200	-1.99E-03 / 1.10E-02 / 268
Rack design	Unpoisoned panels	-1.10E-03 / 7.88E-03 / 142	-2.80E-03 / 1.22E-02 / 252	-3.04E-03 / 1.29E-02 / 285	-2.99E-03 / 1.31E-02 / 286
	Cell pitch increased 0.5 in.	-1.31E-03 / 6.93E-03 / 147	-1.72E-03 / 8.30E-03 / 198	-2.42E-03 / 1.10E-02 / 272	-2.55E-03 / 1.30E-02 / 284
	Poison panel B10 +10%	-1.48E-03 / 7.12E-03 / 134	-1.71E-03 / 8.30E-03 / 198	-1.88E-03 / 1.06E-02 / 250	-2.02E-03 / 1.29E-02 / 281
	Poison panel B10 -10%	-1.47E-03 / 7.10E-03 / 137	-1.74E-03 / 8.50E-03 / 199	-2.11E-03 / 1.10E-02 / 264	-2.08E-03 / 1.29E-02 / 281
Decay time	0 d	-1.46E-03 / 7.83E-03 / 129	-1.71E-03 / 9.03E-03 / 198	-1.79E-03 / 1.06E-02 / 247	-2.10E-03 / 1.30E-02 / 281
	1 year	-1.48E-03 / 7.21E-03 / 129	-1.71E-03 / 8.30E-03 / 198	-1.67E-03 / 1.04E-02 / 241	-2.01E-03 / 1.29E-02 / 281
	5 year	-1.50E-03 / 7.22E-03 / 128	-1.22E-03 / 7.69E-03 / 171	-1.58E-03 / 1.04E-02 / 235	-1.96E-03 / 1.29E-02 / 281
	20 year	-1.51E-03 / 7.28E-03 / 124	-1.32E-03 / 7.57E-03 / 167	-1.69E-03 / 8.30E-03 / 198	-1.91E-03 / 1.29E-02 / 281
	40 year	-1.51E-03 / 7.28E-03 / 124	-1.37E-03 / 7.58E-03 / 166	-1.71E-03 / 8.29E-03 / 197	-1.71E-03 / 1.10E-02 / 274
Soluble boron	1000 ppm[a]	-1.99E-03 / 7.48E-03 / 74	-1.41E-03 / 7.75E-03 / 169	-1.03E-03 / 1.04E-02 / 235	-1.11E-03 / 1.25E-02 / 264
	ppm for k_{eff} = 0.94	-1.62E-03 / 7.30E-03 / 123	-1.70E-03 / 8.30E-03 / 198	-1.48E-03 / 1.04E-02 / 241	-1.74E-03 / 1.25E-02 / 279
Cross-section library[b, c]	ENDF-B/V	-1.84E-03 / 7.34E-03 / 125	N/A	-2.95E-03 / 1.04E-02 / 226	N/A
	ENDF-B/VI	-5.67E-03 / 1.08E-02 / 133	N/A	-6.77E-03 / 1.08E-02 / 234	N/A
Axial burnup	1 node	-1.43E-03 / 7.83E-03 / 138	-1.66E-03 / 9.03E-03 / 181	-1.56E-03 / 1.06E-02 / 205	-1.61E-03 / 1.30E-02 / 213

[a]Parts per million boron by mass.
[b]N/A = not available, only benchmark experiment SDFs using ENDF/B-VII are available.
[c]c_k comparison with benchmark experiment SDFs using ENDF/B-VII, but trending analysis based on ENDF/B-V and ENDF/B-VI.

Table 7.8 Bias and uncertainty based on final plutonium content trending

Description	Change from base	Bias/bias uncertainty (Δk) / No. of experiments with $c_k > 0.8$			
		Final burnup (GWd/MTU)			
		10	25	40[d]	57
PWR SFP model					
Base case	--	5.72E-02 / 7.13E-03 / 134	3.09E-05 / 7.05E-03 / 198	-2.11E-03 / 9.84E-03 / 259	-2.67E-03 / 1.10E-02 / 281
Assembly design	B&W 15×15	6.05E-02 / 7.23E-03 / 91	-1.21E-03 / 7.14E-03 / 168	-1.80E-03 / 9.58E-03 / 232	-2.44E-03 / 9.53E-03 / 237
	W 17×17 no BAs	7.03E-02 / 7.20E-03 / 69	-1.37E-04 / 8.80E-03 / 165	-5.98E-04 / 7.08E-03 / 200	-2.21E-03 / 9.90E-03 / 268
Rack design	Unpoisoned panels	-2.26E-03 / 7.71E-03 / 142	-7.77E-04 / 9.81E-03 / 252	-3.52E-03 / 1.40E-02 / 285	-3.52E-03 / 1.40E-02 / 286
	Cell pitch increased 0.5 in.	5.77E-02 / 6.99E-03 / 147	7.16E-05 / 7.05E-03 / 198	-2.13E-03 / 9.89E-03 / 272	-2.58E-03 / 1.13E-02 / 284
	Poison panel B10 +10%	5.74E-02 / 7.13E-03 / 134	3.43E-05 / 7.05E-03 / 198	-1.93E-03 / 9.60E-03 / 250	-2.67E-03 / 1.10E-02 / 281
	Poison panel B10 -10%	5.66E-02 / 7.12E-03 / 137	-6.72E-05 / 7.22E-03 / 199	-2.09E-03 / 9.88E-03 / 264	-2.67E-03 / 1.10E-02 / 281
Decay time	0 d	5.79E-02 / 7.19E-03 / 129	5.92E-05 / 7.05E-03 / 198	-1.81E-03 / 9.49E-03 / 247	-2.62E-03 / 1.10E-02 / 281
	1 year	5.84E-02 / 7.19E-03 / 129	9.88E-05 / 7.05E-03 / 198	-1.77E-03 / 9.47E-03 / 241	-2.59E-03 / 1.10E-02 / 281
	5 year	5.97E-02 / 7.20E-03 / 128	-1.25E-03 / 7.10E-03 / 171	-1.48E-03 / 9.56E-03 / 235	-2.44E-03 / 1.10E-02 / 281
	20 year	6.23E-02 / 7.24E-03 / 124	-1.43E-03 / 7.50E-03 / 167	-5.52E-04 / 7.05E-03 / 198	-2.14E-03 / 1.10E-02 / 281
	40 year	6.33E-02 / 7.24E-03 / 124	-8.76E-04 / 7.88E-03 / 166	-4.47E-04 / 7.03E-03 / 197	-2.22E-03 / 9.95E-03 / 274
Soluble boron	1000 ppm[a]	6.03E-02 / 7.11E-03 / 74	-1.16E-03 / 7.11E-03 / 169	-1.67E-03 / 9.56E-03 / 235	-2.57E-03 / 1.01E-02 / 264
	ppm for k_{eff} = 0.94	5.78E-02 / 7.25E-03 / 123	3.49E-05 / 7.05E-03 / 198	-1.80E-03 / 9.47E-03 / 241	-2.69E-03 / 1.03E-02 / 279
Cross-section library[b, c]	ENDF-B/V	4.32E-02 / 7.54E-03 / 125	N/A	-1.32E-03 / 9.45E-03 / 226	N/A
	ENDF-B/VI	3.86E-02 / 7.38E-03 / 133	N/A	-5.61E-03 / 9.62E-03 / 234	N/A
Axial burnup	1 node	2.50E-03 / 9.48E-03 / 138	-1.26E-03 / 8.46E-03 / 181	-2.38E-03 / 9.68E-03 / 205	-3.52E-03 / 1.02E-02 / 213

[a]Parts per million boron by mass.
[b]N/A = not available, only benchmark experiment SDFs using ENDF/B-VII are available.
[c]c_k comparison with benchmark experiment SDFs using ENDF/B-VII, but trending analysis based on ENDF/B-V and ENDF/B-VI.
[d]Shaded cells for comparative purposes only but are extrapolations outside range of applicability.

Table 7.9 Bias and uncertainty based on final uranium enrichment trending

Description	Change from base	Bias uncertainty (Δk) / No. of experiments with c_k > 0.8			
		Final burnup (GWd/MTU)			
		10	25	40[d]	57
PWR SFP model					
Base case	--	9.15E-02 / 6.90E-03 / 134	4.26E-04 / 7.26E-03 / 198	2.35E-03 / 9.04E-03 / 259	5.71E-03 / 1.04E-02 / 281
Assembly design	B&W 15×15	-5.47E-01 / 7.14E-03 / 91	-1.12E-04 / 7.56E-03 / 168	-9.29E-03 / 8.78E-03 / 232	-8.98E-03 / 8.79E-03 / 237
	W 17×17 no BAs	1.21E-01 / 7.23E-03 / 69	-1.04E-03 / 8.59E-03 / 165	1.54E-03 / 7.27E-03 / 200	4.01E-03 / 9.09E-03 / 268
Rack design	Unpoisoned panels	1.16E-04 / 8.21E-03 / 142	-6.14E-03 / 9.75E-03 / 252	-5.93E-03 / 1.06E-02 / 285	-5.14E-03 / 1.06E-02 / 286
	Cell pitch increased 0.5 in.	1.47E-01 / 6.75E-03 / 147	1.47E-03 / 7.26E-03 / 198	4.39E-03 / 9.08E-03 / 272	5.72E-03 / 1.05E-02 / 284
	Poison panel B10 +10%	1.03E-01 / 6.90E-03 / 134	5.77E-04 / 7.26E-03 / 198	2.27E-03 / 8.89E-03 / 250	5.71E-03 / 1.04E-02 / 281
	Poison panel B10 -10%	8.02E-02 / 6.89E-03 / 137	3.92E-04 / 7.33E-03 / 199	2.02E-03 / 9.08E-03 / 264	5.27E-03 / 1.04E-02 / 281
Decay time	0 d	8.10E-02 / 6.95E-03 / 129	2.80E-04 / 7.26E-03 / 198	1.67E-03 / 8.81E-03 / 247	5.28E-03 / 1.04E-02 / 281
	1 year	9.48E-02 / 6.96E-03 / 129	7.70E-04 / 7.26E-03 / 198	2.38E-03 / 8.78E-03 / 241	6.16E-03 / 1.04E-02 / 281
	5 year	1.19E-01 / 6.98E-03 / 128	-1.51E-03 / 7.53E-03 / 171	3.79E-03 / 8.79E-03 / 235	6.64E-03 / 1.04E-02 / 281
	20 year	1.45E-01 / 7.02E-03 / 124	-2.01E-03 / 7.95E-03 / 167	4.09E-03 / 7.26E-03 / 198	7.44E-03 / 1.04E-02 / 281
	40 year	1.56E-01 / 7.02E-03 / 124	-1.40E-03 / 8.21E-03 / 166	4.83E-03 / 7.25E-03 / 197	5.70E-03 / 9.12E-03 / 274
Soluble boron	1000 ppm[a]	7.55E-02 / 7.11E-03 / 74	-1.27E-03 / 7.52E-03 / 169	1.95E-03 / 8.79E-03 / 235	5.75E-03 / 9.81E-03 / 264
	ppm for k_{eff} = 0.94	8.80E-02 / 7.04E-03 / 123	3.53E-04 / 7.26E-03 / 198	1.75E-03 / 8.78E-03 / 241	5.76E-03 / 9.84E-03 / 279
Cross-section library[b, c]	ENDF-B/V	1.46E-01 / 7.20E-03 / 125	N/A	4.26E-03 / 8.65E-03 / 226	N/A
	ENDF-B/VI	1.19E-01 / 7.04E-03 / 133	N/A	5.80E-04 / 8.89E-03 / 234	N/A
Axial burnup	1 node	-1.23E-03 / 9.73E-03 / 138	-4.03E-04 / 7.69E-03 / 181	5.91E-04 / 8.82E-03 / 205	-4.63E-04 / 1.02E-02 / 213

[a]Parts per million boron by mass.
[b]N/A = not available, only benchmark experiment SDFs using ENDF/B-VII are available.
[c]c_k comparison with benchmark experiment SDFs using ENDF/B-VII, but trending analysis based on ENDF/B-V and ENDF/B-VI.
[d] Shaded cells for comparative purposes only but are extrapolations outside range of applicability.

7.4.3 Nonapplicable LCE Nuclide Validation Assessment

A principal challenge for crediting FPs in a BUC safety evaluation is the limited availability of relevant FP critical experiments for bias and bias uncertainty determination, and the issue of how to apply the individual FP biases calculated from the experiments to those of the application model. This is the same challenge as for crediting minor actinides such as ^{236}U, ^{243}Am, and ^{237}Np. Neutron energy spectrum shifts, as well as the presence of other materials, may significantly affect the bias associated with any individual isotope of interest. The uncertainties in the computed k_{eff} values due to uncertainties in the cross-section data were computed, as described in Sections 3.2.5 and 6.3, by combining the sensitivity of k_{eff} to the cross-section data with the cross-section covariance data. The TSUNAMI-IP module was used to propagate the poorly validated nuclide (FPs and minor actinide) cross-section uncertainties to k_{eff} uncertainties for each of the parametric models. Table 7.10 provides the results of the cross-section uncertainty analysis for the parametric PWR SFP application models using BUC with actinides and 16 FPs as listed in Section 4. Table 7.11 provides the results of the cross-section uncertainty analysis, in terms of nuclide uncertainty-to-worth ratios, for the base case PWR SFP application model as a function of burnup using all actinides and FPs supported by SCALE. Table 7.12 provides the results of the cross-section uncertainty analysis, in terms of nuclide uncertainty-to-worth ratios, for the cask application model at burnups of 10 and 40 GWd/MTU using all isotopes supported by SCALE, and for the SNF isotopes consisting of actinides and 16 FPs.

Table 7.10 Summary of one sigma uncertainty results for PWR SFP parametric application models

Description	Change from base	Burnup (GWd/MTU)	Parameter			
			Total uncertainty (Δk)	UV[a] uncertainty (Δk)	UV worth (Δk)	UV uncert/worth (%)
Base case	--	10	0.0048	0.0003	-0.0274	1.10
		25	0.0050	0.0006	-0.0483	1.20
		40	0.0051	0.0008	-0.0639	1.28
		57	0.0050	0.0010	-0.0743	1.37
Assembly design	B&W 15×15	10	0.0050	0.0003	-0.0290	1.13
		25	0.0052	0.0006	-0.0503	1.26
		40	0.0052	0.0009	-0.0656	1.37
		57	0.0051	0.0011	-0.0755	1.47
	W 17×17 (No BAs)	10	0.0046	0.0003	-0.0257	1.12
		25	0.0048	0.0006	-0.0461	1.21
		40	0.0048	0.0008	-0.0617	1.31
		57	0.0048	0.0010	-0.0722	1.38
Rack design	Unpoisoned panels	10	0.0066	0.0003	-0.0338	1.01
		25	0.0067	0.0006	-0.0574	1.05
		40	0.0067	0.0008	-0.0759	1.10
		57	0.0065	0.0010	-0.0874	1.15
	Cell pitch increased 0.25 in.	10	0.0046	0.0003	-0.0278	1.10
		25	0.0048	0.0006	-0.0480	1.18
		40	0.0049	0.0008	-0.0630	1.28
		57	0.0049	0.0010	-0.0720	1.34
	Poison panel B10 +10%	10	0.0048	0.0003	-0.0277	1.11
		25	0.0050	0.0006	-0.0480	1.20
		40	0.0050	0.0008	-0.0637	1.29
		57	0.0050	0.0010	-0.0737	1.37

Table 7.10 Summary of one sigma uncertainty results for PWR SFP parametric application models (continued)

Description	Change from base	Burnup (GWd/MTU)	Parameter			
			Total uncertainty (Δk)	UV[a] uncertainty (Δk)	UV worth (Δk)	UV uncert/worth (%)
	Poison panel B10 - 10%	10	0.0048	0.0003	-0.0278	1.10
		25	0.0050	0.0006	-0.0484	1.19
		40	0.0051	0.0008	-0.0643	1.28
		57	0.0050	0.0010	-0.0744	1.36
Decay time	0 d	10	0.0048	0.0003	-0.0249	1.13
		25	0.0050	0.0006	-0.0457	1.23
		40	0.0051	0.0008	-0.0611	1.32
		57	0.0050	0.0010	-0.0714	1.40
	1 year	10	0.0048	0.0003	-0.0310	1.07
		25	0.0049	0.0006	-0.0516	1.16
		40	0.0050	0.0008	-0.0665	1.25
		57	0.0050	0.0010	-0.0759	1.33
	5 year	10	0.0047	0.0003	-0.0316	1.03
		25	0.0049	0.0006	-0.0526	1.11
		40	0.0049	0.0008	-0.0685	1.20
		57	0.0048	0.0010	-0.0754	1.27
	20 year	10	0.0047	0.0003	-0.0315	0.99
		25	0.0048	0.0006	-0.0518	1.08
		40	0.0048	0.0008	-0.0676	1.18
		57	0.0047	0.0009	-0.0755	1.21
	40 year	10	0.0047	0.0003	-0.0311	0.99
		25	0.0047	0.0005	-0.0510	1.08
		40	0.0048	0.0008	-0.0666	1.18
		57	0.0051	0.0010	-0.0792	1.21

Table 7.10 Summary of one sigma uncertainty results for PWR SFP parametric application models (continued)

Description	Change from base	Burnup (GWd/MTU)	Parameter			
			Total uncertainty (Δk)	UV[a] uncertainty (Δk)	UV worth (Δk)	UV uncert/worth (%)
Soluble boron	1000 ppm	10	0.0041	0.0002	-0.0209	1.18
		25	0.0044	0.0005	-0.0377	1.29
		40	0.0045	0.0007	-0.0516	1.39
		57	0.0045	0.0009	-0.0608	1.48
	Search for k_{eff} = 0.94	10	0.0045	0.0003	-0.0254	1.12
		25	0.0047	0.0005	-0.0443	1.22
		40	0.0048	0.0008	-0.0587	1.32
		57	0.0048	0.0010	-0.0678	1.41
Cross-section library	ENDF-B/V	10	0.0048	0.0003	-0.0278	1.12
		25	--	--	--	--
		40	0.0050	0.0008	-0.0632	1.31
		57	--	--	--	--
	ENDF-B/VI	10	0.0048	0.0003	-0.0282	1.11
		25	--	--	--	--
		40	0.0051	0.0008	-0.0648	1.29
		57	--	--	--	--
Axial burnup	1 node	10	0.0052	0.0004	-0.0366	1.12
		25	0.0055	0.0008	-0.0624	1.21
		40	0.0055	0.0011	-0.0810	1.31
		57	0.0057	0.0013	-0.0981	1.36

[a]UV = unvalidated nuclides represented by the 16 FPs and 3 minor actinides (i.e., ^{243}Am, ^{237}Np, and ^{236}U) identified in Section 7.2.

Table 7.11 Unvalidated nuclide uncertainty-to-worth ratios (Δk) results for PWR SFP application model using all isotopes BUC

Burnup (GWd/MTU)	5	10	18	30	40	50	60	70
Minor actinides (3) (%)	3.52	3.52	3.59	3.69	3.80	3.90	3.87	3.82
FP (16) (%)	0.94	0.91	0.92	0.96	0.99	1.02	1.02	1.03
Other actinides (%)	10.43	11.06	13.14	16.59	27.38	28.71	62.92	62.57
Other FP (%)	2.10	1.69	1.68	1.66	1.50	1.69	1.69	1.70
Total UV nuclides in fuel (%)[a]	1.47	1.32	1.35	1.41	1.42	1.50	1.51	1.53

[a] Structural materials need to be accounted for on an application model specific basis.

Table 7.12 Unvalidated nuclide uncertainty to worth ratios (Δk) results for GBC32 application models

BUC isotope set	All nuclides		28 actinides and FPs	
Burnup (GWd/MTU)	10	40	10	40
Minor actinides (3) (%)	3.45	3.74	3.42	3.62
FP (16) (%)	0.85	0.90	0.85	0.89
Other actinides (%)	10.87	11.23	N/A	N/A
Other FP (%)	2.11	2.08	N/A	N/A
Total UV nuclides in fuel (%)[a]	1.15	1.35	1.02	1.18

[a] Structural materials need to be accounted for on an application model specific basis.

7.5 SENSITIVITY ANALYSIS SUMMARY

The bias and bias uncertainty for the various parametric cases were calculated and compared in Section 7.4.1 without the proprietary FP data set. They are presented in Table 7.3 to Table 7.5 based on traditional trending methods as identified in NUREG/CR-6698. When traditional trending parameters are used (i.e., parameters other than c_k), the final plutonium fraction trending parameter provides the most conservative bias and bias uncertainty values for all cases except the different cross-section libraries. PWR SFP calculated bias values ranged from -1.17×10^{-3} to -4.14×10^{-3} with uncertainties ranging from 1.43×10^{-2} to 1.57×10^{-2}. The impacts of SNF system parameter changes on the burnup-dependent base case biases show that the base case bias uncertainty is a factor of ~7 greater than the base case bias and hence subsumes the changes in bias due to the system parameter changes.

The more rigorous, physics-based S/U analysis techniques for critical benchmark selection was utilized in the work reported in Section 7.4.2. As can be seen, the individual application model specific bias and bias uncertainty values are sometimes more limiting than the base case values. This shows that using a more concise set of critical benchmark experiments that exhibit similar sensitivities to nuclear data uncertainty as the application model, yields a more accurate estimate of the application model specific bias and bias uncertainty than the results presented in Section 7.4.1. In Section 7.4.1, the large number of critical experiments obscures application model specific effects because of the inclusion of critical experiments that are not really applicable.

Section 7.4.3 evaluates the parametric variation effects directly on the nuclides (i.e., FPs and minor actinides ^{243}Am, ^{237}Np, and ^{236}U) for which applicable LCE data are not available. TSUNAMI-IP was used to assess the FP and minor actinide uncertainty in k_{eff} based on using the SCALE 44-group cross-section covariance libraries as a bounding method for addressing bias and bias uncertainty for FPs and minor actinides. The TSUNAMI-IP–calculated combined minor actinide and FP uncertainty at a 1σ level based on the cross-section covariance data is presented in Table 7.10. The minor actinide and FP cross-section uncertainty ranges from approximately 1% of the worth at lower burnups (i.e., 10 GWd/MTU) to ~1.5% of the worth at higher burnups (i.e., 57 GWd/MTU). Note that these values are for the BUC isotope set consisting of actinides and 16 FPs. An upper value of 1.5% of the worth is also applicable for SNF isotopic compositions consisting of all nuclides in the SFP configuration, as well as the cask configuration as depicted in Table 7.11 and Table 7.12.

8. CONCLUSIONS AND RECOMMENDATIONS

This report presented a validation approach for BUC criticality safety analyses of commercial SNF storage systems that include credit for fission products. Generic safety application models representative of PWR and BWR fuel storage racks and PWR fuel in a high-capacity dry-storage/transportation cask were used for the demonstration. Models of 609 critical experiment configurations, which are listed in Appendix A, were used to perform this BUC validation study. Included in the validation set were 124 LEU configurations and 194 mixed uranium–plutonium systems described in the IHECSBE (Ref. 9). The validation set also included 156 critical configurations from the French HTC critical experiment series (Refs. 10–13), which used fuel rods with uranium and plutonium compositions designed to be similar to SNF, and 135 critical configurations from the French FP Programme critical experiment series (Refs. 20–24).

As part of the validation study, the critical configurations were used to determine computational bias and bias uncertainty for each of the applications. The impact of application model variations on bias and bias uncertainty was explored, and the results were presented in Section 7.

Based on the analyses performed for this report, it is affirmed that criticality analysts should continue to validate BUC criticality safety evaluations to the extent possible, with the best available critical experiment data. MOX configurations from the IHECSBE and the HTC experiment configurations, collectively, provide sufficient data for validation of BUC analyses with major actinides and hence should be used for validation. LEU critical configurations should not be used in a conventional validation analysis to validate burned fuel systems because they do not include any bias contribution from the plutonium present in burned fuel. The validation statistical analysis should include bias trending analysis as a function of plutonium content, using a trending variable such as plutonium fraction (i.e., gram of Pu per gram of Pu + U).

Critical experiments with uranium, plutonium, and FPs in the correct proportion to support conventional validation of FP BUC are not publicly available. Work was presented in Sections 6.3 and 6.4 that used the available FP critical experiments to estimate bias and bias uncertainty associated with the FPs. Because of the small number of critical experiments, the uncertainty on these FP bias estimates was determined to be significant.

An approach based on calculated sensitivities and nuclear data uncertainties was demonstrated for generating conservative estimates of bias for actinide and FP nuclides for which adequate experimental data are not available. The uncertainty analysis technique yields an application-specific value for the uncertainty in k_{eff} due to the uncertainty in the nuclear data. Other comparisons (Section 3.2.5 and Appendix C) for cases in which adequate critical experiment data are available have demonstrated the validity and conservatism of the approach.

Based on the analyses in this report, a set of recommendations has been developed for validation of SNF BUC criticality calculations:

1. For the primary actinides (i.e., ^{234}U, ^{235}U, ^{238}U, ^{238}Pu, ^{239}Pu, ^{240}Pu, ^{241}Pu, ^{242}Pu, and ^{241}Am), sufficient critical experiment data exist to adequately validate k_{eff} calculations via conventional validation approaches. Therefore, the bias in k_{eff} calculations due to the primary actinide compositions can be determined based on applicable critical experiments, such as the HTC critical experiment data and other MOX critical experiments. Some recommended candidates for mixed uranium-plutonium systems from the IHECSBE are provided in Section 5.2. Note that not all IHECSBE mixed uranium-plutonium systems were

evaluated, and use of other uranium-plutonium LCEs may be appropriate. Use of the HTC and recommended IHECSBE mixed uranium-plutonium systems should provide adequate validation for the primary actinides. Similarity index results for all critical experiments used in this report are provided in Appendix B. It is recommended that critical experiments with c_k values above 0.8 be considered candidates for use in computational method validation.

2. A conservative estimate for the bias associated with minor actinide and FP nuclides of 1.5% of their worth may be used for Δk_x. The range of applicability of this method is limited to low-enriched (<5.0 wt % ^{235}U) LWR UO_x SNF with the ENDF/B-V, -VI, or -VII cross-section libraries and a maximum burnup of 70 GWd/MTU, and a total minor actinide and FP nuclide worth not to exceed 0.1 Δk. Where methods and data similar to those used in this report are applied to models similar to those described in Section 4, uncertainty information from Section 6.3 may be used to cover actinide and fission product nuclides that are not validated via conventional approaches.
3. The bias value determined for the primary actinides, per recommendation #1, and the bias value determined for the remaining actinide and FP nuclides, per recommendation #2, should be combined in an appropriate manner [e.g., using Eq.(3.1)].
4. Structural materials and integral fuel BAs (e.g., steel, aluminum, residual gadolinium in gadolinium fuel rods, other non-fuel materials) need to be accounted for in the criticality safety assessment and validation study. For systems that are similar to the application models in this report, the k_{eff} uncertainties due to nuclear data uncertainties, presented in Section 6.3, can be combined in quadrature and applied to the Δk_p term as illustrated in Section 3.

9. REFERENCES

(1) *Code of Federal Regulations*, Title 10, “Energy” (2011).

(2) “Burnup Credit for LWR Fuel," ANSI/ANS-8.27-2008, an American National Standard, published by the American Nuclear Society, LaGrange Park, IL, 2008.

(3) “Nuclear Criticality Safety in Operations with Fissionable Material Outside Reactors,” ANSI/ANS-8.1-1998; R2007, an American National Standard, published by the American Nuclear Society, LaGrange Park, IL, 1998.

(4) NRC Information Notice 2011-03: “Nonconservative Criticality Safety Analyses for Fuel Storage,” US Nuclear Regulatory Commission (February 16, 2011).

(5) Spent Fuel Project Office, *Interim Staff Guidance—8, rev. 2, Burnup Credit in the Criticality Safety Analyses of PWR Spent Fuel in Transport and Storage Casks*, ISG-8, rev. 2, US Nuclear Regulatory Commission, September 27, 2002.

(6) Letter from L. Kopp to T. Collins, “Guidance on the Regulatory Requirements for Criticality Analysis of Fuel Storage at Light-Water Reactor Power Plants,” US Nuclear Regulatory Commission, August 19, 1998.

(7) C. V. Parks, J. C. Wagner, D. E. Mueller, and I. C. Gauld, “Full Burnup Credit in Transport and Storage Casks—Benefits and Implementation,” *Radwaste Solutions* 14(2), 32–41 (March/April 2007).

(8) G. Radulescu, I.C. Gauld, G. Ilas, and J.C. Wagner, *An Approach for Validating Actinide and Fission Product Burnup Credit Criticality Safety Analyses—Isotopic Composition Predictions*, US Nuclear Regulatory Commission, NUREG/CR-7108, Oak Ridge National Laboratory, Oak Ridge, Tenn. (2012).

(9) *International Handbook of Evaluated Criticality Safety Benchmark Experiments*, NEA/NSC/DOC(95)03, NEA Nuclear Science Committee, September 2009.

(10) F. Fernex, *Programme HTC–Phase 1: Réseaux de Crayons dans l’Eau Pure (Water-Moderated and Reflected Simple Arrays) Reevaluation des Expériences*, DSU/SEC/T/2005-33/D.R, Valduc, France, IRSN (2006). PROPRIETARY document.

(11) F. Fernex, *Programme HTC–Phase 2: Réseaux Simples en Eau Empoisonnée (Bore et Gadolinium) (Reflected Simple Arrays Moderated by Poisoned Water with Gadolinium or Boron) Réévaluation des Experiences*, DSU/SEC/T/2005-38/D.R, Valduc, France, IRSN (2006). PROPRIETARY document.

(12) F. Fernex, *Programme HTC–Phase 3: Configurations “Stockage en Piscine” (Pool Storage) Réévaluation des Experiences*, DSU/SEC/T/2005-37/D.R, Valduc, France, IRSN (2006). PROPRIETARY document.

(13) F. Fernex, *Programme HTC–Phase 4: Configurations “Châteaux de Transport” (Shipping Cask) Réévaluation des Experiences*, DSU/SEC/T/2005-36/D.R., Valduc, France, IRSN (2006). PROPRIETARY document.

(14) *Scale: A Comprehensive Modeling and Simulation Suite for Nuclear Safety Analysis and Design*, ORNL/TM-2005/39, Version 6.1, Oak Ridge National Laboratory, Oak Ridge, Tennessee, June 2011. Available from Radiation Safety Information Computational Center at Oak Ridge National Laboratory as CCC-785.

(15) J. Rhodes, K. Smith, and D. Lee, *CASMO-5/CASMO-5M, A Fuel Assembly Burnup Program, User's Manual*, SSP-07/431 Rev. 0, Studsvik Scandpower, Inc. (2007).

(16) M. Ouisloumen et al., "PARAGON: The New Westinghouse Assembly Lattice Code," in *Proceedings of the ANS International Meeting on Mathematical Methods for Nuclear Applications*, Salt Lake City, Utah, USA (2001).

(17) *MCNP—Monte Carlo N-Particle Transport Code System, Version 5*, Vol. 1: LA-UR-03-1987, Vol. 2: LA-CP-03-0245, and Vol. 3: LA-CP-03-0284, Los Alamos National Laboratory, 2003. Available from Radiation Safety Information Computational Center at Oak Ridge National Laboratory as CCC-740.

(18) V. R. Cain, *A Computer Code to Perform Analyses of Criticality Validation Results*, Y/DD-574, Martin Marietta Energy Systems, Oak Ridge Y-12 Plant, September 1995.

(19) J. J. Lichtenwalter, S. M. Bowman, M. D. DeHart, and C. M. Hopper, *Criticality Benchmark Guide for Light-Water-Reactor Fuel in Transportation and Storage Packages*, NUREG/CR-6361 (ORNL/TM-13211), prepared for the US Nuclear Regulatory Commission by Oak Ridge National Laboratory, Oak Ridge, Tenn., March 1997.

(20) N. Leclaire, "Fission Products Experimental Programme Exploitation, 1st Part, Analysis of the Fission Products experimental programme: Physical type experiments related to the validation of 6 FP absorption cross sections (^{103}Rh, ^{133}Cs, ^{143}Nd, ^{149}Sm, ^{152}Sm, ^{155}Gd) in slightly acidic solutions," DSU/SEC/T/2009-173/D.R.—Index A, Institut de Radioprotection et de Sûreté Nucléaire, 2009. PROPRIETARY document.

(21) N. Leclaire, "Fission Products Experimental Programme Exploitation, 2nd Part, 'Elementary dissolution' type criticality experiments: PWR rods arrays in slightly acidic solutions poisoned or not by fission products," DSU/SEC/T/2009-174/D.R.—Index A, Institut de Radioprotection et de Sûreté Nucléaire, 2009. PROPRIETARY document.

(22) N. Leclaire, "Fission Products Experimental Programme Exploitation, 2nd Part, 'Elementary dissolution' type criticality experiments: PWR rods arrays immersed in depleted uranyl nitrate solutions poisoned or not by fission products (FP)," DSU/SEC/T/2009-175/D.R.—Index A, Institut de Radioprotection et de Sûreté Nucléaire, 2009. PROPRIETARY document.

(23) N. Leclaire, "Fission Products Experimental Programme Exploitation, 3rd Part, 'Dissolution in a large non adjusted tank' type criticality experiments on an array of UO_2 rods, immersed in depleted uranyl nitrate solutions," DSU/SEC/T/2009-176/D.R.—Index A, Institut de Radioprotection et de Sûreté Nucléaire, 2009. PROPRIETARY document.

(24) N. Leclaire, "Fission Products Experimental Programme Exploitation, 3rd Part, 'Advanced dissolution' type criticality experiments: Arrays of HBU rods in depleted uranyl nitrate solutions poisoned or not by fission products," DSU/SEC/T/2009-177/D.R.—Index A, Institut de Radioprotection et de Sûreté Nucléaire, 2009. PROPRIETARY document.

(25) B. L. Broadhead et al., “Sensitivity- and Uncertainty-Based Criticality Safety Validation Techniques,” *Nucl. Sci. Eng.* 146, 340–366 (2004).

(26) B. T. Rearden and D. E. Mueller, “Recent Use of Covariance Data for Criticality Safety Assessment,” *Nuclear Data Sheets* 109, 2739–2744 (2008).

(27) Division of Fuel Cycle Safety and Safeguards, *Interim Staff Guidance—10, rev. 0, Justification for Minimum Margin of Subcriticality for Safety*, ISG-10, rev. 0, US Nuclear Regulatory Commission, June 15, 2006.

(28) J. C. Dean, R. W. Tayloe, Jr., and D. Morey, *Guide for Validation of Nuclear Criticality Safety Calculational Methodology*, NUREG/CR-6698, prepared for the US Nuclear Regulatory Commission by Science Applications International Corporation, Oak Ridge, Tenn., January 2001.

(29) US Nuclear Regulatory Commission, *Standard Review Plan for Spent Fuel Dry Storage Facilities*, NUREG-1567, March 2000.

(30) US Nuclear Regulatory Commission, *Standard Review Plan for Dry Cask Storage Systems*, NUREG-1536, Rev. 1, July 2010.

(31) US Nuclear Regulatory Commission, *Standard Review Plan for Transportation Packages for Spent Nuclear Fuel*, NUREG-1617, March 2000.

(32) RW-859 Nuclear Fuel Data, Energy Information Administration, Washington, D.C. (Oct. 2004).

(33) J. C. Wagner, *Computational Benchmark for Estimation of Reactivity Margin from Fission Products and Minor Actinides in PWR Burnup Credit*, NUREG/CR-6747 (ORNL/TM-2000/306), prepared for the US Nuclear Regulatory Commission by Oak Ridge National Laboratory, Oak Ridge, Tenn., October 2001.

(34) K. W. Cummings and S. E. Turner, “Design of Wet Storage Racks for Spent BWR Fuel”, 35608.pdf in *Proc. 2001 ANS Embedded Topical Meeting on Practical Implementation of Nuclear Criticality Safety*, Reno, NV, November 11–15, 2001.

(35) I. C. Gauld, *Strategies for Application of Isotopic Uncertainties in Burnup Credit*, NUREG/CR-6811 (ORNL/TM-2001/257), prepared for the US Nuclear Regulatory Commission by Oak Ridge National Laboratory, Oak Ridge, Tenn., June 2003. (Table A.1, data point No. 42)

(36) F. Fernex et al. “HTC Experimental Program: Validation and Calculational Analysis,” Institut de Radioprotection et de Sûreté Nucléaire, *Nuc. Sci. Eng.* 162, 1–24 (2009).

(37) D. E. Mueller, K. R. Elam, and P. B. Fox, *Evaluation of the French Haut Taux de Combustion (HTC) Critical Experiment Data*, NUREG/CR-6979 (ORNL/TM-2007/083), prepared for the US Nuclear Regulatory Commission by Oak Ridge National Laboratory, Oak Ridge, Tenn., September 2008.

(38) N. Leclaire et al., “Fission Product Experimental Program: Validation and Computational Analysis,” Institut de Radioprotection et de Sûreté Nucléaire, *Nuc. Sci. Eng.* 161, 188–215 (2009).

(39) R. E. Odeh and D. B. Owen, *Tables for Normal Tolerance Limits, Sampling Plans, and Screening. Statistics, Textbooks and Monographs Volume 32*, New York, New York: Marcel Dekker, 1980.

(40) D. A. Reed, D. F. Hollenbach, and J. M. Scaglione, “Evaluation of French Fission Product Critical Experiment Data,” prepared by Oak Ridge National Laboratory for the US Nuclear Regulatory Commission, draft dated March 29, 2011. PROPRIETARY document.

APPENDIX A
SPENT NUCLEAR FUEL ASSEMBLY BENCHMARK DATA SUMMARY OF EXPERIMENTAL AND CALCULATED RESULTS

Table A.1 Critical experiments from IHECSBE and ENDF/B-VII 238 group library results

Experiment ID	EALF (eV)	Enrich (wt % ^{235}U)	Pu wt. fraction pu/(pu+u)	Sol. boron (ppm)	$k_{eff,\ exp}$	$\sigma_{keff,exp}$	$k_{eff,\ calc}$	$\sigma_{keff,calc}$
LEU-COMP-THERM-001-001	9.61E-02	2.35	0	0	0.9998	0.0031	0.99879	0.00044
LEU-COMP-THERM-001-002	9.54E-02	2.35	0	0	0.9998	0.0031	0.99819	0.00042
LEU-COMP-THERM-001-003	9.45E-02	2.35	0	0	0.9998	0.0031	0.996	0.00048
LEU-COMP-THERM-001-004	9.51E-02	2.35	0	0	0.9998	0.0031	0.99754	0.00048
LEU-COMP-THERM-001-005	9.39E-02	2.35	0	0	0.9998	0.0031	0.99465	0.00043
LEU-COMP-THERM-001-006	9.47E-02	2.35	0	0	0.9998	0.0031	0.99715	0.00048
LEU-COMP-THERM-001-007	9.30E-02	2.35	0	0	0.9998	0.0031	0.9973	0.00046
LEU-COMP-THERM-001-008	9.42E-02	2.35	0	0	0.9998	0.0031	0.99523	0.00045
LEU-COMP-THERM-002-001	1.13E-01	4.31	0	0	0.9997	0.0020	0.99756	0.00012
LEU-COMP-THERM-002-002	1.13E-01	4.31	0	0	0.9997	0.0020	0.99891	0.0001
LEU-COMP-THERM-002-003	1.13E-01	4.31	0	0	0.9997	0.0020	0.99839	0.00011
LEU-COMP-THERM-002-004	1.12E-01	4.31	0	0	0.9997	0.0020	0.9979	0.00011
LEU-COMP-THERM-002-005	1.10E-01	4.31	0	0	0.9997	0.0020	0.99641	0.00012
LEU-COMP-THERM-010-005	3.56E-01	4.31	0	0	1.0000	0.0021	1.000103	0.000095
LEU-COMP-THERM-010-016	2.85E-01	4.31	0	0	1.0000	0.0028	1.002348	0.000099
LEU-COMP-THERM-010-017	2.79E-01	4.31	0	0	1.0000	0.0028	1.001632	0.000097
LEU-COMP-THERM-010-018	2.74E-01	4.31	0	0	1.0000	0.0028	1.001527	0.000099
LEU-COMP-THERM-010-019	2.68E-01	4.31	0	0	1.0000	0.0028	1.001189	0.000098
LEU-COMP-THERM-017-003	9.47E-02	2.35	0	0	1.0000	0.0031	0.998371	0.000099
LEU-COMP-THERM-017-004	2.03E-01	2.35	0	0	1.0000	0.0031	0.997441	0.000098
LEU-COMP-THERM-017-005	1.79E-01	2.35	0	0	1.0000	0.0031	0.998949	0.000099
LEU-COMP-THERM-017-006	1.69E-01	2.35	0	0	1.0000	0.0031	0.999169	0.000095
LEU-COMP-THERM-017-007	1.60E-01	2.35	0	0	1.0000	0.0031	0.999037	0.000096
LEU-COMP-THERM-017-008	1.34E-01	2.35	0	0	1.0000	0.0031	0.996872	0.000099
LEU-COMP-THERM-017-009	1.10E-01	2.35	0	0	1.0000	0.0031	0.996225	0.000094

Table A.1 Critical experiments from IHECSBE and ENDF/B-VII 238 group library results (continued)

Experiment ID	EALF (eV)	Enrich (wt % ^{235}U)	Pu wt. fraction pu/(pu+u)	Sol. boron (ppm)	$k_{eff,\ exp}$	$\sigma_{keff,exp}$	$k_{eff,\ calc}$	$\sigma_{keff,calc}$
LEU-COMP-THERM-017-010	9.98E-02	2.35	0	0	1.0000	0.0031	0.997803	0.000096
LEU-COMP-THERM-017-011	9.80E-02	2.35	0	0	1.0000	0.0031	0.997685	0.000097
LEU-COMP-THERM-017-012	9.67E-02	2.35	0	0	1.0000	0.0031	0.99777	0.000074
LEU-COMP-THERM-017-013	9.53E-02	2.35	0	0	1.0000	0.0031	0.997854	0.000098
LEU-COMP-THERM-017-014	9.46E-02	2.35	0	0	1.0000	0.0031	0.99815	0.000095
LEU-COMP-THERM-017-015	1.78E-01	2.35	0	0	1.0000	0.0028	0.996779	0.000078
LEU-COMP-THERM-017-016	1.71E-01	2.35	0	0	1.0000	0.0028	0.997713	0.000082
LEU-COMP-THERM-017-017	1.66E-01	2.35	0	0	1.0000	0.0028	0.998876	0.000081
LEU-COMP-THERM-017-019	1.62E-01	2.35	0	0	1.0000	0.0028	0.998011	0.000072
LEU-COMP-THERM-017-020	1.61E-01	2.35	0	0	1.0000	0.0028	0.996572	0.000062
LEU-COMP-THERM-017-021	1.59E-01	2.35	0	0	1.0000	0.0028	0.996875	0.000079
LEU-COMP-THERM-017-022	1.58E-01	2.35	0	0	1.0000	0.0028	0.99572	0.000077
LEU-COMP-THERM-017-023	1.69E-01	2.35	0	0	1.0000	0.0028	0.99759	0.000087
LEU-COMP-THERM-017-024	1.64E-01	2.35	0	0	1.0000	0.0028	0.998278	0.000091
LEU-COMP-THERM-017-025	1.57E-01	2.35	0	0	1.0000	0.0028	0.996378	0.000085
LEU-COMP-THERM-017-028	2.81E-01	2.35	0	0	1.0000	0.0028	0.997606	0.000077
LEU-COMP-THERM-017-029	2.52E-01	2.35	0	0	1.0000	0.0028	0.997695	0.000086
LEU-COMP-THERM-022-001	6.69E-01	9.83	0	0	1.0000	0.0046	1.000598	0.000095
LEU-COMP-THERM-022-002	2.83E-01	9.83	0	0	1.0000	0.0046	1.005049	0.000098
LEU-COMP-THERM-022-003	1.24E-01	9.83	0	0	1.0000	0.0036	1.005889	0.000097
LEU-COMP-THERM-022-004	8.25E-02	9.83	0	0	1.0000	0.0037	1.006811	0.000099
LEU-COMP-THERM-022-005	6.86E-02	9.83	0	0	1.0000	0.0038	1.002592	0.000099
LEU-COMP-THERM-022-006	5.45E-02	9.83	0	0	1.0000	0.0046	1.001045	0.000099
LEU-COMP-THERM-022-007	5.40E-02	9.83	0	0	1.0000	0.0046	1.003828	0.000094
LEU-COMP-THERM-023-001	8.21E-02	9.83	0	0	1.0000	0.0044	0.994209	0.000099
LEU-COMP-THERM-023-002	7.62E-02	9.83	0	0	1.0000	0.0044	0.997167	0.000099

Table A.1 Critical experiments from IHECSBE and ENDF/B-VII 238 group library results (continued)

Experiment ID	EALF (eV)	Enrich (wt % ^{235}U)	Pu wt. fraction pu/(pu+u)	Sol. boron (ppm)	$k_{eff,\ exp}$	$\sigma_{keff,exp}$	$k_{eff,\ calc}$	$\sigma_{keff,calc}$
LEU-COMP-THERM-023-003	7.44E-02	9.83	0	0	1.0000	0.0044	0.998395	0.000099
LEU-COMP-THERM-023-004	7.26E-02	9.83	0	0	1.0000	0.0044	1.000376	0.000099
LEU-COMP-THERM-023-005	7.11E-02	9.83	0	0	1.0000	0.0044	1.00118	0.000099
LEU-COMP-THERM-023-006	6.97E-02	9.83	0	0	1.0000	0.0044	1.001677	0.000099
LEU-COMP-THERM-024-001	1.00E+00	9.83	0	0	1.0000	0.0054	0.999404	0.000098
LEU-COMP-THERM-024-002	1.40E-01	9.83	0	0	1.0000	0.0040	1.012075	0.000092
LEU-COMP-THERM-026-003	9.69E-01	4.92	0	0	1.0018	0.0062	1.003422	0.000099
LEU-COMP-THERM-042-001	1.69E-01	2.35	0	0	1.0000	0.0016	0.996729	0.000095
LEU-COMP-THERM-042-002	1.75E-01	2.35	0	0	1.0000	0.0016	0.996887	0.000093
LEU-COMP-THERM-042-003	1.82E-01	2.35	0	0	1.0000	0.0016	0.997765	0.000089
LEU-COMP-THERM-042-004	1.80E-01	2.35	0	0	1.0000	0.0017	0.99861	0.000093
LEU-COMP-THERM-042-005	1.77E-01	2.35	0	0	1.0000	0.0033	0.998294	0.000097
LEU-COMP-THERM-042-006	1.69E-01	2.35	0	0	1.0000	0.0016	0.998138	0.000086
LEU-COMP-THERM-042-007	1.74E-01	2.35	0	0	1.0000	0.0018	0.996322	0.000097
LEU-COMP-THERM-050-001	1.99E-01	4.74	0	0	1.0004	0.0010	0.99735	0.000099
LEU-COMP-THERM-050-002	1.90E-01	4.74	0	0	1.0004	0.0010	0.997352	0.000096
LEU-COMP-THERM-050-003	2.07E-01	4.74	0	822	1.0004	0.0010	0.99787	0.000099
LEU-COMP-THERM-050-004	1.97E-01	4.74	0	822	1.0004	0.0010	0.997357	0.000099
LEU-COMP-THERM-050-005	2.22E-01	4.74	0	5030	1.0004	0.0010	0.998855	0.000099
LEU-COMP-THERM-050-006	2.13E-01	4.74	0	5030	1.0004	0.0010	0.998444	0.0001
LEU-COMP-THERM-050-007	2.09E-01	4.74	0	5030	1.0004	0.0010	0.99875	0.000099
LEU-COMP-THERM-050-008	2.07E-01	4.74	0	0	1.0004	0.0010	0.995679	0.000099
LEU-COMP-THERM-050-009	1.96E-01	4.74	0	0	1.0004	0.0010	0.996095	0.000098
LEU-COMP-THERM-050-010	1.94E-01	4.74	0	0	1.0004	0.0010	0.995822	0.0001
LEU-COMP-THERM-050-011	2.15E-01	4.74	0	0	1.0004	0.0010	0.996621	0.000099
LEU-COMP-THERM-050-012	2.02E-01	4.74	0	0	1.0004	0.0010	0.997669	0.0001

Table A.1 Critical experiments from IHECSBE and ENDF/B-VII 238 group library results (continued)

Experiment ID	EALF (eV)	Enrich (wt % ^{235}U)	Pu wt. fraction pu/(pu+u)	Sol. boron (ppm)	$k_{eff,\ exp}$	$\sigma_{keff,exp}$	$k_{eff,\ calc}$	$\sigma_{keff,calc}$
LEU-COMP-THERM-050-013	1.99E-01	4.74	0	0	1.0004	0.0010	0.997671	0.000099
LEU-COMP-THERM-050-014	2.09E-01	4.74	0	0	1.0004	0.0010	0.9972	0.000099
LEU-COMP-THERM-050-015	2.07E-01	4.74	0	0	1.0004	0.0010	0.997948	0.000096
LEU-COMP-THERM-050-016	2.11E-01	4.74	0	0	1.0004	0.0010	0.999065	0.000099
LEU-COMP-THERM-050-017	2.10E-01	4.74	0	0	1.0004	0.0010	0.998805	0.0001
LEU-COMP-THERM-050-018	2.09E-01	4.74	0	0	1.0004	0.0010	0.998664	0.000099
LEU-COMP-THERM-079-001	2.96E-01	4.31	0	0	0.9999	0.0016	0.997516	0.000099
LEU-COMP-THERM-079-002	2.96E-01	4.31	0	0	1.0002	0.0016	0.99805	0.000099
LEU-COMP-THERM-079-003	3.01E-01	4.31	0	0	1.0005	0.0016	0.998475	0.000099
LEU-COMP-THERM-079-004	3.04E-01	4.31	0	0	1.0004	0.0016	0.998773	0.000099
LEU-COMP-THERM-079-005	3.09E-01	4.31	0	0	1.0004	0.0016	0.998973	0.000099
LEU-COMP-THERM-079-006	1.08E-01	4.31	0	0	0.9994	0.0008	0.998495	0.000099
LEU-COMP-THERM-079-007	1.08E-01	4.31	0	0	1.0003	0.0008	0.999274	0.000099
LEU-COMP-THERM-079-008	1.09E-01	4.31	0	0	1.0008	0.0008	1.000116	0.000099
LEU-COMP-THERM-079-009	1.10E-01	4.31	0	0	1.0003	0.0008	0.999749	0.000099
LEU-COMP-THERM-079-010	1.11E-01	4.31	0	0	1.0009	0.0008	1.000526	0.0001
LEU-MISC-THERM-005-001	1.15E-01	6.00	0	0	1.0000	0.0007	1.002596	0.0001
LEU-MISC-THERM-005-002	1.17E-01	6.00	0	0	1.0001	0.0007	1.002947	0.000099
LEU-MISC-THERM-005-003	1.19E-01	6.00	0	0	0.9999	0.0007	1.003035	0.000099
LEU-MISC-THERM-005-004	1.19E-01	6.00	0	0	1.0000	0.0007	1.002881	0.000099
LEU-MISC-THERM-005-005	1.19E-01	6.00	0	0	1.0000	0.0007	1.003026	0.000099
LEU-MISC-THERM-005-006	1.19E-01	6.00	0	0	1.0000	0.0007	1.003598	0.000099
LEU-MISC-THERM-005-007	1.19E-01	6.00	0	0	0.9999	0.0007	1.003058	0.000099
LEU-MISC-THERM-005-008	1.19E-01	6.00	0	0	0.9999	0.0007	1.002492	0.000099
LEU-MISC-THERM-005-009	1.19E-01	6.00	0	0	0.9999	0.0007	1.003133	0.000099
LEU-MISC-THERM-005-010	1.20E-01	6.00	0	0	0.9998	0.0007	1.002479	0.000099
LEU-MISC-THERM-005-011	1.20E-01	6.00	0	0	0.9999	0.0007	1.002549	0.000099

Table A.1 Critical experiments from IHECSBE and ENDF/B-VII 238 group library results (continued)

Experiment ID	EALF (eV)	Enrich (wt % ^{235}U)	Pu wt. fraction pu/(pu+u)	Sol. boron (ppm)	$k_{eff,\ exp}$	$\sigma_{keff,exp}$	$k_{eff,\ calc}$	$\sigma_{keff,calc}$
LEU-MISC-THERM-005-012	1.20E-01	6.00	0	0	0.9999	0.0007	1.002305	0.000098
LEU-SOL-THERM-002-001	3.75E-02	4.89	0	0	1.0038	0.0040	1.000262	0.000099
LEU-SOL-THERM-002-002	3.93E-02	4.89	0	0	1.0024	0.0037	0.996015	0.000099
LEU-SOL-THERM-002-003	3.85E-02	4.89	0	0	1.0024	0.0044	1.001281	0.000099
LEU-SOL-THERM-003-001	4.02E-02	10.19	0	0	0.9997	0.0039	0.996464	0.000095
LEU-SOL-THERM-003-002	3.84E-02	10.19	0	0	0.9993	0.0042	0.995342	0.000099
LEU-SOL-THERM-003-003	3.81E-02	10.19	0	0	0.9995	0.0042	0.999539	0.000099
LEU-SOL-THERM-003-004	3.80E-02	10.19	0	0	0.9995	0.0042	0.993066	0.000099
LEU-SOL-THERM-003-005	3.54E-02	10.19	0	0	0.9997	0.0048	0.997705	0.000092
LEU-SOL-THERM-003-006	3.51E-02	10.19	0	0	0.9999	0.0049	0.998171	0.000099
LEU-SOL-THERM-003-007	3.49E-02	10.19	0	0	0.9994	0.0049	0.996629	0.000099
LEU-SOL-THERM-003-008	3.39E-02	10.19	0	0	0.9993	0.0052	0.999996	0.000095
LEU-SOL-THERM-003-009	3.38E-02	10.19	0	0	0.9996	0.0052	0.997637	0.000097
LEU-SOL-THERM-004-001	4.08E-02	9.97	0	0	0.9994	0.0008	1.00028	0.00048
LEU-SOL-THERM-004-002	3.98E-02	9.97	0	0	0.9999	0.0009	1.00119	0.00049
LEU-SOL-THERM-004-003	3.86E-02	9.97	0	0	0.9999	0.0009	0.99914	0.00047
LEU-SOL-THERM-004-004	3.78E-02	9.97	0	0	0.9999	0.0010	1.00182	0.00048
LEU-SOL-THERM-004-005	3.73E-02	9.97	0	0	0.9999	0.0010	1.00126	0.00046
LEU-SOL-THERM-004-006	3.68E-02	9.97	0	0	0.9994	0.0011	1.00059	0.00046
LEU-SOL-THERM-004-007	3.65E-02	9.97	0	0	0.9996	0.0011	1.00045	0.00041
MIX-COMP-THERM-001-001	9.48E-01	0.71	2.24E-01	0	1.0000	0.0025	1.000159	0.000099
MIX-COMP-THERM-001-002	2.68E-01	0.71	2.24E-01	0	1.0000	0.0026	0.999358	0.000099
MIX-COMP-THERM-001-003	1.62E-01	0.71	2.24E-01	0	1.0000	0.0032	0.997994	0.000099
MIX-COMP-THERM-001-004	1.13E-01	0.71	2.24E-01	0	1.0000	0.0039	1.000355	0.000099
MIX-COMP-THERM-002-001S	5.29E-01	0.71	2.04E-02	2	1.0024	0.0060	1.000817	0.000099
MIX-COMP-THERM-002-002S	7.01E-01	0.71	2.04E-02	688	1.0009	0.0047	1.001113	0.000099
MIX-COMP-THERM-002-003S	1.85E-01	0.71	2.04E-02	1	1.0042	0.0031	1.002517	0.000099

Table A.1 Critical experiments from IHECSBE and ENDF/B-VII 238 group library results (continued)

Experiment ID	EALF (eV)	Enrich (wt % ^{235}U)	Pu wt. fraction pu/(pu+u)	Sol. boron (ppm)	$k_{eff,\ exp}$	$\sigma_{keff,exp}$	$k_{eff,\ calc}$	$\sigma_{keff,calc}$
MIX-COMP-THERM-002-004S	2.69E-01	0.71	2.04E-02	1090	1.0024	0.0024	1.005391	0.000099
MIX-COMP-THERM-002-005S	1.33E-01	0.71	2.04E-02	2	1.0038	0.0025	1.004704	0.000099
MIX-COMP-THERM-002-006S	1.76E-01	0.71	2.04E-02	767	1.0029	0.0027	1.005547	0.000099
MIX-COMP-THERM-003-001	8.50E-01	0.71	6.59E-02	0	1.0000	0.0072	1.000332	0.000069
MIX-COMP-THERM-003-002	5.17E-01	0.71	6.59E-02	0	1.0000	0.0059	1.001006	0.000069
MIX-COMP-THERM-003-003	6.13E-01	0.71	6.59E-02	337	1.0000	0.0054	1.000343	0.000069
MIX-COMP-THERM-003-004	1.81E-01	0.71	6.59E-02	0	1.0000	0.0031	1.001825	0.000069
MIX-COMP-THERM-003-005	1.50E-01	0.71	6.59E-02	0	1.0000	0.0027	1.001288	0.000069
MIX-COMP-THERM-003-006	9.83E-02	0.71	6.59E-02	0	1.0000	0.0023	1.002059	0.000069
MIX-COMP-THERM-004-001	1.39E-01	0.71	3.00E-02	0	1.0000	0.0046	0.995528	0.000099
MIX-COMP-THERM-004-002	1.38E-01	0.71	2.99E-02	0	1.0000	0.0046	0.996398	0.000099
MIX-COMP-THERM-004-003	1.38E-01	0.71	2.98E-02	0	1.0000	0.0046	0.996654	0.000099
MIX-COMP-THERM-004-004	1.15E-01	0.71	3.00E-02	0	1.0000	0.0039	0.996191	0.000099
MIX-COMP-THERM-004-005	1.14E-01	0.71	2.99E-02	0	1.0000	0.0039	0.997207	0.000099
MIX-COMP-THERM-004-006	1.13E-01	0.71	2.98E-02	0	1.0000	0.0039	0.997597	0.000096
MIX-COMP-THERM-004-007	8.98E-02	0.71	3.00E-02	0	1.0000	0.0040	0.997248	0.000099
MIX-COMP-THERM-004-008	8.95E-02	0.71	2.99E-02	0	1.0000	0.0040	0.997929	0.000099
MIX-COMP-THERM-004-009	8.91E-02	0.71	2.98E-02	0	1.0000	0.0040	0.998696	0.000099
MIX-COMP-THERM-004-010	7.76E-02	0.71	3.00E-02	0	1.0000	0.0051	0.998083	0.000099
MIX-COMP-THERM-004-011	7.73E-02	0.71	2.99E-02	0	1.0000	0.0051	0.99853	0.000099
MIX-COMP-THERM-005-001	3.73E-01	0.71	3.99E-02	0	1.0008	0.0022	1.001774	0.000099
MIX-COMP-THERM-005-002	2.48E-01	0.71	3.99E-02	0	1.0011	0.0026	0.999535	0.000097
MIX-COMP-THERM-005-003	1.71E-01	0.71	3.99E-02	0	1.0016	0.0029	1.006808	0.000098
MIX-COMP-THERM-005-004	1.41E-01	0.71	3.99E-02	0	1.0021	0.0028	1.029384	0.000099
MIX-COMP-THERM-005-005	1.06E-01	0.71	3.99E-02	0	1.0026	0.0036	1.005849	0.000099
MIX-COMP-THERM-005-006	9.17E-02	0.71	3.99E-02	0	1.0033	0.0042	1.005577	0.000095
MIX-COMP-THERM-005-007	8.75E-02	0.71	3.99E-02	0	1.0035	0.0042	1.007526	0.000099

Table A.1 Critical experiments from IHECSBE and ENDF/B-VII 238 group library results (continued)

Experiment ID	EALF (eV)	Enrich (wt % ^{235}U)	Pu wt. fraction pu/(pu+u)	Sol. boron (ppm)	$k_{eff,\ exp}$	$\sigma_{keff,exp}$	$k_{eff,\ calc}$	$\sigma_{keff,calc}$
MIX-COMP-THERM-006-001	3.57E-01	0.71	2.04E-02	0	1.0016	0.0051	0.996918	0.000099
MIX-COMP-THERM-006-002	1.88E-01	0.71	2.04E-02	0	1.0017	0.0036	1.000826	0.000098
MIX-COMP-THERM-006-003	1.37E-01	0.71	2.04E-02	0	1.0026	0.0036	0.99683	0.000087
MIX-COMP-THERM-006-004	1.17E-01	0.71	2.04E-02	0	1.0051	0.0044	1.002949	0.000098
MIX-COMP-THERM-006-005	9.56E-02	0.71	2.04E-02	0	1.0040	0.0054	1.003484	0.000099
MIX-COMP-THERM-006-006	9.06E-02	0.71	2.04E-02	0	1.0055	0.0051	1.00127	0.000098
MIX-COMP-THERM-006-007	1.36E-01	0.71	2.04E-02	0	1.0024	0.0045	0.994319	0.000099
MIX-COMP-THERM-006-008	1.37E-01	0.71	2.04E-02	0	1.0035	0.0044	0.99387	0.000098
MIX-COMP-THERM-006-009	1.37E-01	0.71	2.04E-02	0	1.0035	0.0044	0.993377	0.000097
MIX-COMP-THERM-006-010	1.37E-01	0.71	2.04E-02	0	1.0021	0.0044	0.991588	0.000099
MIX-COMP-THERM-006-011	1.37E-01	0.71	2.04E-02	0	1.0032	0.0044	0.99167	0.000095
MIX-COMP-THERM-006-012	1.38E-01	0.71	2.04E-02	0	1.0032	0.0044	0.991285	0.000099
MIX-COMP-THERM-006-013	1.37E-01	0.71	2.04E-02	0	1.0021	0.0044	0.99269	0.000099
MIX-COMP-THERM-006-014	1.37E-01	0.71	2.04E-02	0	1.0026	0.0044	0.992422	0.000099
MIX-COMP-THERM-006-015	1.37E-01	0.71	2.04E-02	0	1.0033	0.0044	0.992061	0.000098
MIX-COMP-THERM-006-016	1.37E-01	0.71	2.04E-02	0	1.0035	0.0045	0.993068	0.000098
MIX-COMP-THERM-006-017	1.38E-01	0.71	2.04E-02	0	1.0026	0.0046	0.990815	0.000099
MIX-COMP-THERM-006-018	1.38E-01	0.71	2.04E-02	0	1.0023	0.0045	0.989968	0.000098
MIX-COMP-THERM-006-019	1.38E-01	0.71	2.04E-02	0	1.0032	0.0045	0.990804	0.000099
MIX-COMP-THERM-006-020	1.38E-01	0.71	2.04E-02	0	1.0033	0.0045	0.990674	0.000099
MIX-COMP-THERM-006-021	1.38E-01	0.71	2.04E-02	0	1.0030	0.0045	0.989963	0.000099
MIX-COMP-THERM-006-022	1.38E-01	0.71	2.04E-02	0	1.0024	0.0045	0.989822	0.000099
MIX-COMP-THERM-006-023	1.38E-01	0.71	2.04E-02	0	1.0030	0.0045	0.990511	0.000099
MIX-COMP-THERM-006-024	1.38E-01	0.71	2.04E-02	0	1.0030	0.0045	0.990545	0.000097
MIX-COMP-THERM-006-025	1.38E-01	0.71	2.04E-02	0	1.0024	0.0045	0.990283	0.000097
MIX-COMP-THERM-006-026	1.38E-01	0.71	2.04E-02	0	1.0021	0.0045	0.990283	0.000097
MIX-COMP-THERM-006-027	1.38E-01	0.71	2.04E-02	0	1.0033	0.0045	0.990749	0.000099

Table A.1 Critical experiments from IHECSBE and ENDF/B-VII 238 group library results (continued)

Experiment ID	EALF (eV)	Enrich (wt % ^{235}U)	Pu wt. fraction pu/(pu+u)	Sol. boron (ppm)	$k_{eff,\ exp}$	$\sigma_{keff,exp}$	$k_{eff,\ calc}$	$\sigma_{keff,calc}$
MIX-COMP-THERM-006-028	1.38E-01	0.71	2.04E-02	0	1.0033	0.0046	0.990997	0.000099
MIX-COMP-THERM-006-029	9.53E-02	0.71	2.04E-02	0	1.0040	0.0087	0.9986	0.000099
MIX-COMP-THERM-006-030	9.54E-02	0.71	2.04E-02	0	1.0043	0.0087	0.997537	0.000099
MIX-COMP-THERM-006-031	9.55E-02	0.71	2.04E-02	0	1.0045	0.0087	0.996976	0.000099
MIX-COMP-THERM-006-032	9.56E-02	0.71	2.04E-02	0	1.0037	0.0087	0.995413	0.000099
MIX-COMP-THERM-006-033	9.57E-02	0.71	2.04E-02	0	1.0043	0.0087	0.995252	0.000099
MIX-COMP-THERM-006-034	9.58E-02	0.71	2.04E-02	0	1.0037	0.0087	0.994231	0.000099
MIX-COMP-THERM-006-035	9.55E-02	0.71	2.04E-02	0	1.0044	0.0087	0.997611	0.000099
MIX-COMP-THERM-006-036	9.56E-02	0.71	2.04E-02	0	1.0036	0.0087	0.995737	0.000098
MIX-COMP-THERM-006-037	9.58E-02	0.71	2.04E-02	0	1.0041	0.0087	0.995159	0.000098
MIX-COMP-THERM-006-038	9.57E-02	0.71	2.04E-02	0	1.0044	0.0087	0.995777	0.000098
MIX-COMP-THERM-006-039	9.60E-02	0.71	2.04E-02	0	1.0042	0.0088	0.993265	0.000097
MIX-COMP-THERM-006-040	9.60E-02	0.71	2.04E-02	0	1.0038	0.0087	0.992624	0.000099
MIX-COMP-THERM-006-041	9.60E-02	0.71	2.04E-02	0	1.0038	0.0087	0.992568	0.000099
MIX-COMP-THERM-006-042	9.60E-02	0.71	2.04E-02	0	1.0036	0.0087	0.992334	0.000097
MIX-COMP-THERM-006-043	9.59E-02	0.71	2.04E-02	0	1.0044	0.0087	0.993355	0.000092
MIX-COMP-THERM-006-044	9.60E-02	0.71	2.04E-02	0	1.0044	0.0087	0.992866	0.000098
MIX-COMP-THERM-006-045	9.60E-02	0.71	2.04E-02	0	1.0040	0.0087	0.992938	0.000099
MIX-COMP-THERM-006-046	9.60E-02	0.71	2.04E-02	0	1.0040	0.0087	0.992937	0.000099
MIX-COMP-THERM-006-047	9.60E-02	0.71	2.04E-02	0	1.0040	0.0087	0.992773	0.000099
MIX-COMP-THERM-006-048	9.60E-02	0.71	2.04E-02	0	1.0038	0.0087	0.992773	0.000099
MIX-COMP-THERM-006-049	9.60E-02	0.71	2.04E-02	0	1.0039	0.0087	0.992862	0.000096
MIX-COMP-THERM-006-050	9.60E-02	0.71	2.04E-02	0	1.0044	0.0087	0.99344	0.000097
MIX-COMP-THERM-007-001	1.89E-01	0.71	1.99E-02	0	1.0023	0.0035	1.00338	0.000099
MIX-COMP-THERM-007-002	1.38E-01	0.71	1.99E-02	0	1.0024	0.0039	0.998968	0.000099
MIX-COMP-THERM-007-003	1.16E-01	0.71	1.99E-02	0	1.0036	0.0046	1.001016	0.000099
MIX-COMP-THERM-007-004	9.58E-02	0.71	1.99E-02	0	1.0037	0.0057	1.000812	0.000094

Table A.1 Critical experiments from IHECSBE and ENDF/B-VII 238 group library results (continued)

Experiment ID	EALF (eV)	Enrich (wt % ^{235}U)	Pu wt. fraction pu/(pu+u)	Sol. boron (ppm)	$k_{eff,\ exp}$	$\sigma_{keff,exp}$	$k_{eff,\ calc}$	$\sigma_{keff,calc}$
MIX-COMP-THERM-007-005	9.08E-02	0.71	1.99E-02	0	1.0044	0.0061	0.998979	0.000099
MIX-COMP-THERM-008-001	3.79E-01	0.71	2.00E-02	0	0.9997	0.0032	0.997268	0.000095
MIX-COMP-THERM-008-002	1.93E-01	0.71	2.00E-02	0	1.0008	0.0030	0.998639	0.000099
MIX-COMP-THERM-008-003	1.39E-01	0.71	2.00E-02	0	1.0023	0.0038	0.998631	0.000099
MIX-COMP-THERM-008-003_Al	1.38E-01	0.71	2.00E-02	0	1.0023	0.0039	0.996786	0.000095
MIX-COMP-THERM-008-003_B1	1.39E-01	0.71	2.00E-02	0	1.0023	0.0039	0.994897	0.000099
MIX-COMP-THERM-008-003_B2	1.39E-01	0.71	2.00E-02	0	1.0023	0.0039	0.995821	0.000091
MIX-COMP-THERM-008-003_B3	1.39E-01	0.71	2.00E-02	0	1.0023	0.0039	0.9961	0.000099
MIX-COMP-THERM-008-003_B4	1.38E-01	0.71	2.00E-02	0	1.0023	0.0039	0.996278	0.000097
MIX-COMP-THERM-008-003_CdAir	1.39E-01	0.71	2.00E-02	0	1.0023	0.0040	0.995047	0.000093
MIX-COMP-THERM-008-003_CdAl	1.39E-01	0.71	2.00E-02	0	1.0023	0.0041	0.995691	0.000099
MIX-COMP-THERM-008-003_CdB1	1.40E-01	0.71	2.00E-02	0	1.0023	0.0041	0.994727	0.000099
MIX-COMP-THERM-008-003_CdB2	1.40E-01	0.71	2.00E-02	0	1.0023	0.0041	0.995156	0.00009
MIX-COMP-THERM-008-003_CdB3	1.40E-01	0.71	2.00E-02	0	1.0023	0.0041	0.995418	0.000099
MIX-COMP-THERM-008-003_CdB4	1.39E-01	0.71	2.00E-02	0	1.0023	0.0041	0.994738	0.000099
MIX-COMP-THERM-008-003_CdH1	1.40E-01	0.71	2.00E-02	0	1.0023	0.0041	0.995504	0.000095
MIX-COMP-THERM-008-003_CdH2	1.40E-01	0.71	2.00E-02	0	1.0023	0.0041	0.99496	0.000097
MIX-COMP-THERM-008-003_CdH3	1.40E-01	0.71	2.00E-02	0	1.0023	0.0041	0.995141	0.000099
MIX-COMP-THERM-008-003_CdH4	1.40E-01	0.71	2.00E-02	0	1.0023	0.0041	0.995274	0.000099
MIX-COMP-THERM-008-003_CdH5	1.40E-01	0.71	2.00E-02	0	1.0023	0.0041	0.994902	0.000099
MIX-COMP-THERM-008-003_CdWater	1.40E-01	0.71	2.00E-02	0	1.0023	0.0040	0.994952	0.000095
MIX-COMP-THERM-008-003_H1	1.39E-01	0.71	2.00E-02	0	1.0023	0.0039	0.995021	0.000097
MIX-COMP-THERM-008-003_H2	1.39E-01	0.71	2.00E-02	0	1.0023	0.0039	0.995538	0.000097
MIX-COMP-THERM-008-003_H3	1.39E-01	0.71	2.00E-02	0	1.0023	0.0039	0.996075	0.000097
MIX-COMP-THERM-008-003_H4	1.38E-01	0.71	2.00E-02	0	1.0023	0.0039	0.996986	0.000097
MIX-COMP-THERM-008-003_H5	1.38E-01	0.71	2.00E-02	0	1.0023	0.0039	0.997032	0.000097
MIX-COMP-THERM-008-004	1.17E-01	0.71	2.00E-02	0	1.0015	0.0047	1.001757	0.000099

Table A.1 Critical experiments from IHECSBE and ENDF/B-VII 238 group library results (continued)

Experiment ID	EALF (eV)	Enrich (wt % ^{235}U)	Pu wt. fraction pu/(pu+u)	Sol. boron (ppm)	$k_{eff,\ exp}$	$\sigma_{keff,exp}$	$k_{eff,\ calc}$	$\sigma_{keff,calc}$
MIX-COMP-THERM-008-005	9.58E-02	0.71	2.00E-02	0	1.0022	0.0056	1.002015	0.000099
MIX-COMP-THERM-008-006	9.08E-02	0.71	2.00E-02	0	1.0028	0.0065	1.001537	0.000096
MIX-COMP-THERM-009-001	5.17E-01	0.16	1.50E-02	0	1.0003	0.0054	0.999726	0.000092
MIX-COMP-THERM-009-002	3.09E-01	0.16	1.50E-02	0	1.0020	0.0049	0.993582	0.000097
MIX-COMP-THERM-009-003	1.57E-01	0.16	1.50E-02	0	1.0035	0.0050	0.997231	0.000092
MIX-COMP-THERM-009-004	1.18E-01	0.16	1.50E-02	0	1.0046	0.0062	0.99804	0.000086
MIX-COMP-THERM-009-005	9.61E-02	0.16	1.50E-02	0	1.0059	0.0074	1.00071	0.000094
MIX-COMP-THERM-009-006	9.07E-02	0.16	1.50E-02	0	1.0067	0.0080	0.992724	0.000092
MIX-COMP-THERM-011-001	5.46E-01	59.70	2.56E-01	0	1.0000	0.0024	1.002152	0.000099
MIX-COMP-THERM-011-002	5.39E-01	59.70	2.56E-01	0	1.0000	0.0024	1.003254	0.000099
MIX-COMP-THERM-011-003	5.18E-01	59.70	2.56E-01	0	1.0000	0.0025	1.002025	0.000099
MIX-COMP-THERM-011-004	2.46E-01	59.70	2.56E-01	0	1.0000	0.0018	0.999383	0.000098
MIX-COMP-THERM-011-005	2.52E-01	59.70	2.56E-01	0	1.0000	0.0016	0.999688	0.000099
MIX-COMP-THERM-011-006	2.59E-01	59.70	2.56E-01	0	1.0000	0.0016	0.999501	0.000099
MIX-COMP-THERM-012-001	1.33E-01	0.15	7.58E-02	0	1.0052	0.0067	0.97879	0.000099
MIX-COMP-THERM-012-002	1.33E-01	0.15	7.58E-02	0	1.0052	0.0067	0.979883	0.000097
MIX-COMP-THERM-012-003	1.33E-01	0.15	7.58E-02	0	1.0052	0.0067	0.977197	0.000099
MIX-COMP-THERM-012-004	1.34E-01	0.15	7.58E-02	0	1.0052	0.0067	0.981166	0.000099
MIX-COMP-THERM-012-005	1.33E-01	0.15	7.58E-02	0	1.0052	0.0067	0.979784	0.000099
MIX-COMP-THERM-012-006	1.34E-01	0.15	7.58E-02	0	1.0052	0.0075	0.983882	0.000099
MIX-COMP-THERM-012-007	6.44E-02	0.15	7.88E-02	0	1.0053	0.0134	1.033937	0.000099
MIX-COMP-THERM-012-008	6.43E-02	0.15	7.88E-02	0	1.0053	0.0055	1.029094	0.000098
MIX-COMP-THERM-012-009	6.41E-02	0.15	7.88E-02	0	1.0053	0.0055	1.026901	0.000099
MIX-COMP-THERM-012-010	6.41E-02	0.15	7.88E-02	0	1.0053	0.0055	1.026621	0.000099
MIX-COMP-THERM-012-011	6.41E-02	0.15	7.88E-02	0	1.0053	0.0055	1.025248	0.000099
MIX-COMP-THERM-012-012	6.42E-02	0.15	7.88E-02	0	1.0053	0.0055	1.027569	0.000099
MIX-COMP-THERM-012-013	6.45E-02	0.15	7.88E-02	0	1.0053	0.0158	1.036086	0.000099

Table A.1 Critical experiments from IHECSBE and ENDF/B-VII 238 group library results (continued)

Experiment ID	EALF (eV)	Enrich (wt % ^{235}U)	Pu wt. fraction pu/(pu+u)	Sol. boron (ppm)	$k_{eff,\ exp}$	$\sigma_{keff,exp}$	$k_{eff,\ calc}$	$\sigma_{keff,calc}$
MIX-COMP-THERM-012-014	1.38E-01	0.15	1.46E-01	0	1.0012	0.0086	1.025491	0.000098
MIX-COMP-THERM-012-015	1.37E-01	0.15	1.46E-01	0	1.0012	0.0086	1.024827	0.000099
MIX-COMP-THERM-012-016	1.36E-01	0.15	1.46E-01	0	1.0012	0.0086	1.022106	0.000099
MIX-COMP-THERM-012-017	1.35E-01	0.15	1.46E-01	0	1.0012	0.0086	1.021574	0.000099
MIX-COMP-THERM-012-018	1.35E-01	0.15	1.46E-01	0	1.0012	0.0086	1.020982	0.000093
MIX-COMP-THERM-012-019	1.34E-01	0.15	1.46E-01	0	1.0012	0.0086	1.020518	0.000099
MIX-COMP-THERM-012-020	1.89E-01	0.15	1.46E-01	0	1.0014	0.0120	1.019034	0.000098
MIX-COMP-THERM-012-021	1.89E-01	0.15	1.46E-01	0	1.0014	0.0152	1.017898	0.000099
MIX-COMP-THERM-012-022	2.02E-01	0.15	1.46E-01	0	1.0014	0.0086	1.012976	0.000099
MIX-COMP-THERM-012-023	1.58E-01	0.15	3.00E-01	0	1.0007	0.0114	1.015748	0.000099
MIX-COMP-THERM-012-024	1.58E-01	0.15	3.00E-01	0	1.0007	0.0114	1.016363	0.000099
MIX-COMP-THERM-012-025	1.57E-01	0.15	3.00E-01	0	1.0007	0.0114	1.015311	0.000099
MIX-COMP-THERM-012-026	1.54E-01	0.15	3.00E-01	0	1.0007	0.0114	1.013192	0.000099
MIX-COMP-THERM-012-027	1.53E-01	0.15	3.00E-01	0	1.0007	0.0114	1.014137	0.000099
MIX-COMP-THERM-012-028	1.52E-01	0.15	3.00E-01	0	1.0007	0.0114	1.016432	0.000099
MIX-COMP-THERM-012-029	1.51E-01	0.15	3.00E-01	0	1.0007	0.0114	1.015605	0.000099
MIX-COMP-THERM-012-030	1.54E-01	0.15	3.00E-01	0	1.0007	0.0114	1.01417	0.0001
MIX-COMP-THERM-012-031	2.36E-01	0.15	3.00E-01	0	1.0017	0.0151	1.000971	0.000099
MIX-COMP-THERM-012-032	2.36E-01	0.15	3.00E-01	0	1.0017	0.0151	1.001484	0.000099
MIX-COMP-THERM-012-033	2.36E-01	0.15	3.00E-01	0	1.0017	0.0151	0.998008	0.000099
MIX-SOL-THERM-001-001	1.54E-01	0.70	2.19E-01	3	1.0000	0.0016	0.997637	0.000099
MIX-SOL-THERM-001-002	1.55E-01	0.70	2.20E-01	3	1.0000	0.0016	0.997643	0.000099
MIX-SOL-THERM-001-003	1.51E-01	0.70	2.21E-01	3	1.0000	0.0016	0.992688	0.000099
MIX-SOL-THERM-001-004	1.64E-01	0.70	2.22E-01	3	1.0000	0.0016	0.99689	0.000099
MIX-SOL-THERM-001-005	1.68E-01	0.70	2.21E-01	3	1.0000	0.0016	1.001138	0.000098
MIX-SOL-THERM-001-006	1.62E-01	0.70	2.22E-01	3	1.0000	0.0016	1.000883	0.000096
MIX-SOL-THERM-001-007	2.71E-01	2.29	9.68E-01	3	1.0000	0.0016	1.002787	0.000099

Table A.1 Critical experiments from IHECSBE and ENDF/B-VII 238 group library results (continued)

Experiment ID	EALF (eV)	Enrich (wt % ^{235}U)	Pu wt. fraction pu/(pu+u)	Sol. boron (ppm)	$k_{eff,\ exp}$	$\sigma_{keff,exp}$	$k_{eff,\ calc}$	$\sigma_{keff,calc}$
MIX-SOL-THERM-001-008	1.43E-01	2.29	9.67E-01	2	1.0000	0.0016	1.001542	0.000099
MIX-SOL-THERM-001-009	8.95E-02	2.29	9.62E-01	1	1.0000	0.0016	1.000502	0.000099
MIX-SOL-THERM-001-010	1.11E-01	0.70	2.27E-01	2	1.0000	0.0016	1.0018	0.000099
MIX-SOL-THERM-001-011	1.08E-01	0.70	2.27E-01	2	1.0000	0.0050	1.007492	0.000099
MIX-SOL-THERM-001-012	1.05E-01	0.70	2.28E-01	2	1.0000	0.0050	1.008659	0.000098
MIX-SOL-THERM-001-013	8.16E-02	0.70	2.25E-01	2	1.0000	0.0016	0.997657	0.000096
MIX-SOL-THERM-002-001	4.18E-02	0.71	5.18E-01	1	1.0000	0.0024	1.003318	0.000097
MIX-SOL-THERM-002-002	4.17E-02	0.71	5.21E-01	1	1.0000	0.0024	1.003638	0.000092
MIX-SOL-THERM-002-003	4.27E-02	0.44	2.29E-01	1	1.0000	0.0024	1.003091	0.000097
MIX-SOL-THERM-004-001	6.95E-02	0.56	3.97E-01	2	1.0000	0.0033	0.996676	0.000099
MIX-SOL-THERM-004-002	6.55E-02	0.56	3.97E-01	2	1.0000	0.0033	0.996823	0.000099
MIX-SOL-THERM-004-003	6.81E-02	0.56	3.97E-01	2	1.0000	0.0068	0.998696	0.000099
MIX-SOL-THERM-004-004	1.69E-01	0.56	4.06E-01	4	1.0000	0.0078	1.001814	0.0001
MIX-SOL-THERM-004-005	1.54E-01	0.56	4.05E-01	4	1.0000	0.0029	0.997132	0.000099
MIX-SOL-THERM-004-006	1.85E-01	0.56	4.05E-01	4	1.0000	0.0029	0.996693	0.000099
MIX-SOL-THERM-004-007	3.36E-01	0.56	3.96E-01	5	1.0000	0.0026	0.998081	0.000099
MIX-SOL-THERM-004-008	2.55E-01	0.56	3.97E-01	5	1.0000	0.0026	0.998146	0.000099
MIX-SOL-THERM-004-009	2.95E-01	0.56	3.97E-01	5	1.0000	0.0077	0.998954	0.0001
MIX-SOL-THERM-005-001	6.93E-02	0.56	3.95E-01	2	1.0000	0.0037	0.992799	0.000097
MIX-SOL-THERM-005-002	6.50E-02	0.56	3.98E-01	2	1.0000	0.0037	1.000418	0.000098
MIX-SOL-THERM-005-003	1.49E-01	0.56	4.07E-01	4	1.0000	0.0037	1.002735	0.000098
MIX-SOL-THERM-005-004	1.46E-01	0.56	4.07E-01	4	1.0000	0.0037	1.000902	0.000096
MIX-SOL-THERM-005-005	1.86E-01	0.56	4.06E-01	4	1.0000	0.0037	0.988772	0.000096
MIX-SOL-THERM-005-006	3.39E-01	0.56	3.97E-01	5	1.0000	0.0037	0.989047	0.000097
MIX-SOL-THERM-005-007	2.43E-01	0.56	3.96E-01	5	1.0000	0.0037	0.999568	0.000077

Table A.1 Critical experiments from IHECSBE and ENDF/B-VII 238 group library results (continued)

Experiment ID	EALF (eV)	Enrich. (wt % ^{235}U)	Pu wt. Fraction pu/(pu+u)	Sol. Boron (ppm)	$k_{eff,\ exp}$	$\sigma_{keff,exp}$	$k_{eff,\ calc}$	$\sigma_{keff,calc}$
HTC1_01	7.06E-02	1.57	0.01104	0	PI*	PI	1.00031	0.000094
HTC1_02	6.76E-02	1.57	0.01104	0	PI	PI	1.000355	0.0001
HTC1_03	6.74E-02	1.57	0.01104	0	PI	PI	1.000437	0.000099
HTC1_04	8.62E-02	1.57	0.01104	0	PI	PI	1.000128	0.000099
HTC1_05	8.41E-02	1.57	0.01104	0	PI	PI	1.000018	0.000099
HTC1_06	8.33E-02	1.57	0.01104	0	PI	PI	0.999757	0.000099
HTC1_07	1.04E-01	1.57	0.01104	0	PI	PI	0.999781	0.000099
HTC1_08	1.02E-01	1.57	0.01104	0	PI	PI	0.999588	0.000099
HTC1_09	1.01E-01	1.57	0.01104	0	PI	PI	0.999619	0.000099
HTC1_10	1.43E-01	1.57	0.01104	0	PI	PI	0.999817	0.000099
HTC1_11	1.38E-01	1.57	0.01104	0	PI	PI	0.99895	0.000099
HTC1_12	1.36E-01	1.57	0.01104	0	PI	PI	0.998754	0.000092
HTC1_13	2.60E-01	1.57	0.01104	0	PI	PI	0.997985	0.000099
HTC1_14	2.37E-01	1.57	0.01104	0	PI	PI	0.997921	0.000099
HTC1_15	2.33E-01	1.57	0.01104	0	PI	PI	0.998004	0.000099
HTC1_16	1.03E-01	1.57	0.01104	0	PI	PI	0.999508	0.000099
HTC1_17	1.01E-01	1.57	0.01104	0	PI	PI	0.99926	0.0001
HTC1_18	1.03E-01	1.57	0.01104	0	PI	PI	0.997269	0.000099
HTC2B_01	2.50E-01	1.57	0.01104	100	PI	PI	0.998582	0.000099
HTC2B_02	2.48E-01	1.57	0.01104	106	PI	PI	0.997486	0.000099
HTC2B_03	2.58E-01	1.57	0.01104	205	PI	PI	0.998025	0.000099
HTC2B_04	2.67E-01	1.57	0.01104	299	PI	PI	0.998872	0.000099
HTC2B_05	2.78E-01	1.57	0.01104	400	PI	PI	0.998393	0.000099
HTC2B_06	2.74E-01	1.57	0.01104	399	PI	PI	0.998364	0.000099
HTC2B_07	2.83E-01	1.57	0.01104	486	PI	PI	0.999737	0.000099
HTC2B_08	2.90E-01	1.57	0.01104	587	PI	PI	0.998816	0.000099
HTC2B_09	1.68E-01	1.57	0.01104	595	PI	PI	0.999772	0.000097

Table A.1 Critical experiments from IHECSBE and ENDF/B-VII 238 group library results (continued)

Experiment ID	EALF (eV)	Enrich. (wt % ^{235}U)	Pu wt. Fraction pu/(pu+u)	Sol. Boron (ppm)	$k_{eff,\ exp}$	$\sigma_{keff,exp}$	$k_{eff,\ calc}$	$\sigma_{keff,calc}$
HTC2B_10	1.63E-01	1.57	0.01104	499	PI	PI	0.998417	0.000096
HTC2B_11	1.59E-01	1.57	0.01104	393	PI	PI	1.000163	0.000099
HTC2B_12	1.52E-01	1.57	0.01104	295	PI	PI	1.000327	0.000099
HTC2B_13	1.47E-01	1.57	0.01104	200	PI	PI	0.99948	0.000099
HTC2B_14	1.42E-01	1.57	0.01104	89	PI	PI	1.002154	0.000099
HTC2B_15	1.05E-01	1.57	0.01104	90	PI	PI	1.003535	0.000097
HTC2B_16	1.09E-01	1.57	0.01104	194	PI	PI	1.001781	0.000098
HTC2B_17	1.12E-01	1.57	0.01104	286	PI	PI	1.003658	0.000099
HTC2B_18	1.17E-01	1.57	0.01104	415	PI	PI	0.994315	0.000099
HTC2B_19	1.06E-01	1.57	0.01104	100	PI	PI	1.000358	0.000099
HTC2B_20	9.09E-02	1.57	0.01104	220	PI	PI	0.993473	0.000099
HTC2B_21	8.74E-02	1.57	0.01104	110	PI	PI	0.99714	0.000099
HTC2G_01	2.56E-01	1.57	0.01104	0	PI	PI	0.997596	0.000099
HTC2G_02	2.52E-01	1.57	0.01104	0	PI	PI	0.997572	0.000098
HTC2G_03	2.74E-01	1.57	0.01104	0	PI	PI	0.997364	0.000099
HTC2G_04	2.70E-01	1.57	0.01104	0	PI	PI	0.997628	0.000099
HTC2G_05	2.67E-01	1.57	0.01104	0	PI	PI	0.997547	0.000098
HTC2G_06	2.88E-01	1.57	0.01104	0	PI	PI	0.996896	0.000099
HTC2G_07	2.81E-01	1.57	0.01104	0	PI	PI	0.99678	0.000099
HTC2G_08	2.99E-01	1.57	0.01104	0	PI	PI	0.996061	0.000099
HTC2G_09	2.95E-01	1.57	0.01104	0	PI	PI	0.996248	0.0001
HTC2G_10	1.72E-01	1.57	0.01104	0	PI	PI	0.997293	0.000097
HTC2G_11	1.64E-01	1.57	0.01104	0	PI	PI	0.998279	0.000097
HTC2G_12	1.63E-01	1.57	0.01104	0	PI	PI	0.998151	0.000099
HTC2G_13	1.56E-01	1.57	0.01104	0	PI	PI	0.998612	0.0001
HTC2G_14	1.54E-01	1.57	0.01104	0	PI	PI	0.998472	0.000099
HTC2G_15	1.49E-01	1.57	0.01104	0	PI	PI	0.999848	0.000099

Table A.1 Critical experiments from IHECSBE and ENDF/B-VII 238 group library results (continued)

Experiment ID	EALF (eV)	Enrich. (wt % ^{235}U)	Pu wt. Fraction pu/(pu+u)	Sol. Boron (ppm)	$k_{eff,\ exp}$	$\sigma_{keff,exp}$	$k_{eff,\ calc}$	$\sigma_{keff,calc}$
HTC2G_16	1.46E-01	1.57	0.01104	0	PI	PI	0.999841	0.000098
HTC2G_17	1.08E-01	1.57	0.01104	0	PI	PI	1.000852	0.000098
HTC2G_18	8.91E-02	1.57	0.01104	0	PI	PI	1.00129	0.000099
HTC2G_19	1.15E-01	1.57	0.01104	0	PI	PI	0.997328	0.000095
HTC2G_20	1.08E-01	1.57	0.01104	0	PI	PI	1.00078	0.000099
HTC3_01	1.26E-01	1.57	0.01104	0	PI	PI	0.997631	0.000099
HTC3_02	1.44E-01	1.57	0.01104	0	PI	PI	0.999648	0.000099
HTC3_03	1.31E-01	1.57	0.01104	0	PI	PI	0.997088	0.0001
HTC3_04	1.26E-01	1.57	0.01104	0	PI	PI	0.99704	0.000099
HTC3_05	1.38E-01	1.57	0.01104	0	PI	PI	0.996697	0.0001
HTC3_06	1.32E-01	1.57	0.01104	0	PI	PI	0.99968	0.000097
HTC3_07	1.31E-01	1.57	0.01104	0	PI	PI	0.995888	0.000099
HTC3_08	1.42E-01	1.57	0.01104	0	PI	PI	1.003237	0.000099
HTC3_09	1.36E-01	1.57	0.01104	0	PI	PI	0.995853	0.0001
HTC3_10	1.32E-01	1.57	0.01104	0	PI	PI	0.996274	0.000099
HTC3_11	1.40E-01	1.57	0.01104	0	PI	PI	0.995482	0.000099
HTC3_12	1.14E-01	1.57	0.01104	0	PI	PI	0.999308	0.000099
HTC3_13	1.13E-01	1.57	0.01104	0	PI	PI	0.999521	0.000099
HTC3_14	1.13E-01	1.57	0.01104	0	PI	PI	0.999956	0.000099
HTC3_15	1.13E-01	1.57	0.01104	0	PI	PI	0.999398	0.000099
HTC3_16	1.12E-01	1.57	0.01104	0	PI	PI	1.000209	0.000099
HTC3_17	1.10E-01	1.57	0.01104	0	PI	PI	1.00005	0.000099
HTC3_18	1.08E-01	1.57	0.01104	0	PI	PI	1.000185	0.000099
HTC3_19	1.06E-01	1.57	0.01104	0	PI	PI	1.000703	0.000099
HTC3_20	1.04E-01	1.57	0.01104	0	PI	PI	1.000743	0.000099
HTC3_21	1.06E-01	1.57	0.01104	0	PI	PI	0.999992	0.0001
HTC3_22	1.09E-01	1.57	0.01104	0	PI	PI	1.000214	0.0001

Table A.1 Critical experiments from IHECSBE and ENDF/B-VII 238 group library results (continued)

Experiment ID	EALF (eV)	Enrich. (wt % ^{235}U)	Pu wt. Fraction pu/(pu+u)	Sol. Boron (ppm)	$k_{eff,\ exp}$	$\sigma_{keff,exp}$	$k_{eff,\ calc}$	$\sigma_{keff,calc}$
HTC3_23	1.17E-01	1.57	0.01104	0	PI	PI	0.999049	0.000099
HTC3_24	1.53E-01	1.57	0.01104	0	PI	PI	0.998679	0.0001
HTC3_25	1.29E-01	1.57	0.01104	0	PI	PI	0.999733	0.0001
HTC3_26	1.17E-01	1.57	0.01104	0	PI	PI	0.999273	0.0001
HTC4FE_01	1.55E-01	1.57	0.01104	0	PI	PI	1.001338	0.000099
HTC4FE_02	1.52E-01	1.57	0.01104	0	PI	PI	0.997921	0.000099
HTC4FE_03	1.49E-01	1.57	0.01104	0	PI	PI	0.997465	0.000099
HTC4FE_04	1.45E-01	1.57	0.01104	0	PI	PI	0.997726	0.000099
HTC4FE_05	1.42E-01	1.57	0.01104	0	PI	PI	0.997696	0.000099
HTC4FE_06	1.41E-01	1.57	0.01104	0	PI	PI	0.996808	0.000099
HTC4FE_07	1.39E-01	1.57	0.01104	0	PI	PI	0.99634	0.000099
HTC4FE_08	1.38E-01	1.57	0.01104	0	PI	PI	0.9962	0.000099
HTC4FE_09	1.37E-01	1.57	0.01104	0	PI	PI	0.995904	0.000099
HTC4FE_10	1.37E-01	1.57	0.01104	0	PI	PI	0.997785	0.000099
HTC4FE_11	1.34E-01	1.57	0.01104	0	PI	PI	0.998095	0.000099
HTC4FE_12	1.37E-01	1.57	0.01104	0	PI	PI	1.000659	0.000099
HTC4FE_13	1.36E-01	1.57	0.01104	0	PI	PI	0.996201	0.000099
HTC4FE_14	1.52E-01	1.57	0.01104	0	PI	PI	1.006066	0.000099
HTC4FE_15	1.46E-01	1.57	0.01104	0	PI	PI	0.997497	0.000099
HTC4FE_16	1.39E-01	1.57	0.01104	0	PI	PI	0.997434	0.000099
HTC4FE_17	1.38E-01	1.57	0.01104	0	PI	PI	0.995483	0.000099
HTC4FE_18	1.36E-01	1.57	0.01104	0	PI	PI	0.99503	0.000099
HTC4FE_19	1.35E-01	1.57	0.01104	0	PI	PI	0.994927	0.000099
HTC4FE_20	1.34E-01	1.57	0.01104	0	PI	PI	0.99455	0.0001
HTC4FE_21	1.36E-01	1.57	0.01104	0	PI	PI	1.004835	0.000099
HTC4FE_22	1.77E-01	1.57	0.01104	0	PI	PI	0.999606	0.000099
HTC4FE_23	1.68E-01	1.57	0.01104	0	PI	PI	0.999983	0.000099

Table A.1 Critical experiments from IHECSBE and ENDF/B-VII 238 group library results (continued)

Experiment ID	EALF (eV)	Enrich. (wt % ^{235}U)	Pu wt. Fraction pu/(pu+u)	Sol. Boron (ppm)	$k_{eff,\ exp}$	$\sigma_{keff,exp}$	$k_{eff,\ calc}$	$\sigma_{keff,calc}$
HTC4FE_24	1.60E-01	1.57	0.01104	0	PI	PI	0.999222	0.000099
HTC4FE_25	1.59E-01	1.57	0.01104	0	PI	PI	0.999086	0.000097
HTC4FE_26	1.57E-01	1.57	0.01104	0	PI	PI	0.998842	0.000099
HTC4FE_27	1.56E-01	1.57	0.01104	0	PI	PI	0.998697	0.000099
HTC4FE_28	1.55E-01	1.57	0.01104	0	PI	PI	0.998726	0.000099
HTC4FE_29	1.46E-01	1.57	0.01104	0	PI	PI	0.999267	0.000099
HTC4FE_30	1.36E-01	1.57	0.01104	0	PI	PI	0.999734	0.000099
HTC4FE_31	1.30E-01	1.57	0.01104	0	PI	PI	0.999448	0.000099
HTC4FE_32	1.26E-01	1.57	0.01104	0	PI	PI	0.999482	0.000099
HTC4FE_33	1.24E-01	1.57	0.01104	0	PI	PI	0.999645	0.000099
HTC4PB_01	1.55E-01	1.57	0.01104	0	PI	PI	1.001169	0.000099
HTC4PB_02	1.51E-01	1.57	0.01104	0	PI	PI	0.998384	0.000099
HTC4PB_03	1.47E-01	1.57	0.01104	0	PI	PI	0.998223	0.0001
HTC4PB_04	1.44E-01	1.57	0.01104	0	PI	PI	0.998542	0.000099
HTC4PB_05	1.41E-01	1.57	0.01104	0	PI	PI	0.998287	0.000099
HTC4PB_06	1.36E-01	1.57	0.01104	0	PI	PI	0.998541	0.000099
HTC4PB_07	1.34E-01	1.57	0.01104	0	PI	PI	0.99892	0.000099
HTC4PB_08	1.40E-01	1.57	0.01104	0	PI	PI	0.997751	0.000099
HTC4PB_09	1.39E-01	1.57	0.01104	0	PI	PI	0.997326	0.000099
HTC4PB_10	1.38E-01	1.57	0.01104	0	PI	PI	0.996814	0.000099
HTC4PB_11	1.37E-01	1.57	0.01104	0	PI	PI	0.996884	0.000099
HTC4PB_12	1.37E-01	1.57	0.01104	0	PI	PI	1.000861	0.000099
HTC4PB_13	1.37E-01	1.57	0.01104	0	PI	PI	1.000935	0.000099
HTC4PB_14	1.36E-01	1.57	0.01104	0	PI	PI	1.000094	0.000099
HTC4PB_15	1.32E-01	1.57	0.01104	0	PI	PI	0.996566	0.000099
HTC4PB_16	1.35E-01	1.57	0.01104	0	PI	PI	0.996709	0.000099
HTC4PB_17	1.51E-01	1.57	0.01104	0	PI	PI	1.005001	0.000099

Table A.1 Critical experiments from IHECSBE and ENDF/B-VII 238 group library results (continued)

Experiment ID	EALF (eV)	Enrich. (wt % ^{235}U)	Pu wt. Fraction pu/(pu+u)	Sol. Boron (ppm)	$k_{eff,\ exp}$	$\sigma_{keff,exp}$	$k_{eff,\ calc}$	$\sigma_{keff,calc}$
HTC4PB_18	1.44E-01	1.57	0.01104	0	PI	PI	0.998171	0.000099
HTC4PB_19	1.38E-01	1.57	0.01104	0	PI	PI	0.998562	0.000099
HTC4PB_20	1.35E-01	1.57	0.01104	0	PI	PI	0.999268	0.000099
HTC4PB_21	1.36E-01	1.57	0.01104	0	PI	PI	0.997242	0.000096
HTC4PB_22	1.35E-01	1.57	0.01104	0	PI	PI	0.996525	0.0001
HTC4PB_23	1.34E-01	1.57	0.01104	0	PI	PI	0.9963	0.000099
HTC4PB_24	1.34E-01	1.57	0.01104	0	PI	PI	0.995791	0.000099
HTC4PB_25	1.32E-01	1.57	0.01104	0	PI	PI	0.998796	0.000099
HTC4PB_26	1.30E-01	1.57	0.01104	0	PI	PI	0.99942	0.000099
HTC4PB_27	1.76E-01	1.57	0.01104	0	PI	PI	0.998982	0.000099
HTC4PB_28	1.67E-01	1.57	0.01104	0	PI	PI	0.999809	0.000099
HTC4PB_29	1.59E-01	1.57	0.01104	0	PI	PI	0.99925	0.000099
HTC4PB_30	1.45E-01	1.57	0.01104	0	PI	PI	0.999831	0.000099
HTC4PB_31	1.36E-01	1.57	0.01104	0	PI	PI	1.000141	0.000099
HTC4PB_32	1.30E-01	1.57	0.01104	0	PI	PI	1.000319	0.000099
HTC4PB_33	1.27E-01	1.57	0.01104	0	PI	PI	1.00058	0.000099
HTC4PB_34	1.25E-01	1.57	0.01104	0	PI	PI	1.000403	0.0001
HTC4PB_35	1.58E-01	1.57	0.01104	0	PI	PI	0.999679	0.000099
HTC4PB_36	1.56E-01	1.57	0.01104	0	PI	PI	0.999908	0.000099
HTC4PB_37	1.55E-01	1.57	0.01104	0	PI	PI	0.999861	0.000099
HTC4PB_38	1.54E-01	1.57	0.01104	0	PI	PI	0.999602	0.000099

Table A.1 Critical experiments from IHECSBE and ENDF/B-VII 238 group library results (continued)

Experiment ID	EALF (eV)	Enrich. (wt % ^{235}U)	Pu wt. fraction pu/(pu+u)	Sol. boron (ppm)	Fission product	$k_{eff,\ exp}$	$\sigma_{keff,exp}$	$k_{eff,\ calc}$	$\sigma_{keff,calc}$
FP1_173_01	2.05E-01	4.74	0	0	^{103}Rh	PI	PI	1.000236	0.000099
FP1_173_02	2.15E-01	4.74	0	0	^{103}Rh	PI	PI	1.000398	0.000099
FP1_173_03	2.15E-01	4.74	0	0	^{103}Rh	PI	PI	0.999587	0.000099
FP1_173_05	1.98E-01	4.74	0	0	^{103}Rh	PI	PI	0.999666	0.000099
FP1_173_06	2.07E-01	4.74	0	0	^{133}Cs	PI	PI	0.999615	0.000099
FP1_173_07	1.98E-01	4.74	0	0	^{133}Cs	PI	PI	0.999313	0.000099
FP1_173_08	2.15E-01	4.74	0	0	^{133}Cs	PI	PI	0.999542	0.000099
FP1_173_09	1.99E-01	4.74	0	0	^{133}Cs	PI	PI	0.999228	0.000099
FP1_173_10	1.97E-01	4.74	0	0	^{133}Cs	PI	PI	0.999176	0.000099
FP1_173_11	2.15E-01	4.74	0	0	^{133}Cs	PI	PI	0.999242	0.000099
FP1_173_12	2.07E-01	4.74	0	0	^{133}Cs	PI	PI	0.999723	0.000099
FP1_173_13	2.15E-01	4.74	0	0	^{133}Cs	PI	PI	0.999589	0.000099
FP1_173_14	2.16E-01	4.74	0	0	^{133}Cs	PI	PI	0.999293	0.000099
FP1_173_15	1.97E-01	4.74	0	0	^{133}Cs	PI	PI	0.999559	0.000099
FP1_173_16	2.16E-01	4.74	0	0	^{nat}Nd	PI	PI	0.999607	0.000099
FP1_173_17	1.98E-01	4.74	0	0	^{nat}Nd	PI	PI	0.999663	0.000098
FP1_173_18	2.14E-01	4.74	0	0	^{152}Sm	PI	PI	0.999589	0.000099
FP1_173_19	2.12E-01	4.74	0	0	^{152}Sm	PI	PI	0.999196	0.000099
FP1_173_20	2.10E-01	4.74	0	0	^{152}Sm	PI	PI	0.999549	0.000099
FP1_173_21	2.06E-01	4.74	0	0	^{152}Sm	PI	PI	1.000071	0.000099
FP1_173_22	2.04E-01	4.74	0	0	^{152}Sm	PI	PI	0.999738	0.000099
FP1_173_23	2.07E-01	4.74	0	0	^{155}Gd	PI	PI	0.999457	0.000098
FP1_173_24	2.04E-01	4.74	0	0	^{155}Gd	PI	PI	0.998935	0.000099
FP1_173_25	2.02E-01	4.74	0	0	^{155}Gd	PI	PI	0.998953	0.000099

Table A.1 Critical experiments from IHECSBE and ENDF/B-VII 238 group library results (continued)

Experiment ID	EALF (eV)	Enrich. (wt % ^{235}U)	Pu wt. fraction pu/(pu+u)	Sol. boron (ppm)	Fission product	$k_{eff,\ exp}$	$\sigma_{keff,exp}$	$k_{eff,\ calc}$	$\sigma_{keff,calc}$
FP1_173_26	1.96E-01	4.74	0	0	^{155}Gd	PI	PI	0.999467	0.000099
FP1_173_27	1.98E-01	4.74	0	0	^{155}Gd	PI	PI	0.999579	0.000099
FP1_173_28	2.15E-01	4.74	0	0	Mixt.	PI	PI	0.999899	0.000099
FP1_173_29	2.05E-01	4.74	0	0	Mixt.	PI	PI	1.000094	0.000099
FP1_173_30	2.03E-01	4.74	0	0	Mixt.	PI	PI	0.999855	0.000099
FP1_173_31	2.02E-01	4.74	0	0	^{149}Sm	PI	PI	0.999498	0.00010
FP1_173_32	2.07E-01	4.74	0	0	^{149}Sm	PI	PI	0.999878	0.000099
FP1_173_34	2.07E-01	4.74	0	820.1	^{nat}B	PI	PI	1.000193	0.000099
FP1_173_35	2.15E-01	4.74	0	0	HNO_3	PI	PI	0.998491	0.00010
FP1_173_36	1.91E-01	4.74	0	0	HNO_3	PI	PI	0.99814	0.000099
FP1_173_37	2.15E-01	4.74	0	0	HNO_3	PI	PI	0.99903	0.000099
FP1_173_38	2.07E-01	4.74	0	0	HNO_3	PI	PI	0.999412	0.000099
FP1_173_39	1.99E-01	4.74	0	0	HNO_3	PI	PI	0.999646	0.000099
FP1_173_40	1.98E-01	4.74	0	0	HNO_3	PI	PI	0.999741	0.000099
FP1_173_41	2.13E-01	4.74	0	0	HNO_3	PI	PI	0.999031	0.000099
FP1_173_42	2.12E-01	4.74	0	0	HNO_3	PI	PI	0.999045	0.00010
FP1_173_43	2.06E-01	4.74	0	0	HNO_3	PI	PI	0.999446	0.000099
FP1_173_44	2.05E-01	4.74	0	0	HNO_3	PI	PI	0.999462	0.00010
FP1_173_45	2.04E-01	4.74	0	0	HNO_3	PI	PI	0.9994	0.000099
FP1_173_46	1.99E-01	4.74	0	0	HNO_3	PI	PI	0.999826	0.000099
FP1_173_47	2.04E-01	4.74	0	0	HNO_3	PI	PI	0.999773	0.000099
FP3_176_01	2.93E-01	4.74	0	0	DUN	PI	PI	0.997286	0.000099
FP3_176_02	2.82E-01	4.74	0	0	DUN	PI	PI	0.999111	0.00010
FP3_176_03	2.83E-01	4.74	0	0	DUN	PI	PI	0.998792	0.000099
FP3_176_04	2.39E-01	4.74	0	0	DUN	PI	PI	0.998628	0.00010
FP3_176_05	2.39E-01	4.74	0	0	DUN	PI	PI	0.998734	0.000099

Table A.1 Critical experiments from IHECSBE and ENDF/B-VII 238 group library results (continued)

Experiment ID	EALF (eV)	Enrich. (wt % ^{235}U)	Pu wt. fraction pu/(pu+u)	Sol. boron (ppm)	Fission product	$k_{eff,\ exp}$	$\sigma_{keff,exp}$	$k_{eff,\ calc}$	$\sigma_{keff,calc}$
FP3_176_06	2.38E-01	4.74	0	0	DUN	PI	PI	0.998557	0.000099
FP3_176_07	2.40E-01	4.74	0	0	DUN	PI	PI	0.998195	0.000099
FP3_177_01	1.52E-01	1.57	1.05	0	DUN	PI	PI	1.003851	0.000099
FP3_177_02	1.52E-01	1.57	1.05	0	DUN	PI	PI	1.003307	0.000099
FP3_177_03	1.51E-01	1.57	1.05	0	DUN	PI	PI	1.003781	0.000099
FP3_177_04	1.38E-01	1.57	1.05	0	DUN	PI	PI	1.003398	0.000099
FP3_177_05	1.38E-01	1.57	1.05	0	DUN	PI	PI	1.003332	0.000099
FP3_177_06	1.38E-01	1.57	1.05	0	DUN	PI	PI	1.00364	0.00010
FP3_177_07	1.38E-01	1.57	1.05	0	DUN	PI	PI	1.003592	0.000098
FP2_174_HBC_01	2.34E-01	1.57	1.06	0	^{103}Rh	PI	PI	0.998117	0.000099
FP2_174_HBC_02	2.26E-01	1.57	1.06	0	^{103}Rh	PI	PI	0.997367	0.000099
FP2_174_HBC_03	2.33E-01	1.57	1.06	0	^{155}Gd	PI	PI	1.000577	0.000099
FP2_174_HBC_04	2.28E-01	1.57	1.06	0	^{155}Gd	PI	PI	1.000232	0.00010
FP2_174_HBC_05	2.32E-01	1.57	1.06	0	^{149}Sm	PI	PI	1.001045	0.000099
FP2_174_HBC_06	2.27E-01	1.57	1.06	0	^{149}Sm	PI	PI	1.001075	0.00010
FP2_174_HBC_07	2.26E-01	1.57	1.06	0	Mixt.	PI	PI	1.000533	0.000099
FP2_174_HBC_08	2.35E-01	1.57	1.06	0	HNO_3	PI	PI	0.999143	0.00010
FP2_174_HBC_09	2.21E-01	1.57	1.06	0	HNO_3	PI	PI	0.999661	0.000099
FP2_174_HBC_10	2.28E-01	1.57	1.06	0	HNO_3	PI	PI	0.999531	0.000099
FP2_174_HBC_11	2.31E-01	1.57	1.06	0	HNO_3	PI	PI	0.999087	0.000099
FP2_174_HBC_12	2.31E-01	1.57	1.06	0	HNO_3	PI	PI	0.99935	0.000099
FP2_174_HBC_13	2.31E-01	1.57	1.06	0	HNO_3	PI	PI	0.999602	0.000099
FP2_174_HBC_14	2.30E-01	1.57	1.06	0	HNO_3	PI	PI	0.999353	0.00010
FP2_174_UO2_01	2.34E-01	1.57	1.06	0	^{133}Cs	PI	PI	1.000927	0.000099
FP2_174_UO2_02	2.33E-01	1.57	1.06	0	^{133}Cs	PI	PI	1.000483	0.000099
FP2_174_UO2_03	2.26E-01	1.57	1.06	0	^{133}Cs	PI	PI	1.000571	0.000099

Table A.1 Critical experiments from IHECSBE and ENDF/B-VII 238 group library results (continued)

Experiment ID	EALF (eV)	Enrich. (wt % ^{235}U)	Pu wt. fraction pu/(pu+u)	Sol. boron (ppm)	Fission product	$k_{eff,\ exp}$	$\sigma_{keff,exp}$	$k_{eff,\ calc}$	$\sigma_{keff,calc}$
FP2_174_UO2_04	2.30E-01	1.57	1.06	0	^{133}Cs	PI	PI	1.000531	0.000099
FP2_174_UO2_05	2.29E-01	1.57	1.06	0	^{133}Cs	PI	PI	1.000465	0.000099
FP2_174_UO2_06	2.41E-01	1.57	1.06	0	^{103}Rh	PI	PI	0.996885	0.000099
FP2_174_UO2_07	2.41E-01	1.57	1.06	0	^{103}Rh	PI	PI	0.996620	0.000099
FP2_174_UO2_08	2.37E-01	1.57	1.06	0	^{103}Rh	PI	PI	0.997042	0.000099
FP2_174_UO2_09	2.31E-01	1.57	1.06	0	^{103}Rh	PI	PI	0.997044	0.000099
FP2_174_UO2_10	2.29E-01	1.57	1.06	0	^{103}Rh	PI	PI	0.996799	0.000099
FP2_174_UO2_11	2.29E-01	1.57	1.06	0	^{nat}Nd	PI	PI	1.000237	0.000099
FP2_174_UO2_12	2.29E-01	1.57	1.06	0	^{nat}Nd	PI	PI	1.000076	0.000099
FP2_174_UO2_13	2.38E-01	1.57	1.06	0	^{149}Sm	PI	PI	1.001628	0.000100
FP2_174_UO2_14	2.36E-01	1.57	1.06	0	^{149}Sm	PI	PI	1.001914	0.000099
FP2_174_UO2_15	2.33E-01	1.57	1.06	0	^{149}Sm	PI	PI	1.000559	0.000099
FP2_174_UO2_16	2.30E-01	1.57	1.06	0	^{149}Sm	PI	PI	1.001505	0.000100
FP2_174_UO2_17	2.25E-01	1.57	1.06	0	^{149}Sm	PI	PI	1.000368	0.000100
FP2_174_UO2_18	2.33E-01	1.57	1.06	0	^{152}Sm	PI	PI	1.000790	0.000098
FP2_174_UO2_19	2.28E-01	1.57	1.06	0	^{152}Sm	PI	PI	1.000522	0.000099
FP2_174_UO2_20	2.41E-01	1.57	1.06	0	^{155}Gd	PI	PI	1.001308	0.000099
FP2_174_UO2_21	2.33E-01	1.57	1.06	0	^{155}Gd	PI	PI	0.999476	0.000099
FP2_174_UO2_22	2.31E-01	1.57	1.06	0	^{155}Gd	PI	PI	0.999607	0.000099
FP2_174_UO2_23	2.34E-01	1.57	1.06	0	Mixt.	PI	PI	1.000041	0.000097
FP2_174_UO2_24	2.29E-01	1.57	1.06	0	Mixt.	PI	PI	1.000291	0.000096
FP2_174_UO2_25	2.47E-01	1.57	1.06	0	Mixt.	PI	PI	1.002539	0.000099
FP2_174_UO2_26	2.41E-01	1.57	1.06	0	Mixt.	PI	PI	1.002514	0.000100
FP2_174_UO2_27	2.50E-01	1.57	1.06	0	Mixt.	PI	PI	1.003020	0.000099
FP2_174_UO2_28	2.47E-01	1.57	1.06	0	Mixt.	PI	PI	1.002835	0.000099
FP2_174_UO2_29	2.57E-01	1.57	1.06	0	HNO_3	PI	PI	0.994993	0.000099
FP2_174_UO2_30	2.57E-01	1.57	1.06	0	HNO_3	PI	PI	0.996099	0.000099
FP2_174_UO2_31	2.43E-01	1.57	1.06	0	HNO_3	PI	PI	0.998027	0.000099

Table A.1 Critical experiments from IHECSBE and ENDF/B-VII 238 group library results (continued)

Experiment ID	EALF (eV)	Enrich. (wt % ^{235}U)	Pu wt. fraction pu/(pu+u)	Sol. boron (ppm)	Fission product	$k_{eff,\ exp}$	$\sigma_{keff,exp}$	$k_{eff,\ calc}$	$\sigma_{keff,calc}$
FP2_174_UO2_32	2.30E-01	1.57	1.06	0	HNO_3	PI	PI	0.998988	0.000100
FP2_174_UO2_33	2.30E-01	1.57	1.06	0	HNO_3	PI	PI	0.998961	0.000099
FP2_174_UO2_34	2.35E-01	1.57	1.06	0	HNO_3	PI	PI	0.997965	0.000099
FP2_174_UO2_35	2.30E-01	1.57	1.06	0	HNO_3	PI	PI	0.998289	0.000099
FP2_174_UO2_36	2.30E-01	1.57	1.06	0	HNO_3	PI	PI	0.998183	0.000099
FP2_174_UO2_37	2.33E-01	1.57	1.06	0	HNO_3	PI	PI	0.998126	0.000099
FP2_174_UO2_38	2.34E-01	1.57	1.06	0	HNO_3	PI	PI	0.997780	0.000099
FP2_174_UO2_39	2.32E-01	1.57	1.06	0	HNO_3	PI	PI	0.997914	0.000099
FP2_174_UO2_40	2.31E-01	1.57	1.06	0	HNO_3	PI	PI	0.998199	0.000100
FP2_174_UO2_41	2.37E-01	1.57	1.06	0	HNO_3	PI	PI	0.997925	0.000099
FP2_174_UO2_42	2.46E-01	1.57	1.06	0	HNO_3	PI	PI	0.996647	0.000099
FP2_174_UO2_43	2.46E-01	1.57	1.06	0	HNO_3	PI	PI	0.997186	0.000100
FP2_174_UO2_44	2.30E-01	1.57	1.06	0	HNO_3	PI	PI	0.998279	0.000098
FP2_174_UO2_45	2.47E-01	1.57	1.06	0	HNO_3	PI	PI	0.996273	0.000099
FP2_174_UO2_46	2.45E-01	1.57	1.06	0	HNO_3	PI	PI	0.997414	0.000099
FP2_174_UO2_47	2.29E-01	1.57	1.06	0	HNO_3	PI	PI	0.997995	0.000099
FP2_174_UO2_48	2.29E-01	1.57	1.06	0	HNO_3	PI	PI	0.998076	0.000099
FP2_174_UO2_49	2.33E-01	1.57	1.06	0	HNO_3	PI	PI	0.998455	0.000099
FP2_174_UO2_50	2.44E-01	1.57	1.06	0	HNO_3	PI	PI	0.997616	0.000099
FP2_174_UO2_51	2.52E-01	1.57	1.06	0	HNO_3	PI	PI	0.995679	0.000099
FP2_174_UO2_52	2.55E-01	1.57	1.06	0	HNO_3	PI	PI	0.996030	0.000099
FP2_174_UO2_53	2.34E-01	1.57	1.06	0	HNO_3	PI	PI	0.997929	0.000099
FP2_174_UO2_54	2.32E-01	1.57	1.06	0	HNO_3	PI	PI	0.998125	0.000099
FP2_175_01	2.40E-01	1.57	1.06	0	HNO_3	PI	PI	0.997611	0.000099
FP2_175_09	2.40E-01	1.57	1.06	0	DUN	PI	PI	1.000922	0.000097
FP2_175_10	2.37E-01	1.57	1.06	0	DUN	PI	PI	1.000756	0.000099
FP2_175_11	2.32E-01	1.57	1.06	0	DUN	PI	PI	1.000685	0.000099
FP2_175_12	2.28E-01	1.57	1.06	0	DUN	PI	PI	1.0012	0.00010

Table A.1 Critical experiments from IHECSBE and ENDF/B-VII 238 group library results (continued)

Experiment ID	EALF (eV)	Enrich. (wt % ^{235}U)	Pu wt. fraction pu/(pu+u)	Sol. boron (ppm)	Fission product	$k_{eff,\ exp}$	$\sigma_{keff,exp}$	$k_{eff,\ calc}$	$\sigma_{keff,calc}$
FP2_175_13	2.35E-01	1.57	1.06	0	DUN+^{149}Sm	PI	PI	1.00201	0.000099
FP2_175_14	2.33E-01	1.57	1.06	0	DUN+FP Mix	PI	PI	1.001594	0.000099
FP2_175_15	2.28E-01	1.57	1.06	0	DUN+FP Mix	PI	PI	1.001308	0.000099

* PI = proprietary information

APPENDIX B
SIMILARITY ASSESSMENT RESULTS

Table B.1 Critical experiment similarity assessment c_k values for applications

No.	Experiment ID	PWR SFP 10 GWd/MTU	PWR SFP 40 GWd/MTU	GBC-32 10 GWd/MTU	GBC-32 40 GWd/MTU	BWR SFP 11 GWd/MTU
1	LEU-COMP-THERM-001-001	0.554	0.459	0.611	0.521	0.450
2	LEU-COMP-THERM-001-002	0.573	0.471	0.625	0.529	0.476
3	LEU-COMP-THERM-001-003	0.585	0.478	0.634	0.534	0.493
4	LEU-COMP-THERM-001-004	0.574	0.472	0.626	0.529	0.477
5	LEU-COMP-THERM-001-005	0.592	0.482	0.638	0.536	0.503
6	LEU-COMP-THERM-001-006	0.580	0.475	0.630	0.532	0.486
7	LEU-COMP-THERM-001-007	0.594	0.483	0.640	0.536	0.507
8	LEU-COMP-THERM-001-008	0.590	0.481	0.637	0.535	0.500
9	LEU-COMP-THERM-002-001	0.420	0.373	0.495	0.451	0.298
10	LEU-COMP-THERM-002-002	0.422	0.374	0.497	0.453	0.301
11	LEU-COMP-THERM-002-003	0.428	0.378	0.502	0.455	0.309
12	LEU-COMP-THERM-002-004	0.452	0.394	0.521	0.467	0.341
13	LEU-COMP-THERM-002-005	0.464	0.402	0.531	0.473	0.357
14	LEU-COMP-THERM-010-005	0.628	0.510	0.661	0.553	0.576
15	LEU-COMP-THERM-010-016	0.496	0.432	0.568	0.507	0.393
16	LEU-COMP-THERM-010-017	0.493	0.429	0.566	0.505	0.389
17	LEU-COMP-THERM-010-018	0.493	0.429	0.565	0.504	0.388
18	LEU-COMP-THERM-010-019	0.484	0.423	0.556	0.498	0.375
19	LEU-COMP-THERM-017-003	0.603	0.489	0.647	0.541	0.520
20	LEU-COMP-THERM-017-004	0.681	0.537	0.703	0.570	0.632
21	LEU-COMP-THERM-017-005	0.660	0.524	0.689	0.563	0.599
22	LEU-COMP-THERM-017-006	0.652	0.520	0.684	0.560	0.588
23	LEU-COMP-THERM-017-007	0.648	0.517	0.680	0.558	0.582
24	LEU-COMP-THERM-017-008	0.627	0.504	0.664	0.549	0.553
25	LEU-COMP-THERM-017-009	0.599	0.487	0.644	0.539	0.514
26	LEU-COMP-THERM-017-010	0.629	0.507	0.671	0.556	0.560
27	LEU-COMP-THERM-017-011	0.623	0.502	0.666	0.553	0.549
28	LEU-COMP-THERM-017-012	0.620	0.501	0.663	0.551	0.545
29	LEU-COMP-THERM-017-013	0.616	0.498	0.659	0.548	0.539
30	LEU-COMP-THERM-017-014	0.611	0.495	0.654	0.545	0.531
31	LEU-COMP-THERM-017-015	0.646	0.521	0.688	0.571	0.578
32	LEU-COMP-THERM-017-016	0.641	0.518	0.685	0.569	0.570
33	LEU-COMP-THERM-017-017	0.640	0.517	0.683	0.568	0.567
34	LEU-COMP-THERM-017-019	0.636	0.515	0.680	0.566	0.561
35	LEU-COMP-THERM-017-020	0.631	0.512	0.676	0.563	0.553
36	LEU-COMP-THERM-017-021	0.629	0.511	0.673	0.561	0.550
37	LEU-COMP-THERM-017-022	0.612	0.499	0.659	0.553	0.524
38	LEU-COMP-THERM-017-023	0.622	0.505	0.665	0.555	0.541

Table B.1 Critical experiment similarity assessment c_k values for applications (continued)

No.	Experiment ID	PWR SFP 10 GWd/MTU	PWR SFP 40 GWd/MTU	GBC-32 10 GWd/MTU	GBC-32 40 GWd/MTU	BWR SFP 11 GWd/MTU
39	LEU-COMP-THERM-017-024	0.620	0.504	0.663	0.554	0.537
40	LEU-COMP-THERM-017-025	0.626	0.507	0.668	0.557	0.544
41	LEU-COMP-THERM-017-028	0.685	0.544	0.711	0.578	0.630
42	LEU-COMP-THERM-017-029	0.675	0.537	0.704	0.575	0.615
43	LEU-COMP-THERM-022-001	0.384	0.359	0.472	0.446	0.297
44	LEU-COMP-THERM-022-002	0.358	0.336	0.447	0.425	0.261
45	LEU-COMP-THERM-022-003	0.339	0.315	0.422	0.399	0.246
46	LEU-COMP-THERM-022-004	0.342	0.313	0.417	0.390	0.261
47	LEU-COMP-THERM-022-005	0.354	0.318	0.422	0.389	0.281
48	LEU-COMP-THERM-022-006	0.418	0.356	0.468	0.412	0.379
49	LEU-COMP-THERM-022-007	0.424	0.360	0.472	0.415	0.388
50	LEU-COMP-THERM-023-001	0.352	0.318	0.424	0.392	0.278
51	LEU-COMP-THERM-023-002	0.345	0.313	0.417	0.387	0.268
52	LEU-COMP-THERM-023-003	0.344	0.312	0.416	0.386	0.267
53	LEU-COMP-THERM-023-004	0.345	0.312	0.416	0.386	0.269
54	LEU-COMP-THERM-023-005	0.347	0.314	0.418	0.387	0.271
55	LEU-COMP-THERM-023-006	0.349	0.315	0.419	0.388	0.275
56	LEU-COMP-THERM-024-001	0.403	0.372	0.486	0.456	0.327
57	LEU-COMP-THERM-024-002	0.365	0.334	0.445	0.415	0.283
58	LEU-COMP-THERM-026-003	0.520	0.453	0.582	0.519	0.441
59	LEU-COMP-THERM-042-001	0.643	0.520	0.688	0.571	0.575
60	LEU-COMP-THERM-042-002	0.658	0.529	0.697	0.575	0.597
61	LEU-COMP-THERM-042-003	0.666	0.534	0.703	0.578	0.610
62	LEU-COMP-THERM-042-004	0.667	0.534	0.703	0.578	0.610
63	LEU-COMP-THERM-042-005	0.665	0.533	0.701	0.577	0.607
64	LEU-COMP-THERM-042-006	0.647	0.522	0.689	0.570	0.580
65	LEU-COMP-THERM-042-007	0.657	0.528	0.696	0.574	0.595
66	LEU-COMP-THERM-050-001	0.416	0.376	0.498	0.460	0.288
67	LEU-COMP-THERM-050-002	0.418	0.377	0.499	0.460	0.291
68	LEU-COMP-THERM-050-003	0.432	0.387	0.511	0.469	0.309
69	LEU-COMP-THERM-050-004	0.438	0.391	0.516	0.472	0.318
70	LEU-COMP-THERM-050-005	0.450	0.400	0.526	0.479	0.334
71	LEU-COMP-THERM-050-006	0.456	0.404	0.531	0.482	0.342
72	LEU-COMP-THERM-050-007	0.459	0.406	0.533	0.483	0.347
73	LEU-COMP-THERM-050-008	0.429	0.386	0.509	0.468	0.305
74	LEU-COMP-THERM-050-009	0.435	0.389	0.514	0.470	0.313
75	LEU-COMP-THERM-050-010	0.437	0.391	0.515	0.471	0.316
76	LEU-COMP-THERM-050-011	0.436	0.391	0.515	0.472	0.314
77	LEU-COMP-THERM-050-012	0.447	0.398	0.523	0.477	0.329

Table B.1 Critical experiment similarity assessment c_k values for applications (continued)

No.	Experiment ID	PWR SFP 10 GWd/MTU	PWR SFP 40 GWd/MTU	GBC-32 10 GWd/MTU	GBC-32 40 GWd/MTU	BWR SFP 11 GWd/MTU
78	LEU-COMP-THERM-050-013	0.447	0.398	0.524	0.477	0.330
79	LEU-COMP-THERM-050-014	0.456	0.405	0.531	0.483	0.342
80	LEU-COMP-THERM-050-015	0.461	0.407	0.535	0.485	0.348
81	LEU-COMP-THERM-050-016	0.455	0.403	0.530	0.482	0.340
82	LEU-COMP-THERM-050-017	0.458	0.406	0.533	0.484	0.344
83	LEU-COMP-THERM-050-018	0.457	0.405	0.532	0.483	0.343
84	LEU-COMP-THERM-079-001	0.408	0.373	0.496	0.461	0.271
85	LEU-COMP-THERM-079-002	0.409	0.374	0.497	0.462	0.272
86	LEU-COMP-THERM-079-003	0.418	0.380	0.504	0.467	0.284
87	LEU-COMP-THERM-079-004	0.423	0.384	0.508	0.470	0.292
88	LEU-COMP-THERM-079-005	0.430	0.390	0.514	0.475	0.302
89	LEU-COMP-THERM-079-006	0.413	0.368	0.491	0.449	0.289
90	LEU-COMP-THERM-079-007	0.411	0.367	0.489	0.448	0.286
91	LEU-COMP-THERM-079-008	0.424	0.376	0.499	0.455	0.304
92	LEU-COMP-THERM-079-009	0.427	0.379	0.503	0.458	0.309
93	LEU-COMP-THERM-079-010	0.440	0.388	0.513	0.464	0.326
94	LEU-MISC-THERM-005-001	0.466	0.410	0.538	0.486	0.360
95	LEU-MISC-THERM-005-002	0.471	0.414	0.542	0.489	0.367
96	LEU-MISC-THERM-005-003	0.479	0.420	0.549	0.493	0.378
97	LEU-MISC-THERM-005-004	0.480	0.421	0.549	0.494	0.379
98	LEU-MISC-THERM-005-005	0.481	0.422	0.551	0.495	0.381
99	LEU-MISC-THERM-005-006	0.484	0.424	0.552	0.497	0.384
100	LEU-MISC-THERM-005-007	0.486	0.426	0.554	0.498	0.387
101	LEU-MISC-THERM-005-008	0.491	0.429	0.558	0.501	0.394
102	LEU-MISC-THERM-005-009	0.489	0.429	0.557	0.501	0.393
103	LEU-MISC-THERM-005-010	0.489	0.429	0.557	0.501	0.393
104	LEU-MISC-THERM-005-011	0.488	0.428	0.556	0.500	0.390
105	LEU-MISC-THERM-005-012	0.489	0.429	0.557	0.501	0.392
106	LEU-SOL-THERM-002-001	0.538	0.435	0.563	0.470	0.503
107	LEU-SOL-THERM-002-002	0.509	0.418	0.543	0.461	0.458
108	LEU-SOL-THERM-002-003	0.521	0.425	0.551	0.465	0.476
109	LEU-SOL-THERM-003-001	0.403	0.345	0.446	0.395	0.346
110	LEU-SOL-THERM-003-002	0.423	0.357	0.460	0.404	0.375
111	LEU-SOL-THERM-003-003	0.429	0.361	0.465	0.406	0.384
112	LEU-SOL-THERM-003-004	0.432	0.363	0.468	0.408	0.389
113	LEU-SOL-THERM-003-005	0.489	0.397	0.508	0.429	0.473
114	LEU-SOL-THERM-003-006	0.498	0.403	0.514	0.432	0.487
115	LEU-SOL-THERM-003-007	0.506	0.407	0.519	0.434	0.499
116	LEU-SOL-THERM-003-008	0.542	0.426	0.541	0.441	0.559

Table B.1 Critical experiment similarity assessment c_k values for applications (continued)

No.	Experiment ID	PWR SFP 10 GWd/MTU	PWR SFP 40 GWd/MTU	GBC-32 10 GWd/MTU	GBC-32 40 GWd/MTU	BWR SFP 11 GWd/MTU
117	LEU-SOL-THERM-003-009	0.544	0.427	0.542	0.441	0.564
118	LEU-SOL-THERM-004-001	0.418	0.355	0.459	0.404	0.368
119	LEU-SOL-THERM-004-002	0.429	0.362	0.467	0.408	0.385
120	LEU-SOL-THERM-004-003	0.441	0.369	0.475	0.412	0.403
121	LEU-SOL-THERM-004-004	0.454	0.377	0.484	0.417	0.423
122	LEU-SOL-THERM-004-005	0.464	0.383	0.491	0.420	0.439
123	LEU-SOL-THERM-004-006	0.473	0.388	0.497	0.423	0.453
124	LEU-SOL-THERM-004-007	0.482	0.393	0.503	0.426	0.466
125	MIX-COMP-THERM-001-001	0.538	0.719	0.609	0.763	0.296
126	MIX-COMP-THERM-001-002	0.516	0.690	0.584	0.733	0.283
127	MIX-COMP-THERM-001-003	0.515	0.686	0.580	0.726	0.286
128	MIX-COMP-THERM-001-004	0.522	0.692	0.584	0.728	0.295
129	MIX-COMP-THERM-002-001S	0.673	0.827	0.744	0.867	0.402
130	MIX-COMP-THERM-002-002S	0.699	0.852	0.759	0.880	0.439
131	MIX-COMP-THERM-002-003S	0.629	0.785	0.706	0.833	0.353
132	MIX-COMP-THERM-002-004S	0.697	0.852	0.748	0.871	0.446
133	MIX-COMP-THERM-002-005S	0.630	0.785	0.703	0.829	0.359
134	MIX-COMP-THERM-002-006S	0.693	0.846	0.740	0.862	0.445
135	MIX-COMP-THERM-003-001	0.585	0.762	0.662	0.809	0.317
136	MIX-COMP-THERM-003-002	0.569	0.746	0.648	0.796	0.302
137	MIX-COMP-THERM-003-003	0.576	0.755	0.654	0.802	0.310
138	MIX-COMP-THERM-003-004	0.542	0.713	0.617	0.762	0.286
139	MIX-COMP-THERM-003-005	0.542	0.712	0.616	0.759	0.289
140	MIX-COMP-THERM-003-006	0.558	0.725	0.623	0.763	0.312
141	MIX-COMP-THERM-004-001	0.625	0.789	0.698	0.832	0.357
142	MIX-COMP-THERM-004-002	0.628	0.792	0.700	0.834	0.360
143	MIX-COMP-THERM-004-003	0.629	0.793	0.701	0.835	0.362
144	MIX-COMP-THERM-004-004	0.625	0.787	0.695	0.828	0.360
145	MIX-COMP-THERM-004-005	0.626	0.788	0.696	0.829	0.361
146	MIX-COMP-THERM-004-006	0.629	0.791	0.698	0.831	0.365
147	MIX-COMP-THERM-004-007	0.629	0.789	0.694	0.825	0.370
148	MIX-COMP-THERM-004-008	0.631	0.791	0.695	0.826	0.372
149	MIX-COMP-THERM-004-009	0.632	0.792	0.696	0.827	0.374
150	MIX-COMP-THERM-004-010	0.640	0.798	0.699	0.828	0.386
151	MIX-COMP-THERM-004-011	0.642	0.800	0.700	0.828	0.388
152	MIX-COMP-THERM-005-001	0.613	0.785	0.690	0.831	0.340
153	MIX-COMP-THERM-005-002	0.599	0.770	0.676	0.818	0.327
154	MIX-COMP-THERM-005-003	0.594	0.764	0.669	0.810	0.327
155	MIX-COMP-THERM-005-004	0.602	0.771	0.673	0.812	0.338

Table B.1 Critical experiment similarity assessment c_k values for applications (continued)

No.	Experiment ID	PWR SFP 10 GWd/MTU	PWR SFP 40 GWd/MTU	GBC-32 10 GWd/MTU	GBC-32 40 GWd/MTU	BWR SFP 11 GWd/MTU
156	MIX-COMP-THERM-005-005	0.612	0.778	0.675	0.812	0.356
157	MIX-COMP-THERM-005-006	0.635	0.798	0.687	0.819	0.387
158	MIX-COMP-THERM-005-007	0.647	0.807	0.693	0.822	0.404
159	MIX-COMP-THERM-006-001	0.649	0.805	0.726	0.851	0.372
160	MIX-COMP-THERM-006-002	0.628	0.785	0.706	0.833	0.352
161	MIX-COMP-THERM-006-003	0.626	0.781	0.700	0.826	0.354
162	MIX-COMP-THERM-006-004	0.633	0.787	0.703	0.828	0.365
163	MIX-COMP-THERM-006-005	0.650	0.800	0.711	0.832	0.390
164	MIX-COMP-THERM-006-006	0.657	0.806	0.714	0.834	0.401
165	MIX-COMP-THERM-006-007	0.626	0.781	0.700	0.826	0.355
166	MIX-COMP-THERM-006-008	0.627	0.782	0.701	0.827	0.356
167	MIX-COMP-THERM-006-009	0.628	0.783	0.702	0.828	0.357
168	MIX-COMP-THERM-006-010	0.628	0.783	0.702	0.828	0.357
169	MIX-COMP-THERM-006-011	0.629	0.784	0.703	0.829	0.358
170	MIX-COMP-THERM-006-012	0.630	0.785	0.703	0.829	0.359
171	MIX-COMP-THERM-006-013	0.627	0.781	0.701	0.827	0.355
172	MIX-COMP-THERM-006-014	0.628	0.783	0.702	0.828	0.357
173	MIX-COMP-THERM-006-015	0.629	0.784	0.703	0.829	0.358
174	MIX-COMP-THERM-006-016	0.629	0.784	0.703	0.829	0.358
175	MIX-COMP-THERM-006-017	0.630	0.785	0.704	0.830	0.359
176	MIX-COMP-THERM-006-018	0.631	0.786	0.704	0.830	0.360
177	MIX-COMP-THERM-006-019	0.631	0.786	0.704	0.830	0.360
178	MIX-COMP-THERM-006-020	0.631	0.786	0.704	0.830	0.360
179	MIX-COMP-THERM-006-021	0.632	0.787	0.704	0.830	0.361
180	MIX-COMP-THERM-006-022	0.631	0.786	0.704	0.830	0.360
181	MIX-COMP-THERM-006-023	0.631	0.786	0.704	0.830	0.360
182	MIX-COMP-THERM-006-024	0.631	0.786	0.704	0.830	0.360
183	MIX-COMP-THERM-006-025	0.631	0.786	0.704	0.830	0.360
184	MIX-COMP-THERM-006-026	0.631	0.786	0.704	0.830	0.360
185	MIX-COMP-THERM-006-027	0.631	0.786	0.704	0.830	0.360
186	MIX-COMP-THERM-006-028	0.632	0.787	0.704	0.830	0.361
187	MIX-COMP-THERM-006-029	0.650	0.801	0.711	0.832	0.390
188	MIX-COMP-THERM-006-030	0.651	0.801	0.711	0.833	0.391
189	MIX-COMP-THERM-006-031	0.651	0.802	0.712	0.833	0.392
190	MIX-COMP-THERM-006-032	0.651	0.802	0.712	0.833	0.392
191	MIX-COMP-THERM-006-033	0.652	0.802	0.712	0.833	0.393
192	MIX-COMP-THERM-006-034	0.652	0.802	0.712	0.834	0.393
193	MIX-COMP-THERM-006-035	0.651	0.801	0.711	0.833	0.391
194	MIX-COMP-THERM-006-036	0.651	0.802	0.712	0.833	0.392

Table B.1 Critical experiment similarity assessment c_k values for applications (continued)

No.	Experiment ID	PWR SFP 10 GWd/MTU	PWR SFP 40 GWd/MTU	GBC-32 10 GWd/MTU	GBC-32 40 GWd/MTU	BWR SFP 11 GWd/MTU
195	MIX-COMP-THERM-006-037	0.652	0.802	0.712	0.833	0.393
196	MIX-COMP-THERM-006-038	0.652	0.802	0.712	0.834	0.393
197	MIX-COMP-THERM-006-039	0.652	0.803	0.712	0.834	0.393
198	MIX-COMP-THERM-006-040	0.653	0.803	0.713	0.834	0.394
199	MIX-COMP-THERM-006-041	0.653	0.803	0.713	0.834	0.394
200	MIX-COMP-THERM-006-042	0.653	0.803	0.713	0.834	0.394
201	MIX-COMP-THERM-006-043	0.653	0.804	0.713	0.834	0.394
202	MIX-COMP-THERM-006-044	0.653	0.804	0.713	0.834	0.394
203	MIX-COMP-THERM-006-045	0.653	0.803	0.713	0.834	0.394
204	MIX-COMP-THERM-006-046	0.653	0.803	0.713	0.834	0.394
205	MIX-COMP-THERM-006-047	0.653	0.803	0.713	0.834	0.393
206	MIX-COMP-THERM-006-048	0.653	0.803	0.713	0.834	0.393
207	MIX-COMP-THERM-006-049	0.653	0.803	0.713	0.834	0.394
208	MIX-COMP-THERM-006-050	0.653	0.804	0.713	0.834	0.394
209	MIX-COMP-THERM-007-001	0.655	0.809	0.729	0.853	0.380
210	MIX-COMP-THERM-007-002	0.651	0.804	0.723	0.846	0.380
211	MIX-COMP-THERM-007-003	0.657	0.808	0.724	0.846	0.390
212	MIX-COMP-THERM-007-004	0.674	0.821	0.730	0.849	0.416
213	MIX-COMP-THERM-007-005	0.681	0.827	0.733	0.850	0.427
214	MIX-COMP-THERM-008-001	0.700	0.851	0.766	0.885	0.432
215	MIX-COMP-THERM-008-002	0.670	0.823	0.742	0.864	0.396
216	MIX-COMP-THERM-008-003	0.669	0.821	0.737	0.859	0.398
217	MIX-COMP-THERM-008-003_Al	0.669	0.821	0.737	0.859	0.399
218	MIX-COMP-THERM-008-003_B1	0.672	0.824	0.739	0.861	0.403
219	MIX-COMP-THERM-008-003_B2	0.672	0.824	0.739	0.861	0.403
220	MIX-COMP-THERM-008-003_B3	0.670	0.822	0.738	0.860	0.401
221	MIX-COMP-THERM-008-003_B4	0.669	0.821	0.737	0.859	0.399
222	MIX-COMP-THERM-008-003_CdAir	0.673	0.825	0.740	0.862	0.404
223	MIX-COMP-THERM-008-003_CdAl	0.673	0.825	0.740	0.862	0.404
224	MIX-COMP-THERM-008-003_CdB1	0.673	0.824	0.740	0.861	0.403
225	MIX-COMP-THERM-008-003_CdB2	0.673	0.825	0.740	0.862	0.404
226	MIX-COMP-THERM-008-003_CdB3	0.673	0.825	0.740	0.862	0.404
227	MIX-COMP-THERM-008-003_CdB4	0.673	0.824	0.740	0.861	0.404
228	MIX-COMP-THERM-008-003_CdH1	0.673	0.825	0.740	0.862	0.404
229	MIX-COMP-THERM-008-003_CdH2	0.673	0.825	0.740	0.862	0.405
230	MIX-COMP-THERM-008-003_CdH3	0.674	0.826	0.740	0.862	0.405
231	MIX-COMP-THERM-008-003_CdH4	0.673	0.825	0.740	0.862	0.405
232	MIX-COMP-THERM-008-003_CdH5	0.673	0.825	0.740	0.862	0.404
233	MIX-COMP-THERM-008-003_CdWater	0.673	0.825	0.740	0.862	0.404

Table B.1 Critical experiment similarity assessment c_k values for applications (continued)

No.	Experiment ID	PWR SFP 10 GWd/MTU	PWR SFP 40 GWd/MTU	GBC-32 10 GWd/MTU	GBC-32 40 GWd/MTU	BWR SFP 11 GWd/MTU
234	MIX-COMP-THERM-008-003_H1	0.671	0.823	0.739	0.861	0.402
235	MIX-COMP-THERM-008-003_H2	0.672	0.824	0.739	0.861	0.403
236	MIX-COMP-THERM-008-003_H3	0.671	0.822	0.738	0.860	0.401
237	MIX-COMP-THERM-008-003_H4	0.671	0.822	0.738	0.860	0.401
238	MIX-COMP-THERM-008-003_H5	0.670	0.822	0.738	0.860	0.400
239	MIX-COMP-THERM-008-004	0.675	0.825	0.739	0.859	0.409
240	MIX-COMP-THERM-008-005	0.692	0.838	0.745	0.861	0.437
241	MIX-COMP-THERM-008-006	0.699	0.843	0.747	0.860	0.449
242	MIX-COMP-THERM-009-001	0.716	0.860	0.768	0.880	0.458
243	MIX-COMP-THERM-009-002	0.660	0.807	0.720	0.835	0.400
244	MIX-COMP-THERM-009-003	0.647	0.796	0.708	0.828	0.382
245	MIX-COMP-THERM-009-004	0.647	0.797	0.706	0.826	0.385
246	MIX-COMP-THERM-009-005	0.655	0.803	0.708	0.826	0.398
247	MIX-COMP-THERM-009-006	0.657	0.804	0.708	0.825	0.401
248	MIX-COMP-THERM-011-001	0.481	0.615	0.562	0.679	0.287
249	MIX-COMP-THERM-011-002	0.481	0.615	0.562	0.679	0.287
250	MIX-COMP-THERM-011-003	0.482	0.616	0.563	0.680	0.288
251	MIX-COMP-THERM-011-004	0.517	0.648	0.593	0.707	0.319
252	MIX-COMP-THERM-011-005	0.516	0.648	0.593	0.707	0.318
253	MIX-COMP-THERM-011-006	0.516	0.647	0.593	0.707	0.319
254	MIX-COMP-THERM-012-001	0.600	0.776	0.654	0.801	0.360
255	MIX-COMP-THERM-012-002	0.600	0.776	0.654	0.801	0.360
256	MIX-COMP-THERM-012-003	0.600	0.776	0.654	0.801	0.360
257	MIX-COMP-THERM-012-004	0.599	0.776	0.654	0.801	0.359
258	MIX-COMP-THERM-012-005	0.600	0.776	0.654	0.801	0.359
259	MIX-COMP-THERM-012-006	0.599	0.776	0.654	0.801	0.359
260	MIX-COMP-THERM-012-007	0.565	0.729	0.618	0.754	0.334
261	MIX-COMP-THERM-012-008	0.565	0.729	0.618	0.755	0.335
262	MIX-COMP-THERM-012-009	0.568	0.732	0.620	0.757	0.337
263	MIX-COMP-THERM-012-010	0.568	0.732	0.620	0.757	0.338
264	MIX-COMP-THERM-012-011	0.567	0.731	0.619	0.756	0.336
265	MIX-COMP-THERM-012-012	0.567	0.731	0.619	0.756	0.336
266	MIX-COMP-THERM-012-013	0.565	0.729	0.618	0.755	0.335
267	MIX-COMP-THERM-012-014	0.543	0.712	0.599	0.742	0.318
268	MIX-COMP-THERM-012-015	0.544	0.714	0.600	0.744	0.319
269	MIX-COMP-THERM-012-016	0.545	0.715	0.601	0.745	0.320
270	MIX-COMP-THERM-012-017	0.546	0.716	0.602	0.746	0.321
271	MIX-COMP-THERM-012-018	0.548	0.718	0.603	0.747	0.322
272	MIX-COMP-THERM-012-019	0.549	0.720	0.604	0.748	0.324

Table B.1 Critical experiment similarity assessment c_k values for applications (continued)

No.	Experiment ID	PWR SFP 10 GWd/MTU	PWR SFP 40 GWd/MTU	GBC-32 10 GWd/MTU	GBC-32 40 GWd/MTU	BWR SFP 11 GWd/MTU
273	MIX-COMP-THERM-012-020	0.531	0.701	0.590	0.734	0.307
274	MIX-COMP-THERM-012-021	0.531	0.700	0.590	0.734	0.307
275	MIX-COMP-THERM-012-022	0.525	0.686	0.569	0.704	0.320
276	MIX-COMP-THERM-012-023	0.518	0.687	0.573	0.717	0.304
277	MIX-COMP-THERM-012-024	0.519	0.688	0.573	0.718	0.304
278	MIX-COMP-THERM-012-025	0.521	0.690	0.575	0.719	0.306
279	MIX-COMP-THERM-012-026	0.524	0.694	0.578	0.722	0.308
280	MIX-COMP-THERM-012-027	0.527	0.697	0.580	0.725	0.311
281	MIX-COMP-THERM-012-028	0.528	0.698	0.581	0.726	0.312
282	MIX-COMP-THERM-012-029	0.530	0.700	0.583	0.728	0.313
283	MIX-COMP-THERM-012-030	0.525	0.694	0.578	0.723	0.309
284	MIX-COMP-THERM-012-031	0.502	0.670	0.559	0.703	0.291
285	MIX-COMP-THERM-012-032	0.503	0.671	0.560	0.704	0.292
286	MIX-COMP-THERM-012-033	0.502	0.670	0.559	0.703	0.292
287	MIX-SOL-THERM-001-001	0.539	0.711	0.595	0.742	0.318
288	MIX-SOL-THERM-001-002	0.539	0.711	0.595	0.741	0.318
289	MIX-SOL-THERM-001-003	0.524	0.694	0.584	0.728	0.306
290	MIX-SOL-THERM-001-004	0.539	0.712	0.596	0.742	0.318
291	MIX-SOL-THERM-001-005	0.549	0.723	0.604	0.751	0.327
292	MIX-SOL-THERM-001-006	0.523	0.693	0.583	0.728	0.304
293	MIX-SOL-THERM-001-007	0.494	0.666	0.548	0.697	0.292
294	MIX-SOL-THERM-001-008	0.495	0.665	0.550	0.696	0.289
295	MIX-SOL-THERM-001-009	0.506	0.675	0.561	0.706	0.295
296	MIX-SOL-THERM-001-010	0.539	0.711	0.595	0.740	0.319
297	MIX-SOL-THERM-001-011	0.547	0.719	0.601	0.746	0.325
298	MIX-SOL-THERM-001-012	0.539	0.710	0.594	0.739	0.319
299	MIX-SOL-THERM-001-013	0.544	0.714	0.598	0.742	0.322
300	MIX-SOL-THERM-002-001	0.568	0.734	0.612	0.749	0.340
301	MIX-SOL-THERM-002-002	0.569	0.735	0.613	0.750	0.341
302	MIX-SOL-THERM-002-003	0.576	0.741	0.619	0.755	0.347
303	MIX-SOL-THERM-004-001	0.485	0.646	0.543	0.682	0.274
304	MIX-SOL-THERM-004-002	0.496	0.658	0.554	0.693	0.284
305	MIX-SOL-THERM-004-003	0.501	0.665	0.558	0.698	0.288
306	MIX-SOL-THERM-004-004	0.494	0.661	0.552	0.696	0.286
307	MIX-SOL-THERM-004-005	0.489	0.655	0.548	0.691	0.281
308	MIX-SOL-THERM-004-006	0.476	0.641	0.536	0.679	0.270
309	MIX-SOL-THERM-004-007	0.485	0.653	0.545	0.690	0.277
310	MIX-SOL-THERM-004-008	0.496	0.665	0.555	0.701	0.286
311	MIX-SOL-THERM-004-009	0.501	0.671	0.559	0.706	0.291

Table B.1 Critical experiment similarity assessment c_k values for applications (continued)

No.	Experiment ID	PWR SFP 10 GWd/MTU	PWR SFP 40 GWd/MTU	GBC-32 10 GWd/MTU	GBC-32 40 GWd/MTU	BWR SFP 11 GWd/MTU
312	MIX-SOL-THERM-005-001	0.500	0.664	0.557	0.697	0.287
313	MIX-SOL-THERM-005-002	0.523	0.689	0.579	0.720	0.307
314	MIX-SOL-THERM-005-003	0.510	0.679	0.568	0.712	0.300
315	MIX-SOL-THERM-005-004	0.515	0.684	0.572	0.717	0.304
316	MIX-SOL-THERM-005-005	0.493	0.661	0.552	0.696	0.285
317	MIX-SOL-THERM-005-006	0.500	0.671	0.559	0.706	0.291
318	MIX-SOL-THERM-005-007	0.519	0.691	0.577	0.724	0.308
319	HTC1_01	0.842	0.913	0.878	0.927	0.629
320	HTC1_02	0.839	0.910	0.877	0.926	0.626
321	HTC1_03	0.840	0.911	0.877	0.926	0.627
322	HTC1_04	0.783	0.869	0.848	0.912	0.538
323	HTC1_05	0.783	0.869	0.848	0.911	0.539
324	HTC1_06	0.783	0.869	0.848	0.911	0.539
325	HTC1_07	0.761	0.851	0.834	0.902	0.507
326	HTC1_08	0.761	0.851	0.835	0.902	0.508
327	HTC1_09	0.762	0.852	0.835	0.903	0.508
328	HTC1_10	0.751	0.843	0.830	0.899	0.492
329	HTC1_11	0.752	0.844	0.830	0.900	0.494
330	HTC1_12	0.753	0.845	0.831	0.900	0.495
331	HTC1_13	0.771	0.861	0.846	0.912	0.520
332	HTC1_14	0.772	0.862	0.846	0.913	0.520
333	HTC1_15	0.772	0.862	0.846	0.913	0.520
334	HTC1_16	0.769	0.858	0.840	0.907	0.516
335	HTC1_17	0.772	0.860	0.843	0.909	0.521
336	HTC1_18	0.772	0.861	0.843	0.910	0.520
337	HTC2B_01	0.788	0.877	0.858	0.924	0.540
338	HTC2B_02	0.789	0.878	0.859	0.925	0.542
339	HTC2B_03	0.801	0.889	0.868	0.932	0.557
340	HTC2B_04	0.815	0.903	0.878	0.942	0.577
341	HTC2B_05	0.828	0.914	0.886	0.949	0.594
342	HTC2B_06	0.828	0.914	0.886	0.949	0.594
343	HTC2B_07	0.841	0.926	0.895	0.956	0.612
344	HTC2B_08	0.851	0.935	0.901	0.961	0.628
345	HTC2B_09	0.861	0.945	0.906	0.966	0.640
346	HTC2B_10	0.845	0.931	0.897	0.959	0.615
347	HTC2B_11	0.828	0.916	0.887	0.951	0.591
348	HTC2B_12	0.811	0.901	0.875	0.941	0.568
349	HTC2B_13	0.793	0.884	0.862	0.929	0.544
350	HTC2B_14	0.774	0.866	0.848	0.916	0.521

Table B.1 Critical experiment similarity assessment c_k values for applications (continued)

No.	Experiment ID	PWR SFP 10 GWd/MTU	PWR SFP 40 GWd/MTU	GBC-32 10 GWd/MTU	GBC-32 40 GWd/MTU	BWR SFP 11 GWd/MTU
351	HTC2B_15	0.791	0.879	0.858	0.923	0.544
352	HTC2B_16	0.813	0.900	0.873	0.937	0.573
353	HTC2B_17	0.837	0.921	0.889	0.950	0.605
354	HTC2B_18	0.857	0.939	0.900	0.959	0.635
355	HTC2B_19	0.795	0.883	0.861	0.926	0.550
356	HTC2B_20	0.846	0.926	0.891	0.948	0.623
357	HTC2B_21	0.818	0.901	0.873	0.934	0.583
358	HTC2G_01	0.795	0.884	0.863	0.929	0.550
359	HTC2G_02	0.794	0.884	0.863	0.929	0.549
360	HTC2G_03	0.813	0.901	0.876	0.940	0.574
361	HTC2G_04	0.813	0.902	0.877	0.941	0.575
362	HTC2G_05	0.813	0.902	0.877	0.941	0.574
363	HTC2G_06	0.829	0.916	0.887	0.950	0.596
364	HTC2G_07	0.831	0.918	0.888	0.951	0.599
365	HTC2G_08	0.846	0.932	0.898	0.959	0.621
366	HTC2G_09	0.846	0.932	0.898	0.959	0.622
367	HTC2G_10	0.862	0.946	0.906	0.966	0.642
368	HTC2G_11	0.837	0.925	0.892	0.956	0.604
369	HTC2G_12	0.838	0.926	0.892	0.956	0.605
370	HTC2G_13	0.812	0.902	0.875	0.941	0.569
371	HTC2G_14	0.813	0.903	0.876	0.942	0.570
372	HTC2G_15	0.783	0.875	0.854	0.923	0.532
373	HTC2G_16	0.785	0.876	0.856	0.924	0.534
374	HTC2G_17	0.804	0.892	0.867	0.932	0.561
375	HTC2G_18	0.836	0.917	0.884	0.943	0.608
376	HTC2G_19	0.840	0.925	0.891	0.953	0.611
377	HTC2G_20	0.808	0.896	0.870	0.934	0.566
378	HTC3_01	0.817	0.903	0.878	0.941	0.575
379	HTC3_02	0.821	0.907	0.882	0.945	0.580
380	HTC3_03	0.824	0.910	0.883	0.946	0.584
381	HTC3_04	0.823	0.908	0.882	0.945	0.582
382	HTC3_05	0.824	0.910	0.884	0.946	0.584
383	HTC3_06	0.832	0.916	0.889	0.949	0.595
384	HTC3_07	0.821	0.907	0.882	0.944	0.580
385	HTC3_08	0.826	0.912	0.886	0.948	0.587
386	HTC3_09	0.826	0.911	0.885	0.947	0.587
387	HTC3_10	0.826	0.911	0.885	0.947	0.587
388	HTC3_11	0.824	0.910	0.884	0.946	0.584
389	HTC3_12	0.771	0.861	0.844	0.911	0.517

Table B.1 Critical experiment similarity assessment c_k values for applications (continued)

No.	Experiment ID	PWR SFP 10 GWd/MTU	PWR SFP 40 GWd/MTU	GBC-32 10 GWd/MTU	GBC-32 40 GWd/MTU	BWR SFP 11 GWd/MTU
390	HTC3_13	0.780	0.869	0.851	0.917	0.528
391	HTC3_14	0.792	0.879	0.860	0.924	0.543
392	HTC3_15	0.797	0.883	0.863	0.927	0.549
393	HTC3_16	0.803	0.889	0.868	0.930	0.557
394	HTC3_17	0.811	0.895	0.873	0.934	0.567
395	HTC3_18	0.821	0.903	0.879	0.939	0.581
396	HTC3_19	0.816	0.899	0.875	0.935	0.576
397	HTC3_20	0.818	0.900	0.876	0.936	0.579
398	HTC3_21	0.784	0.871	0.852	0.917	0.535
399	HTC3_22	0.770	0.859	0.842	0.909	0.517
400	HTC3_23	0.761	0.852	0.836	0.905	0.506
401	HTC3_24	0.776	0.866	0.850	0.917	0.523
402	HTC3_25	0.804	0.890	0.869	0.931	0.558
403	HTC3_26	0.793	0.880	0.860	0.925	0.543
404	HTC4FE_01	0.836	0.920	0.893	0.953	0.602
405	HTC4FE_02	0.836	0.920	0.893	0.953	0.602
406	HTC4FE_03	0.837	0.920	0.893	0.953	0.602
407	HTC4FE_04	0.837	0.920	0.893	0.953	0.602
408	HTC4FE_05	0.836	0.919	0.892	0.953	0.601
409	HTC4FE_06	0.834	0.918	0.891	0.952	0.599
410	HTC4FE_07	0.835	0.919	0.891	0.952	0.599
411	HTC4FE_08	0.833	0.918	0.890	0.951	0.597
412	HTC4FE_09	0.832	0.916	0.889	0.950	0.594
413	HTC4FE_10	0.833	0.917	0.890	0.951	0.596
414	HTC4FE_11	0.830	0.914	0.889	0.949	0.593
415	HTC4FE_12	0.844	0.926	0.897	0.955	0.612
416	HTC4FE_13	0.840	0.922	0.894	0.953	0.606
417	HTC4FE_14	0.842	0.925	0.897	0.956	0.609
418	HTC4FE_15	0.838	0.921	0.894	0.954	0.603
419	HTC4FE_16	0.834	0.918	0.891	0.952	0.598
420	HTC4FE_17	0.833	0.917	0.891	0.951	0.597
421	HTC4FE_18	0.833	0.917	0.890	0.951	0.595
422	HTC4FE_19	0.832	0.916	0.889	0.950	0.594
423	HTC4FE_20	0.830	0.914	0.888	0.949	0.591
424	HTC4FE_21	0.839	0.922	0.895	0.954	0.605
425	HTC4FE_22	0.801	0.888	0.870	0.933	0.556
426	HTC4FE_23	0.804	0.891	0.872	0.935	0.560
427	HTC4FE_24	0.811	0.896	0.876	0.938	0.569
428	HTC4FE_25	0.810	0.896	0.876	0.938	0.567

Table B.1 Critical experiment similarity assessment c_k values for applications (continued)

No.	Experiment ID	PWR SFP 10 GWd/MTU	PWR SFP 40 GWd/MTU	GBC-32 10 GWd/MTU	GBC-32 40 GWd/MTU	BWR SFP 11 GWd/MTU
429	HTC4FE_26	0.810	0.895	0.875	0.937	0.567
430	HTC4FE_27	0.808	0.894	0.874	0.936	0.565
431	HTC4FE_28	0.809	0.894	0.874	0.936	0.565
432	HTC4FE_29	0.822	0.905	0.883	0.943	0.583
433	HTC4FE_30	0.825	0.908	0.885	0.945	0.586
434	HTC4FE_31	0.820	0.904	0.882	0.943	0.579
435	HTC4FE_32	0.812	0.897	0.877	0.939	0.568
436	HTC4FE_33	0.807	0.893	0.873	0.936	0.562
437	HTC4PB_01	0.831	0.916	0.889	0.950	0.595
438	HTC4PB_02	0.831	0.916	0.889	0.950	0.594
439	HTC4PB_03	0.832	0.917	0.889	0.950	0.595
440	HTC4PB_04	0.833	0.917	0.889	0.950	0.596
441	HTC4PB_05	0.831	0.916	0.888	0.949	0.594
442	HTC4PB_06	0.828	0.913	0.886	0.948	0.590
443	HTC4PB_07	0.827	0.912	0.885	0.947	0.587
444	HTC4PB_08	0.832	0.916	0.888	0.950	0.594
445	HTC4PB_09	0.830	0.915	0.888	0.949	0.592
446	HTC4PB_10	0.832	0.916	0.889	0.950	0.594
447	HTC4PB_11	0.829	0.914	0.887	0.948	0.591
448	HTC4PB_12	0.841	0.923	0.895	0.953	0.607
449	HTC4PB_13	0.841	0.923	0.895	0.954	0.608
450	HTC4PB_14	0.841	0.923	0.894	0.953	0.606
451	HTC4PB_15	0.836	0.919	0.891	0.951	0.600
452	HTC4PB_16	0.837	0.920	0.892	0.951	0.602
453	HTC4PB_17	0.835	0.919	0.892	0.952	0.600
454	HTC4PB_18	0.833	0.917	0.890	0.951	0.597
455	HTC4PB_19	0.830	0.915	0.888	0.949	0.592
456	HTC4PB_20	0.829	0.914	0.887	0.948	0.591
457	HTC4PB_21	0.831	0.916	0.889	0.950	0.593
458	HTC4PB_22	0.831	0.915	0.888	0.949	0.593
459	HTC4PB_23	0.830	0.915	0.888	0.949	0.592
460	HTC4PB_24	0.829	0.914	0.887	0.949	0.590
461	HTC4PB_25	0.827	0.912	0.886	0.947	0.588
462	HTC4PB_26	0.825	0.910	0.885	0.946	0.585
463	HTC4PB_27	0.795	0.883	0.864	0.929	0.547
464	HTC4PB_28	0.798	0.885	0.866	0.930	0.550
465	HTC4PB_29	0.804	0.891	0.870	0.933	0.559
466	HTC4PB_30	0.817	0.901	0.878	0.939	0.575
467	HTC4PB_31	0.819	0.902	0.879	0.940	0.577

Table B.1 Critical experiment similarity assessment c_k values for applications (continued)

No.	Experiment ID	PWR SFP 10 GWd/MTU	PWR SFP 40 GWd/MTU	GBC-32 10 GWd/MTU	GBC-32 40 GWd/MTU	BWR SFP 11 GWd/MTU
468	HTC4PB_32	0.812	0.897	0.874	0.936	0.568
469	HTC4PB_33	0.805	0.891	0.869	0.932	0.558
470	HTC4PB_34	0.799	0.886	0.865	0.929	0.551
471	HTC4PB_35	0.805	0.891	0.870	0.934	0.560
472	HTC4PB_36	0.804	0.890	0.870	0.933	0.559
473	HTC4PB_37	0.804	0.890	0.870	0.933	0.559
474	HTC4PB_38	0.804	0.890	0.870	0.933	0.559

APPENDIX C
BIAS AND BIAS UNCERTAINTY USING GLLSM

C.1 GENERALIZED LINEAR LEAST-SQUARES METHOD (GLLSM) BIAS ESTIMATES

A new capability for SCALE allows the prediction of computational biases and bias uncertainties with the SCALE TSURFER program (Ref. 14, Section M21), which applies a generalized linear least-squares method (GLLSM) (Ref. 25) technique using the k_{eff} sensitivity data, calculated k_{eff} values, expected k_{eff} values, experimental uncertainty information, and cross-section covariance data to generate cross-section adjustments that minimize the overall chi-square (χ^2) statistic for the system of critical experiments. Cross-section covariance data are used as a restraint on cross-section adjustments. Benchmark-model k_{eff} uncertainty values and user-specified correlation data for benchmark model k_{eff} values are used as restraints on benchmark-model k_{eff} adjustments. The cross-section adjustments are then combined with the k_{eff} sensitivity data for the safety analysis model(s) to produce bias estimates. If similar experiments are available to validate the use of a particular nuclide in the application, the uncertainty of the bias for this nuclide is reduced through the GLLSM procedure. In TSURFER, experiments that are dissimilar from the application can still provide useful information for bias assessment if at least one material demonstrates similar sensitivities to those of the experiments that are similar to the application. If similar experiments are not available to validate a particular nuclide, the uncertainty in the bias for the given nuclide is determined using the unadjusted SCALE cross-section covariance data (or for nuclides and reactions not present in the covariance file, user-specified values may be used). A recent detailed derivation of the GLLSM formalism is given in Ref. 25. The general formalism allows cross correlations between the initial integral experiment measurements and the original nuclear data, such as would be present if the calculations used a previously “adjusted” library of nuclear data.

The TSURFER procedure for bias and bias uncertainty assessment is quite different from those traditionally used in criticality-safety evaluations based on interpolation or extrapolation of a trend line with a confidence band treating uncertainties in the data as well as uncertainties in the trend line itself. Instead of trending the data, TSURFER assimilates individual data components, rejecting inconsistent components based on user input criteria. Historically, the validity of a calculation performed for some application has been established by considering how well the same calculational methods and nuclear data perform for a set of representative benchmark experiments. While a simple comparison of the computed and experimental results is very informative, it does not fully take advantage of the valuable information provided by the measured integral responses. If the original sets of calculated and experimental responses are consolidated in a consistent manner (i.e., correctly accounting for uncertainties), then the “adjusted” results should be a better estimate of the true responses because the revised response values are based upon more information than was available in either the original calculations or measurements alone. This is essentially a statement of the Bayes Theorem from probability theory, which indicates how prior information (calculated responses) can be evolved by incorporating additional information (integral measurements) into more reliable posterior results (the adjusted responses). The equations used for the GLLSM are provided in Broadhead et al. (Ref. 25).

TSURFER performs an assessment of sources of the computational bias by multiplying the individual sensitivities of the application by the cross-section adjustments that are performed within its implementation. Hence, TSURFER can predict individual biases in application k_{eff} values associated with individual reactions, such as (n,γ) absorptions by FP nuclides. In addition to generating cross-section adjustments, TSURFER calculates the reduction in the nuclear data uncertainty that results from application of the GLLSM, generating a set of revised cross-section covariance data. As a result of application of the chi-squared minimization technique, the

revised covariance data include many more correlations between neutron energy groups, reactions, and nuclides than were present in the unmodified covariance data. The revised covariance data can be applied to the k_{eff} sensitivity data of the safety analysis model(s) to quantify the residual uncertainty in k_{eff} due to the post-adjustment uncertainty in the nuclear data. One of the challenges yet to be resolved prior to TSURFER's being recommended for criticality safety assessments is that it is not presently clear how the residual uncertainty in k_{eff} should be modified or used to support compliance with the 10 CFR 50.68 requirements for use of a 95% probability with a 95% confidence bias and uncertainty. Another limitation is the lack of experimental correlation data. Uncertainties in benchmark experiments are rigorously quantified and documented in the IHECSBE and other experiment documents. Where experiments use the same materials or same measurement devices, uncertainties quantified for different experiments will be correlated. Of the approximately 4000 experiments in IHECSBE, only about 60 have experimental correlations quantified. Hence, TSURFER can currently be used only to confirm bias and bias uncertainty results obtained using other methods.

C.2 GENERALIZED LINEAR LEAST-SQUARES METHODS

The analysis is conducted with a suite of benchmark experiments for which the benchmark k_{eff} values and their uncertainties, as well as correlations in uncertainties between benchmarks, are quantified. The unbiased or adjusted k_{eff} for the application is computed through sensitivity coefficients, not through a criticality calculation using adjusted nuclear data. Thus, with a complete set of experiments to validate important components in the application, a precise bias with a small uncertainty can be predicted. Where the experimental coverage is lacking, a bias can be predicted with an appropriately large uncertainty.

The TSURFER method is much more suitable than traditional bias estimation techniques, given the limited number of directly comparable experiments (with and without FPs) and the unresolved nature of some observed trends or differences in the FP data. Also, TSURFER is better suited to use experiments involving mixtures of FPs than are conventional techniques.

A significant benefit of the TSURFER technique is that it provides a means to use information from experiments that have low (<0.8) TSUNAMI-IP–determined similarity coefficients (i.e., c_k values) with respect to a given application model. Traditional validation techniques necessitate high similarity in order to develop appropriate biases.

C.3 GLLSM RESULTS

Bias and bias uncertainty results of the TSURFER analyses are provided in Table C.1 for the PWR SFP BUC application models using actinides plus 16 FPs. From Table C.1, note that with the exception of ^{103}Rh, the FP biases are positive and that the overall bias for the seven FPs evaluated is positive.

Table C.1 TSURFER results using actinide + 16 FP isotopes

Configuration	**PWR SFP**	**PWR SFP**	**PWR SFP**	**PWR SFP**
Fuel burnup (GWd/MTU)	**10**	**25**	**40**	**57**
Initial application k_{eff}	0.99039	0.98991	0.98997	0.99006
Initial uncertainty (Δk) for application k_{eff}	0.00480	0.00506	0.00506	0.00501
Total bias (Δk) in initial k_{eff}	0.00189	0.00156	0.00172	0.00188
Adjusted application k_{eff}	0.98852	0.98834	0.98824	0.98816
Uncertainty for adjusted k_{eff} (Δk)	0.00074	0.00065	0.00067	0.00072
Bias (Δk) in initial k_{eff} by FP nuclide				
^{103}Rh	–0.00013	–0.00037	–0.00054	–0.00066
^{133}Cs	0.00009	0.00022	0.00032	0.00039
^{143}Nd	0.00019	0.00045	0.00063	0.00076
^{145}Nd	0.00005	0.00013	0.00020	0.00025
^{149}Sm	0.00042	0.00048	0.00054	0.00054
^{152}Sm	0.00004	0.00010	0.00014	0.00017
^{155}Gd	0.00000	0.00000	0.00000	0.00000
Total FP bias (Δk) in initial k_{eff}	0.00066	0.00101	0.00129	0.00145
Residual uncertainty (Δk) for adjusted k_{eff} by FP nuclide[a]				
^{103}Rh	7.3×10^{-6}	2.1×10^{-5}	3.1×10^{-5}	3.8×10^{-5}
^{133}Cs	8.1×10^{-6}	2.0×10^{-5}	2.9×10^{-5}	3.6×10^{-5}
^{143}Nd	5.7×10^{-5}	1.3×10^{-4}	1.8×10^{-4}	2.1×10^{-4}
^{145}Nd	4.2×10^{-5}	1.0×10^{-4}	1.6×10^{-4}	2.0×10^{-4}
^{149}Sm	4.0×10^{-5}	4.5×10^{-5}	5.0×10^{-5}	5.1×10^{-5}
^{152}Sm	8.7×10^{-6}	2.1×10^{-5}	2.9×10^{-5}	3.4×10^{-5}
^{155}Gd	--	--	--	--
Residual uncertainty (Δk) in adjusted k_{eff} for 7 FP nuclides	8.3×10^{-5}	1.7×10^{-4}	2.5×10^{-4}	3.0×10^{-4}

[a]Bias uncertainty data are 1-σ and are based on (n,γ) reactions only.

The TSURFER calculated total bias and residual nuclear data uncertainty for the various parametric application models are provided in Table C.2. The impacts of the parametric variations on the FP biases are presented in Table C.3 with residual FP nuclear data uncertainty values provided in Table C.4. Only the six FPs that are present in the critical benchmark experiment suite are listed. The 0 decay time cases were not evaluated with TSURFER.

Because the FP experiment data are proprietary and most applicants will not have access to them, and other publicly available FP experiments are limited in quantity, the TSUNAMI-IP results in Table C.5 were compared with the TSURFER results. These results are presented in Figure C.1, showing that the base case FP uncertainty based on the cross-section covariance data at a 1σ confidence level is bounding of the true FP bias and bias uncertainty based on experimental data, as calculated using GLLSM techniques.

Table C.2 TSURFER total bias and bias uncertainty (1σ)

Description	Change from base	Bias / residual nuclear data uncertainty (Δk)			
		Final BU (GWd/MTU)			
		10	25	40	57
PWR SFP model					
Assembly design	B&W 15×15	1.99E-03 / 7.99E-04	1.76E-03 / 6.96E-04	2.03E-03 / 7.36E-04	2.30E-03/7.92E-04
	W 17×17 no BAs	2.01E-03 / 7.49E-04	1.73E-03 / 6.30E-04	1.88E-03 / 6.52E-04	1.92E-03/6.88E-04
Rack design	Unpoisoned panels	5.48E-04 / 1.36E-03	1.29E-04 / 1.21E-03	4.01E-04 / 1.17E-03	6.18E-04/1.16E-03
	Cell pitch increased 0.5 in.	1.54E-03 / 6.88E-04	1.36E-03 / 5.96E-04	1.55E-03 / 6.38E-04	1.58E-03/6.73E-04
	Poison panel B10 +10%	1.82E-03 / 7.44E-04	1.59E-03 / 6.40E-04	1.77E-03 / 6.75E-04	1.94E-03/7.25E-04
	Poison panel B10 -10%	1.80E-03 / 7.40E-04	1.54E-03 / 6.31E-04	1.77E-03 / 6.68E-04	1.94E-03/7.20E-04
Decay time	1 yr	1.89E-03 / 7.34E-04	1.69E-03 / 6.28E-04	1.91E-03 / 6.60E-04	2.06E-03/7.04E-04
	5 yr	1.98E-03 / 7.29E-04	2.02E-03 / 6.19E-04	2.40E-03 / 6.49E-04	2.50E-03/6.79E-04
	20 yr	2.16E-03 / 7.27E-04	2.57E-03 / 6.27E-04	3.28E-03 / 6.85E-04	3.44E-03/7.04E-04
	40 yr	2.24E-03 / 7.25E-04	2.81E-03 / 6.41E-04	3.68E-03 / 7.21E-04	3.89E-03/7.53E-04
Soluble boron	1000 ppm[a]	1.75E-03 / 6.91E-04	1.41E-03 / 6.15E-04	1.56E-03 / 6.55E-04	1.67E-03/7.02E-04
	ppm for k_{eff} = 0.94	1.79E-03 / 7.02E-04	1.52E-03 / 6.12E-04	1.67E-03 / 6.53E-04	1.80E-03/7.03E-04
Axial burnup	1 node	1.94E-03 / 7.51E-04	2.09E-03 / 7.20E-04	2.45E-03 / 8.25E-04	2.56E-03/9.66E-04

[a]Parts per million boron by mass.

Table C.3 TSURFER FP isotope bias

Description	Change from base	Burnup (GWd/MTU)	FP isotope bias (Δk)[a]							
			^{103}Rh	^{133}Cs	^{143}Nd	^{145}Nd	^{149}Sm	^{152}Sm	^{155}Gd	Total
Base case	--	10	−0.00013	0.00009	0.00019	0.00005	0.00042	0.00004	0.00000	0.00066
		25	−0.00037	0.00022	0.00045	0.00013	0.00048	0.00010	0.00000	0.00101
		40	−0.00054	0.00032	0.00063	0.00020	0.00054	0.00014	0.00000	0.00129
		57	−0.00066	0.00039	0.00076	0.00025	0.00054	0.00017	0.00000	0.00145
Assembly design	B&W 15×15	10	−0.00013	0.00008	0.00009	0.00003	0.00036	0.00002	0.00000	0.00045
		25	−0.00032	0.00017	0.00019	0.00008	0.00041	0.00004	0.00000	0.00058
		40	−0.00045	0.00025	0.00027	0.00012	0.00043	0.00006	0.00000	0.00068
		57	−0.00053	0.00030	0.00032	0.00015	0.00044	0.00007	0.00000	0.00076
	W 17×17 (No BAs)	10	−0.00008	0.00006	0.00007	0.00003	0.00037	0.00002	0.00000	0.00046
		25	−0.00024	0.00015	0.00017	0.00007	0.00044	0.00004	0.00000	0.00062
		40	−0.00037	0.00022	0.00024	0.00010	0.00048	0.00005	0.00000	0.00073
		57	−0.00045	0.00026	0.00030	0.00013	0.00048	0.00006	0.00000	0.00078
Rack design	Unpoisoned panels	10	−0.00010	0.00006	0.00009	0.00003	0.00047	0.00002	0.00000	0.00057
		25	−0.00027	0.00014	0.00018	0.00007	0.00052	0.00004	0.00000	0.00068
		40	−0.00039	0.00021	0.00025	0.00010	0.00056	0.00006	0.00000	0.00080
		57	−0.00046	0.00026	0.00031	0.00012	0.00056	0.00006	0.00000	0.00085
	Cell pitch increased 0.25 in.	10	−0.00009	0.00006	0.00007	0.00003	0.00041	0.00002	0.00000	0.00050
		25	−0.00024	0.00014	0.00016	0.00006	0.00050	0.00004	0.00000	0.00066
		40	−0.00036	0.00021	0.00023	0.00010	0.00053	0.00005	0.00000	0.00076
		57	−0.00043	0.00024	0.00028	0.00012	0.00053	0.00006	0.00000	0.00080
	Poison panel B10 +10%	10	−0.00009	0.00006	0.00007	0.00003	0.00041	0.00002	0.00000	0.00050
		25	−0.00026	0.00015	0.00017	0.00007	0.00046	0.00004	0.00000	0.00063
		40	−0.00038	0.00022	0.00024	0.00010	0.00051	0.00005	0.00000	0.00076
		57	−0.00046	0.00027	0.00029	0.00013	0.00052	0.00006	0.00000	0.00082

Table C.3 TSURFER FP isotope bias (continued)

Description	Change from base	Burnup (GWd/MTU)	FP isotope bias (Δk)[a]							
			^{103}Rh	^{133}Cs	^{143}Nd	^{145}Nd	^{149}Sm	^{152}Sm	^{155}Gd	Total
	Poison panel B10 -10%	10	−0.00009	0.00006	0.00007	0.00003	0.00041	0.00002	0.00000	0.00050
		25	−0.00026	0.00015	0.00017	0.00007	0.00046	0.00004	0.00000	0.00063
		40	−0.00038	0.00022	0.00024	0.00010	0.00052	0.00005	0.00000	0.00076
		57	−0.00046	0.00027	0.00030	0.00013	0.00052	0.00006	0.00000	0.00082
Decay time	1 year	10	−0.00013	0.00006	0.00008	0.00003	0.00048	0.00002	0.00000	0.00053
		25	−0.00030	0.00015	0.00017	0.00007	0.00054	0.00004	0.00001	0.00068
		40	−0.00042	0.00022	0.00024	0.00010	0.00057	0.00005	0.00001	0.00078
		57	−0.00049	0.00027	0.00029	0.00013	0.00057	0.00006	0.00002	0.00084
	5 year	10	−0.00013	0.00006	0.00008	0.00003	0.00047	0.00002	0.00001	0.00053
		25	−0.00029	0.00015	0.00017	0.00007	0.00053	0.00004	0.00003	0.00069
		40	−0.00041	0.00022	0.00024	0.00010	0.00056	0.00005	0.00004	0.00080
		57	−0.00047	0.00026	0.00028	0.00012	0.00055	0.00006	0.00006	0.00086
	20 year	10	−0.00012	0.00006	0.00007	0.00003	0.00046	0.00002	0.00002	0.00053
		25	−0.00027	0.00014	0.00016	0.00006	0.00052	0.00004	0.00004	0.00068
		40	−0.00038	0.00021	0.00023	0.00010	0.00055	0.00005	0.00007	0.00082
		57	−0.00043	0.00024	0.00026	0.00011	0.00053	0.00006	0.00009	0.00086
	40 year	10	−0.00012	0.00006	0.00007	0.00003	0.00046	0.00001	0.00002	0.00053
		25	−0.00026	0.00014	0.00015	0.00006	0.00052	0.00003	0.00004	0.00068
		40	−0.00038	0.00021	0.00022	0.00010	0.00055	0.00005	0.00007	0.00081
		57	−0.00041	0.00023	0.00026	0.00011	0.00052	0.00005	0.00009	0.00085
Soluble boron	1000 ppm	10	−0.00008	0.00006	0.00006	0.00002	0.00030	0.00001	0.00000	0.00037
		25	−0.00022	0.00013	0.00013	0.00006	0.00036	0.00003	0.00000	0.00050
		40	−0.00033	0.00020	0.00020	0.00009	0.00040	0.00005	0.00000	0.00060
		57	−0.00041	0.00024	0.00025	0.00011	0.00041	0.00006	0.00000	0.00066

Table C.3 TSURFER FP isotope bias (continued)

Description	Change from base	Burnup (GWd/MTU)	FP isotope bias (Δk)[a]							
			^{103}Rh	^{133}Cs	^{143}Nd	^{145}Nd	^{149}Sm	^{152}Sm	^{155}Gd	Total
	Search for k_{eff} = 0.94	10	−0.00009	0.00006	0.00007	0.00003	0.00037	0.00002	0.00000	0.00046
		25	−0.00024	0.00014	0.00015	0.00006	0.00043	0.00004	0.00000	0.00059
		40	−0.00036	0.00021	0.00022	0.00010	0.00046	0.00005	0.00000	0.00069
		57	−0.00044	0.00026	0.00027	0.00012	0.00047	0.00006	0.00000	0.00075
Cross-section library	ENDF-B/V	10	N/A[b]	N/A	N/A	N/A	N/A	N/A	N/A	N/A
		25	N/A	N/A	N/A	N/A	N/A	N/A	N/A	N/A
		40	N/A	N/A	N/A	N/A	N/A	N/A	N/A	N/A
		57	N/A	N/A	N/A	N/A	N/A	N/A	N/A	N/A
	ENDF-B/VI	10	N/A	N/A	N/A	N/A	N/A	N/A	N/A	N/A
		25	N/A	N/A	N/A	N/A	N/A	N/A	N/A	N/A
		40	N/A	N/A	N/A	N/A	N/A	N/A	N/A	N/A
		57	N/A	N/A	N/A	N/A	N/A	N/A	N/A	N/A
Axial burnup	1 node	10	−0.00013	0.00009	0.00010	0.00004	0.00050	0.00003	0.00000	0.00063
		25	−0.00034	0.00020	0.00022	0.00009	0.00057	0.00005	0.00000	0.00079
		40	−0.00048	0.00028	0.00031	0.00014	0.00059	0.00007	0.00000	0.00091
		57	−0.00057	0.00033	0.00039	0.00017	0.00059	0.00008	0.00000	0.00100

[a]Bias data based on (n, γ) reactions only.
[b]N/A = not available because sensitivity data files have been generated only for ENDF/B-VII cross-section library.

Table C.4 TSURFER FP residual uncertainty (1σ)

Description	Change from base	Burnup (GWd/MTU)	FP isotope residual uncertainty (Δk)[a]							
			^{103}Rh	^{133}Cs	^{143}Nd	^{145}Nd	^{149}Sm	^{152}Sm	^{155}Gd	Total
Base case	--	10	7.3E-06	8.1E-06	5.7E-05	4.2E-05	4.0E-05	8.7E-06	--	8.3E-05
		25	2.1E-05	2.0E-05	1.3E-04	1.0E-04	4.5E-05	2.1E-05	--	1.7E-04
		40	3.1E-05	2.9E-05	1.8E-04	1.6E-04	5.0E-05	2.9E-05	--	2.5E-04
		57	3.8E-05	3.6E-05	2.1E-04	2.0E-04	5.1E-05	3.4E-05	--	3.0E-04
Assembly design	B&W 15×15	10	2.5E-05	2.4E-05	1.0E-04	5.5E-05	5.9E-05	1.9E-05	--	1.4E-04
		25	5.9E-05	5.4E-05	2.1E-04	1.3E-04	6.8E-05	4.1E-05	--	2.7E-04
		40	8.3E-05	7.7E-05	2.9E-04	1.9E-04	7.1E-05	5.4E-05	1.5E-06	3.8E-04
		57	9.7E-05	9.3E-05	3.4E-04	2.4E-04	7.1E-05	6.2E-05	2.5E-06	4.5E-04
	W 17×17 (No BAs)	10	1.6E-05	1.9E-05	8.8E-05	4.4E-05	6.1E-05	1.5E-05	--	1.2E-04
		25	4.5E-05	4.5E-05	1.9E-04	1.1E-04	7.3E-05	3.5E-05	--	2.5E-04
		40	6.8E-05	6.7E-05	2.7E-04	1.7E-04	7.8E-05	4.9E-05	--	3.5E-04
		57	8.3E-05	8.2E-05	3.3E-04	2.1E-04	7.9E-05	5.7E-05	1.1E-06	4.2E-04
Rack design	Unpoisoned panels	10	1.9E-05	2.1E-05	1.2E-04	4.8E-05	7.7E-05	1.9E-05	--	1.5E-04
		25	5.2E-05	4.6E-05	2.4E-04	1.1E-04	8.5E-05	4.1E-05	--	2.9E-04
		40	7.4E-05	6.7E-05	3.2E-04	1.6E-04	9.2E-05	5.3E-05	--	3.9E-04
		57	8.7E-05	8.1E-05	3.8E-04	2.0E-04	9.2E-05	6.1E-05	1.3E-06	4.6E-04
	Cell pitch increased 0.25 in.	10	1.7E-05	2.0E-05	8.9E-05	4.6E-05	6.7E-05	1.6E-05	--	1.2E-04
		25	4.5E-05	4.4E-05	1.9E-04	1.0E-04	8.2E-05	3.3E-05	--	2.4E-04
		40	6.7E-05	6.4E-05	2.7E-04	1.6E-04	8.7E-05	4.6E-05	--	3.4E-04
		57	8.0E-05	7.6E-05	3.2E-04	1.9E-04	8.6E-05	5.2E-05	1.3E-06	4.0E-04
	Poison panel B10 +10%	10	1.7E-05	2.0E-05	8.9E-05	4.6E-05	6.7E-05	1.6E-05	--	1.2E-04
		25	4.8E-05	4.7E-05	2.0E-04	1.1E-04	7.5E-05	3.6E-05	--	2.5E-04
		40	7.0E-05	6.8E-05	2.7E-04	1.7E-04	8.4E-05	4.9E-05	--	3.5E-04
		57	8.5E-05	8.3E-05	3.2E-04	2.1E-04	8.5E-05	5.7E-05	1.3E-06	4.2E-04

Table C.4 TSURFER FP residual uncertainty (1σ) (continued)

Description	Change from base	Burnup (GWd/MTU)	FP isotope residual uncertainty (Δk)[a]							
			^{103}Rh	^{133}Cs	^{143}Nd	^{145}Nd	^{149}Sm	^{152}Sm	^{155}Gd	Total
	Poison panel B10 -10%	10	1.7E-05	2.0E-05	9.0E-05	4.5E-05	6.7E-05	1.6E-05	--	1.2E-04
		25	4.8E-05	4.7E-05	2.0E-04	1.1E-04	7.5E-05	3.6E-05	--	2.5E-04
		40	7.0E-05	6.8E-05	2.7E-04	1.7E-04	8.4E-05	4.9E-05	--	3.5E-04
		57	8.6E-05	8.3E-05	3.3E-04	2.1E-04	8.5E-05	5.7E-05	1.3E-06	4.2E-04
Decay time	1 year	10	2.5E-05	2.0E-05	9.8E-05	4.5E-05	7.8E-05	1.5E-05	2.1E-06	1.4E-04
		25	5.6E-05	4.7E-05	2.0E-04	1.1E-04	8.9E-05	3.5E-05	5.4E-06	2.6E-04
		40	7.7E-05	6.8E-05	2.7E-04	1.6E-04	9.3E-05	4.8E-05	9.1E-06	3.5E-04
		57	9.1E-05	8.3E-05	3.2E-04	2.1E-04	9.2E-05	5.6E-05	1.2E-05	4.2E-04
	5 year	10	2.4E-05	2.0E-05	9.5E-05	4.4E-05	7.7E-05	1.5E-05	7.4E-06	1.3E-04
		25	5.4E-05	4.6E-05	1.9E-04	1.1E-04	8.7E-05	3.4E-05	1.9E-05	2.5E-04
		40	7.6E-05	6.7E-05	2.7E-04	1.6E-04	9.2E-05	4.7E-05	3.1E-05	3.4E-04
		57	8.7E-05	8.0E-05	3.1E-04	2.0E-04	9.0E-05	5.4E-05	4.2E-05	4.0E-04
	20 year	10	2.3E-05	1.9E-05	9.1E-05	4.2E-05	7.5E-05	1.4E-05	1.3E-05	1.3E-04
		25	5.0E-05	4.4E-05	1.8E-04	1.0E-04	8.5E-05	3.2E-05	3.0E-05	2.4E-04
		40	7.1E-05	6.5E-05	2.5E-04	1.6E-04	9.0E-05	4.5E-05	4.9E-05	3.3E-04
		57	8.0E-05	7.4E-05	2.9E-04	1.9E-04	8.6E-05	5.1E-05	6.7E-05	3.8E-04
	40 year	10	2.2E-05	1.9E-05	8.9E-05	4.1E-05	7.5E-05	1.4E-05	1.3E-05	1.3E-04
		25	4.9E-05	4.3E-05	1.8E-04	9.9E-05	8.4E-05	3.1E-05	3.0E-05	2.3E-04
		40	7.0E-05	6.4E-05	2.4E-04	1.5E-04	9.0E-05	4.4E-05	4.9E-05	3.2E-04
		57	7.7E-05	7.2E-05	2.8E-04	1.8E-04	8.4E-05	4.9E-05	6.9E-05	3.7E-04
Soluble boron	1000 ppm	10	1.5E-05	1.7E-05	6.8E-05	3.9E-05	4.9E-05	1.4E-05	--	9.6E-05
		25	4.1E-05	4.1E-05	1.5E-04	9.4E-05	5.9E-05	3.1E-05	--	2.0E-04
		40	6.2E-05	6.1E-05	2.2E-04	1.5E-04	6.5E-05	4.3E-05	--	2.9E-04
		57	7.6E-05	7.5E-05	2.7E-04	1.9E-04	6.7E-05	5.1E-05	9.7E-07	3.5E-04

Table C.4 TSURFER FP residual uncertainty (1σ) (continued)

Description	Change from base	Burnup (GWd/MTU)	FP isotope residual uncertainty (Δk)[a]							
			^{103}Rh	^{133}Cs	^{143}Nd	^{145}Nd	^{149}Sm	^{152}Sm	^{155}Gd	Total
	Search for k_{eff} = 0.94	10	1.6E-05	1.9E-05	8.2E-05	4.4E-05	6.1E-05	1.5E-05	--	1.1E-04
		25	4.5E-05	4.5E-05	1.8E-04	1.0E-04	7.1E-05	3.4E-05	--	2.3E-04
		40	6.7E-05	6.5E-05	2.5E-04	1.6E-04	7.6E-05	4.7E-05	--	3.2E-04
		57	8.1E-05	7.9E-05	3.0E-04	2.0E-04	7.7E-05	5.4E-05	1.1E-06	3.9E-04
Cross-section library	ENDF-B/V	10	N/A	N/A	N/A	N/A	N/A	N/A	N/A	N/A
		25	N/A	N/A	N/A	N/A	N/A	N/A	N/A	N/A
		40	N/A	N/A	N/A	N/A	N/A	N/A	N/A	N/A
		57	N/A	N/A	N/A	N/A	N/A	N/A	N/A	N/A
	ENDF-B/VI	10	N/A	N/A	N/A	N/A	N/A	N/A	N/A	N/A
		25	N/A	N/A	N/A	N/A	N/A	N/A	N/A	N/A
		40	N/A	N/A	N/A	N/A	N/A	N/A	N/A	N/A
		57	N/A	N/A	N/A	N/A	N/A	N/A	N/A	N/A
Axial burnup	1 node	10	2.5E-05	2.9E-05	1.3E-04	6.8E-05	8.1E-05	2.4E-05	--	1.7E-04
		25	6.3E-05	6.3E-05	2.6E-04	1.5E-04	9.3E-05	4.8E-05	--	3.3E-04
		40	8.9E-05	8.7E-05	3.5E-04	2.2E-04	9.7E-05	6.1E-05	--	4.5E-04
		57	1.1E-04	1.0E-04	4.3E-04	2.8E-04	9.7E-05	7.1E-05	1.6E-06	5.5E-04

[a]Bias uncertainty data based on (n, γ) reactions only.
[b]N/A = not available because sensitivity data files have been generated only for ENDF/B-VII cross-section library.

Table C.5 TSUNAMI-IP seven FP bounding uncertainty in k_{eff} at 1σ confidence

Description	Change from base	Burnup (GWd/MTU)	FP isotope nuclear data uncertainty (Δk)							
			^{103}Rh	^{133}Cs	^{143}Nd	^{145}Nd	^{149}Sm	^{152}Sm	^{155}Gd	Total
Base case	--	10	4.6E-05	5.0E-05	1.1E-04	4.7E-05	1.5E-04	2.0E-05	1.3E-07	2.1E-04
		25	1.3E-04	1.2E-04	2.5E-04	1.2E-04	1.7E-04	4.7E-05	4.3E-07	3.8E-04
		40	1.9E-04	1.7E-04	3.5E-04	1.7E-04	1.9E-04	6.4E-05	9.0E-07	5.1E-04
		57	2.3E-04	2.1E-04	4.2E-04	2.2E-04	1.9E-04	7.4E-05	1.6E-06	6.0E-04
Assembly design	B&W 15×15	10	6.8E-05	6.1E-05	1.3E-04	5.8E-05	1.4E-04	2.5E-05	2.5E-07	2.2E-04
		25	1.6E-04	1.4E-04	2.7E-04	1.4E-04	1.5E-04	5.2E-05	8.7E-07	4.0E-04
		40	2.3E-04	1.9E-04	3.8E-04	2.0E-04	1.6E-04	7.0E-05	1.8E-06	5.5E-04
		57	2.7E-04	2.3E-04	4.5E-04	2.5E-04	1.6E-04	7.9E-05	3.1E-06	6.5E-04
	W 17×17 (No BAs)	10	4.3E-05	4.9E-05	1.1E-04	4.6E-05	1.4E-04	2.0E-05	1.1E-07	2.0E-04
		25	1.3E-04	1.2E-04	2.5E-04	1.1E-04	1.7E-04	4.6E-05	3.6E-07	3.7E-04
		40	1.9E-04	1.7E-04	3.6E-04	1.7E-04	1.8E-04	6.4E-05	7.6E-07	5.1E-04
		57	2.3E-04	2.1E-04	4.4E-04	2.2E-04	1.8E-04	7.4E-05	1.3E-06	6.1E-04
Rack design	Unpoisoned panels	10	5.8E-05	6.0E-05	1.6E-04	5.2E-05	1.8E-04	2.8E-05	1.4E-07	2.6E-04
		25	1.5E-04	1.3E-04	3.1E-04	1.1E-04	1.9E-04	5.4E-05	4.7E-07	4.3E-04
		40	2.1E-04	1.8E-04	4.2E-04	1.7E-04	2.1E-04	7.1E-05	9.5E-07	5.7E-04
		57	2.5E-04	2.2E-04	4.9E-04	2.1E-04	2.1E-04	8.0E-05	1.6E-06	6.7E-04
	Cell pitch increased 0.25 in.	10	4.4E-05	4.8E-05	1.1E-04	4.5E-05	1.6E-04	1.9E-05	1.4E-07	2.1E-04
		25	1.3E-04	1.1E-04	2.5E-04	1.1E-04	1.9E-04	4.3E-05	4.5E-07	3.7E-04
		40	1.9E-04	1.6E-04	3.5E-04	1.7E-04	2.0E-04	5.9E-05	9.5E-07	5.0E-04
		57	2.2E-04	1.9E-04	4.2E-04	2.0E-04	2.0E-04	6.7E-05	1.6E-06	5.9E-04
	Poison panel B10 +10%	10	4.7E-05	5.1E-05	1.1E-04	4.8E-05	1.5E-04	2.1E-05	1.3E-07	2.1E-04
		25	1.3E-04	1.2E-04	2.5E-04	1.2E-04	1.7E-04	4.7E-05	4.3E-07	3.8E-04
		40	1.9E-04	1.7E-04	3.6E-04	1.7E-04	1.9E-04	6.3E-05	9.0E-07	5.1E-04
		57	2.3E-04	2.1E-04	4.3E-04	2.2E-04	1.9E-04	7.3E-05	1.6E-06	6.1E-04

Table C.5 TSUNAMI-IP seven FP bounding uncertainty in k_{eff} at 1σ confidence (continued)

Description	Change from base	Burnup (GWd/MTU)	FP isotope nuclear data uncertainty (Δk)							
			^{103}Rh	^{133}Cs	^{143}Nd	^{145}Nd	^{149}Sm	^{152}Sm	^{155}Gd	Total
	Poison panel B10 -10%	10	4.7E-05	5.1E-05	1.2E-04	4.7E-05	1.5E-04	2.1E-05	1.3E-07	2.1E-04
		25	1.3E-04	1.2E-04	2.6E-04	1.2E-04	1.7E-04	4.7E-05	4.3E-07	3.8E-04
		40	1.9E-04	1.7E-04	3.6E-04	1.7E-04	1.9E-04	6.4E-05	9.0E-07	5.2E-04
		57	2.4E-04	2.1E-04	4.3E-04	2.2E-04	1.9E-04	7.4E-05	1.6E-06	6.1E-04
Decay time	1 year	10	6.9E-05	5.2E-05	1.3E-04	4.6E-05	1.8E-04	2.0E-05	2.5E-06	2.4E-04
		25	1.5E-04	1.2E-04	2.6E-04	1.1E-04	2.0E-04	4.5E-05	6.7E-06	4.0E-04
		40	2.1E-04	1.7E-04	3.6E-04	1.7E-04	2.1E-04	6.2E-05	1.1E-05	5.3E-04
		57	2.5E-04	2.1E-04	4.3E-04	2.2E-04	2.1E-04	7.2E-05	1.5E-05	6.2E-04
	5 year	10	6.7E-05	5.1E-05	1.2E-04	4.5E-05	1.8E-04	1.9E-05	9.1E-06	2.4E-04
		25	1.5E-04	1.2E-04	2.5E-04	1.1E-04	2.0E-04	4.4E-05	2.3E-05	3.9E-04
		40	2.1E-04	1.7E-04	3.5E-04	1.7E-04	2.1E-04	6.1E-05	3.8E-05	5.2E-04
		57	2.4E-04	2.0E-04	4.1E-04	2.1E-04	2.0E-04	6.9E-05	5.1E-05	6.0E-04
	20 year	10	6.3E-05	4.8E-05	1.2E-04	4.3E-05	1.7E-04	1.8E-05	1.6E-05	2.3E-04
		25	1.4E-04	1.1E-04	2.3E-04	1.0E-04	1.9E-04	4.1E-05	3.7E-05	3.7E-04
		40	2.0E-04	1.6E-04	3.3E-04	1.6E-04	2.1E-04	5.8E-05	6.1E-05	5.0E-04
		57	2.2E-04	1.8E-04	3.8E-04	1.9E-04	2.0E-04	6.5E-05	8.3E-05	5.6E-04
	40 year	10	6.2E-05	4.8E-05	1.2E-04	4.3E-05	1.7E-04	1.8E-05	1.6E-05	2.3E-04
		25	1.4E-04	1.1E-04	2.3E-04	1.0E-04	1.9E-04	4.0E-05	3.7E-05	3.6E-04
		40	1.9E-04	1.6E-04	3.2E-04	1.6E-04	2.0E-04	5.7E-05	6.1E-05	4.9E-04
		57	2.1E-04	1.8E-04	3.7E-04	1.9E-04	1.9E-04	6.3E-05	8.6E-05	5.5E-04
Soluble boron	1000 ppm	10	4.0E-05	4.4E-05	8.7E-05	4.1E-05	1.1E-04	1.8E-05	9.4E-08	1.6E-04
		25	1.1E-04	1.0E-04	2.0E-04	9.8E-05	1.3E-04	4.0E-05	3.2E-07	3.0E-04
		40	1.7E-04	1.5E-04	2.8E-04	1.5E-04	1.5E-04	5.5E-05	6.9E-07	4.3E-04
		57	2.1E-04	1.8E-04	3.5E-04	1.9E-04	1.5E-04	6.4E-05	1.2E-06	5.1E-04

Table C.5 TSUNAMI-IP seven FP bounding uncertainty in k_{eff} at 1σ confidence (continued)

Description	Change from base	Burnup (GWd/MTU)	FP isotope nuclear data uncertainty (Δk)							
			^{103}Rh	^{133}Cs	^{143}Nd	^{145}Nd	^{149}Sm	^{152}Sm	^{155}Gd	Total
	Search for k_{eff} = 0.94	10	4.5E-05	4.9E-05	1.1E-04	4.5E-05	1.4E-04	2.0E-05	1.2E-07	1.9E-04
		25	1.2E-04	1.1E-04	2.3E-04	1.1E-04	1.6E-04	4.4E-05	3.8E-07	3.5E-04
		40	1.8E-04	1.6E-04	3.2E-04	1.7E-04	1.7E-04	6.0E-05	8.0E-07	4.8E-04
		57	2.2E-04	2.0E-04	3.9E-04	2.1E-04	1.8E-04	6.9E-05	1.4E-06	5.6E-04
Cross-section library	ENDF-B/V	10	4.5E-05	4.3E-05	1.1E-04	4.4E-05	1.5E-04	1.9E-05	1.4E-07	2.0E-04
		25	--	--	--	--	--	--	--	--
		40	1.9E-04	1.4E-04	3.3E-04	1.6E-04	1.9E-04	5.9E-05	9.3E-07	4.8E-04
		57	--	--	--	--	--	--	--	--
	ENDF-B/VI	10	4.4E-05	4.8E-05	1.1E-04	4.5E-05	1.5E-04	1.9E-05	1.3E-07	2.0E-04
		25	--	--	--	--	--	--	--	--
		40	1.9E-04	1.7E-04	3.3E-04	1.7E-04	1.9E-04	6.1E-05	8.8E-07	4.9E-04
		57	--	--	--	--	--	--	--	--
Axial burnup	1 node	10	6.9E-05	7.5E-05	1.6E-04	7.1E-05	1.8E-04	3.2E-05	1.4E-07	2.8E-04
		25	1.8E-04	1.6E-04	3.4E-04	1.6E-04	2.1E-04	6.2E-05	5.2E-07	4.9E-04
		40	2.5E-04	2.2E-04	4.6E-04	2.3E-04	2.2E-04	7.9E-05	1.1E-06	6.6E-04
		57	2.9E-04	2.7E-04	5.7E-04	2.9E-04	2.2E-04	9.2E-05	2.0E-06	7.9E-04

The TSURFER results for the application models show the combined FP bias values ranging from 3.7×10^{-4} to 1.45×10^{-3}. The TSURFER FP bias values are essentially equal to or less than the 3 sigma error band of the cross-section covariance uncertainty. The results indicate that the FP cross sections consistently overpredict k_{eff} when combined, hence confirming the validity of using the cross-section covariance data to bound the bias because no credit for positive bias is taken.

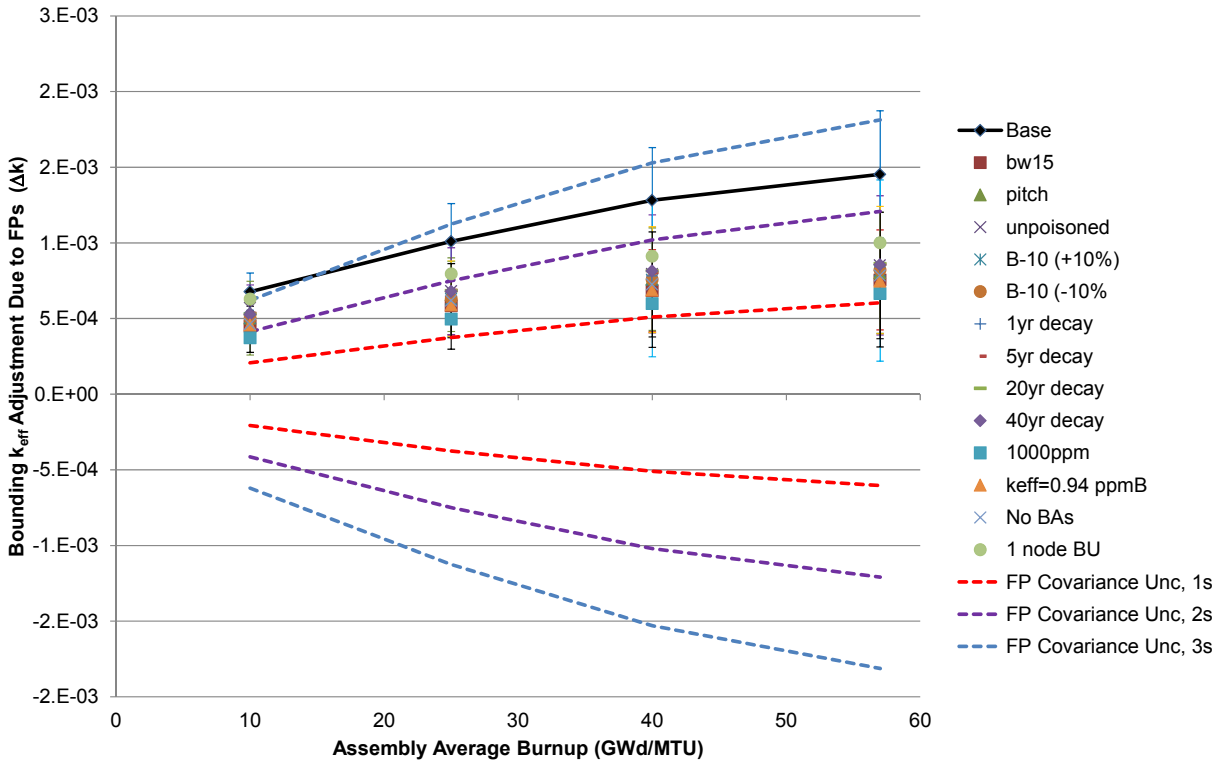

Figure C.1 Net FP bias and bias uncertainty compared against bounding FP covariance uncertainty.

APPENDIX D
EXAMPLE TRITON DEPLETION CODE INPUT

PWR Assembly

```
=t-depl parm=(centrm,addnux=3)
PWR Westinghouse OFA 17x17 with WABA, 1/4 assembly model, 4.0 wt% enriched
v7-238
read comp
'
'fuel 1.0 wt%
 uo2 1 den=10.5216 1 1100 92235 4.0
 92238 96.0 end
'clad
 zirc4 2 1 620 end
'water moderator with 1000 ppm soluble boron
 h2o 3 den=0.63 1 610 end
 arbmb 0.63 1 1 0 0 5000 100 3 1000e-06 610 end
'gap
 n 4 den=0.00125 1 620 end
'guide tube
 zirc4 5 1 610 end
'
'WABA inner water moderator with 1000 ppm soluble boron
 h2o 10 den=0.63 1 610 end
 arbmb 0.63 1 1 0 0 5000 100 10 1000e-06 610 end
'WABA inner cladding
 zirc4 11 1 610 end
'WABA inner gap
 n 12 den=0.00125 1 610 end
'WABA Al2O3-B4C
 b-10 13 0 3.0697E-3 610.0 end
 b-11 13 0 1.2753E-2 610.0 end
 c 13 0 3.9521E-3 610.0 end
 al 13 0 2.6344E-2 610.0 end
 o 13 0 3.9506E-2 610.0 end
'WABA Al2O3-B4C
 b-10 14 0 3.0697E-3 610.0 end
 b-11 14 0 1.2753E-2 610.0 end
 c 14 0 3.9521E-3 610.0 end
 al 14 0 2.6344E-2 610.0 end
 o 14 0 3.9506E-2 610.0 end
'WABA Al2O3-B4C
 b-10 15 0 3.0697E-3 610.0 end
 b-11 15 0 1.2753E-2 610.0 end
 c 15 0 3.9521E-3 610.0 end
 al 15 0 2.6344E-2 610.0 end
 o 15 0 3.9506E-2 610.0 end
'WABA Al2O3-B4C
 b-10 16 0 3.0697E-3 610.0 end
 b-11 16 0 1.2753E-2 610.0 end
 c 16 0 3.9521E-3 610.0 end
 al 16 0 2.6344E-2 610.0 end
 o 16 0 3.9506E-2 610.0 end
'WABA Al2O3-B4C
 b-10 17 0 3.0697E-3 610.0 end
 b-11 17 0 1.2753E-2 610.0 end
 c 17 0 3.9521E-3 610.0 end
 al 17 0 2.6344E-2 610.0 end
```

```
 o 17 0 3.9506E-2 610.0 end
'WABA outer gap
 n 18 den=0.00125 1 610 end
'WABA outer cladding
 zirc4 19 1 610 end
'WABA outer water moderator with 1000 ppm soluble boron
 h2o 20 den=0.63 1 610 end
 arbmb 0.63 1 1 0 0 5000 100 20 1000e-06 610 end
'WABA guide tube
 zirc4 21 1 610 end
'WABA pitch water moderator with 1000 ppm soluble boron
 h2o 22 den=0.63 1 610 end
 arbmb 0.63 1 1 0 0 5000 100 22 1000e-06 610 end
'ring around WABA for centrm 4.0 wt%
 uo2 23 den=10.5216 1 1100 92235 4.0
 92238 96.0 end
'
end comp
' ----------------------------------------------------------------
' Cell data
' ----------------------------------------------------------------
read celldata
 latticecell squarepitch pitch=1.2598 3
 fueld=0.7844 1
 gapd=0.8001 4
 cladd=0.9144 2 end
 multiregion cylindrical right_bdy=white end
 10 0.28575 11 0.33910 12 0.35305 13 0.35767
 14 0.36690 15 0.38999 16 0.39923 17 0.40385
 18 0.41785 19 0.48387 20 0.56135 21 0.60200
 22 0.71077 23 0.80 end zone
end celldata
' ----------------------------------------------------------------
' Depletion data
' ----------------------------------------------------------------
read depletion
 1 flux 13 14 15 16 17
end depletion
' ----------------------------------------------------------------
' Burn data
' ----------------------------------------------------------------
read burndata
 power=60.0 burn=1500 down=0 nlib=30 end
end burndata
' ----------------------------------------------------------------
' NEWT model data
' ----------------------------------------------------------------
read model
Westinghouse OFA 17x17, 4.0 wt% uo2
read parm
 run=yes
end parm
read materials
 1 1 ! fuel ! end
 2 1 ! clad ! end
 3 2 ! water ! end
 4 0 ! gap ! end
```

```
 5 1 ! guide tube ! end
 10 2 ! WABA inner water ! end
 11 1 ! WABA clad ! end
 12 0 ! WABA inner gap ! end
 13 2 ! WABA poison rod ! end
 14 2 ! WABA poison rod ! end
 15 2 ! WABA poison rod ! end
 16 2 ! WABA poison rod ! end
 17 2 ! WABA poison rod ! end
 18 0 ! WABA gap ! end
 19 1 ! WABA outer clad ! end
 20 2 ! WABA outer water ! end
 21 1 ! WABA guide tube ! end
 22 2 ! WABA pitch water ! end
end materials
read geom
unit 1
com='fuel rod'
 cylinder 10 .3922
 cylinder 20 .40005
 cylinder 30 .4572
 cuboid 40 4p0.6299
 media 1 1 10
 media 4 1 20 -10
 media 2 1 30 -20
 media 3 1 40 -30
 boundary 40 4 4
unit 5
com='guide tube'
 cylinder 10 .28575
 cylinder 20 .33910
 cylinder 30 .35305
 cylinder 40 .35767
 cylinder 50 .36690
 cylinder 60 .38999
 cylinder 70 .39923
 cylinder 80 .40385
 cylinder 90 .41785
 cylinder 100 .48387
 cylinder 110 .56135
 cylinder 120 .602
 cuboid 130 4p0.6299
 media 10 1 10
 media 11 1 20 -10
 media 12 1 30 -20
 media 13 1 40 -30
 media 14 1 50 -40
 media 15 1 60 -50
 media 16 1 70 -60
 media 17 1 80 -70
 media 18 1 90 -80
 media 19 1 100 -90
 media 20 1 110 -100
 media 21 1 120 -110
 media 22 1 130 -120
 boundary 130 4 4
unit 11
```

```
com='right half of fuel rod'
 cylinder 10 .3922 chord +x=0
 cylinder 20 .40005 chord +x=0
 cylinder 30 .4572 chord +x=0
 cuboid 40 0.6299 0.0 2p0.6299
 media 1 1 10
 media 4 1 20 -10
 media 2 1 30 -20
 media 3 1 40 -30
 boundary 40 2 4
unit 12
com='top half of fuel rod'
 cylinder 10 .3922 chord +y=0
 cylinder 20 .40005 chord +y=0
 cylinder 30 .4572 chord +y=0
 cuboid 40 2p0.6299 0.6299 0.0
 media 1 1 10
 media 4 1 20 -10
 media 2 1 30 -20
 media 3 1 40 -30
 boundary 40 4 2
unit 51
com='right half of guide tube'
 cylinder 10 .28575 chord +x=0.0
 cylinder 20 .33910 chord +x=0.0
 cylinder 30 .35305 chord +x=0.0
 cylinder 40 .35767 chord +x=0.0
 cylinder 50 .36690 chord +x=0.0
 cylinder 60 .38999 chord +x=0.0
 cylinder 70 .39923 chord +x=0.0
 cylinder 80 .40385 chord +x=0.0
 cylinder 90 .41785 chord +x=0.0
 cylinder 100 .48387 chord +x=0.0
 cylinder 110 .56135 chord +x=0.0
 cylinder 120 .602 chord +x=0.0
 cuboid 130 0.6299 0.0 2p0.6299
 media 10 1 10
 media 11 1 20 -10
 media 12 1 30 -20
 media 13 1 40 -30
 media 14 1 50 -40
 media 15 1 60 -50
 media 16 1 70 -60
 media 17 1 80 -70
 media 18 1 90 -80
 media 19 1 100 -90
 media 20 1 110 -100
 media 21 1 120 -110
 media 22 1 130 -120
 boundary 130 2 4
unit 52
com='top half of guide tube'
 cylinder 10 .28575 chord +y=0.0
 cylinder 20 .33910 chord +y=0.0
 cylinder 30 .35305 chord +y=0.0
 cylinder 40 .35767 chord +y=0.0
 cylinder 50 .36690 chord +y=0.0
```

```
 cylinder 60 .38999 chord +y=0.0
 cylinder 70 .39923 chord +y=0.0
 cylinder 80 .40385 chord +y=0.0
 cylinder 90 .41785 chord +y=0.0
 cylinder 100 .48387 chord +y=0.0
 cylinder 110 .56135 chord +y=0.0
 cylinder 120 .602 chord +y=0.0
 cuboid 130 2p0.6299 0.6299 0.0
 media 10 1 10
 media 11 1 20 -10
 media 12 1 30 -20
 media 13 1 40 -30
 media 14 1 50 -40
 media 15 1 60 -50
 media 16 1 70 -60
 media 17 1 80 -70
 media 18 1 90 -80
 media 19 1 100 -90
 media 20 1 110 -100
 media 21 1 120 -110
 media 22 1 130 -120
 boundary 130 4 2
unit 53
com='1/4 instrument tube'
 cylinder 10 .56135 chord +x=0 chord +y=0
 cylinder 20 .602 chord +x=0 chord +y=0
 cuboid 40 0.6299 0.0 0.6299 0.0
 media 3 1 10
 media 5 1 20 -10
 media 3 1 40 -20
 boundary 40 2 2
global unit 10
 cuboid 10 10.7083 0.0 10.7083 0.0
 array 1 10 place 1 1 0 0
 media 3 1 10
 boundary 10 34 34
end geom
read array
 ara=1 nux=9 nuy=9 typ=cuboidal
 fill
 53 12 12 52 12 12 52 12 12
 11 1 1 1 1 1 1 1 1
 11 1 1 1 1 1 1 1 1
 51 1 1 5 1 1 5 1 1
 11 1 1 1 1 1 1 1 1
 11 1 1 1 1 5 1 1 1
 51 1 1 5 1 1 1 1 1
 11 1 1 1 1 1 1 1 1
 11 1 1 1 1 1 1 1 1
 end fill
end array
read bounds
 all=refl
end bounds
end model
end
=shell
```

```
 cp ft33f001.cmbined $RTNDIR/origenlib-4.0
end
```

BWR Assembly

```
=t-depl parm=(centrm, addnux=3, weight)
BWR GE 10×10 fuel assembly - averaged assembly, uo2-gd pin - 5
v7-238
' generic ge10x120-8, 3wt% Gd rods, fuel assembly

read comp
' water channel clad
zirc2 1 1.0 567 end
' water Channel coolant
h2o 2 den=0.776 1.0 512 end
' Coolant between assemblies
h2o 3 den=0.776 1.0 512 end
' Assembly channel
zirc2 4 1.0 512 end
' fuel, no-Gd
uo2 10 den=10.41 1.00 840 92235 5 92238 95 end
' fuel, with Gd
uo2 20 den=10.41 0.97 840 92235 5 92238 95 end
gd2o3 20 den=10.41 0.03 840 end
uo2 21 den=10.41 0.97 840 92235 5 92238 95 end
gd2o3 21 den=10.41 0.03 840 end
uo2 22 den=10.41 0.97 840 92235 5 92238 95 end
gd2o3 22 den=10.41 0.03 840 end
uo2 23 den=10.41 0.97 840 92235 5 92238 95 end
gd2o3 23 den=10.41 0.03 840 end
uo2 24 den=10.41 0.97 840 92235 5 92238 95 end
gd2o3 24 den=10.41 0.03 840 end
' cladding & moderator
zirc2 5 1.0 567 end
h2o 6 den=0.776 1.0 512 end
zirc2 7 1.0 567 end
h2o 8 den=0.776 1.0 512 end
end comp
' ----------------------------------------------------------------
' Cell data
' ----------------------------------------------------------------
read celldata
latticecell squarepitch pitch=1.295 6
 fueld=0.876 10
 gapd=0.894 0
 cladd=1.026 5 end
 centrmdata alump=0.3 pmc_omit=1 nmf6=-1 end centrmdata
multiregion cylindrical left_bdy=reflected right_bdy=white end
 20 0.19588
 21 0.27702
 22 0.33927
 23 0.39176
 24 0.438
 0 0.447
 7 0.513
 8 0.73062 end zone
 centrmdata alump=0.3 pmc_omit=1 nmf6=-1 end centrmdata
end celldata
' ----------------------------------------------------------------
```

```
' Depletion data
' ----------------------------------------------------------------
read depletion
 10 flux 20 21 22 23 24 end
end depletion
' ----------------------------------------------------------------
' Burn data
' ----------------------------------------------------------------
read burndata
 power=26.44 burn=2 nlib=1 down=0 end
 power=26.44 burn=200 nlib=10 down=0 end
 power=26.44 burn=200 nlib=10 down=3 end
end burndata
read opus
 title= Masses of Fuel Nuclides
 units=grams
 time=days
 typarms=nucl
 libtype=all
 symnuc=
 u-234 u-235 u-236 u-238
 np-237
 pu-238 pu-239 pu-240 pu-241 pu-242
 am-241 am-243
 mo-95 tc-99 ag-109 ru-101 rh-103 cs-133
 nd-143 nd-145 eu-151 eu-153
 gd-154 gd-155 gd-156 gd-157 gd-158 gd-160
 sm-147 sm-148 sm-149 sm-150 sm-151 sm-152 end
end opus
' ----------------------------------------------------------------
' NEWT model data
' ----------------------------------------------------------------
read model
BWR GE 10×10 fuel assembly - averaged assembly, uo2-gd pin - 5
read parm
 run=yes
 cmfd=1
 xycmfd=2
 drawit=yes
 epsilon=1e-5
 converg=mix
 inners=6
 therm=yes
 therms=1
 outers=9999
end parm
read materials
 1 1 ! WC-Zr ! end
 2 3 ! WC-W ! end
 3 3 ! As-W ! end
 4 1 ! As-Zr ! end
 10 1 ! fuel ! end
 20 1 ! fuel-gd ! end
 21 1 ! fuel-gd ! end
 22 1 ! fuel-gd ! end
 23 1 ! fuel-gd ! end
 24 1 ! fuel-gd ! end
```

```
 5 1 ! clad ! end
 6 3 ! mod ! end
 7 1 ! clad ! end
 8 3 ! mod ! end
end materials
read geom
unit 1
com='UO2 fuel pin'
 cylinder 10 0.438
 cylinder 20 0.447
 cylinder 30 0.513
 cuboid 40 4p0.6475
 media 10 1 10
 media 0 1 20 -10
 media 5 1 30 -20
 media 6 1 40 -30
 boundary 40 4 4
unit 2
com='gd-UO2 fuel pin'
 cylinder 6 0.19588
 cylinder 7 0.27702
 cylinder 8 0.33927
 cylinder 9 0.39176
 cylinder 10 0.438
 cylinder 20 0.447
 cylinder 30 0.513
 cuboid 40 4p0.6475
 media 20 1 6
 media 21 1 7 -6
 media 22 1 8 -7
 media 23 1 9 -8
 media 24 1 10 -9
 media 0 1 20 -10
 media 7 1 30 -20
 media 8 1 40 -30
 boundary 40 4 4
unit 3
com='water filled position'
 cuboid 10 4p0.6475
 media 2 1 10
 boundary 10 4 4
unit 4
com='water rod'
 cylinder 10 1.161
 cylinder 20 1.261
 media 2 1 10
 media 1 1 20 -10
 boundary 20 8 8
global unit 10
com='assembly'
 cuboid 10 4p6.475
 cuboid 20 4p6.675
 cuboid 30 4p7.62
 array 1 10 place 1 1 -5.8275 -5.8275
 hole 4 origin x=1.295 y=1.295
 hole 4 origin x=-1.295 y=-1.295
 media 4 1 20 -10
```

```
 media 3 1 30 -20
 boundary 30 12 12
end geom
read array
 ara=1 nux=10 nuy=10
 fill
 1 1 1 1 1 1 1 1 1 1
 1 1 1 1 1 2 1 1 1 1
 1 1 1 1 1 1 2 1 1 1
 1 1 2 3 3 1 1 2 1 1
 1 1 1 3 3 1 1 1 2 1
 1 1 2 1 1 3 3 1 1 1
 1 1 1 1 1 3 3 1 1 1
 1 1 1 1 2 1 2 1 1 1
 1 1 1 1 1 1 1 1 1 1
 1 1 1 1 1 1 1 1 1 1 end fill
end array
read bounds
 all=refl
end bounds
end data
end
' ----------------------------------------------------------------
=shell
 mkdir $RTNDIR/${CASE_NAME}_compositions
 cp StdCmpMix* $RTNDIR/${CASE_NAME}_compositions/
end
```

NRC FORM 335
(12-2010)
NRCMD 3.7

U.S. NUCLEAR REGULATORY COMMISSION

BIBLIOGRAPHIC DATA SHEET

(See instructions on the reverse)

1. REPORT NUMBER
(Assigned by NRC, Add Vol., Supp., Rev., and Addendum Numbers, if any.)

NUREG/CR-7109

2. TITLE AND SUBTITLE

An Approach for Validating Actinide and Fission Product Burnup Credit Criticality Safety Analyses – Criticality (keff) Predictions

3. DATE REPORT PUBLISHED

MONTH	YEAR
04	2012

4. FIN OR GRANT NUMBER

JCN V6005

5. AUTHOR(S)

J. M. Scaglione, D. E. Mueller, J. C. Wagner, and W. J. Marshall

6. TYPE OF REPORT

Technical

7. PERIOD COVERED *(Inclusive Dates)*

8. PERFORMING ORGANIZATION - NAME AND ADDRESS *(If NRC, provide Division, Office or Region, U.S. Nuclear Regulatory Commission, and mailing address; if contractor, provide name and mailing address.)*

Oak Ridge National Laboratory
Managed by UT-Battelle, LLC
Oak Ridge, TN 37831-6170

9. SPONSORING ORGANIZATION - NAME AND ADDRESS *(If NRC, type "Same as above"; if contractor, provide NRC Division, Office or Region, U.S. Nuclear Regulatory Commission, and mailing address.)*

Division of Systems Analysis, Office of Nuclear Regulatory Research
U.S. Nuclear Regulatory Commission
Washington, DC 20666-0002

10. SUPPLEMENTARY NOTES

D. Algama, NRC Project Manager

11. ABSTRACT *(200 words or less)*

Taking credit for the reduced reactivity potential of spent fuel in criticality analyses is referred to as burnup credit (BUC). Criticality safety evaluations require validation of the calculational method with critical experiments that are as similar as possible to the safety analysis models, and for which the keff values are known. This poses a challenge for validation of BUC criticality analyses, as critical experiments with actinide and fission product (FP) nuclides similar to spent nuclear fuel (SNF) are not available. To address the issue of validation for nuclides that lack experimental data (e.g., minor actinides and FPs) the US Nuclear Regulatory Commission (NRC) initiated a project with the Oak Ridge National Laboratory (ORNL) to establish and demonstrate an approach that could be used for commercial SNF criticality safety evaluations based on best-available data and methods. This report describes how model-specific sensitivity data can be used to translate nuclear data uncertainties into uncertainty in the model keff value.

12. KEY WORDS/DESCRIPTORS *(List words or phrases that will assist researchers in locating the report.)*

Burnup credit, validation, criticality safety, spent fuel, fission products

13. AVAILABILITY STATEMENT

unlimited

14. SECURITY CLASSIFICATION

(This Page)

unclassified

(This Report)

unclassified

15. NUMBER OF PAGES

16. PRICE

Printed
on recycled
paper

Federal Recycling Program

UNITED STATES
NUCLEAR REGULATORY COMMISSION
WASHINGTON, DC 20555-0001

OFFICIAL BUSINESS

NUREG/CR-7109

An Approach for Validating Actinide and Fission Product Burnup Credit Criticality Safety Analyses—Criticality (K_{eff}) Predictions

April 2012